The electrical and optical properties of cadmium selenide

Kindleysides, L.

The Electrical and Optical Properties of Cadmium Selenide

by

L. Kindleysides, Dip. Tech.

Presented in candidature for the degree of Doctor of Philosophy in the University of Durham.

February, 1969

ACKNOWLEDGEMENTS

The author expresses his gratitude to Dr.J. Woods for his supervision, inspiration and invaluable advice throughout both the course of the research and the preparation of this thesis. He wishes to thank S.R.C. for their financial support during the work and Professor D.A. Wright for the use of his laboratory facilities. He would also like to thank all of his colleagues in the department for many useful discussions. The help of the workshop staff, headed by Mr. F. Spence, in the construction of equipment is gratefully acknowledged.

ABSTRACT

Measurements of thermally stimulated currents, photoconductivity and photoluminescence have been used to study the imperfection centres in photosensitive CdSe crystals. These crystals were grown from the elements using a flow technique.

Seven closely spaced, discrete sets of traps, with concentrations between 10^{12} and 10^{14} cm^{-3}, lie between 0.15 and 0.36 ev below the conduction band. They empty in the temperature range 90 to 210°K. Two other groups of traps are found after illumination at various temperatures with intense white light.

(1) Illumination between 250 and 275°K creates four new sets of traps with associated T.S.C. peaks at 215, 230, 250 and 270°K. Also in this temperature range holes are thermally freed from sensitising centres which lie 0.6 ev above the valence band. The consequent increased recombination substantially modifies the T.S.C. peak shapes and no sensible values of the trapping parameters can be obtained from T.S.C. curve analysis. Illumination at higher temperatures destroys these four centres.

(2) Three further T.S.C. peaks appear at 295, 335 and 365°K as a result of illumination above 250°K. They increase in height with increasing temperature of illumination. Such behaviour can be attributed to either the photochemical creation of traps or the existence of traps surrounded by repulsive potential barriers. The traps have depths of 0.43, 0.52 and 0.63 ev.

They have capture cross sections of about 10^{-20} cm^2 and densities of up to 10^{19} cm^{-3}.

Illumination at increasing temperatures in the range 90 to $400^{o}K$ results in a progressive reduction in the free electron lifetime. This is due to the photochemical creation of class 1 fast recombination centres. Simultaneously the intensity of a 1.15 μ luminescence emission band increases and that of a 0.95 μ band decreases. There is no direct evidence to suggest that these effects are related.

CONTENTS

CHAPTER 1

General Properties of CdSe

1.1 Introduction

Cadmium selenide is a semi-insulating material which belongs to the group of II-VI compounds known as the chalcegonides (sulphides, selenides and tellurides) of zinc and cadmium. These materials have been studied for over 40 years because of their interesting photoconductive and luminescent properties. However much of the work on these materials has been concerned with zinc sulphide and cadmium sulphide. Cadmium selenide has been comparatively neglected in contrast with these two compounds.

Possible applications of these materials are quite varied. Zinc sulphide phosphors are used in the manufacture of the screens of cathode ray tubes. There is also considerable interest at the moment in the possibility of making ZnS electroluminescent display devices. The high photosensitivities that can be achieved in CdS and CdSe make these materials suitable for use in commercial photocells and possibly as infra red and gamma ray detectors. Shimizu and Kiuchi (1967) have described a vidicon camera tube which uses CdSe as a target material and which is about 10 times more sensitive than a conventional tube. More recently attention has been directed to II-VI compounds in regard to their possible use as acousto-electric devices and thin film transistors.

The electrical and optical properties of II-VI compounds are considerably influenced by the presence of trapping and recombination centres due to either impurities or native defects. These give rise to energy levels within the forbidden gap. Much of the work carried out on these materials is devoted to elucidating the nature and role of native defects.

The purpose of the research reported in this thesis was essentially to identify imperfection centres in highly photosensitive cadmium selenide crystals. The crystals were small rods grown from the vapour phase by a flow technique which is described in Chapter 4.

Thermally stimulated current measurements, described in Chapters 6 to 9, were used to obtain information concerning the trapping centres present. Measurements of photoconductivity and luminescence are reported in Chapters 10 to 12 and these give information related to the recombination centres. Photochemical changes in the defect structure of II-VI compounds appear to be important. Therefore the effect of illumination at different temperatures on the various traps and recombination centres was also examined. Discussions of the results are included in the appropriate chapters.

In order to present a reasonable background upon which to consider the results of the different measurements some general properties of CdSe are described in Chapter 1. Chapter 2 deals with theory associated with photoconductivity. This is

important not only because some of the theory is needed in an analysis of later results but because an understanding of photoconductivity is essential in any consideration of a highly photosensitive material such as CdSe. In Chapter 3 the theory required for the interpretation of thermally stimulated current data is presented.

1.2 Native defects

The II-VI compounds are regarded as having a mixture of ionic and covalent bonding. On a simple ionic picture the point defects which can give rise to donor and acceptor levels in CdSe are:

(1) Cadmium interstitials - donors.

(2) Cadmium vacancies - acceptors.

(3) Selenium interstitials - acceptors.

(4) Selenium vacancies - donors.

These defects can be neutral, singly charged or doubly charged. Of course the introduction of any electrically active defect into a crystal lattice implies that some form of compensation occurs in order to maintain charge neutrality. An example of this is the Schottky type defect consisting of a pair of oppositely charged vacancies. The process of auto - compensation in II-VI compounds is by no means understood.

The identification of point defects in II-VI compounds is not simple. An example of this is demonstrated by the difficulty encountered in growing stoichiometric crystals of

these materials. It is well known that they tend to grow with an excess of the group 11 element (cadmium in the case of CdSe). If this non-stoichiometric excess is appreciable the resultant crystals are semi-conducting (resistivities 1Ωcm or lower) and are not significantly photosensitive. Stoichiometric crystals are of the insulating type (with resistivities $10^{10}\Omega$ cms or greater) and are usually highly photosensitive. The high conductivity of non-stoichiometric crystals is attributed to the presence of shallow donors. However the identification of the defects responsible for these donor levels is ambiguous. Tubota et al (1960) have assigned the shallow donors in CdSe to selenium vacancies whereas Burmeister and Stevenson (1967) suggested that they were singly ionised cadmium interstitials.

Woodbury and Hall (1967) studied the diffusion of the chalcogens in several II-VI compounds. They suggested that the only electrically active defects are vacancies. However they also concluded that the mobile defects during diffusion are neutral interstitials.

Point defects are not stationary entities, except perhaps at low temperatures. The energies required for their movement through the crystal lattice are typically a few tenths of an electron volt. As a result of this they can migrate through the lattice and perhaps form associations with other defects or impurities. The possibility that some of the imperfection centres found in II-VI compounds consist of such complexes makes

the interpretation of the defect structure difficult.

Optical irradiation of II-VI compounds can produce centres that were not present before the illumination or perhaps destroy centres that did exist. Photochemical effects of this sort have been reported in the literature. For example Korsunskaya et al (1966) reported the photochemical creation of trapping centres and recombination centres in CdS crystals as a result of irradiation in the temperature range 170 to 290°K. The action of the illumination in producing changes in the defect structure can take three forms:

(1) The photon energy may assist the migration of defects to regions where they can associate with other defects.

(2) The charge state of defects may change under illumination. For example if a defect captures an electron it may then be able to combine with a positively charged imperfection which it would otherwise repel.

(3) The photon energy may be sufficient to cause the dissociation of existing complexes.

1.3 The band structure of cadmium selenide

Cadmium selenide usually crystallises in the hexagonal wurtzite structure. In this structure each cadmium ion is bonded to four selenium ions, one at each corner of a tetrahedron. Similarly each selenium ion is bonded to four cadmium ions which lie at the corners of a tetrahedron. This crystal form is illustrated in figure 1.3.1.

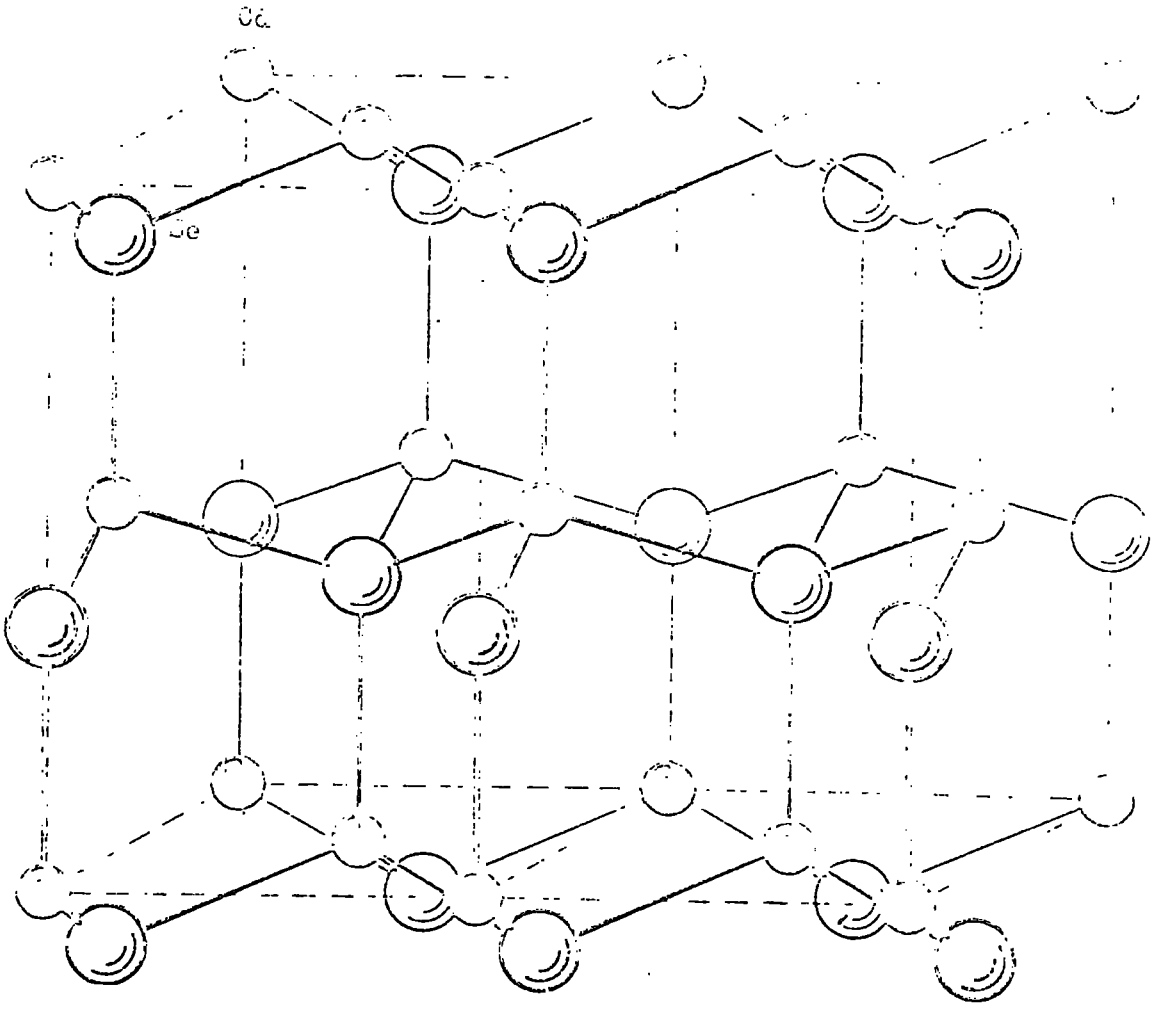

FIGURE 1.3.1 Hexagonal CdSe structure.

The band structure of crystals with the wurtzite structure derived by Birman (1959) is shown in figure 1.3.2. The band maxima and minima lie at k = 0,0,0. The conduction band is formed from s states of the cations (cadmium in the case of CdSe). The valence bands are formed from the p states of the anions (selenium in the case of CdSe). Three valence bands are produced from the p orbitals by the action of crystal field splitting and spin orbit coupling.

From the symmetries of the bands (marked in figure 1.3.2) Birman deduced the selection rules governing the transitions between the bands. The allowed transitions for different polarisations of the photon electric vector, E, with respect to the crystal c-axis are as follows:

(a) E parallel to the c-axis, Γ_1-Γ_1.

(b) E perpendicular to the c-axis, Γ_1-Γ_7 and Γ_4-Γ_7.

The separations of the various bands in CdSe at 4.2°K are shown in figure 1.3.3. These were derived by Wheeler and Dimmock (1961 and 1962) from a study of absorption and reflection spectra and the Zeeman splitting of free exciton lines. They observed a crystal field splitting of the valence bands of 0.025 ev and a spin orbit splitting of 0.432 ev. Wheeler and Dimmock also derived the following values for the effective electron and hole masses.

(a) m_e^*/m_o = 0.13 both parallel and perpendicular to the c-axis i.e. no anisotropy.

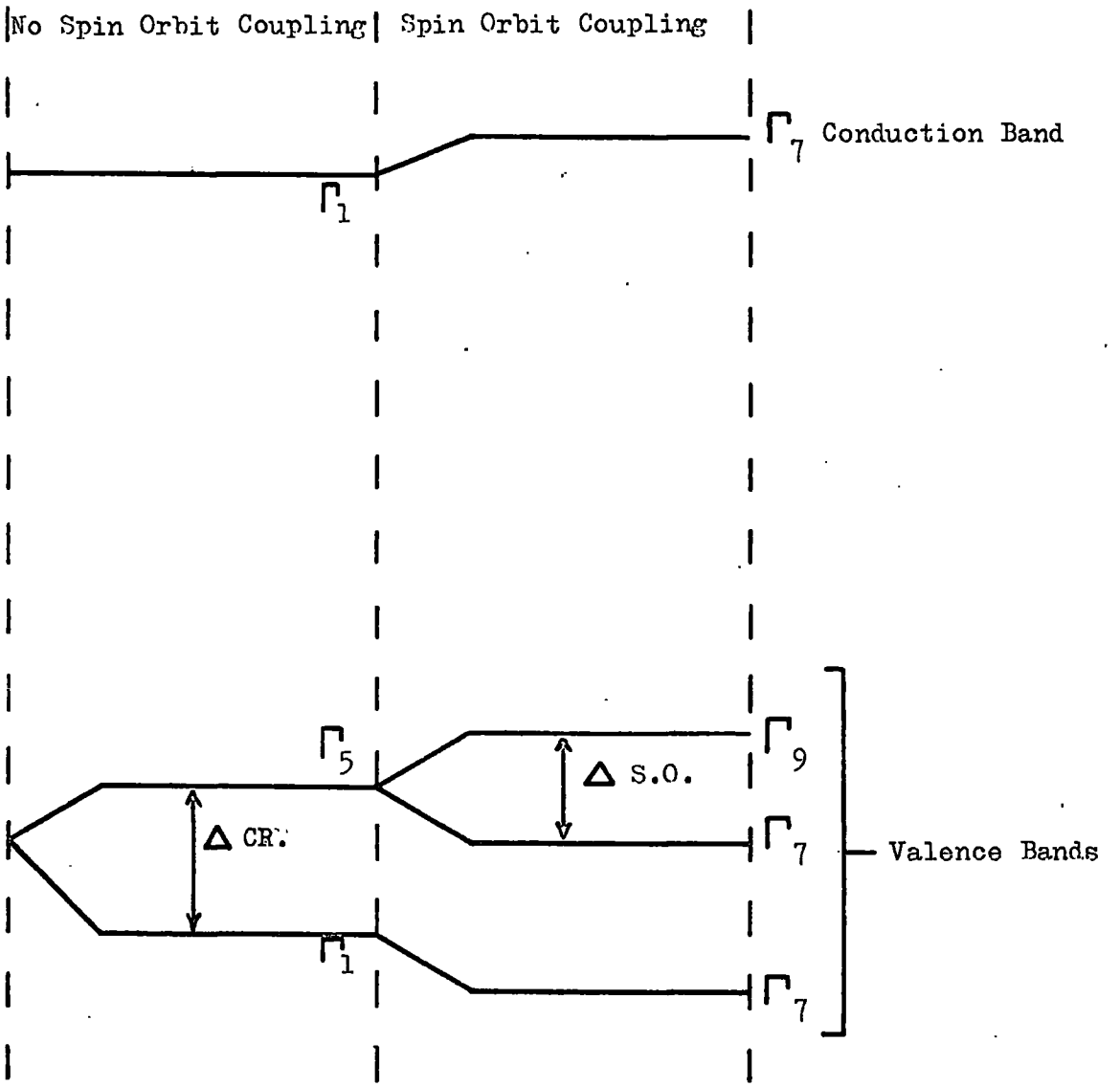

Δ CR. = Crystal Field Splitting

Δ S.O. = Spin Orbit Splitting

FIGURE 1.3.2 Band structure and symmetries of Wurtzite (after Birman, 1959).

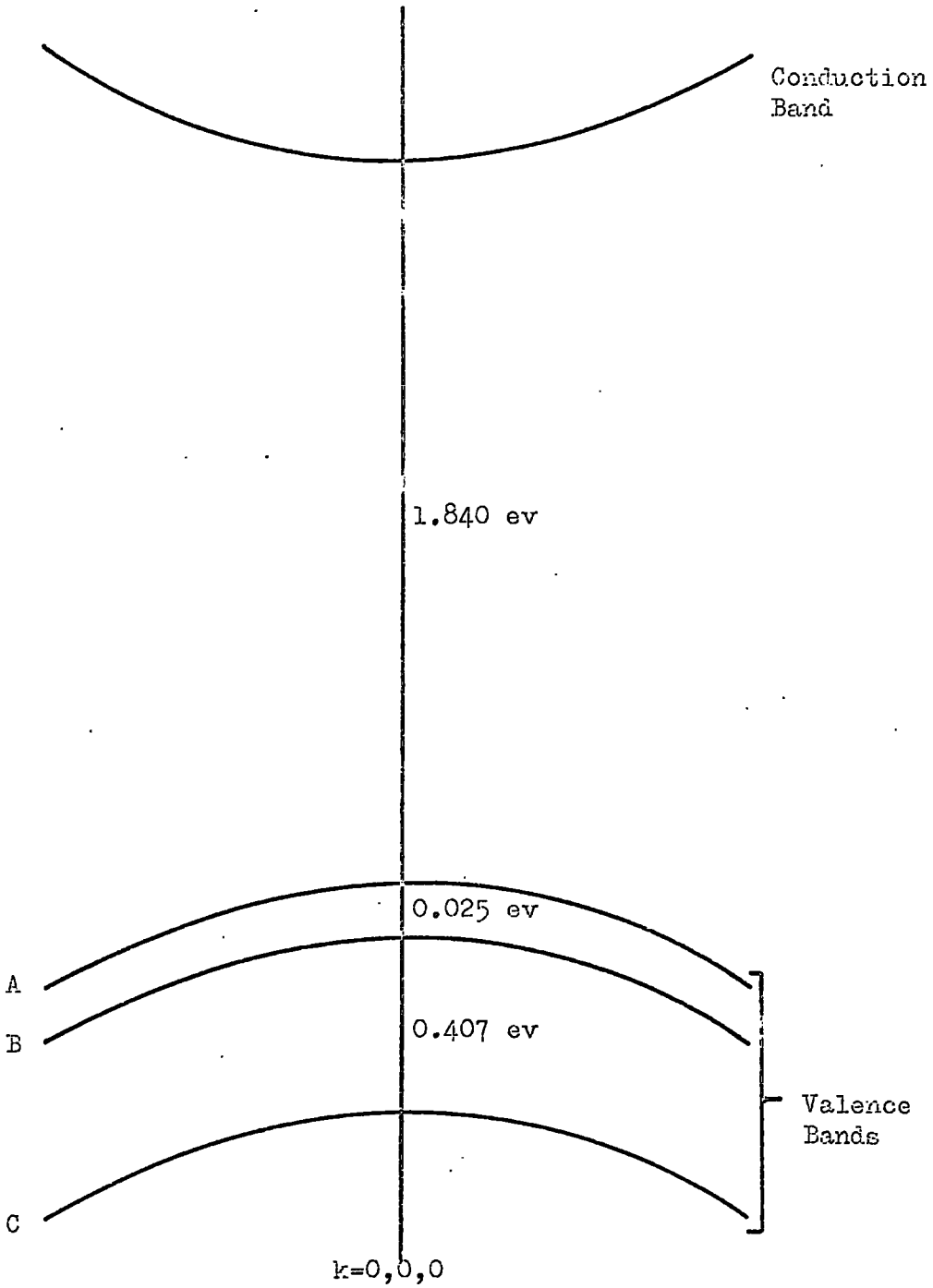

FIGURE 1.3.3 Band structure of CdSe at 4.2°K, after Wheeler and Dimmock (1961 and 1962).

(b) m_h^*/m_o = 0.45 perpendicular to the c-axis

= > 1 parallel to the c-axis

i.e. a large degree of anisotropy.

From reflectivity measurements on CdSe Ginter (1965) found anisotropy in the effective electron mass values. He observed that

$$\frac{m^*_{\text{perpendicular}}}{m^*_{\text{parallel}}} = 1.035$$

His average value of effective mass, m_e^*/m_o = 0.125, is in good agreement with that of Wheeler and Dimmock.

1.4 Conductivity and mobility in CdSe

Cadmium selenide is always n type, there has been no report of the p type material being prepared. This is assumed to be because shallow acceptors cannot be introduced without auto-compensation occurring through the creation of donor centres. Highly conducting n type CdSe can be made insulating by the incorporation of acceptor centres (by copper doping or annealing in selenium vapour for example). However it does not seem possible to extend this treatment to obtain p type crystals. A similar situation exists in CdS. Woodbury (1964) studied the diffusion of cadmium in CdS and one of his conclusions was that the concentration of cadmium vacancies (which give rise to acceptor levels) was always determined by the concentration of impurity donors present.

Reported measurements of conductivity and

mobility in CdSe are few and have been almost exclusively made on semi-conducting material. Heinz and Banks (1956) studied the temperature dependence of the resistivities of crystals with room temperature carrier densities in the range 3×10^{17} to 4×10^{18} cm^{-3}. They observed that the resistivities of such crystals were essentially constant over the temperature range 100 to 370°K. This behaviour is typical of that of degenerate semi-conductors. Measurements of resistivity both along the c-axis and normal to it showed little anisotropy. Heinz and Banks also made electron mobility measurements. They found room temperature values between 390 and 900 cm^2/V sec but did not study the temperature dependence of μ .

A more comprehensive study of the electrical properties of cadmium selenide has been carried out by Burmeister and Stevenson (1967). The crystals examined were again of the semi-conducting type, with room temperature carrier concentrations of 10^{16} to 10^{17} cm^{-3} (corresponding to resistivities of about $10^{-1}\Omega$ cms). These workers analysed their carrier concentration against temperature data in terms of a model consisting of single donor levels and compensating acceptors. Theoretical curves were fitted to the experimental points. The model which yielded the best fitting curve was that for 3.1×10^{16} cm^{-3} donors lying 0.014 ev below the conduction band and 2.0×10^{15} cm^{-3} acceptors. Measurements of carrier concentration in the range 20 to 100°K indicated the existence

of impurity band conduction below about 77°K. Burmeister and Stevenson observed little anisotropy of the electrical properties, the following ratios of electron mobility perpendicular to the c-axis (μ_1) and parallel to the c-axis (μ_3) being found.

(a) At room temperature, $\mu_1/\mu_3 = 1.06$

(b) At 77°K, $\mu_1/\mu_3 = 1.01$

Measurements of the variation of electron mobility with temperature made by Burmeister and Stevenson are shown in figure 1.4.1. These workers also calculated the variation of mobility that would be expected theoretically from a consideration of the types of scattering likely to be dominant in a partially ionic material such as CdSe. The agreement between the theoretical curve and the experimental values is quite good as can be seen in figure 1.4.1. These results show that above 100°K the dominant mechanism is polar optical mode scattering with a small contribution from piezoelectric scattering. Below 100°K ionised impurity scattering becomes predominant.

The experimental values of mobility shown in figure 1.4.1 were used when results presented later in this thesis required such values in their evaluation. It must be mentioned that the values in figure 1.4.1 are probably not strictly applicable to the crystals examined in connection with the work reported in this thesis. These crystals exhibited dark

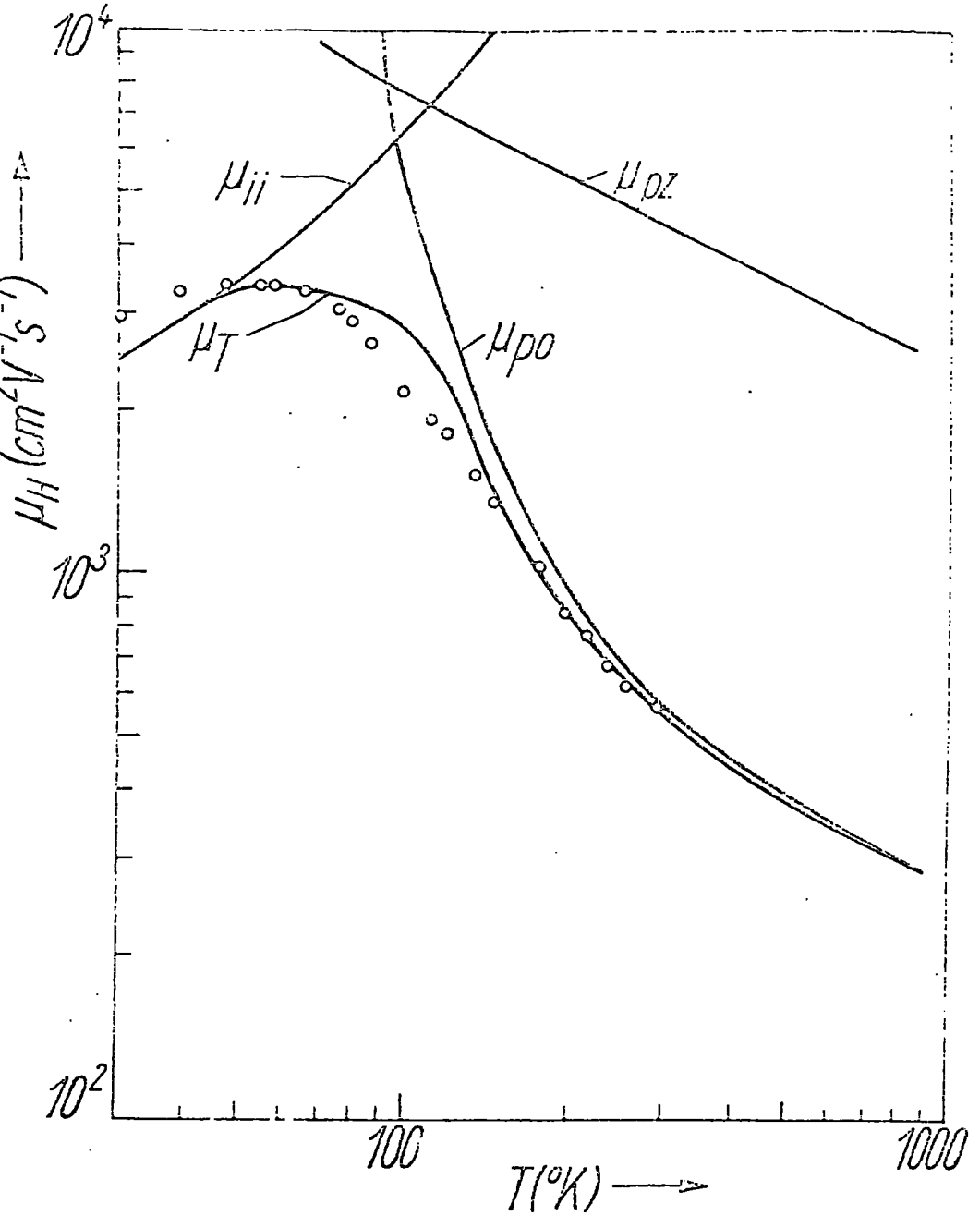

FIGURE 1.4.1 Electron mobility in CdSe after Rumeister and Stevenson (1967).

resistivities of $10^{10}\Omega$cms or greater and were highly photosensitive, properties which were quite different from those of the crystals studied by Burmeister and Stevenson. It is not known to what extent this difference in properties invalidates the mobility values given in figure 1.4.1. A possible deviation is at low temperatures as ionised impurity scattering may not be predominant in high resistivity crystals unless such impurities are compensated. The values in figure 1.4.1 were used in practice simply because of the lack of data pertaining to insulating type crystals.

1.5 The role of excitons in photoconductivity

Highly photosensitive materials such as cadmium selenide usually exhibit maximum sensitivity when excited by light with wavelengths lying close to the fundamental absorption edge. Until recently this has been attributed to the direct excitation of electrons from the valence band to the conduction band. However an idea gaining more acceptance recently is that although this creation of free electron-hole pairs does take place, excitons play a principal part in the excitation of photoconductivity. This is well demonstrated by the work of Park and Reynolds (1963). They examined the exciton structure in the spectral response of photoconductivity curves of CdS, CdSe and a range of CdS_xSe_{1-x} crystals. Typical spectra obtained by them for CdSe at 77^oK and 4.2^oK are shown in figure 1.5.1. The positions of the photoconductivity maxima in the spectra

corresponded to exciton lines observed by other workers (Wheeler and Dimmock in the case of CdSe) in absorption and reflection spectra. Park and Reynolds concluded that:

(1) The background level of photocurrent and the observation of an exciton series limit in the spectra indicated that the direct excitation of free pairs occurred.

(2) The major contribution to the photoconductivity came from excitons.

As excitons are neutral it is necessary that they dissociate into free carriers before they can give rise to a photocurrent. The three processes by which this can occur are:

(a) Interaction with phonons - the excitons need not be mobile for this to occur.

(b) Interaction with impurity centres - the excitons must be mobile for this to occur.

(c) Interaction with other excitons - the excitons again must be mobile.

Whichever of the mechanisms discussed above causes the generation of carriers in practice, it is the subsequent behaviour of the free carriers which determines the photoconductive properties of a material. Photoconductivity is the topic of the next chapter.

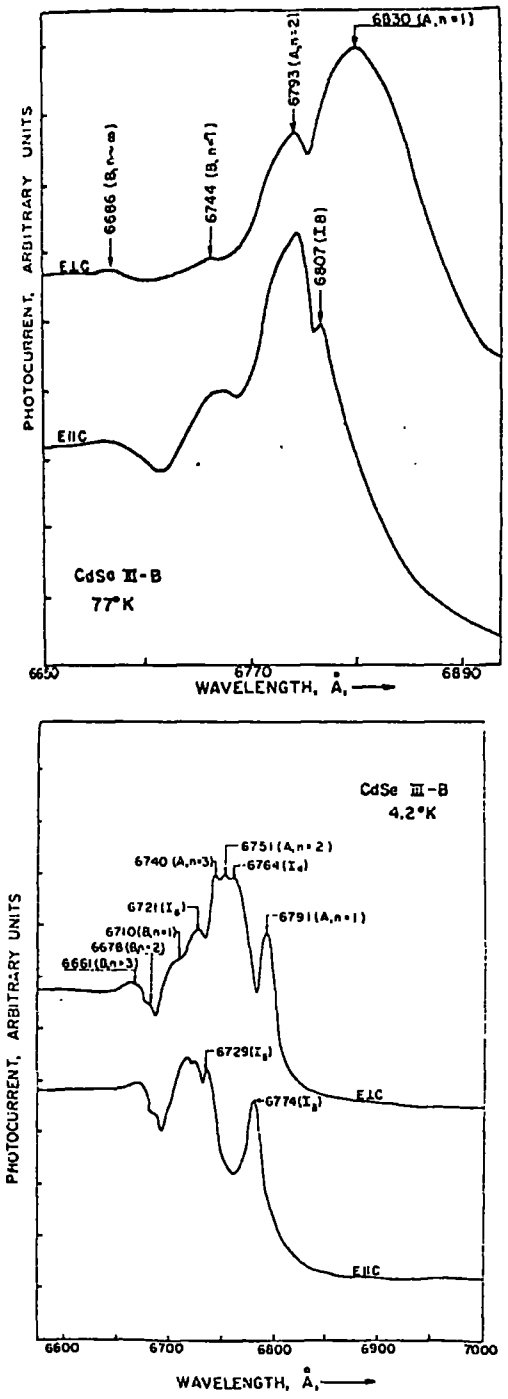

FIGURE 1.5.1 Exciton structure in the spectral dependence of photoconductivity of CdSe, after Park and Reynolds (1963).

References

Birman, J.L., 1959, Phys. Rev., 114, 1490.

Birman, J.L., 1959, Phys. Rev. Letters, 2, 157.

Burmeister, R.A., and Stevenson, D.A. 1967, Phys. Stat. Sol., 24, 683.

Dimmock, J.O., and Wheeler, R.G., 1961, J. Appl. Phys., 32, 2271.

Ginter, J., 1965, Phys. Stat, Sol., 8, K141.

Heinz, D.M., and Banks, E., 1956, J. Chem. Phys., 24, 391.

Korsunskaya, N.E., et. al., 1966, Phys. Stat. Sol., 13, 25.

Park, Y.S., and Reynolds, D.C., 1963, Phys. Rev., 132, 2450.

Shimizu, K., and Kuichi, Y., 1967, Japan. J. Appl. Phys., 6, 1089.

Tubota, H., et. al., 1960, J. Phys. Soc. Japan, 15, 1701.

Wheeler, R.G., and Dimmock, J.O., 1962, Phys. Rev., 125, 1805.

Woodbury, H.H., 1964, Phys. Rev., 134, A492.

Woodbury, H.H., and Hall, R.B., 1967, Phys. Rev., 157, 641.

CHAPTER 2

Photoconductivity and trapping effects

2.1 Free carrier lifetime

An important concept in a consideration of photoconductivity is that of the free carrier lifetime. This is defined as the time a photo-excited carrier exists in its appropriate band and is thus able to contribute to the photocurrent. Usually the lifetime of a carrier ends when it recombines with a carrier of opposite charge. In cadmium selenide free holes have short lifetimes of about 10^{-8} secs because they are quickly captured by recombination centres. The free electron lifetime is usually several orders of magnitude larger than this and can be as long as 10^{-2} secs. Thus photoconductivity in CdSe is governed by the behaviour of the free electrons and this fact is implicit in the discussion of photoconductivity given in this chapter.

The free electron lifetime does not include the time an electron may spend in a trap before being thermally released to the conduction band. However trapping affects the response time as is discussed in section 2.3.

The following fundamental relationships (for the steady state) are important when considering photoconductivity.

$$n = F\tau_n \qquad 2.1.1$$

Where, n is the free electron density.

F is the rate of excitation of free electrons per unit

volume.

τ_n is the free electron lifetime.

Similarly the free hole density is given by

$$p = F \tau_p \qquad 2.1.2$$

where τ_p is the free hole lifetime.

The photoconductive gain, G, is defined as

$$G = \tau_n / T_r \qquad 2.1.3$$

where T_r is the transit time for electrons to pass between electrodes of separation L with a potential of V volts applied. If f photons per second are incident on a photoconductor and each photon excites one free pair (as is generally assumed for light of band gap energy) then

$$G = I/ef \qquad 2.1.4$$

where, I is the photocurrent generated.

e is the electronic charge.

The gain is related to the lifetime by the expression

$$G = \tau_n \mu_n V/L^2 \qquad 2.1.5$$

where μ_n is the electron mobility.

2.2 The capture and thermal freeing of carriers at imperfection centres

Centres with energy levels lying within the forbidden gap can act either as traps (for electrons or holes) or as recombination centres and in both states influence the properties of a photoconductor. The important parameter of any centre is the capture cross section it presents to mobile

carriers. Usually the cross section for electrons, S_n, is different from that for holes, S_p.

Consider the case for electron capture by a discrete set of centres. If there is a density of N empty levels then

Rate of capture of electrons = $NS_n vn$ 2.2.1

where v is the thermal velocity of the electrons. The lifetime is given by

$$\tau_n = (NS_n v)^{-1} \qquad 2.2.2$$

If the centres lie at a depth E below the conduction band then the probability, p, of a captured electron being thermally freed is

$$p = \nu \exp(-E/kT) \qquad 2.2.3$$

where, k is the Boltzmann constant.

T is the absolute temperature.

ν is the attempt to escape frequency of the electron (this will be less than 10^{12} sec^{-1} i.e. the vibrational frequency of the crystal lattice).

Also $$\nu = S_n v N_c \qquad 2.2.4$$

where N_c is the effective density of states in the conduction band.

2.3 Response time

The response time of a photoconductor is usually defined as the time taken, after the removal of the exciting illumination, for a photocurrent to decay to 1/e of its initial steady state value. For a material containing shallow trapping

levels (which applies to most photoconductors in practice) the response time is usually longer than the free carrier lifetime. This is because the density of trapped electrons usually exceeds the density of free electrons ($n_t \gg n$) so that the decay of the photocurrent is limited by the thermal release of electrons from the traps. Only at high light intensities, where $n \geqslant n_t$, does the response time approach the lifetime. The growth of photocurrent is also affected by shallow traps. This is because in order to increase the density of free electrons the density of electrons trapped in the shallow levels must be increased in the same proportion. Again the influence of the traps is reduced at high illumination intensities.

If the decay or response time, τ_o, is defined as the time for the photocurrent to fall to 1/e of its initial value, then

$$\tau_o = (n_t)_{kT}/N_r S_n v n \qquad 2.3.1$$

where, N_r is the density of empty recombination centres.

$(n_t)_{kT}$ defines the density of electrons trapped in a kT wide portion of the band gap in the neighbourhood of the steady state Fermi level.

Substitution of 2.2.2 in 2.3.1 yields

$$\tau_o = (n_t)_{kT}\, \tau_n/n$$

and hence

$$\tau_o/\tau_n = (n_t)_{kT}/n \qquad 2.3.2$$

The response times in CdSe can be of the order of seconds. However the time required for a photocurrent either to rise or decay to a steady level can be many minutes. This is

especially the case for low light intensities when the traps are initially empty.

2.4 The gain-bandwidth relationship

A consideration of equation 2.1.5 appears to indicate that the photoconductive gain can be made indefinitely large simply by increasing the applied voltage. However this is not the case. When the applied potential reaches a sufficiently high value a space charge limited current (S.C.L.C.), equal in magnitude to the photocurrent, begins to flow. This S.C.L.C. limits the maximum gain obtainable.

Under the condition of S.C.L.C. flow the transit time is equal to the dielectric relaxation time i.e. $T_r = \tau_r$.

Substitution of this expression in 2.1.3 yields the maximum gain obtainable.

$$G_{max} = \tau_n / \tau_r \qquad 2.4.1$$

Equation 2.4.1 describes the case where the response time is equal to the lifetime. When the response time is different from the lifetime i.e. there is a significant density of trapped electrons, 2.4.1 becomes

$$G_{max} = \tau_o / \tau_r \qquad 2.4.2$$

Equation 2.4.2 is the gain-bandwidth relationship. It can be further modified for the case of a photoconductor containing deep recombination centres. Then

$$G_{max} = (\tau_o / \tau_r)M \qquad 2.4.3$$

where $M = n_t(E_f, E_{fn}) / n_t(E_{fn})$ and $M \gg 1$ 2.4.4

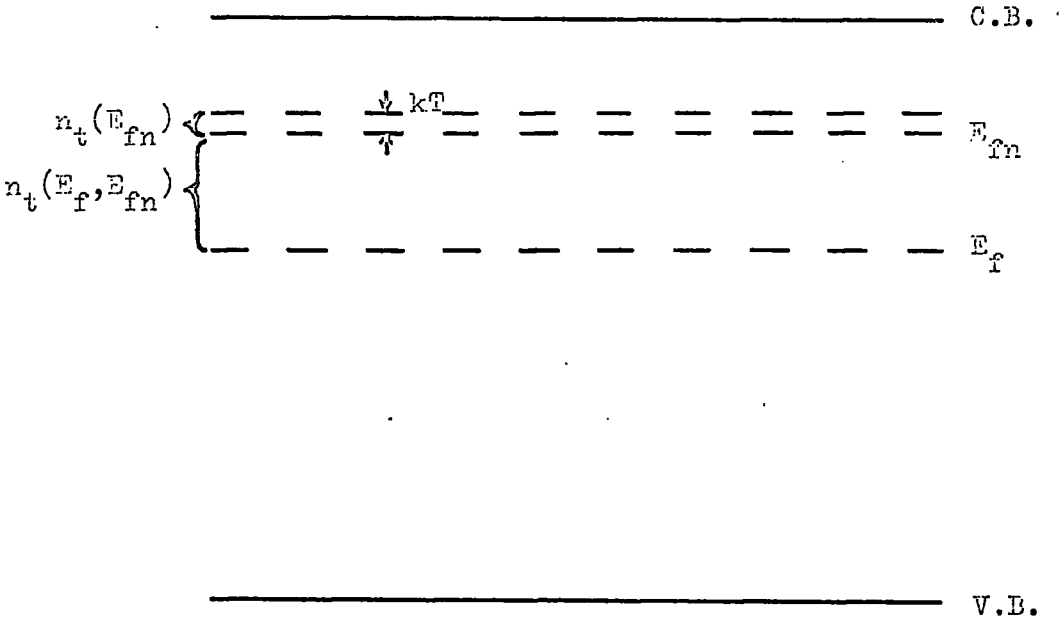

E_f is the dark equilibrium Fermi level.

E_{fn} is the steady state Fermi level under illumination.

FIGURE 2.4.1 Definition of E_f and E_{fn}.

With reference to figure 2.4.1, $n_t(E_f,E_{fn})$ defines the density of centres lying between the dark equilibrium Fermi level and the steady state Fermi level under illumination. $n_t(E_{fn})$ refers to the density of traps in a kT wide portion of the band gap at the steady state Fermi level.

Values of M as large as 500 have been reported for sensitive photoconductors.

2.5 Demarcation levels

The distinction between trapping centres and recombination centres is not rigid. Any particular centre can act either as a trap or as a recombination centre under different conditions of temperature and illumination. For a given set of conditions the following definitions apply to a discrete set of centres lying at a depth E below the conduction band and having an electron occupancy of n_t.

(1) The centres act as electron traps if - the captured electrons have a greater probability of being thermally freed to the conduction band than of recombining with holes at the centres.

i.e. $$n_t p v S_p \ll n_t v S_n N_c \exp(-E/kT) \qquad 2.5.1$$

(2) The centres act as recombination centres if - the captured electrons have a greater probability of recombining with holes at the centres than of being thermally freed to the conduction band.

i.e. $$n_{tpv}S_p \gg n_t v S_n N_c \exp(-E/kT) \qquad 2.5.2$$

Similar definitions distinguish between hole traps and recombination centres. We can also define demarcation levels:
(a) When an electron is located at the electron demarcation level, E_{dn}, it has an equal probability of being thermally freed to the conduction band or of recombining with a free hole.
(b) When a hole is located at the hole demarcation level, E_{dp}, it has an equal probability of being thermally freed to the valence band or of recombining with a free electron.

The demarcation levels are related to the steady state Fermi levels (E_{fn} and E_{fp}) by the following expressions.

$$E_{dn} = E_{fn} + kT \ln(N_n/N_p) \qquad 2.5.3$$

$$E_{dp} = E_{fp} - kT \ln(N_n/N_p) \qquad 2.5.4$$

Where, N_n is the available density of recombination centres for holes i.e. the density of centres which have captured electrons.

N_p is the available density of recombination centres for electrons i.e. the density of centres which have captured holes.

The Fermi and demarcation levels for an insulator such as CdSe are illustrated in figure 2.5.1. With reference to this diagram:

Region A - Centres in this region act as electron traps.

Region B - Although centres in this region are above the electron demarcation level they are below the electron Fermi level. They will therefore have

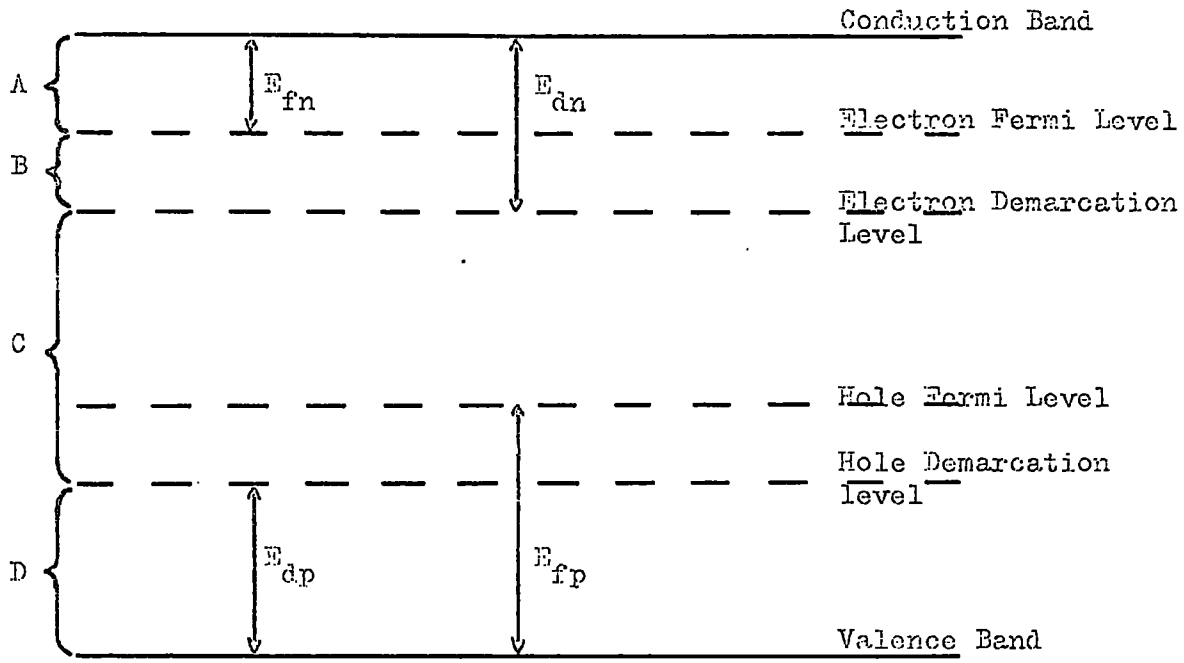

FIGURE 2.5.1 Fermi and demarcation levels for an insulator.

a high degree of electron occupancy and will take part in recombination with free holes.

Region C - Centres in this region are recombination centres.

Region D - Centres in this region act as hole traps.

Finally the change in the position of the demarcation levels corresponding to changes in temperature and intensity of illumination can be considered. If the temperature increases or the intensity of illumination decreases both demarcation levels move towards the centre of the band gap. A decrease in temperature or an increase in the light intensity results in both demarcation levels moving towards their respective band edges.

2.6 Sensitising centres

Sensitive photoconductors contain two types of recombination centre, which have opposing effects on the photosensitivity. Class 1 levels are fast recombination centres. These quickly capture free holes. Free electrons then readily recombine with these holes. Thus the action of these centres is to reduce the free carrier lifetime. Class 1 centres are characterised by large capture cross sections for both electrons and holes, perhaps 10^{-15} cm^2 or greater. However the effect of the class 11 centres, known as sensitising centres, is to increase the free electron lifetime. This is because these centres have a small capture cross section for electrons; values of 10^{-21} cm^2 have been measured. Thus although the

class 11 centres can readily capture holes the subsequent recombination rate of electrons with these holes is very small. Sensitising centres are formed by the introduction of compensated acceptor levels. These acceptors can be either native defects or impurities.

The process of sensitisation is illustrated in figure 2.6.1 (a), (b) and (c).

(a) This is the case where only fast recombination centres are present. The photoexcited carriers quickly recombine, with a resultant short lifetime. The photoconductor is insensitive in this condition.

(b) If class 11 centres are present but lie below the hole demarcation level (i.e. for high temperatures and/or low light intensities) they simply act as hole traps and do not significantly affect the photoconductive gain. This is again limited by recombination via the class 1 centres and the photoconductor is still insensitive.

(c) For low temperatures and/or high light intensities the sensitising centres lie above the hole demarcation level. Holes captured by these centres do not recombine with electrons as quickly as holes captured by class 1 centres. The net result is that the class 11 centres become mainly occupied by holes and the class 1 centres become mainly occupied by electrons. Free electrons can then essentially only recombine with holes at centres which have a small capture cross section

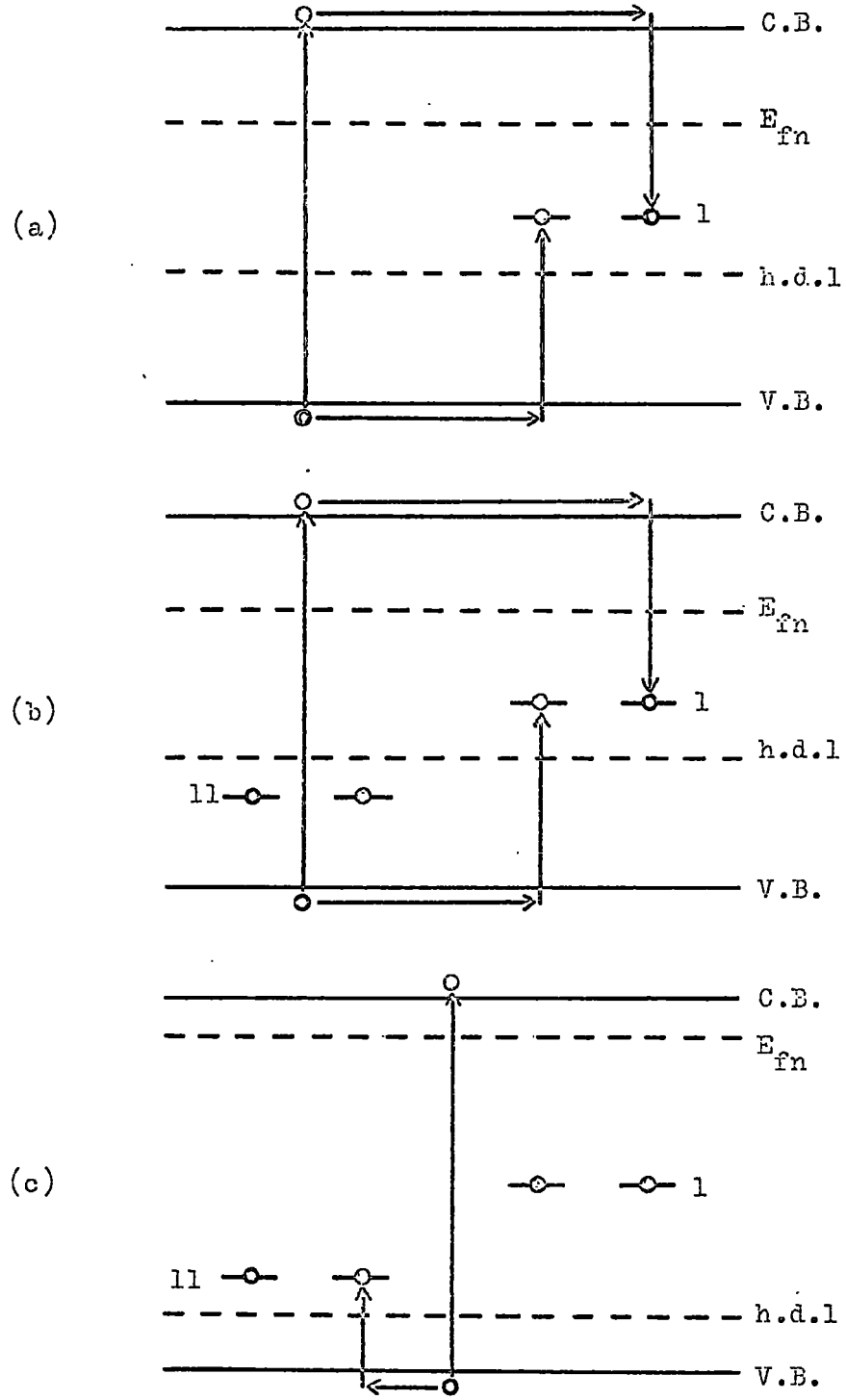

FIGURE 2.6.1 Sensitisation process.

for electrons. Consequently the lifetime of the electrons is increased and the photoconductor becomes highly photosensitive. Sensitisation only occurs if the density of class 1 and class 11 centres is substantially greater than the density of free carriers (this is usually the case in practice). If this criterion does not apply then both types of centre become filled by holes and there is no sensitisation.

As well as giving rise to large photoconductive gains, the incorporation of sensitising centres into a material results in three interesting effects; (a) superlinearity (b) thermal quenching, and (c) infra red quenching. These effects are important as their study yields information concerning the sensitising centres. The following three sections are devoted to a discussion of these effects.

2.7 Superlinearity

Consider the case of an n type photoconductor containing one set of class 1 centres and no sensitising centres. In the steady state, neglecting any trapping effects, the rate of optical excitation of electrons balances the rate of recombination of electrons at the centres.

$$\text{i.e.} \quad F = nNS_n v \qquad 2.7.1$$

N is the density of recombination centres containing holes. As there is only one set of centres then N = n.

$$\text{Thus} \quad F = n^2 S_n v$$

$$\text{Therefore} \quad n = (F/S_n v)^{\frac{1}{2}} \qquad 2.7.2$$

From 2.7.2 it is seen that the photocurrent (proportional to n) varies as the square root of the light intensity (assuming that the intensity is proportional to F).

Equation 2.7.2 only applies to a simple model. The square root relationship is not usually found in practice as it is modified by the presence of trapping levels and sensitising centres. In particular, sensitising centres lead to a superlinear dependence of photocurrent on light intensity i.e. $n \propto F^x$ where $x > 1$. This superlinearity exists only over a certain range of illumination intensity as is illustrated in figure 2.7.1. The superlinear range generally covers orders of magnitude of both current and intensity.

The occurrence of superlinearity can be thought of simply in terms of the following picture. When the intensity of illumination is increased, at a constant temperature, the hole demarcation level (h.d.l.) moves towards the valence band edge. As the h.d.l. passes through the class 11 levels these centres become occupied by holes and sensitisation occurs. The sharp increase in lifetime that accompanies this sensitisation results in superlinearity of the measured photocurrent. Superlinearity ends when the sensitisation process is essentially complete i.e. the transfer of holes from the class 1 to the class 11 centres is finished.

An analysis of superlinear behaviour requires a model containing at least two different sets of centres. Klasens

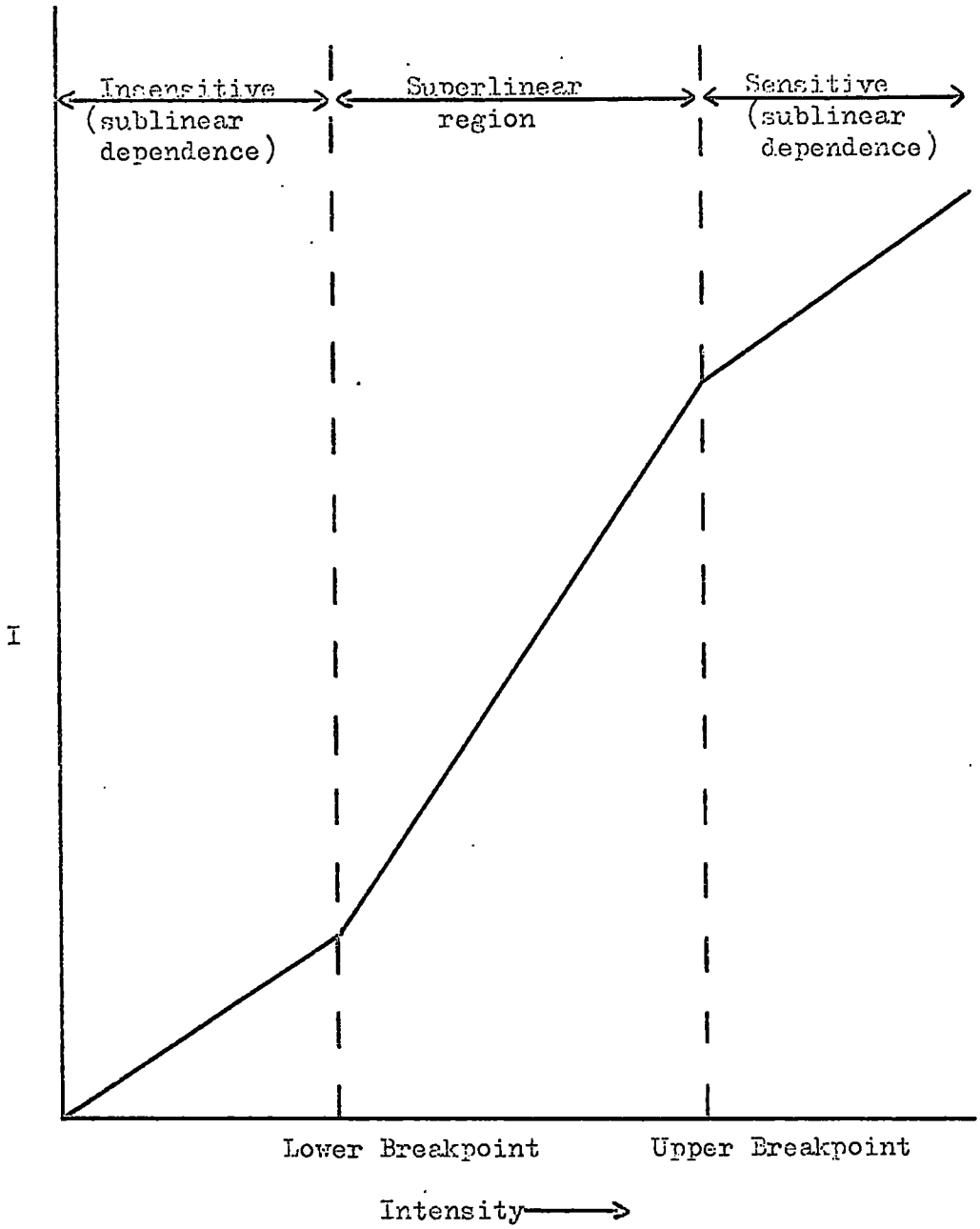

FIGURE 2.7.1 Illustration of superlinearity.

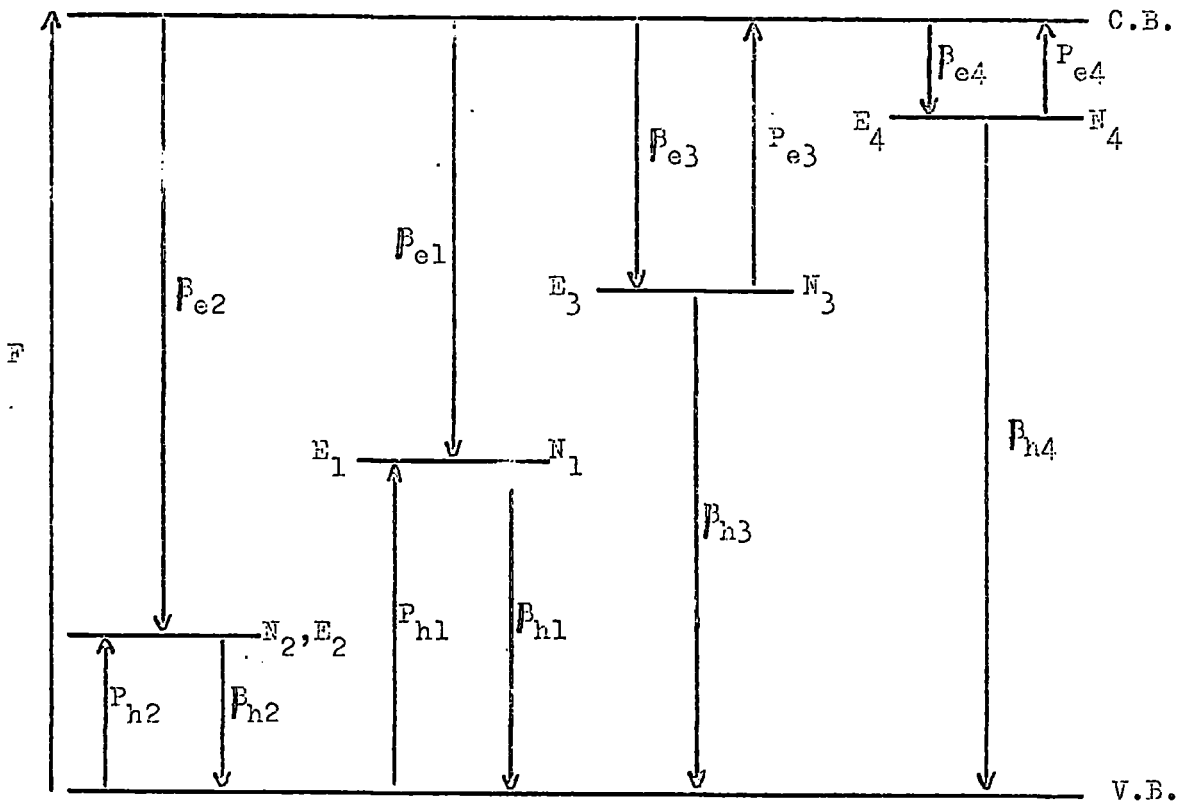

FIGURE 2.7.2 Four centre model for the analysis of superlinearity, after Dussel and Bube (1966).

(1958) has considered a two centre model and Bube (1957) analysed a three centre model. More recently Dussel and Bube (1966) evaluated a four centre model which could also be extended to cover the case of distributions of traps. This four level model is shown in figure 2.7.2. The centres considered are class 1 (denoted by index 1) and class 11 (index 2) recombination centres, deep traps (index 3) and shallow traps (index 4).

The following notation applies to the model illustrated in figure 2.7.2.

F is the density of free electron - hole pairs created per second by the illumination.

n is the free electron density.

p is the free hole density.

N_i is the density of centres i.

n_i is the density of centres i occupied by electrons.

E_i is the depth of centres i below the conduction band when i = 3 or 4 and the height of centres i above the valence band when i = 1 or 2.

β_{ei} is the capture probability for electrons at an empty centre i.

$$\beta_{ei} = s_{ni} v$$

β_{hi} is the capture probability for holes at a centre i occupied by an electron.

$$\beta_{hi} = s_{pi} v$$

P_{ei} is the probability of thermal excitation of an electron from a centre i (for i = 3 or 4) to the conduction band.

$$P_{ei} = N_c \beta_{ei} \exp(-E_i/kT)$$

Where N_c is the effective density of states in the conduction band.

P_{hi} is the probability of thermal excitation of a hole from a centre i (for i = 1 or 2) to the valence band.

$$P_{hi} = N_v \beta_{hi} \exp(-E_i/kT)$$

Where N_v is the effective density of states in the valence band.

The following equations describe the steady state kinetics involving the various centres.

For the free electrons

$$F = \beta_{e1} n(N_1 - n_1) + \beta_{e2} n(N_2 - n_2) + \beta_{e3} n(N_3 - n_3) + \beta_{e4} n(N_4 - n_4) - P_{e3} n_3 - P_{e4} n_4 \qquad 2.7.3$$

For the centres, 1

$$\beta_{e1} n(N_1 - n_1) + P_{h1}(N_1 - n_1) = \beta_{h1} n_1 p \qquad 2.7.4$$

For the centres, 2

$$\beta_{e2} n(N_2 - n_2) + P_{h2}(N_2 - n_2) = \beta_{h2} n_2 p \qquad 2.7.5$$

For the centres, 3

$$\beta_{e3} n(N_3 - n_3) = \beta_{h3} n_3 p + P_{e3} n_3 \qquad 2.7.6$$

For the centres, 4

$$\beta_{e4} n(N_4 - n_4) = \beta_{h4} n_4 p + P_{e4} n_4 \qquad 2.7.7$$

Also, in order to maintain charge neutrality

$$p + (N_1 - n_1) + (N_2 - n_2) = n + n_3 + n_4 \qquad 2.7.8$$

The above six equations can be solved to give the following two relationships.

$$F = \sum_i R_i = np \sum_i \left[\frac{\beta_{ei}\beta_{hi}N_i}{\beta_{hi}p + \beta_{ei}n + P_i} \right] \qquad 2.7.9$$

Where, R_i is the recombination rate through centres i.

P_i is P_{ei} for i = 3 and 4.

P_i is P_{hi} for i = 1 and 2.

and

$$p\left[1 + \frac{\beta_{h1}N_1}{\beta_{h1}p + \beta_{e1}n + P_{h1}} + \frac{\beta_{h2}N_2}{\beta_{h2}p + \beta_{e2}n + P_{h2}}\right] =$$

$$n\left[1 + \frac{\beta_{e3}N_3}{\beta_{h3}p + \beta_{e3}n + P_{e3}} + \frac{\beta_{e4}N_4}{\beta_{h4}p + \beta_{e4}n + P_{e4}}\right] \qquad 2.7.10$$

The solution of 2.7.9 and 2.7.10 to give n as a function of F is obviously very involved. The procedure adopted by Dussel and Bube was to simplify the expressions by considering only the dominant terms under various conditions. For example, under low intensities of illumination traps 3 and 4 are empty and centres 1 and 2 are in thermal equilibrium with the valence band. The dominant recombination path is via the class 1 centres. 2.7.10 now reduces to

$$p(\beta_{h1}N_1/P_{h1}) = n(\beta_{e3}N_3/P_{e3}) \qquad 2.7.11$$

and 2.7.9 becomes

$$F = R_1 = np(\beta_{e1}\beta_{h1}N_1/P_{h1}) \qquad 2.7.12$$

From 2.7.11 and 2.7.12

$$F = (\beta_{e1}\beta_{e3}N_3/P_{e3})n^2 \qquad 2.7.13$$

i.e. $n \propto F^{\frac{1}{2}}$

This is the same variation of n with F as that given in 2.7.2 for the case of a single set of recombination centres. This is to be expected because for low light intensities the recombination kinetics are essentially those for a one centre model.

Dussel and Bube examined the conditions for the onset and end of superlinearity in detail. They considered models both for discrete and quasi-continuous trap distributions. They found that in order for superlinearity to occur three conditions must be fulfilled.

(1) Centres 1 must not be in thermal equilibrium with the valence band.

$$\text{i.e. } n > P_{h1}/\beta_{e1}$$

(2) Holes must be mainly in centres 2.

$$\text{i.e. } (N_2 - n_2) > (N_1 - n_1)$$

(3) Traps 3 must be filled.

$$\text{i.e. } n > P_{e3}/\beta_{e3}$$

This last condition does not apply if there is a continuous distribution of traps.

A feature to note is that the shallow traps (levels 4) do not affect the onset of superlinearity. This is because they are substantially empty at the comparatively low intensities of illumination associated with the onset of superlinearity. They therefore do not take part in the recombination process.

The lower breakpoint of superlinearity (reference figure

2.7.1) is defined by whichever of the three conditions given above is last met as the light intensity is increased. This is the condition which occurs at the highest value of n.

Dussel and Bube derived three basic conditions that could cause the end of superlinearity. These are:

(1) A shift in the recombination path from centres 1 to centres 2.

$$\text{i.e. } R_2 > R_1$$

(2) The electron occupancy of centres 2 being determined by recombination rather than by thermal excitation from the valence band.

$$\text{i.e. } n > P_{h2}/\beta_{e2}$$

(3) A shift in the recombination path from centres 1 to centres 4 when $n_4 > N_3$.

$$\text{i.e. } R_4 > R_1$$

There is a fourth condition which applies only if centres 4 consist of a shallow exponential trap distribution.

(4) A shift in the recombination path from centres 4 to centres 2.

$$\text{i.e. } R_2 > R_4$$

It is seen that the cessation of superlinearity can be influenced by the shallow traps (4) if they play a significant part in recombination at the fairly high light intensities involved.

Any of the four conditions listed above can cause the end

of superlinearity. In practice the one which defines the upper breakpoint is that which is first fulfilled as the light intensity is increased. This is the condition which occurs at the lowest value of n.

The procedure used in an analysis of superlinearity data is illustrated by the following example. Measurements of n as a function of F are obtained at different temperatures. These measurements will result in a set of curves such as is shown in figure 2.7.3. If traps 3 and 4 are discrete levels and the upper breakpoints of superlinearity are defined by the condition $R_2 > R_1$, then the values of n at these breakpoints are given by

$$n_{ub} = (\beta_{h1} N_1 / \beta_{h2} \beta_{e2} N_2) P_{h2} \qquad 2.7.14$$

and since $$P_{h2} = N_v \beta_{h2} \exp(-E_2/kT)$$

2.7.14 then becomes $$n_{ub} = (\beta_{h1} N_1 N_v / \beta_{e2} N_2) \exp(-E_2/kT) \qquad 2.7.15$$

Therefore a plot of ln n_{ub} against 1/T yields a straight line of slope $-E_2/k$. If the upper breakpoints are limited by a condition other than $R_2 > R_1$ then the slope of the ln n_{ub} vs 1/T line will be associated with that particular limiting condition. The various conditions and slopes derived by Dussel and Bube are listed in table 2.1.

The lower breakpoints of superlinearity can be treated in a similar fashion to that given above for the upper breakpoints. Table 2.2 summarises the lower breakpoint characteristics

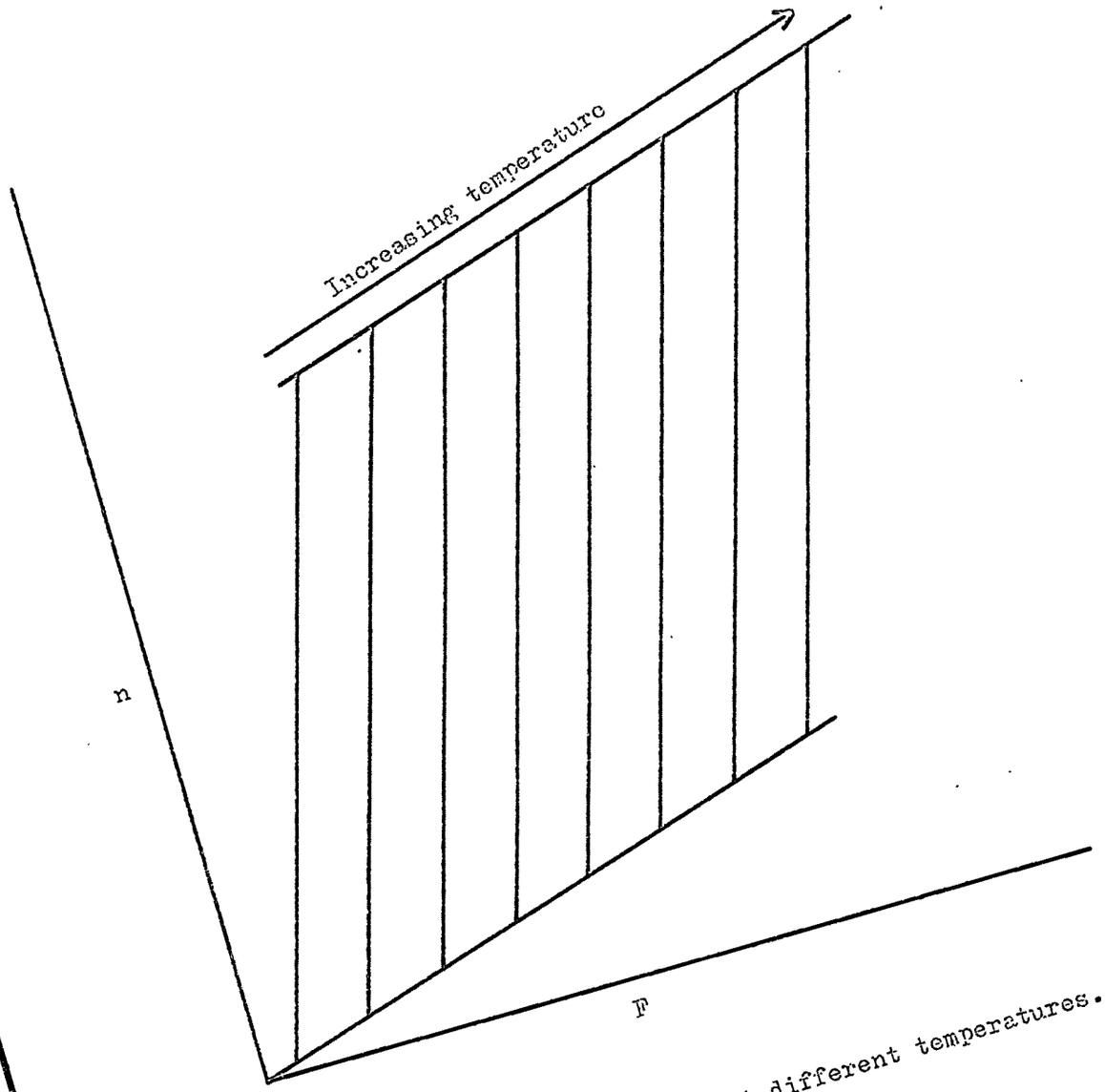

FIGURE 2.7.3 Superlinearity at different temperatures.

Table 2.1. Upper breakpoint characteristics.

Assumptions	Cause of end of superlinearity	Slope of $\ln n_{1o}$ vs $1/T$
N_3 and N_4 discrete	$R_2 > R_1$	$-E_2$
	$n > P_{h2}/\beta_{e2}$	$-E_2$
	$R_4 > R_1$	$-E_4$
N_3 discrete, N_4 an exponential distribution	$R_2 > R_1$	$-E_2$
	$n > P_{h2}/\beta_{e2}$	$-E_2$
	$R_4 > R_1$	$-kT^*\ln(\ldots)$
	$N_2 > R_4$	No linear dependence

The exponential trap distribution is defined by

$$N_4(E) = N_o \exp(-E/kT^*)$$

$$N_4 = \int_o^\infty N_4(E)dE$$

$$N_T = N_4(T^*/T^* - T)$$

where T^* is the characteristic temperature of the distribution.

Table 2.2. Lower breakpoint characteristics.

Assumptions	Cause of onset of superlinearity	Slope of $\ln n_{1o}$ vs $1/T$
N_3 discrete	$(N_2 - n_2) > (N_1 - n_1)$	$-E_2$
	$n > P_{e3}/\beta_{e3}$	$-E_3$
	$n > P_{h1}/\beta_{e1}$	$-E_1$
N_3 continuous	$(N_2 - n_2) > (N_1 - n_1)$	$-E_2$
	$n > P_{h1}/\beta_{e1}$	$-E_1$

derived by Dussel and Bube.

2.8 Thermal quenching of photoconductivity

Thermal quenching of photoconductivity can occur when a photoconductor is in the sensitive state i.e. when the class 11 centres are occupied by holes. If the temperature is raised, while a constant intensity of illumination is maintained, then above a certain temperature the photocurrent rapidly decreases by several orders of magnitude. The threshold of the quenching occurs at progressively higher temperatures as the illumination intensity is increased. This behaviour is illustrated in figure 2.8.1.

As the temperature is increased the hole demarcation level moves towards the centre of the band gap. Thermal quenching corresponds to the large decrease in lifetime which occurs as the h.d.l. passes through the class 11 levels i.e. as the material becomes desensitised. The quenching ends when the class 11 centres are effectively in thermal equilibrium with the valence band and thus behave as hole traps. The offset of the quenching threshold to higher temperatures with an increase in light intensity is readily explained in terms of the opposing effects of temperature and illumination (reference section 2.5). An increase in illumination intensity shifts the h.d.l. towards the valence band edge and thus a higher temperature is required to move this level to the position of the class 11 centres.

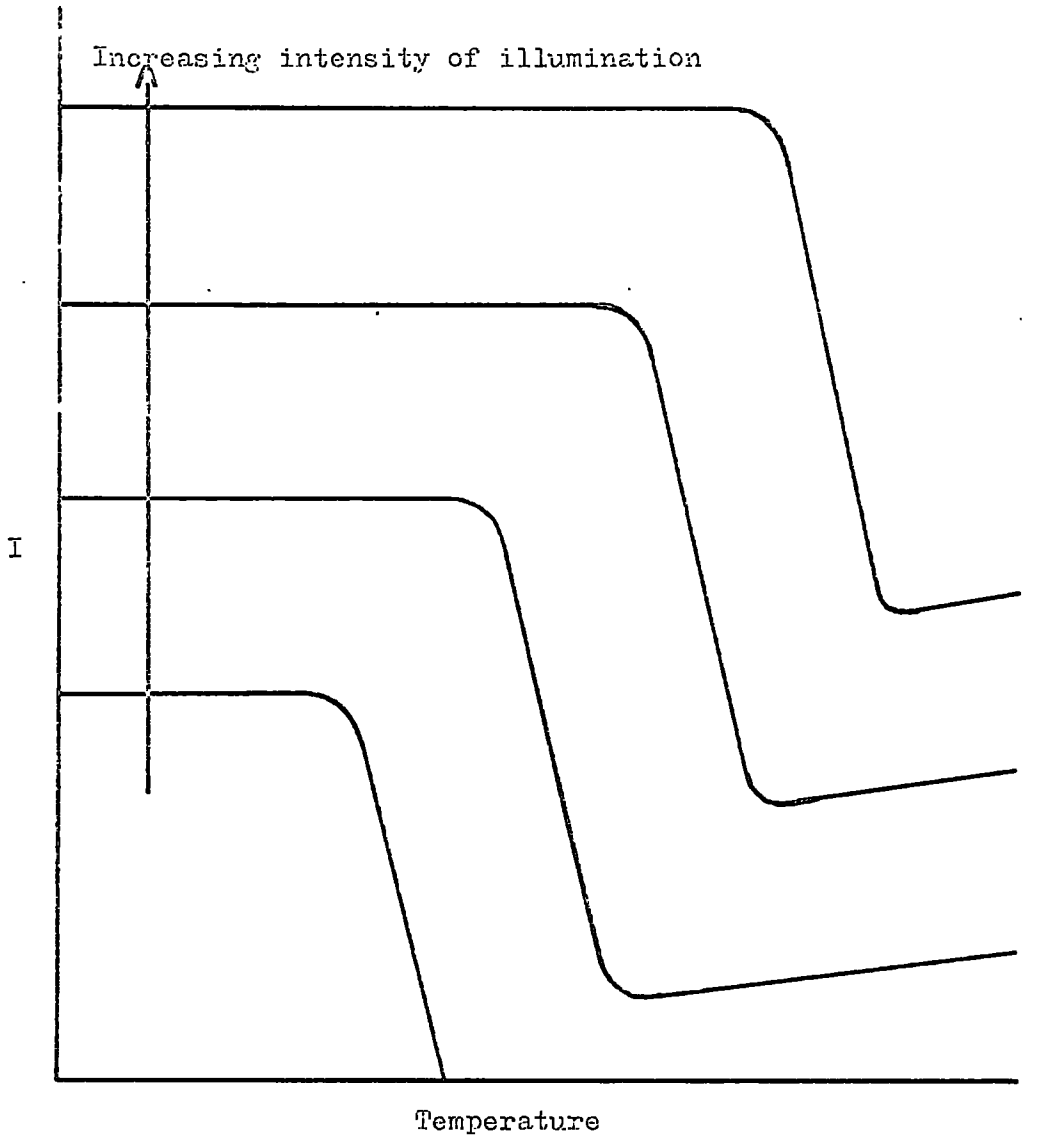

FIGURE 2.8.1 Thermal quenching of photoconductivity.

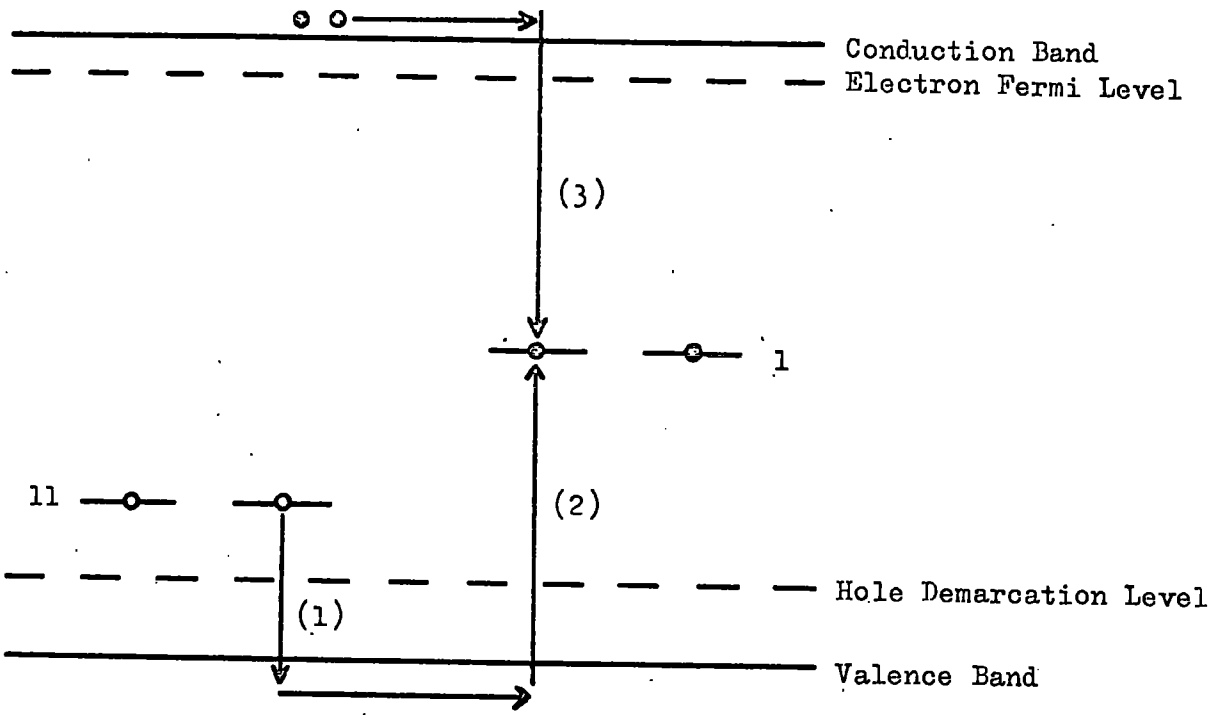

Figure 2.9.1 The transitions involved in the infra red quenching of photoconductivity.

The slow increase in photocurrent which often follows the end of thermal quenching is due to a gradual change in the recombination kinetics associated with the class 1 centres. As the h.d.l. moves towards these levels with an increase in temperature their occupancy is increasingly determined by thermal exchange with the valence band. The rate of recombination via these centres consequently decreases, albeit slowly, and there is an increase in free electron lifetime.

The low and high temperature limits of the thermal quenching range for a particular light intensity correspond respectively to the upper and lower breakpoints of superlinearity discussed in the previous section.

2.9 Infra red quenching of photoconductivity

The phenomenon of infra red quenching is the reduction in photocurrent that is sometimes observed when a photoconductor in the sensitised state is illuminated with secondary radiation in a particular wavelength range. The secondary irradiation which produces this effect is often in the infra red region. The mechanism of infra red quenching is illustrated in figure 2.9.1. Electrons are excited to the class 11 centres by the secondary radiation (transition 1 in figure 2.9.1). The resultant freed holes are quickly captured by the class 1 centres (transition 2). Free electrons can then recombine with these holes (transition 3) and the free electron lifetime is consequently reduced. A quenching of the photocurrent

results.

In order for I.R. quenching to occur the secondary radiation must have sufficient energy to excite electrons from the valence band to the sensitising centres. Measurements of the spectral response of the quenching should therefore display a threshold at a photon energy corresponding to the height of the sensitising centres above the valence band.

This chapter has been concerned with various aspects of photoconductivity. In sections 2.3 and 2.4 it was shown that response time and gain are influenced by the presence of trapping centres. In the following chapter the techniques used in the evaluation of the parameters of such centres (trap depth, capture cross section and density) are discussed.

References

Bube, R.H., 1957, J. Phys. Chem. Solids, 1, 234.

Dussel, G.A., and Bube, R.H., 1966, J. Appl. Phys., 37, 13.

Klasens, H.A., 1958, J. Phys. Chem. Solids, 7, 175.

CHAPTER 3

Theory associated with the analysis of thermally stimulated currents (T.S.C.)

3.1 Introduction

Carriers captured at either electron or hole traps can be thermally released by heating the material through an appropriate temperature range. The current which results from this freeing of carriers rises to a maximum and then decays as the temperature is increased. The measurement and analysis of such thermally stimulated currents is widely used in the evaluation of trapping parameters. Nicholas and Woods (1964) have reviewed a variety of techniques by which thermally stimulated current curves can be analysed to yield information concerning the associated traps.

In this chapter the recombination kinetics associated with the thermal release of electrons from traps is considered (a similar treatment applies to hole traps). Finally the various techniques which have been employed in the analysis of T.S.C. results discussed in later chapters are described.

3.2 Recombination kinetics

The simple model considered consists of one set of discrete traps and one set of recombination centres. S_t and S_r are the capture cross sections for electrons of the traps and the recombination centres respectively. The traps lie at a depth of E below the conduction band.

The probability, p, of an electron escaping from a trap at a temperature T has been given in 2.2.3.

$$p = \nu \exp(-E/kT)$$

After being released from a trap an electron stays in the conduction band until it either recombines or is retrapped. The relative probabilities of these two processes occurring are determined by the respective capture cross sections of the traps and the recombination centres and their occupancy. The rate of change of the trapped electron density, n_t, is given by

$$dn_t/dt = - n_t \nu \exp(-E/kT) + n_c(N_t - n_t)S_t v \qquad 3.2.1$$

where n_c is the density of electrons in the conduction band. The rate of change of n_c is given by

$$\frac{dn_c}{dt} = - \frac{n_c}{\tau_n} - \frac{dn_t}{dt} \qquad 3.2.2$$

Assuming that τ_n is short and therefore that $dn_c/dt \ll n_c/\tau_n$, 3.2.2 becomes

$$n_c = -\tau_n(dn_t/dt) \qquad 3.2.3$$

Three limiting cases of the recombination kinetics are usually considered.

(1) Monomolecular kinetics

Under these conditions there is no appreciable retrapping of freed electrons i.e. $S_t \ll S_r$.

3.2.1 simplifies to

$$dn_t/dt = -n_t \nu \exp(-E/kT) \qquad 3.2.4$$

If the temperature at the start of the heating is T_o and

the density of filled traps at this temperature is n_{to}, then from 3.2.3 and 3.2.4

$$\sigma = n_{to} \tau_n e \mu_n \nu \exp\left[-(E/kT) - \int_{T_o}^{T} \frac{\nu}{\beta} \exp(-E/kT)dT\right] \qquad 3.2.5$$

where σ is the thermally stimulated conductivity at a temperature T and β is the constant heating rate employed.

(2) Bimolecular kinetics

The bimolecular case is defined by $S_t = S_r$.

3.2.1 becomes

$$dn_t/dt = -(n_t^2/N_t)\nu \exp(-E/kT) \qquad 3.2.6$$

Solving 3.2.6 and substituting the result in 3.2.3 gives the expression for the conductivity under bimolecular conditions.

$$\sigma = \frac{n_{to}^2 \tau_n e \mu_n \nu \exp(-E/kT)}{N_t\left[1 + \frac{n_{to}\nu}{N_t\beta}\int_{T_o}^{T} \exp(-E/kT)dT\right]^2} \qquad 3.2.7$$

Where N_t is the total density of traps.

(3) Fast retrapping

Under these conditions a freed electron has a high probability of being retrapped i.e. $S_t \gg S_r$.

As the trapped electrons are affectively in thermal equilibrium with the conduction electrons

$$n_c/N_c = (n_t/N_t) \exp(-E/kT) \qquad 3.2.8$$

3.2.3 and 3.2.8 can be solved to give the thermally stimulated conductivity under conditions of fast retrapping.

$$\sigma = \frac{N_c n_{to} e \mu_n}{N_t} \exp\left[-(E/kT) - \frac{1}{N_t \beta \tau_n} \int_{T_o}^{T} N_c \exp(-E/kT) dT \right] \quad 3.2.9$$

3.3 The Garlick and Gibson technique

The technique devised by Garlick and Gibson (1948) for the analysis of T.S.C. curves is independent of the recombination kinetics operative during trap emptying. In the initial stages of the release of electrons from traps the integrals in 3.2.5, 3.2.7 and 3.2.9 are negligible. Therefore the thermally stimulated conductivity for all three cases can be described by an expression of the form

$$\sigma = \text{constant} \times \exp(-E/kT) \quad 3.3.1$$

where the constant is different in the three cases.

If it is assumed that $N_c \mu_n$ is independent of temperature then a plot of ln current against $1/T$ for the initial part of the rising side of a T.S.C. peak should give a straight line of slope $-E/k$. Thus the depth of the trap below the conduction band is obtained.

3.4 Grossweiner's technique

This method is only applicable when the traps empty under monomolecular conditions. Grossweiner (1953) showed that the trap depth is given by

$$E = 1.51\, kT^{*}T'/(T^{*} - T') \quad 3.4.1$$

where, T^{*} is the temperature at the maximum of the T.S.C. peak.

T' is the temperature at which the conductivity, on the

rising side of the peak, is half the value at the maximum.

Equation 3.4.1 gives the trap depth to an accuracy of better than 10% provided that $(E/kT^*) > 20$ and $(N_c v s_t/\beta) > 10^7$. Grossweiner also derived the following expression for the capture cross section of the traps.

$$s_t = \frac{3T'\beta \exp(E/kT^*)}{2N_c v T^*(T^* - T')} \qquad 3.4.2$$

3.5 The Fermi level method

This method is only valid when the traps empty under conditions of fast retrapping. Bube (1955) proposed that in these circumstances, at the T.S.C. peak maximum, the quasi Fermi level coincides with the position of the traps. The trap depth is therefore given by

$$E = kT^* \ln(N_c/n_c^*) \qquad 3.5.1$$

where n_c^* is the free electron density corresponding to the conductivity at the peak maximum.

This method is suspect owing to the arbitrary nature of the basic assumption that the Fermi level corresponds to the position of the traps. Haering and Adams (1960) considered the errors involved in this assumption. They concluded that the minimum error in trap depths evaluated using 3.5.1 is $-\frac{1}{2}kT^*$. This amounts to about 0.01 ev when T^* is 200°K.

3.6 Curve fitting

The technique of curve fitting developed by Cowell and Woods (1967) is used in later chapters as the principal method

in the analysis of T.S.C. curves. This method is essentially one of fitting theoretical curves to the experimental data. Its advantage over methods such as those described in the three previous sections is that it utilises the whole of the experimental curve and not just a part of it. The technique as applied to the case of monomolecular recombination kinetics is illustrated below.

The expression for the thermally stimulated conductivity is given in 3.2.5. Cowell and Woods rewrote this equation in the following form:

$$\sigma = A \exp\left[-t + B\int_{to}^{t} \exp(-t)t^{-2}dt\right] \qquad 3.6.1$$

Where, $t = E/kT$

$$A = \text{constant} = n_{to}\tau_n e\,\mu_n\nu \qquad 3.6.2$$

$$B = \text{constant} = \nu E/\beta k \qquad 3.6.3$$

In deriving 3.6.1 it is assumed that ν is independent of temperature and that the variations of μ_n and τ_n with temperature over the span of the T.S.C. peak can be neglected. 3.6.1 can be expanded using repeated integration by parts to give

$$\sigma = A \exp\left[-t - B\left\{\exp(-t)t^{-2} - 2\exp(-t)t^{-3} + 6\exp(-t)t^{-4}.....\right\}_{to}^{t}\right] \qquad 3.6.4$$

It is found that the bottom limit of the expansion cancels out during the normalisation of the theoretical curve to the experimental curve (see later) using the constant A. Cowell

and Woods neglected all but the first term in the above expansion. They considered that this did not introduce errors greater than 5% in the calculated values of trap depth. However in the present work the first four terms in the expansion were used. 3.6.4 becomes

$$\sigma = A \exp\left[-t - B \exp(-t)t^{-2}\left\{1 - 2t^{-1} + 6t^{-2} - 24t^{-3}\right\}\right] \qquad 3.6.5$$

At the maximum of the T.S.C. peak $t = t^{*} = E/kT^{*}$. Differentiating 3.6.1 and equating the result to zero yields the following expression for B.

$$B = \exp(t^{*})t^{*2} \qquad 3.6.6$$

The theoretical curve corresponding to any particular values of trap depth, E, and temperature at the peak maximum, T^{*}, is then described by equations 3.6.5 and 3.6.6.

In practice the trap depth associated with an experimental T.S.C. curve was derived in the following fashion. An initial value of E was obtained using, for example, Grossweiner's technique. Theoretical curves for a range of energies about this value were then calculated with the aid of a computer (the computer programme used is given in Appendix III at the end of this thesis). The parameter A was simply adjusted to normalise the theoretical curves to the experimental curve at the maximum. The theoretical curve that gave the best fit to the experimental data was then obtained and the value of E associated with this curve was taken to be the required trap depth. It must be noted here that it was often difficult to decide which of two or

three curves gave the best fit. The error that resulted from this ambiguity was of the order of $\pm$ 0.01 ev.

Once the trap depth had been determined, 3.6.3 and 3.6.6 were used to give a value of ν . This in turn yielded a value of the capture cross section, S_t, of the traps, since $\nu = N_c v S_t$ (reference 2.2.4). 3.6.2 was also used to calculate the initial density of filled traps, n_{to}.

A similar treatment to that given above can be applied to the case of traps which empty with fast retrapping. The relevant expressions are then:

$$\sigma = C \exp\left[-t - D \exp(-t) t^{-7/2}\left\{1 - 3.5t^{-1} + 15.75t^{-2} - 86.625t^{-3}\right\}\right] \qquad 3.6.7$$

$$D = \exp(t^*)t^{*7/2} = \frac{N_c E^{5/2}}{N_t \beta T^{*3/2} k^{5/2} \tau_n} = \text{constant} \qquad 3.6.8$$

$$C = \text{constant} = N_c e \mu_n n_{to}/N_t \qquad 3.6.9$$

3.7 Trap density

The total density of filled traps can readily be derived from the area under an experimental T.S.C. curve provided that the photoconductive gain, G, is known. The procedure is to plot the curve as current against time. Integration of the area under this curve yields the total charge, Q, freed during the heating. If the crystal volume is V then the density of filled traps is given by

$$n_{to} = Q/eVG \qquad 3.7.1$$

3.8 Constant temperature method

A method of T.S.C. analysis which does not require the measurement of current against temperature has been proposed by Haine and Carley Read (1968). In this method the temperature is held at a value less than that at the T.S.C. maximum and the decay of the thermally stimulated current with time is observed.

A trapping factor θ is defined such that

$$\theta = (N_c/N_t)\ \exp(-E/kT) \qquad 3.8.1$$

The rate of decay of the current at a fixed temperature is defined by

$$\frac{dn_c}{dt} = \frac{n_t\theta}{\tau_t} - \frac{n_c}{\tau_t}\left[1 - \frac{n_t}{N_t}\right] - \frac{n_c}{\tau_n} \qquad 3.8.2$$

where the trapping time, $\tau_t = 1/N_t S_t v$ 3.8.3

dn_c/dt can be neglected with respect to the other terms so 3.8.2 becomes

$$n_t\theta = n_c\left[1 + \frac{\tau_t}{\tau_n} - \frac{n_t}{N_t}\right] \qquad 3.8.4$$

Also, $$n_t = n_{to} - \int \frac{n_c\,dt}{\tau_n} \qquad 3.8.5$$

If $n_t \doteq N_t$ the solution of 3.8.4 and 3.8.5 is

$$n_c = n_{to}\theta\,(\tau_n/\tau_t)\ \exp(-t\theta/\tau_t) \qquad 3.8.6$$

If $n_t \ll N_t$ the solution of 3.8.4 and 3.8.5 is

$$n_c = n_{to}\theta\left[\frac{\tau_n}{\tau_n + \tau_t}\right]\ \exp\left[\frac{-t\theta}{\tau_n + \tau_t}\right] \qquad 3.8.7$$

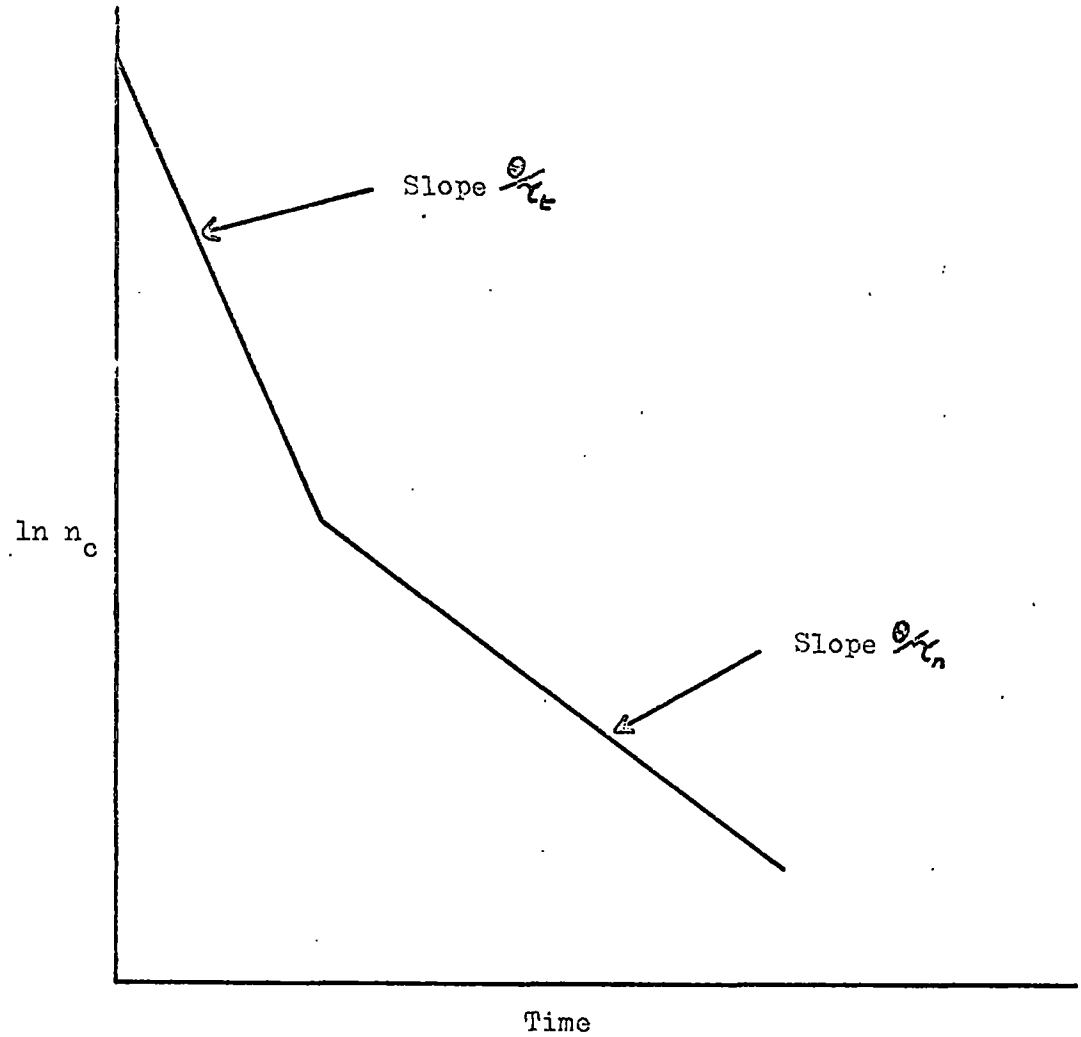

FIGURE 3.8.1 Decay of T.S.C. with time for the case of fast retrapping with the traps initially full (after Haine and Carley Read, 1968).

The cases of trap emptying without retrapping or with fast retrapping are now considered.

(a) Monomolecular kinetics

Under these conditions $\tau_t \gg \tau_n$ and 3.8.7 reduces to 3.8.6. Thus a plot of ln n_c against time should give a straight line of slope $-\theta/\tau_t$.

(b) Fast retrapping

Under these conditions $\tau_t \ll \tau_n$ and 3.8.7 becomes

$$n_c = n_{to}\theta \exp(-t\,\theta / \tau_n) \qquad 3.8.8$$

Two different modes of behaviour can be distinguished for the case of fast retrapping. If the initial fraction of filled traps is small ($n_t \ll N_t$) then 3.8.8 describes the decay of the current. A plot of ln n_c against t should then give a straight line of slope $-\theta/\tau_n$. However if the traps are initially full ($n_t \doteq N_t$) a plot of ln n_c against t should give 2 lines, of slopes $-\theta/\tau_t$ and $-\theta/\tau_n$, as illustrated in figure 3.8.1. The breakpoint in the two slopes corresponds to the transition from 3.8.6 to 3.8.8 as the fraction of filled traps becomes small.

A great deal of information concerning the traps can be obtained from a curve such as that shown in figure 3.8.1 provided that the free electron lifetime is independently measured. From the two slopes and the zero time intercept the values of E, S_t, N_t, τ_t and θ can be calculated using equations 3.8.1 and 3.8.3. These results are used in section

7.3 to calculate the parameters associated with traps which give rise to a T.S.C. peak at 105°K.

3.9 Summary

In order for the methods of T.S.C. analysis described in this chapter to be valid several assumptions must be made. These are that ν, μ_n and τ_n do not vary with temperature over the range of the experimental curves. During the interpretation of T.S.C. data presented in later chapters these assumptions have been made except in the case of the temperature dependence of the lifetime. It was possible to study this variation of lifetime and where it was significant suitable corrections were made.

References

Bube, R.H., 1955, J. Chem. Phys., 23, 18.

Cowell, T.A.T., and Woods, J., 1967, Brit. J. Appl. Phys., 18, 1045.

Garlick, G.F.J., and Gibson, A.F., 1948, Proc. Phys. Soc., 60, 574.

Grossweiner, L.I., 1953, J. Appl. Phys., 24, 1306.

Haering, R.R., and Adams, E.N., 1960, Phys. Rev., 117, 451.

Haine, M.E., and Carley Read, R.E., 1968, Brit. J. Appl. Phys. (J.Phys.D), 1, 1257.

Nicholas, K.H., and Woods, J., 1964, Brit. J. Appl. Phys., 15, 783.

CHAPTER 4

Crystal Growth

4.1 Introduction

Crystals of the chalcegonides of cadmium and zinc are usually grown from the vapour phase as they do not melt at normal pressure but dissociate and sublime. They can be grown from the melt but high temperatures and pressures are required. Kubo and Amemiya (1965) grew large crystals of cadmium selenide from the melt at 1200°C under a pressure of 70 atmospheres of argon. Fahrig (1963) compared large crystals of cadmium sulphide grown from the melt and vapour phase. He found that the properties of crystals grown from the melt were more uniform throughout a crystal. However the vapour phase grown crystals were usually of higher resistivity and photosensitivity and had better purity and stoichiometry.

A difficulty encountered in the growth of crystals of II-VI compounds is that of obtaining stoichiometry. The effects of non-stoichiometry on crystal properties have been mentioned in section 1.2. The aim of the present work was predominantly to examine the properties of insulating type crystals. Thus the method of growth used had to provide a good degree of control over the growth conditions so that reasonably stoichiometric crystals were obtained. A vapour phase technique was used.

4.2 Vapour phase growth techniques

Many types of vapour phase growth involve some variation

of the Frerichs flow method (Frerichs 1947). In these techniques the vapourised material is carried along a heated tube by a carrier gas to a region where crystal growth takes place. Frerichs used hydrogen to transport cadmium vapour which reacted with a stream of hydrogen sulphide to produce cadmium sulphide. Fahrig (1963) and Hoschl and Konak (1963) used inert carrier gases passing over separate charges of the elements to grow cadmium sulphide and selenide respectively. Stanley (1956) and Fochs (1960) used powder charges of cadmium sulphide with either inert carrier gases or hydrogen sulphide. An advantage of these flow methods is that the sublimation process possesses an inherent degree of self purification. The more volatile impurities in the starting charge tend to be driven off at the beginning of a growth run and the heavier impurities remain behind in the residue of the charge. The disadvantages of the various flow methods are that the crystals grown are small and also it is difficult to control the growth conditions sufficiently so that reproducible batches of stoichiometric crystals are obtained.

Other methods (Piper and Polich, 1961; Fahrig, 1963; and Clark, 1966) have been used to grow larger crystals of cadmium sulphide than can be obtained using flow methods. These techniques involve growth in a closed system where a powder charge of CdS is sublimed down a temperature gradient. Sometimes the growth tube is slowly pulled through the

temperature gradient during growth. Growth can be carried out either in vacuum or in an inert gas atmosphere. Again control of the growth conditions is difficult.

4.3 Growth of Cadmium Selenide from the elements

Crystals were grown from the elements by a flow technique using argon as the carrier gas. Figure 4.3.1 shows the arrangement used. The temperature profile of the furnace is shown in figure 4.3.2. A three zone furnace was used, each zone having a separate heater winding of Kanthal 'A' resistance wire. There was a $\frac{1}{4}$ inch gap only between the adjacent zone windings and as a result the heating in one zone affected the other zones to a certain extent. Therefore the controlled temperatures of each zone could not be varied entirely independently of each other. The total power consumption under typical conditions was approximately $\frac{3}{4}$ KW.

Three identical control circuits were used for the different zones. Power was obtained from the 240V A.C. mains supply and adjusted using 'Regavolt' voltage regulators. 'Ether' on-off controllers activated mercury switch relays. These in turn switched the zone currents on and off and thus controlled the various temperatures. The temperature control points corresponded to the positions of the charge centres in the first two zones and the maximum temperature position in the last zone. Temperatures, measured with Platinum/Platinum 13% Rhodium thermocouples, were controlled at 485°C, 540°C and

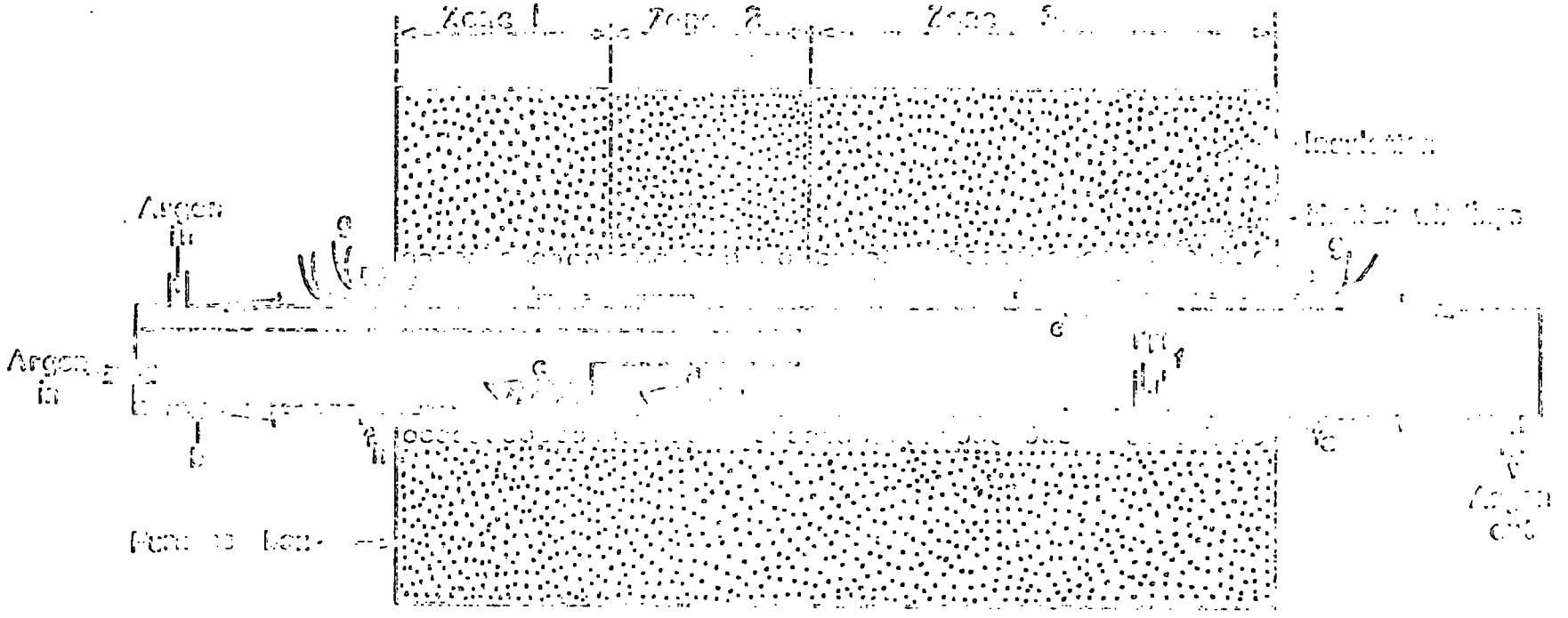

KEY

a	Grading tube	e	Liner
b	Separating tube	f	Crystals
c	Soldering charge	g	Thermocouple
d	Soldering charge	h	Ferrule tube

FIGURE 4.3.1. GROWTH OF [illegible]

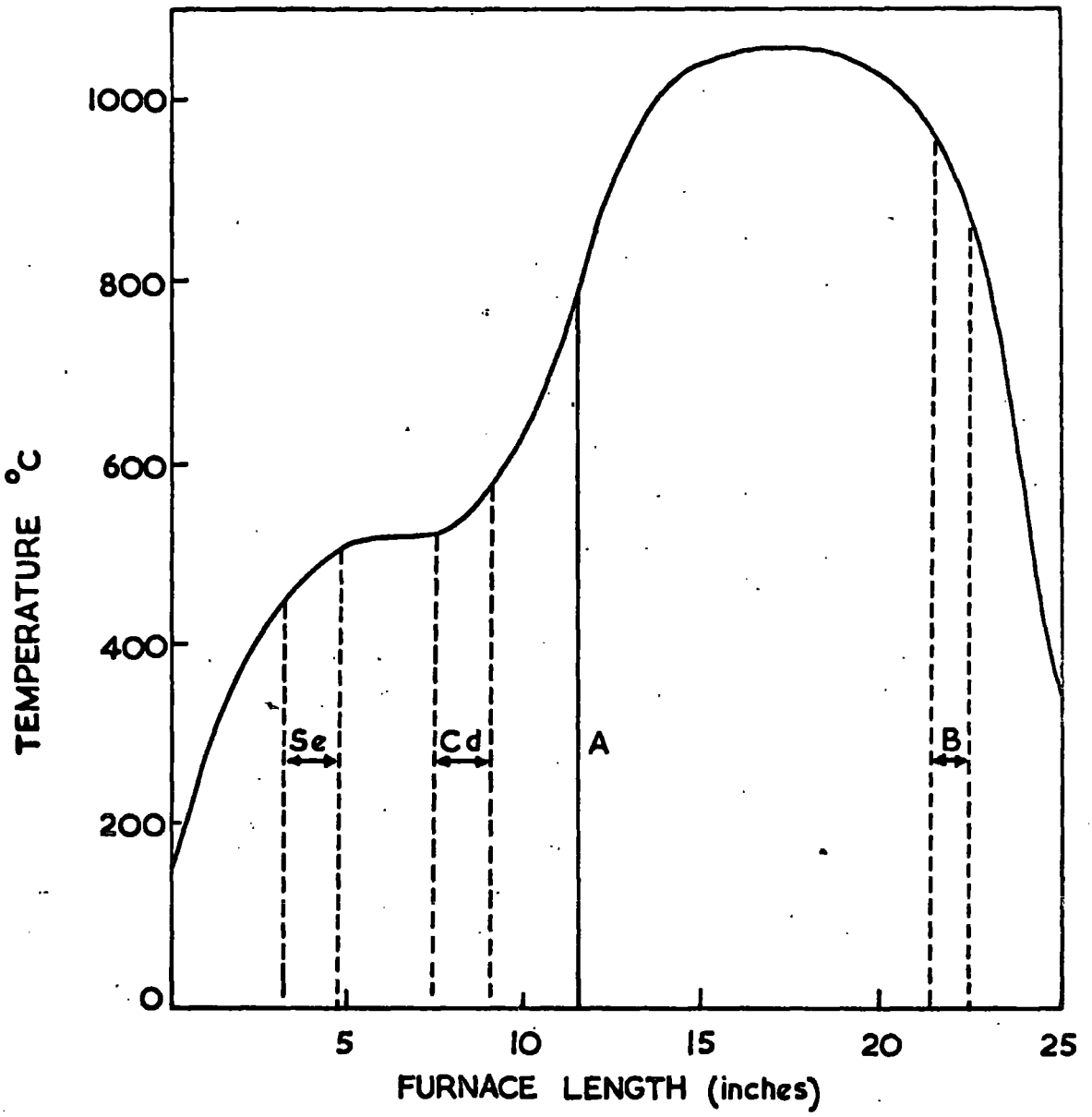

Se - Selenium charge

Cd - Cadmium charge

A - End of separating tube

B - Crystal growth

FIGURE 4.3.2. Temperature profile of 3 zone furnace used to grow CdSe.

1065°C respectively to an accuracy of ± 5°C. The thermocouples were placed outside the growing tube in the gap above it. The temperature profile shown in figure 4.3.2 was measured inside the growing tube, with the gas flows on, using a thermocouple and potentiometer.

The cadmium and selenium charges ('Light's' 6N and 5N shot respectively) were held in silica combustion boats inside a 25 mm diameter silica growing tube. The selenium boat was contained within a smaller silica tube, the separating tube. There were two inlet gas flows. One led directly into the growing tube and provided the carrier gas for the cadmium vapour. The other passed into the separating tube and over the selenium charge. The two streams met and mixed approximately half way down the growing tube and then flowed into the reaction zone where crystal growth took place on a cylindrical silica liner. Inlet and outlet gas flows passed through cone and socket joints at each end of the growing tube. The joints were sealed with 'Apiezon' grease and held tight against each other with light springs. A clear, flat end was provided on the outlet socket to enable the crystal growth to be observed.

99.995% pure argon was used as a carrier gas. This was further purified by passing it through (1) a drying tower containing a molecular sieve (aluminium calcium silicate) to remove water vapour, and (2) a heated tube (400°C) containing copper pellets to remove oxygen. The gas flow was then divided

to provide the separate streams for the two charges. Each flow was controlled with a needle valve (to $\pm$ 2 mls/min) and measured with a 'Rotameter' flow gauge. Toxic H_2Se, Cd and Se vapours were removed from the outlet gas by passing it into a 2 litre condensing flask and through a wash bottle containing concentrated sodium hydroxide solution. Finally the gas was expelled into the atmosphere outside the building. The flask also acted as a reservoir to reduce the pressure fluctuations in the gas flow caused by bubbling it through the sodium hydroxide. Connections between the various components of the gas flow system were made with clear PVC tubing.

After loading the charges into the growing tube the system was flushed with argon for half an hour to remove any air present. Flushing was continued for a further quarter of an hour while the copper furnace heated to 400°C. The main furnace was then switched on. $2\frac{1}{2}$ hours were required for all three zones to reach their correct temperature and the temperature profile to stabilise. During this time the gas flows were set at 15 mls/min. This did not produce sufficient transport for any appreciable crystal growth to take place but allowed a crystalline substrate to be built up on the liner. When the correct conditions for growth had been established both flows were increased to 100 mls/min and growth was allowed to proceed for 2 hours. After this time crystals almost completely blocked the liner and the furnace was then switched

off.

The gas flows were also stopped when the furnace was switched off. This was to prevent two effects which would otherwise have occurred as the furnace cooled down to room temperature (a process which took about 12 hours).

(a) Further crystal growth taking place under conditions which were different to those required for stoichiometric growth.

(b) Annealing of the crystals in a flow of excess cadmium vapour as the cadmium charge cooled more slowly than the selenium charge.

The outlet from the growing tube was closed during the cooling to prevent contamination of the crystals by water vapour from the wash bottle.

4.4 Growth habit

Crystal growth took place over the last inch of the liner. The crystals tended to grow radially across the liner from a microcrystalline substrate. The yield of crystals from a typical run was quite small, approximately 1 gram. Three main growth habits were observed.

(1) Plates with areas from 1 mm^2 to 1 cm^2 and 10 to 100 μ thick.

(2) Rods about 1 cm long, up to 1 mm wide and 100 μ to 1 mm thick. These were the crystals which were used for the measurements described in later chapters.

(3) Fine whiskers up to $1\frac{1}{2}$ cms long.

Table 4.1. Growth conditions

	Crystal growth-mid-point temperature (°C)	Selenium charge-mid-point temperature (°C)	Cadmium charge-mid-point temperature (°C)
Present Work	925	485	540
Hoschl & Konak	940	500	585
	Crystal growth-temperature spread (°C)	Selenium charge-temperature spread (°C)	Cadmium charge-temperature spread (°C)
Present Work	875 to 970	445 to 505	525 to 570
Hoschl & Konak	930 to 980	490 to 510	575 to 590
	Maximum temperature in reaction zone (°C)	Flow over selenium charge (mls/min)	Flow over cadmium charge (mls/min)
Present Work	1065	100	100
Hoschl & Konak	1100	50	150

Table 4.2. Comparative amounts of charges transported.

	Weight of charge evaporated (gms)	Atomic weight	$\frac{\text{Weight of charge}}{\text{atomic weight}}$
Selenium	2.57	79	0.032
Cadmium	1.43	112	0.013

Table 4.3. Impurities in starting materials for crystal growth.

Impurity element	Amount present in 5N Selenium shot (ppm)	Amount present in 6N Cadmium shot (ppm)
Aluminium	< 3	
Silver	< 3	< 0.1
Copper	1	< 0.1
Iron	2	
Manganese	< 5	0.3
Lead	1	0.3
Bismuth		0.2
Calcium		0.1
Silicon		0.2

The crystals were semi-insulating, with a room temperature dark resistivity of 10^{11} to $10^{12}\Omega$cms, suggesting that they were reasonably stoichiometric. They were also highly photosensitive, having gains of up to 10^{4}.

The growth conditions are summarised in table 4.1. Also listed in this table are the conditions used by Hoschl and Konak (1963) for the growth of CdSe from the elements. They derived these conditions from a study of the thermodynamics of the growth process. The two sets of conditions are fairly similar, although the temperature ranges over the charge and growth regions obtained by Hoschl and Konak were smaller than those found with the furnace described in the preceding section. Surprisingly these large spreads of temperature did not affect the reproducibility of the crystals i.e. batches of crystals whose properties varied from semiconducting to semi-insulating were not obtained.

This reproducibility can perhaps be understood when the weight of the charges evaporated during a typical run is considered. This data is given in table 4.2. It was found that there was more transport of selenium than of cadmium. As the flow rates over the two charges were equal it follows that the mixture of vapours flowing into the growth region contained an excess of selenium. This does not mean that the crystals grew containing an excess of selenium. However it does mean that there would be little tendency for them to grow with an

excess of cadmium which would have resulted in low resistivity crystals. Semiconducting crystals were grown if the temperature of the cadmium charge was increased to above 570°C. This was presumably because they then grew containing an excess of cadmium.

An X-ray powder photograph was taken in order to verify that the crystals grown were CdSe. The diffraction pattern obtained was compared to the ASTM data for CdSe and this showed that the crystals were indeed cadmium selenide with the usual hexagonal structure. No extra lines due to either cadmium or selenium were found in the diffraction pattern.

The impurity content of the crystals was not known as there were no mass spectrographic analysis facilities available. However the manufacturers of the materials used as starting charges quoted typical impurity contents of the materials. These are reproduced in table 4.3 and give an indication of the nature and quantity of some of the impurities that may have been present in the crystals. It must be noted that the silicon content of the crystals might have been quite high as a result of the charges being contained in silica combustion boats and the crystals growing on a silica liner.

Although the research reported in this thesis was mainly concerned with the properties of as grown crystals, low resistance crystals which had been treated in various ways after growth to increase their resistivity were also examined. The

two types of treatment used are described in the following sections.

4.5 Heat treatment in selenium vapour

The resistivity of semiconducting crystals could be increased from about 1Ωcm to 10^{10}Ωcms (at room temperature) by annealing them in selenium vapour. This treatment introduced acceptor centres in the form of either cadmium vacancies or selenium interstitials. The annealing procedure was as follows.

Crystals to be treated were sealed in a heavy walled silica tube, which had previously been evacuated to a pressure of 10^{-5} torr, together with one pellet of 5N selenium (approximate weight 0.2 gms). The tube was then enclosed within a stainless steel tube as protection against an explosion resulting from high selenium vapour pressures. After loading the tube into a furnace it was heated up to 800°C and held at this temperature for 24 hours. The corresponding vapour pressure of selenium at this temperature is approximately 5 atmospheres. At the end of this annealing period the crystals were quickly quenched to room temperature by pushing the tube out of the furnace into cold water.

4.6 Copper doping

Copper acts as an acceptor impurity in cadmium selenide and is thus suitable for doping crystals to increase their resistance. Doping was done by immersing crystals in a 1 part

in 10^6 solution of copper sulphate for $\frac{1}{2}$ hour. This produced a layer of copper selenide on the surfaces of the crystals. The copper was then diffused into the crystals by heating them at $500^{\circ}C$ in an evacuated silica tube (10^{-5} torr) for 5 hours. This treatment increased resistivities from 1Ω cm to $10^6\Omega$ cms at room temperature.

References

Clark, L., and Woods, J., 1966, Brit. J. Appl. Phys., 17, 319.

Fahrig, R.H., 1963, Electrochemical Technology, 1, 362.

Fochs, P.D., 1960, J. Appl. Phys., 31, 1733.

Frerichs, R., 1947, Phys. Rev., 72, 594.

Hoschl, P., and Konak, C., 1963, Czech. J. Phys. B, 13, 364.

Kubo, S., and Amemiya, M., 1965, Japan. J. Appl. Phys., 4, 941.

Piper, W.W., and Polich, S.J., 1961, J. Appl. Phys., 32, 1278.

Stanley, J.M., 1956, J. Chem. Phys., 24, 1279.

CHAPTER 5

Experimental Techniques

5.1 Mounting the crystals

Measurements were carried out on rod type crystals. Contacts were made by evaporating indium over about 1 mm. at each end of the rods. Indium was used as it is generally accepted as making an ohmic contact to materials such as CdSe. The evaporation was done at a pressure of 10^{-5}torr, obtained with a mercury diffusion pumping system and a cold trap. No prior treatment was given to the crystals before making the contacts.

As measurements were made over a temperature range of 90°K to 400°K it was necessary to mount the crystals in a cryostat. In fact three cryostats were used for different types of measurements and these are described in the appropriate sections below. However a common method of mounting the crystals was utilised in all the cryostats.

The crystals were first fixed onto thin silica slides (Dimensions 7/8 x 7/16 inch x 0.5 mms) by melting strips of indium onto the evaporated contacts and the slides. Prior to this the slides were subjected to ion bombardment in a hydrogen atmosphere for ten minutes to ensure that the indium made a good bond to the glass. The indium was melted on at a temperature of 200°C for 1 minute under an atmosphere of oxygen free nitrogen. The slides provided electrical insulation from the

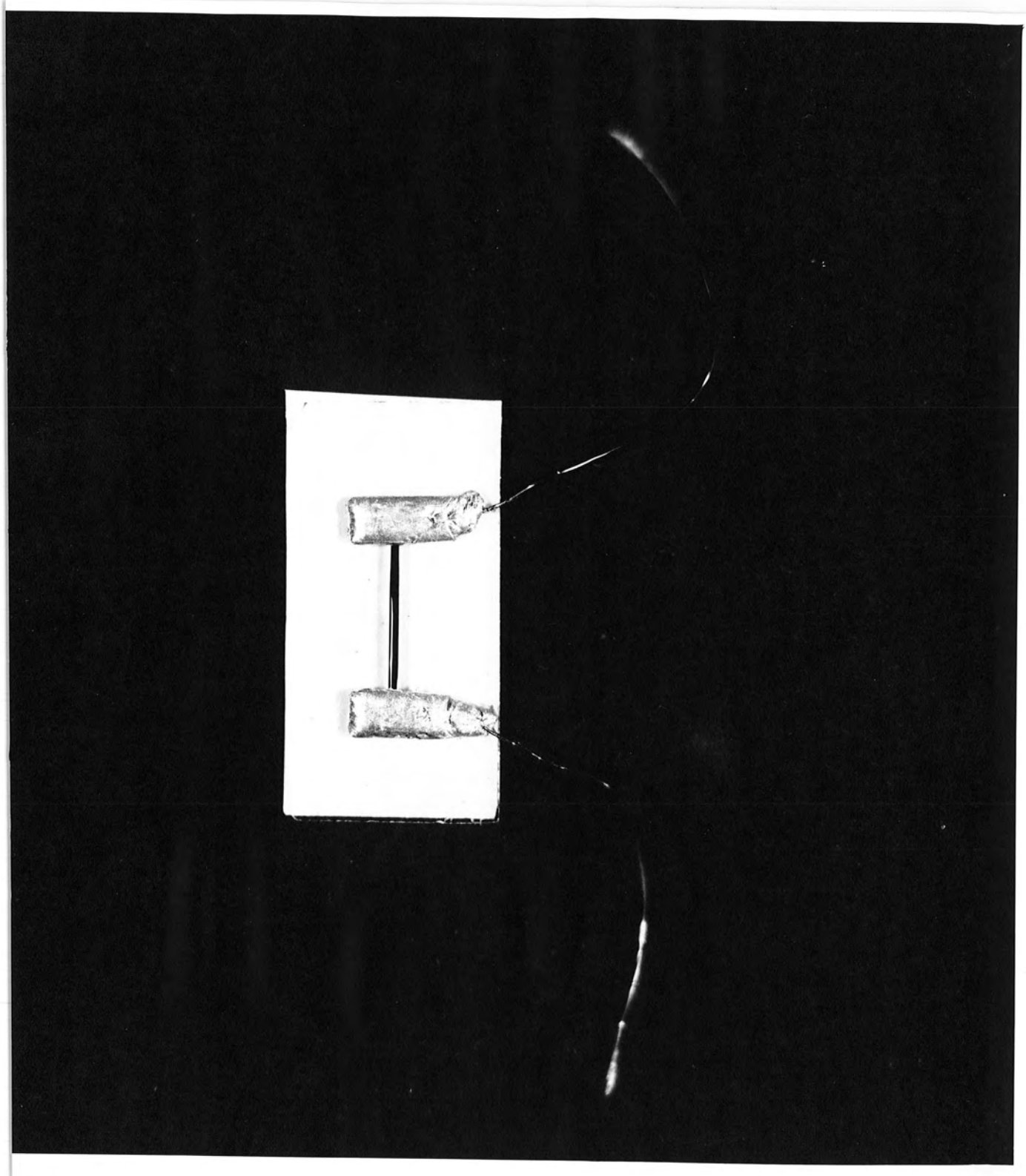

FIGURE 5.1.1 Mounted crystal.

cryostat block while still allowing reasonable thermal conduction. Silica was used to prevent cracking as a result of thermal cycling during the measurements.

Thin copper leads were attached to the ends of the indium strips using a miniature soldering iron. Care was taken not to melt that part of the indium attached to the crystal. A mounted crystal is shown in figure 5.1.1. The slides were held on the cryostat blocks by small clips. A thin layer of silicone grease was introduced between the slide and the block to improve thermal conduction.

Great care was taken during both contacting and mounting the crystals to ensure that no contamination occurred, with finger grease for example, which would give rise to significant leakage currents. This was necessary because of the high resistances of the crystals.

The technique described above resulted in good electrical contacts which were also mechanically strong. After mounting a crystal a V-I curve under illumination (maximum applied potential 120 V) was measured. A linear relationship was generally found and reversing the polarity of the applied voltage did not cause any change in the characteristic. Although not conclusive, these checks suggested that the contacts were reasonably ohmic.

5.2 Temperature variation and measurement

The vacuum jackets of the cryostats were usually evacuated

using a rotary pump which produced a pressure of approximately 10^{-1} torr. Cooling of the cryostat block (made of copper) was achieved by the introduction of liquid nitrogen into an attached reservoir. To heat the crystal a wire coil, insulated by a silica tube, was inserted into a hole in the centre of the block. The heater was supplied from a 12 volt transformer and adjusted with a 'Variac' control.

The temperature of a crystal was measured using a copper/constantan thermocouple in conjunction with a potentiometer (Tinsley Model 3387B). The cold junction was held at room temperature in a small water bath. Each cryostat was provided with a thermocouple which was indium soldered onto the silica slide close to the crystal during the mounting procedure. It was not possible to attach the thermocouple to the crystal because the resultant pick up of electrical noise interfered with the measurement of small currents.

5.3 D.C. measurements

Most of the electrical measurements made were D.C. e.g. thermally stimulated currents and photoconductivity. The circuit used is shown schematically in figure 5.3.1. The applied voltage was derived from an H.T. battery and could be varied between 0 and 120 volts. A suitably shunted moving coil meter, contained in the power supply box, measured currents greater than 1 μA.

Currents in the range 10^{-13} to 10^{-6} A were measured using a

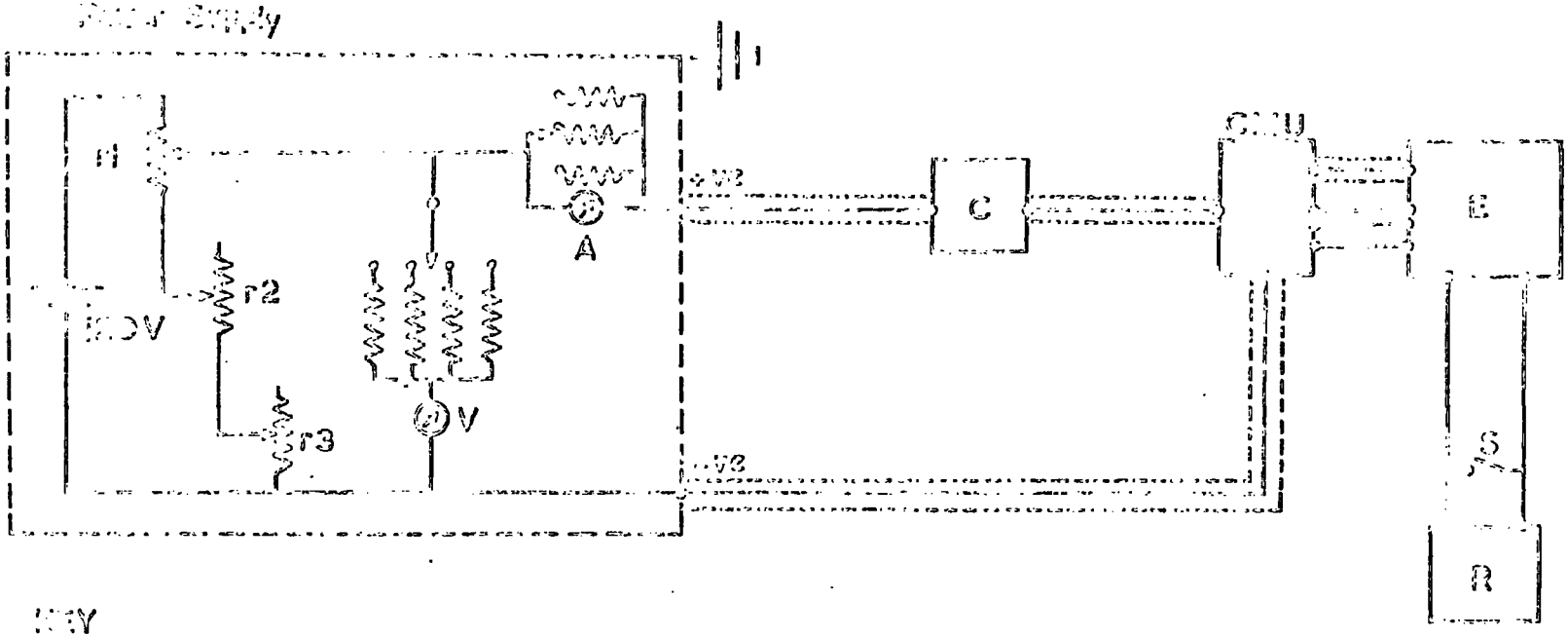

KEY

r1	Coarse voltage control	CMU	Current measuring unit
r2	Medium " "	C	Crystal mounted in cryostat
r3	Fine " "	E	Vibron electrometer
A	Ammeter with ranges 50μA, 500μA, 5mA, 50mA.	R	Chart recorder
V	Voltmeter with ranges 5V, 50V, 100V, 250V.	S	Switching switch

FIGURE 6.3.1. Circuit for D.C. measurements.

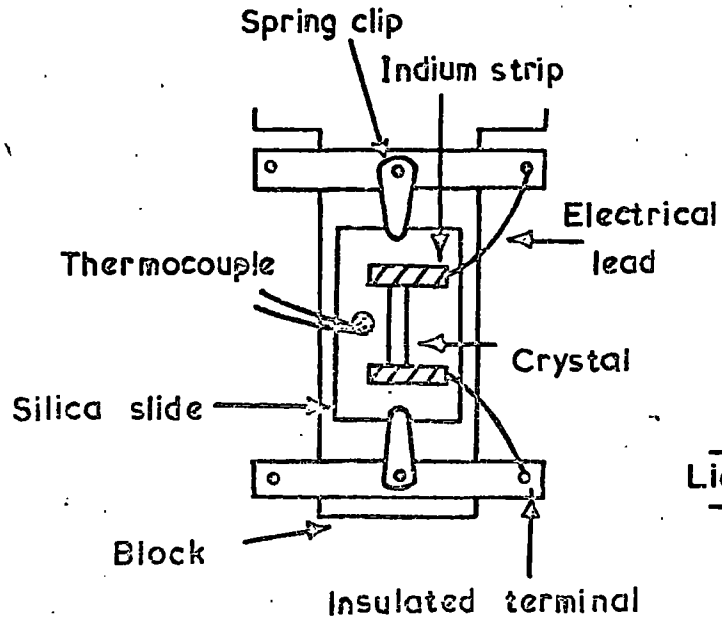

FIGURE 5.4.1(b) METHOD OF MOUNTING CRYSTAL ON BLOCK

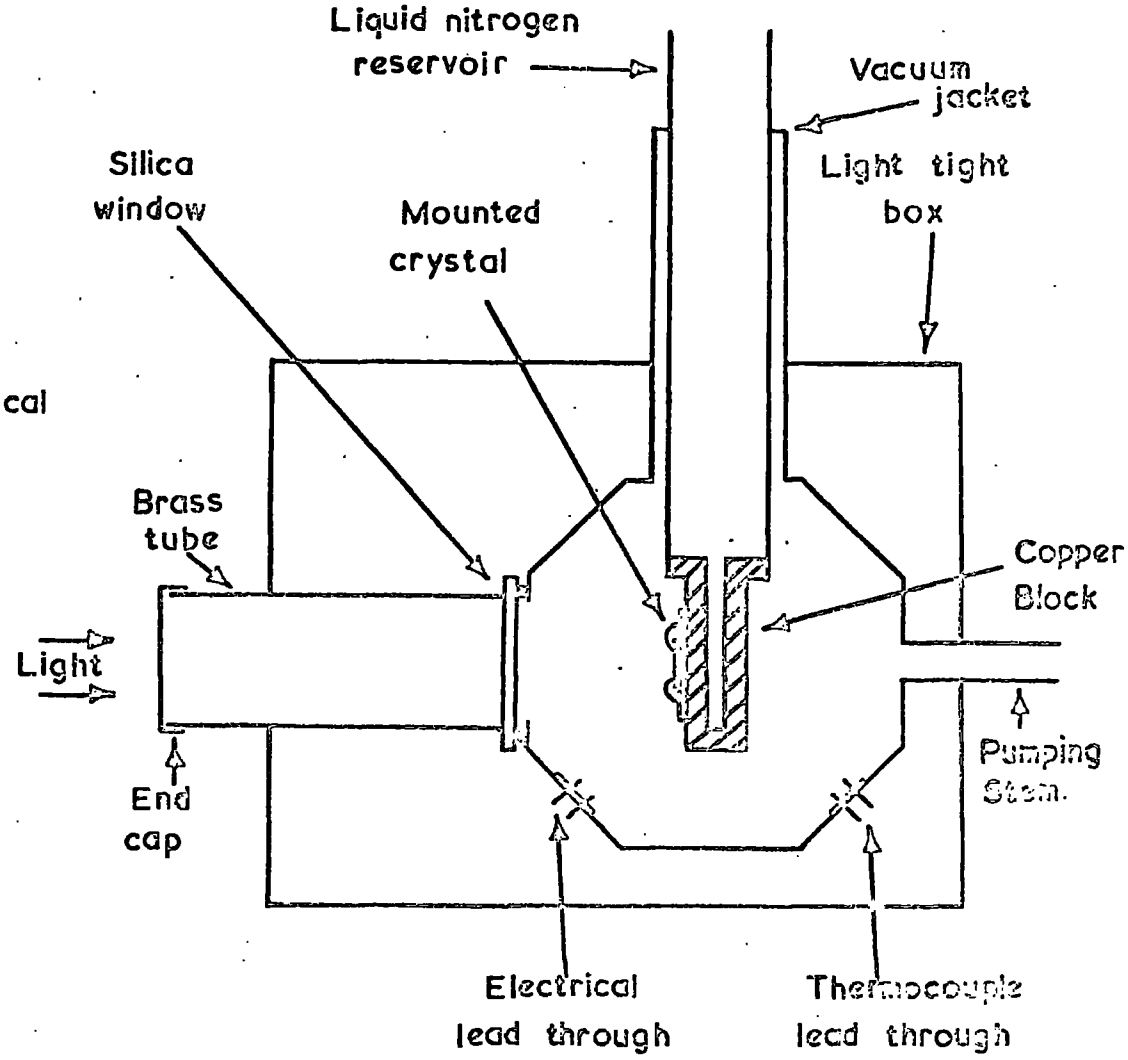

FIGURE 5. 4. 1(a) CRYOSTAT IN T.S.C. MEASUREMENTS

Vibron electrometer (Model 33B) with a matched current measuring unit (Model A33B) containing high stability resistances. The Vibron reading was displayed on a chart recorder. This enabled currents to be continuously monitored against temperature, time or wavelength of illumination. The recorder input could be shorted out by means of a switch. This produced a blip on the trace so that the point corresponding to a particular temperature, for example, could be marked.

Non-microphonic co-axial cable and B.N.C. sockets and plugs were used for the external connections in order to minimise both noise and leakage currents. It was found that the total leakage current in the circuit was less than 10^{-13}A with 50 volts applied.

5.4 Thermally stimulated currents

A diagram of the cryostat used in the measurement of thermally stimulated currents is shown in figure 5.4.1(a). Figure 5.4.1(b) illustrates in more detail the method of mounting a crystal on the cryostat block. The cryostat body was enclosed within a box to prevent stray light reaching the crystal. Illumination, from a 750 W tungsten lamp, was introduced through a brass tube. This tube was provided with a light tight end cap which was simply removed to allow light to fall on a crystal as required. Thermocouple and electrical leads were introduced into the cryostat by means of glass to metal seals. The electrical leads were led to P.T.F.E.

insulated terminals mounted on bars attached to the block. The leads from the crystal were in turn connected to these terminals.

Ideally the measurement of thermally stimulated currents requires a constant heating rate. However this is not simple to achieve. In practice, as a crystal was heated up from 90°K to 400°K, the heater current was increased four times to counteract the decrease in heating rate. This did not produce a uniform rate of heating, for typical measurements a variation between 0.14 and 0.24°K/sec. was found over the whole temperature range.

The procedure adopted in the measurement of thermally stimulated currents is described in section 6.1.

5.5 Spectral response of photoconductivity and infra red quenching

Monochromatic illumination, for the measurement of spectral response of photoconductivity and infra red quenching, was obtained using a Barr and Stroud double monochromator type VL2. Quartz prisms (spectrosil 'A' quality) were used and these enabled measurements to be made out to 4 μ if necessary. A 500 W tungsten lamp provided the light source at the input slit of the monochromator. The lamp was run from a 240 V stabilised A.C. supply and its intensity was varied by altering the filament current with a 'Variac' control.

A cryostat was required which would permit a crystal to be

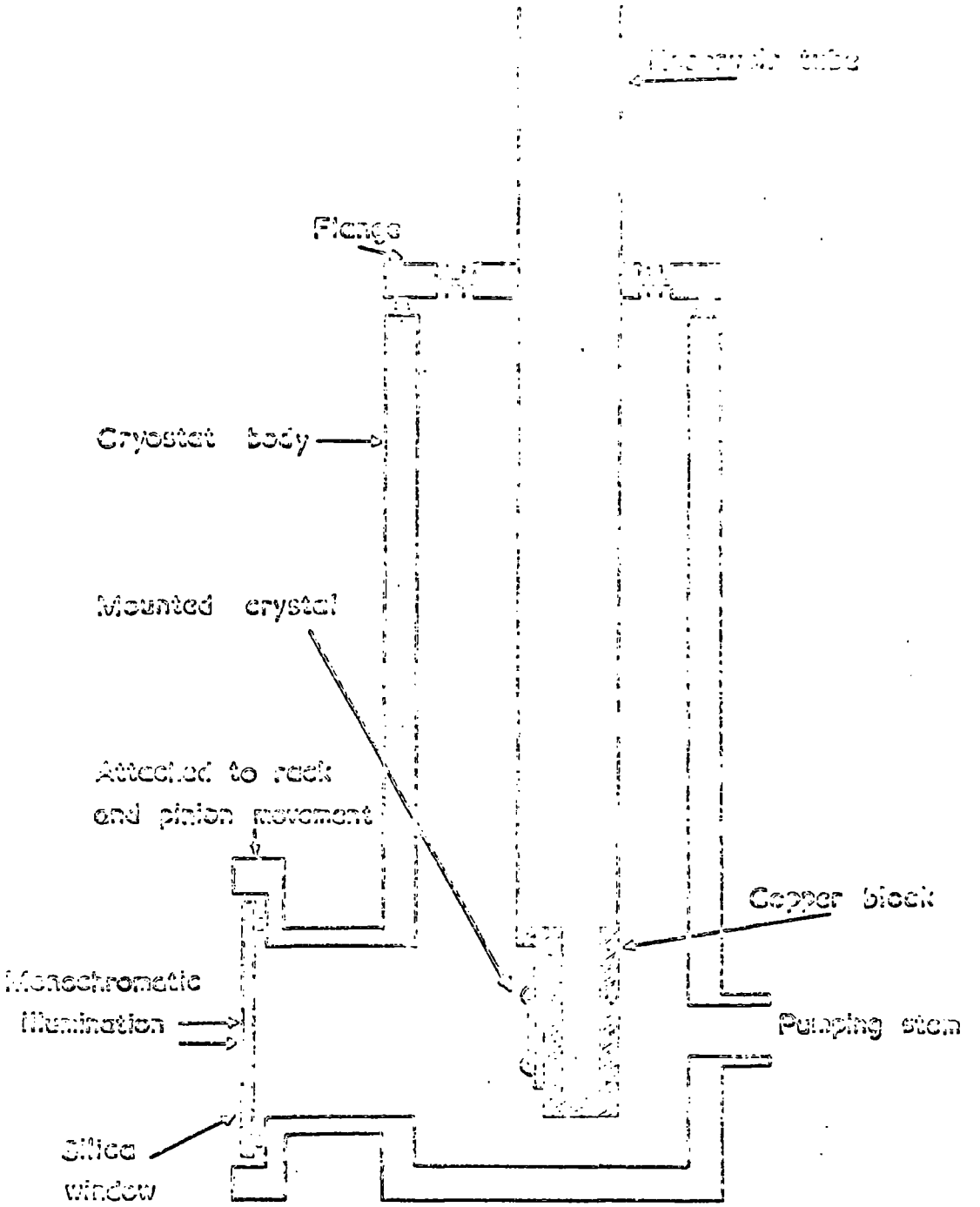

FIGURE 5.5.1. CRYOSTAT FOR USE WITH MONOCHROMATOR

aligned with the monochromator output slit. The design used is shown in figure 5.5.1. The body of the cryostat fitted onto the slit by means of a special adaptor. A rack and pinion movement enabled the cryostat to be raised or lowered with respect to the slit thus providing adjustment in the vertical direction. Horizontal adjustment was obtained by rotating the flange attached to the reservoir tube, which was mounted eccentrically in the flange. This eccentricity magnified the horizontal movement of the crystal obtained by rotating the flange. In practice a crystal was aligned with the slit by adjusting it in the two directions until a maximum photoresponse was obtained. The rack and pinion movement was not completely light tight and had to be covered with black cloth to eliminate stray light. In the cryostat shown in figure 5.5.1. the electrical leads were not taken to insulated terminals but were directly attached to the melted indium contacts after mounting the crystal in the cryostat.

For measurements of infra red quenching it was necessary to illuminate a crystal with a primary light source as well as with monochromatic radiation. Primary illumination was introduced onto the crystal via a light pipe mounted in the side of the cryostat body. The illumination was obtained from a tungsten lamp, filtered to remove all but the red radiation (of about band gap energy). A 1 cm wide glass cell containing water, plus two HA1 and one OR2 Chance glass filters, were used

to remove the unwanted longer wavelengths.

More details regarding the techniques employed in measuring spectral response and infra red quenching are described in Chapter 10, which is concerned with results obtained from measurements of this nature.

The cryostat and monochromator described above were also used in the measurement of thermally stimulated currents after illumination with monochromatic light and for photocurrent against temperature measurements.

5.6 Photoluminescence

A schematic illustration of the arrangement used for the excitation and detection of photoluminescence is presented in figure 5.6.1. Crystals were mounted in a similar cryostat to that shown in figure 5.4.1(a) although it was not enclosed within a light tight box. The cryostat was provided with two silica windows to permit the entry of exciting illumination and the exit of the luminescent emission. One side of the cryostat block was angled at about 60^{o} so that a crystal presented a large area to both the exciting radiation and the focussing mirrors.

Luminescence was excited using a 250 W high pressure mercury lamp. This was used because it was found to excite about 8 times more emission than could be obtained with a 750 W tungsten lamp. Infra red radiation was filtered out of the mercury lamp spectrum using copper sulphate solution and

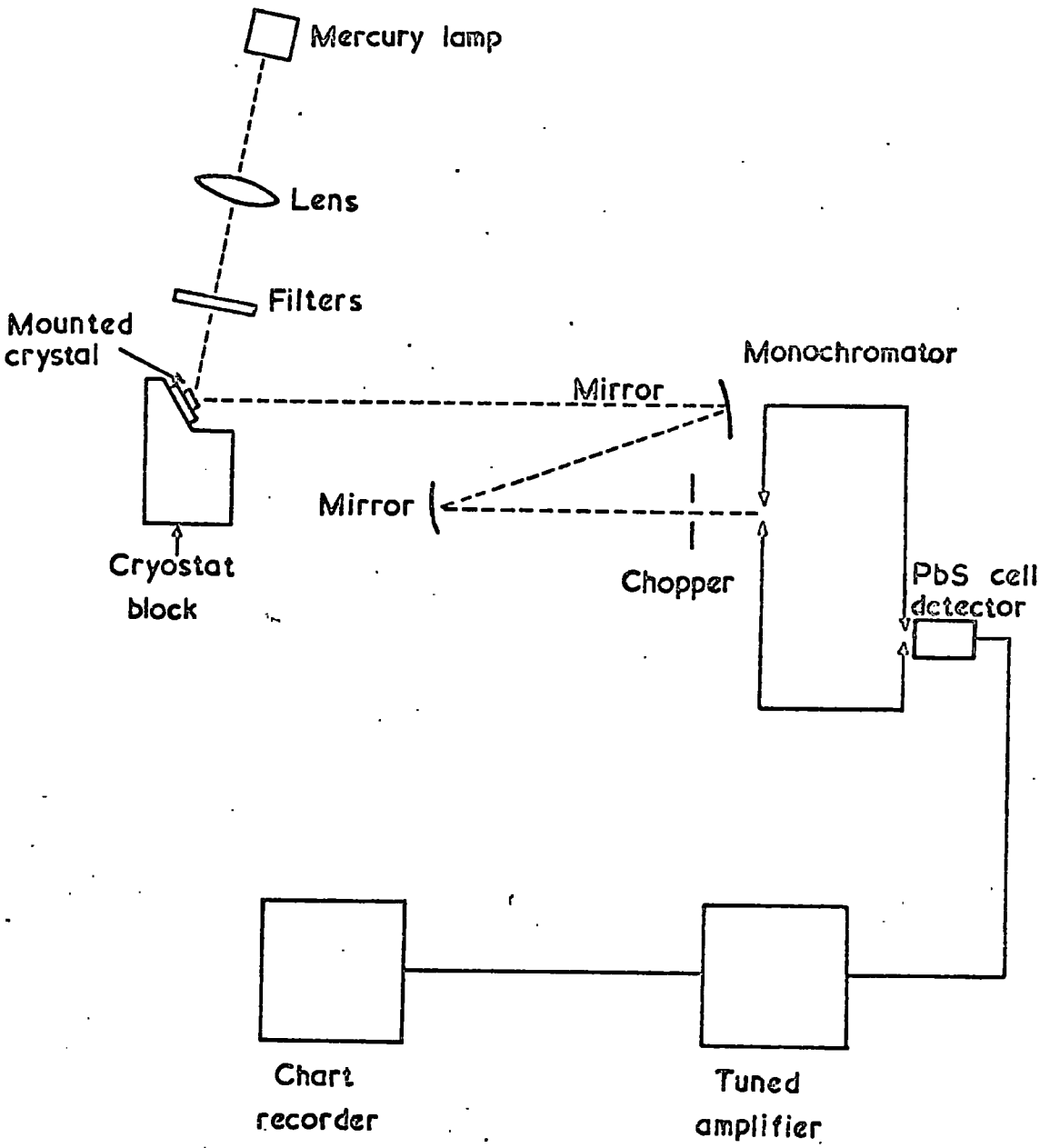

FIGURE 5.6.1. MEASUREMENT OF PHOTOLUMINESCENCE.

two HA1 Chance glass filters. This was done to prevent these wavelengths from being reflected and masking the luminescence emitted from a crystal. The luminescence was focussed onto the monochromator input slit by two mirrors. The emission was modulated at 800 c/s using a mechanically driven chopper located in front of the input slit.

The spectrum of the luminescence was analysed with the monochromator mentioned in the previous section and detected with a lead sulphide cell (Mullard 61SV). The output from this detector was amplified by a Barr & Stroud tuned amplifier (Model EL7921) and then displayed on a chart recorder. During measurements of luminescence the monochromator was automatically scanned through the required wavelength range and the spectrum was recorded on a chart. A marker pen, activated by a switch on the monochromator, marked the chart at regular intervals to enable the emission wavelengths to be identified.

5.7 Calibration of light intensities

For an analysis of photoconductivity results (see Chapters 10 and 11) it was necessary to know the intensity of the incident monochromatic illumination. To measure this the tungsten lamp illumination entering the monochromator was chopped at a frequency of 10 c/s. The monochromatic light was detected with a thermopile (Hilger & Watts FT.16.301) and the output from this was amplified by the tuned amplifier. A

knowledge of the thermopile sensitivity and the amplifier gain then allowed the intensity of the monochromatic radiation to be calculated.

The spectral response of the lead sulphide cell used to detect luminescence was also calibrated against the thermopile.

CHAPTER 6

Thermally stimulated current measurements

6.1 Introduction

The following experimental procedure was used to measure thermally stimulated currents (T.S.C.) over the temperature range 90°K to 400°K. The crystal was first heated in the dark to 400°K to empty the traps and then cooled to 90°K. This cooling was done either in the dark or under illumination which could be switched on at any required temperature. After cooling, the crystal was illuminated for 10 minutes in order to complete the trap filling. Next a voltage was applied with the crystal in the dark and the thermally stimulated current was monitored as the crystal was heated up.

Illumination was provided by an unfiltered, focussed, 750 W tungsten lamp which gave an illumination intensity on the crystal of about 2400 ft. candles. An applied potential of 50 volts was used. The average heating rate was 0.17°K/sec. Although this varied between 0.14 and 0.24°K/sec. during a run it was substantially constant over the range of temperatures covering any particular T.S.C. peak. Thus the variation in heating rate did not invalidate the analysis of any peak. The background pressure in the cryostat was 2×10^{-1} torr.

6.2 As grown crystals

In order to obtain reproducible T.S.C. curves it was found necessary, before making any measurements, to heat the crystal

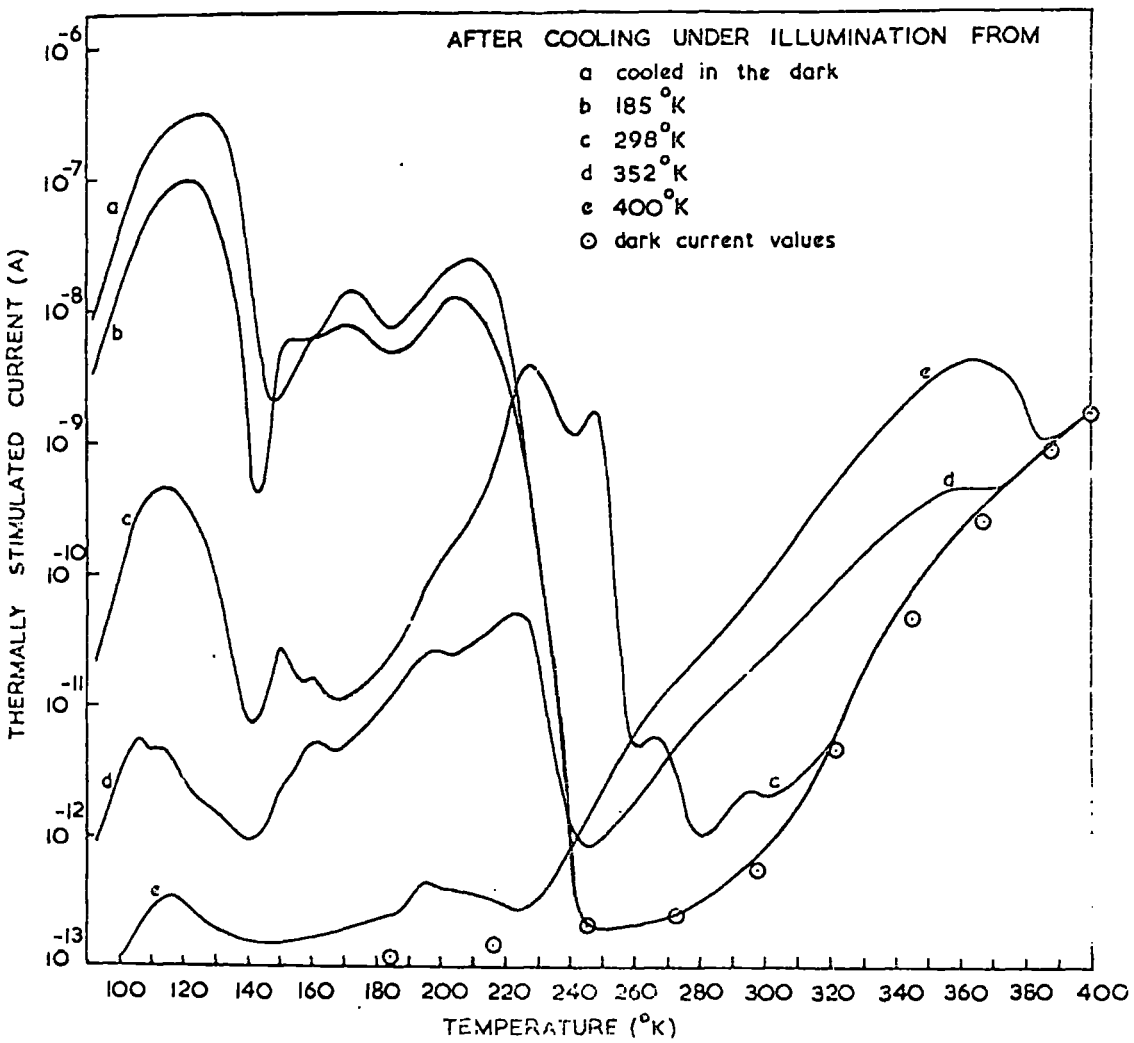

Fig. 6.2.1. Thermally stimulated current curves after cooling from various temperatures under white light illumination

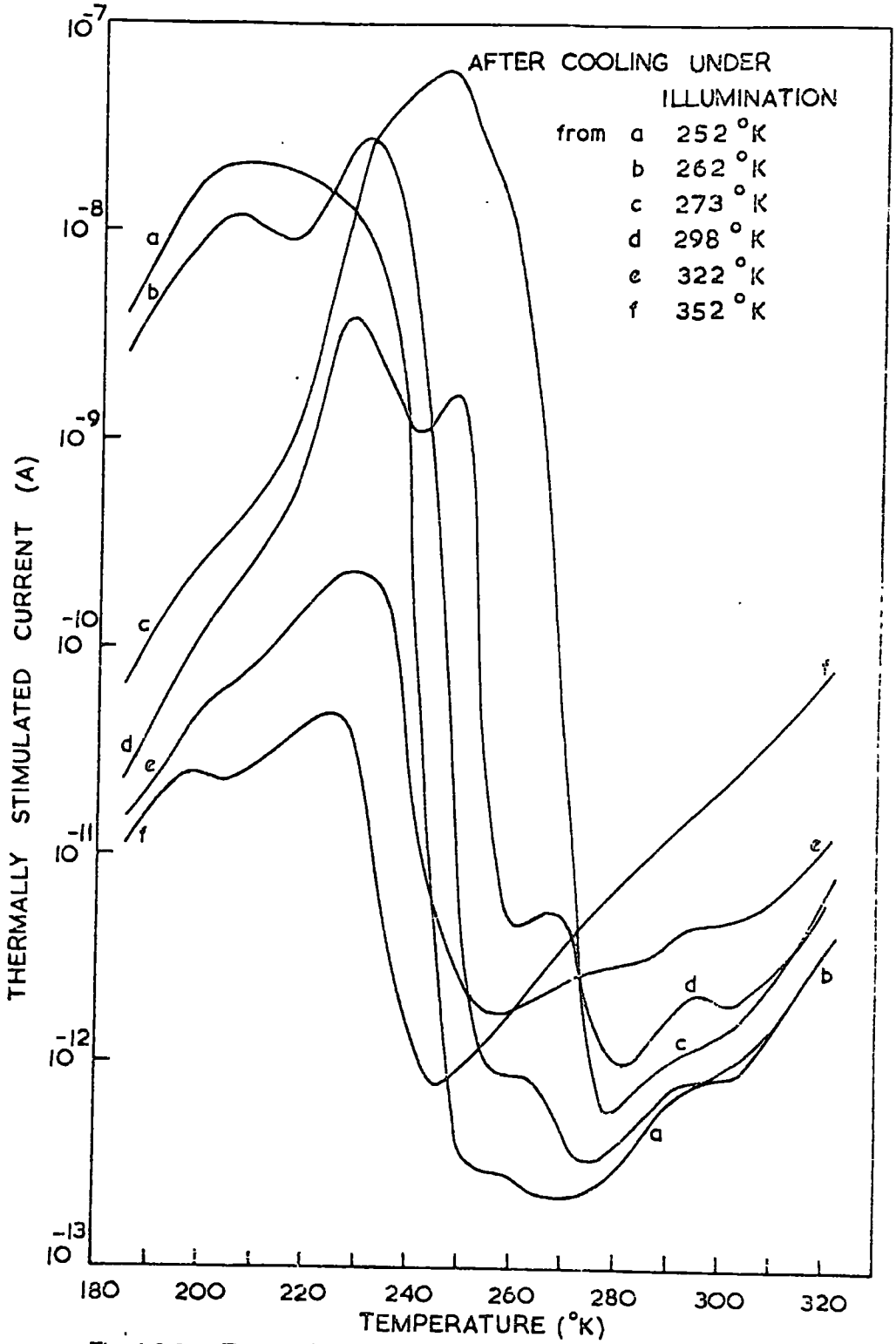

Fig. 6.2.2. Thermally stimulated current measurements in the intermediate temperature range.

in vacuum at 400°K in the dark for 1 hour. Figure 6.2.1 shows a typical set of T.S.C. curves obtained from a high resistance, highly photosensitive, as grown crystal. The curves were obtained after cooling under illumination from different temperatures, T_s. The resultant T.S.C. curve was strongly dependent on the value of T_s. Heating to 400°K put the crystal into a standard, stable state which was then modified by the next cooling schedule used. Some of the variations in the T.S.C. curves obtained are shown in more detail in figure 6.2.2.

Three sets of T.S.C. peaks were found:-

(1) The low temperature peaks in the range up to about 210°K. These decreased in magnitude as T_s was increased.

(2) The intermediate temperature peaks in the range 210°K to 280°K. These appeared and increased in magnitude as T_s was increased between 250°K and 275°K and then decreased with higher values of T_s.

(3) The high temperature peaks in the range above 280°K. These appeared and gradually increased in height as T_s was increased above 250°K.

Above 260°K, when no T.S.C. peaks were found, the current closely followed the dark current. For temperatures below about 180°K the dark current was too small to be measured i.e. it was less than 10^{-13}A.

The traps which give rise to the various peaks are

discussed in more detail in following chapters.

6.3 Thermally stimulated currents after illumination with monochromatic light

T.S.C. spectra were measured following illumination with monochromatic light obtained from a monochromator with a tungsten lamp source as described in section 5.5. The energy flux (.022 $\mu w/mm^2$) and band width (480 A^o) were the same for each wavelength. Because of the low intensity of excitation the crystal was illuminated for 20 minutes after cooling to complete the trap filling. T.S.C. curves obtained after cooling in the dark are shown in figure 6.3.1. It was found that illumination with wavelengths shorter than 1.05 μ was required before any trap filling was obtained. This corresponds to an energy threshold of 1.18 ev which is considerably less than the band gap energy of CdSe at 90°K (1.82 ev). This threshold is discussed further, in connection with the spectral response of photoconductivity, in section 10.5. With wavelengths shorter than the threshold the efficiency of trap filling progressively increased until maximum filling was achieved with wavelengths of 0.8 μ and shorter.

Figure 6.3.2 shows T.S.C. spectra obtained after cooling a crystal from 400°K under monochromatic illumination. Only a small reduction in the low temperature peaks was found, the largest effect being obtained with radiation of band gap

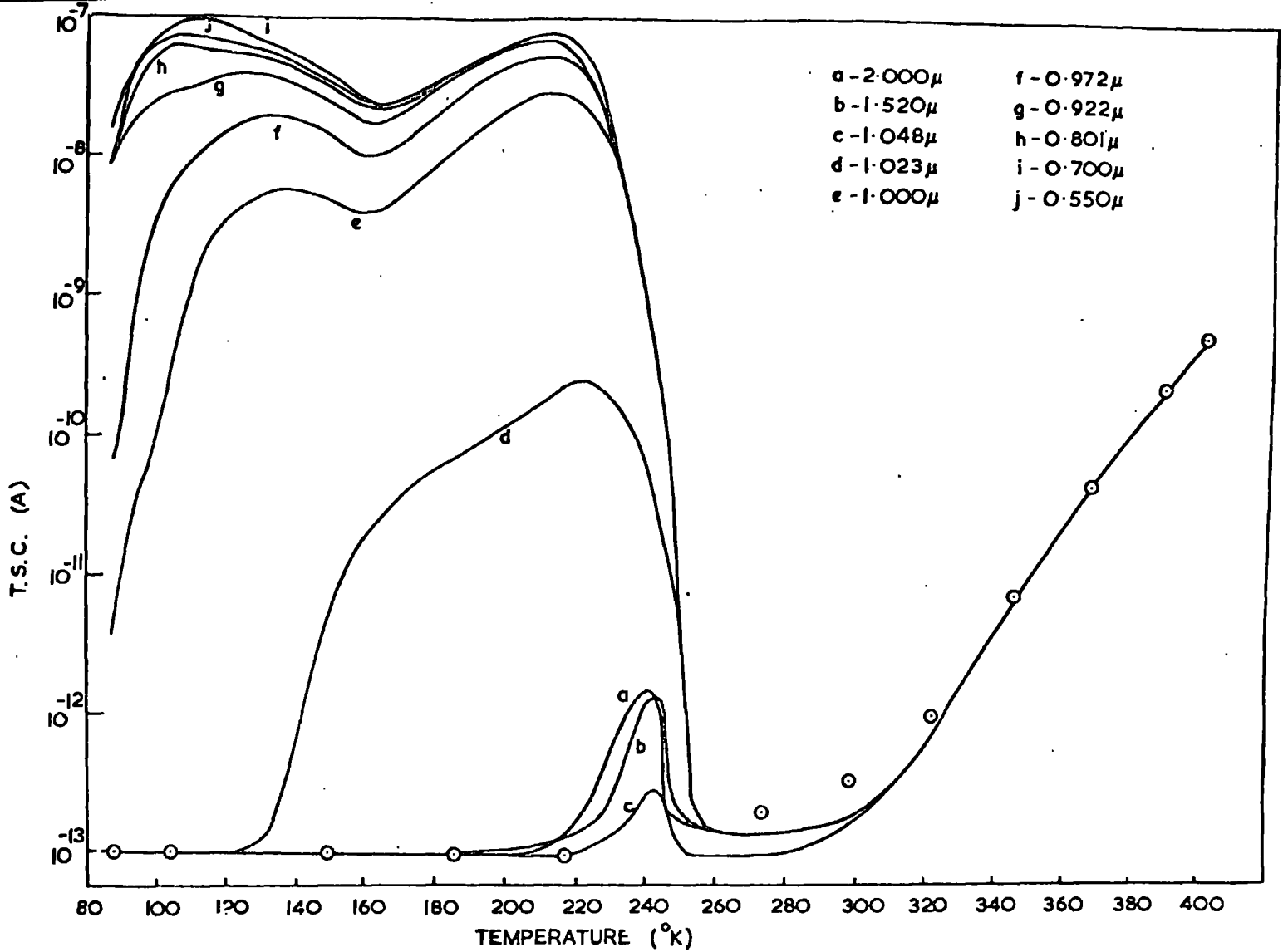

FIGURE 6.3.1. T.S.C. curves obtained after cooling in the dark and then illuminating with monochromatic radiation. Dark current values are marked ⊙.

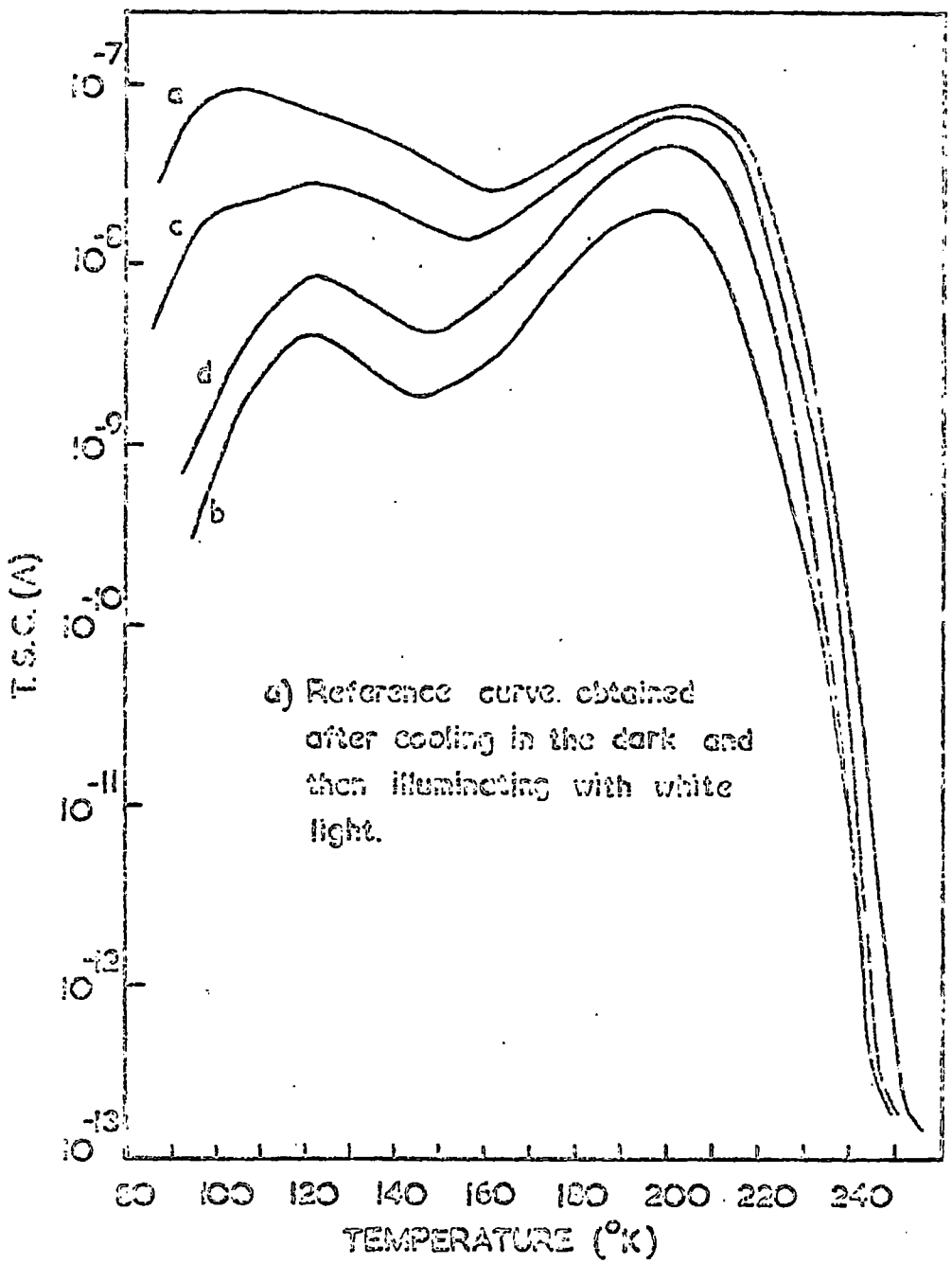

FIGURE 6.3.2. T.S.C. curves after cooling from 400°K under monochromatic illumination of wavelengths b)0·700μ c)0·847μ d)0·550μ

energy (wavelength 0.7 μ) i.e. for light strongly absorbed throughout the crystal. No high temperature peaks were found. T.S.C. measurements made after cooling from 273°K under illumination showed no reduction in the low temperature peaks and no intermediate temperature peaks. As the intensity of the monochromatic radiation was less than that of the white light it appeared that the variations in T.S.C. curves with cooling schedule were intensity dependent. This was verified by making T.S.C. measurements after irradiation with white light of about 10% of the usual intensity. This decrease in intensity reduced the magnitude of the observed changes with cooling schedule. Cooling from 400°K under this weaker illumination resulted in high temperature peaks with about $\frac{1}{2}$ of their usual height and low temperature peaks about $1\frac{1}{2}$ orders of magnitude larger than those obtained with maximum light intensity. The intermediate temperature peaks, obtained after cooling from 273°K under illumination, were reduced in height by about $\frac{2}{3}$.

6.4 Changes in the T.S.C. spectra

Three different processes have been postulated by previous authors to explain variations in T.S.C. curves of the type described in section 6.2. These are:

(a) Photochemical effects which lead to changes in trap density or perhaps the creation of new traps. Such effects have been reported for CdS by Woods and Nicholas (1964) and Korsunskaya et al (1966).

(b) Changes in free carrier lifetime or mobility (again photochemically caused). These would affect the magnitude of the observed thermally stimulated currents. Cowell and Woods (1967) found photo-induced changes in lifetime in CdS.
(c) When a trap is surrounded by a coulombic repulsive barrier the efficiency of trap filling increases as the temperature at which illumination is carried out is raised. This mechanism would explain the behaviour of the high temperature traps but not of other traps. Bube et al (1966) have reported traps of this type in various CdS_xSe_{1-x} crystals.

These possible effects are discussed in more detail with respect to the different traps later in this chapter and in following chapters.

6.5 Photocurrent vs Temperature measurements

In measurements of photocurrent against temperature at a constant level of illumination i.e. a constant rate of excitation of carriers, a variation of either carrier lifetime or mobility with temperature will be seen as a corresponding change in current. Measurements of this type were made after crystals had been subjected to different cooling treatments as for the T.S.C. runs. Monochromatic illumination of approximately band gap energy (0.69 μ) was used to excite the photocurrent.

It was found that an increase in the temperature at which

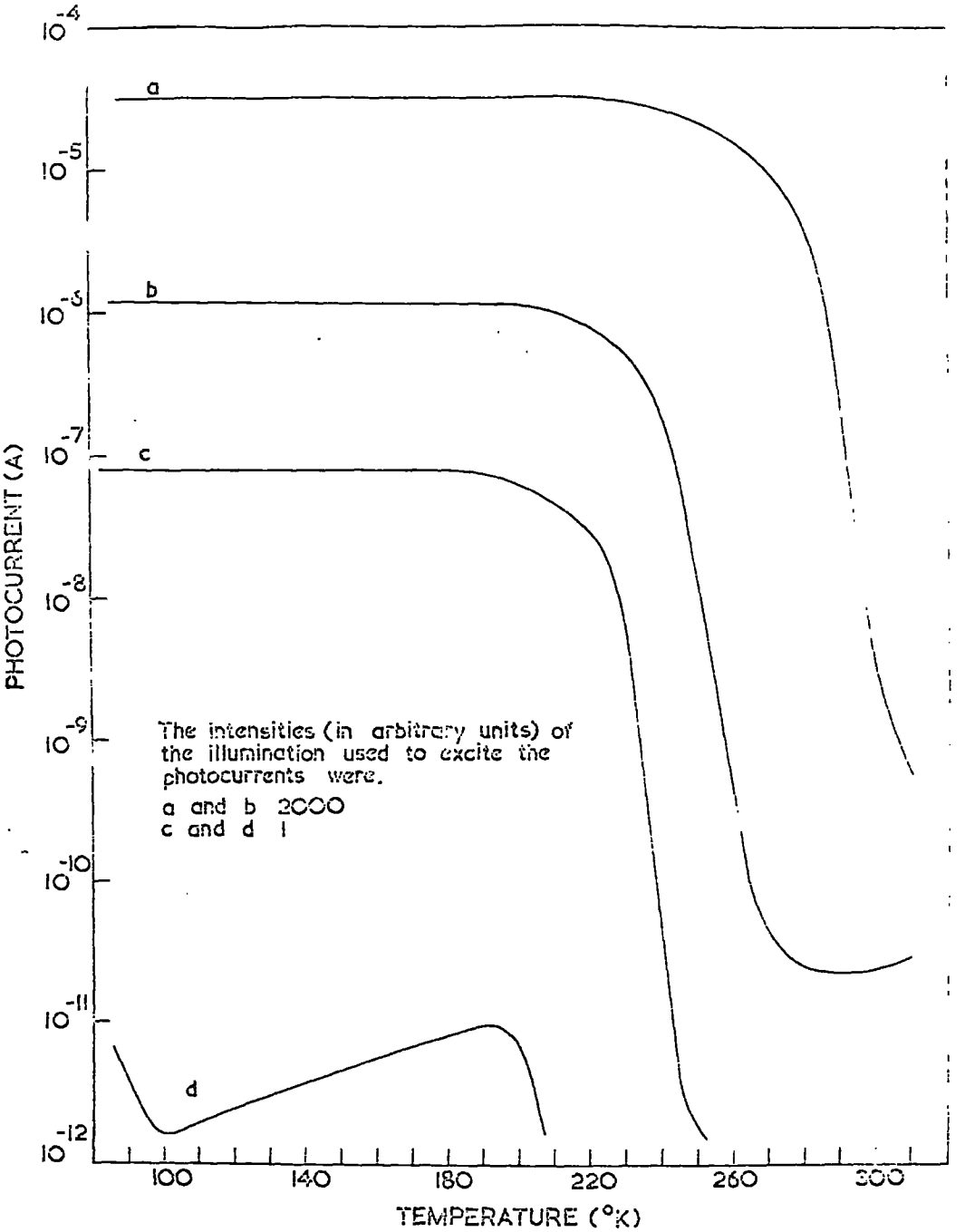

FIGURE 6.5.1. Photocurrent against temperature measurements obtained after cooling in the dark (curves a and c) and after cooling from 400 °K under continuous illumination (curves b and d)

irradiation was started during cooling resulted in a decrease in the magnitude of the photocurrent subsequently measured. This is illustrated in figure 6.5.1. Curves (a) and (c) were obtained after cooling in the dark and curves (b) and (d) after cooling from 400°K under illumination. The observed decrease in photocurrent was greatest at low excitation intensities. There are nearly 4 orders of magnitude difference between the current levels of curves (c) and (d). These were similar to the T.S.C. magnitudes measured after corresponding cooling treatments. This difference is too large to be associated with a change in mobility and therefore must be attributed to a decrease in carrier lifetime. Thus the fall in the heights of the low temperature T.S.C. peaks, which occurs as a result of cooling from progressively higher temperatures under illumination, is due to a reduction in carrier lifetime caused by the illumination at the higher temperatures. This phenomenon is discussed further in Chapter 11, where it will be shown that the reduction in lifetime is associated with the photochemical creation of fast recombination centres.

The behaviour of the intermediate and high temperature T.S.C. peaks with changes in the cooling treatment cannot be accounted for by lifetime variations.

Measurements of photocurrent against temperature given in curves (c) and (d) of figure 6.5.1 show a thermal quenching threshold at about 200°K. There is a subsequent decrease in

lifetime of about 6 orders of magnitude in the temperature range 200°K to 280°K. This accounts for the sharp collapse of thermally stimulated currents in this range. The manifestation of thermal quenching indicates the existence of sensitising centres in the as grown crystals.

6.6 Crystals treated after growth

As stated in section 4.5 crystals with low resistivity as grown could be made more insulating by annealing them in selenium vapour. T.S.C. curves for such a crystal are shown in figure 6.6.1. A broad distribution of low temperature peaks was observed. Photocurrent measurements showed that, as with as grown crystals, the fall in the magnitude of these peaks when illumination was started at progressively higher temperatures during cooling was due to a decrease in lifetime. A small peak, which was essentially unaffected by the cooling schedule used, was also found at 240°K.

Some initially low resistance crystals were also doped with copper (as described in section 4.6) which increased their resistivity to about $10^6 \Omega$ cm at room temperature. T.S.C. measurements made on a crystal treated in this way are shown in figure 6.6.2. Again a distribution of low temperature peaks was observed. Also an intermediate temperature peak appeared at 230°K after cooling schedules similar to those which led to the appearance of that peak in the T.S.C. spectra of as grown crystals.

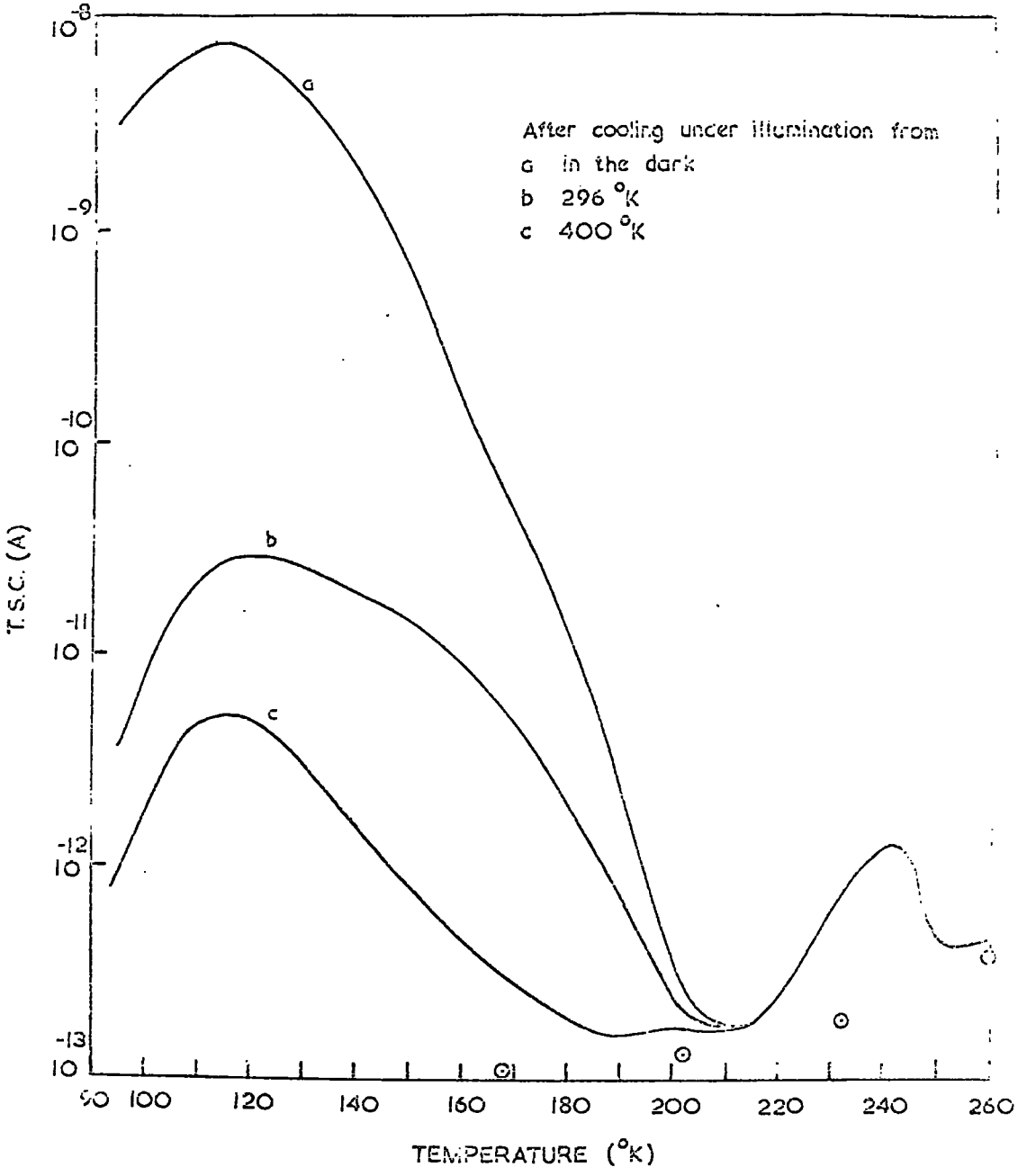

FIGURE 6.6.1. T.S.C. measurements obtained from a crystal annealed in selenium vapour. Dark current values are denoted by ⊙.

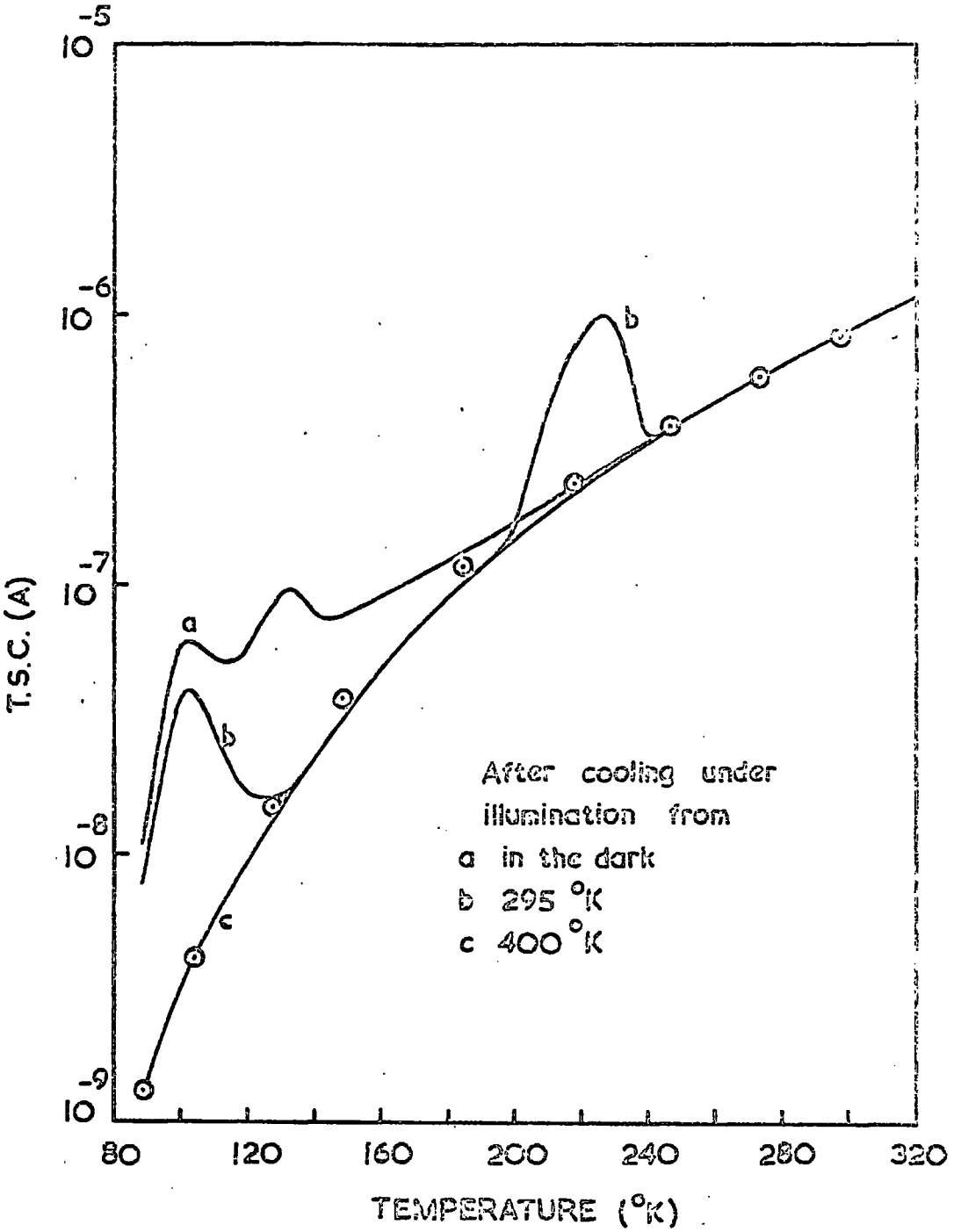

FIGURE 6.6.2. T.S.C. measurements obtained from a copper doped crystal. Dark current values are denoted by ⊙.

6.7 Surface effects

Photo-induced absorption and desorption of oxygen on the surface of II-VI compounds is well known. Williams (1962), Bube (1963) and Mark (1964) have studied the effect in CdS; Bube (1957) and Somorjai (1963) in CdSe; and Kabayashi and Kawaji (1956) in ZnS. Both Bube and Mark reported an increase in trap density in CdS due to oxygen desorption and Mark attributed an observed increase in carrier lifetime to such desorption. In order to try to establish whether any of the traps found from T.S.C. measurements were associated with such surface effects, T.S.C. measurements were made using an improved vacuum in the cryostat. A pressure of 2×10^{-5} torr was achieved using an oil diffusion pump and cold trap. However the T.S.C. spectra obtained with this high vacuum were not significantly different from those found with pressures of 2×10^{-1} torr. Before being able to conclude definitely that none of the traps are surface states affected by the ambient atmosphere measurements made under better still vacuum are required.

An argument against the decrease in lifetime, discussed in section 6.5, being connected with photo-assisted surface effects is that Bube (1957) showed that illumination of CdSe at high temperatures (about $100^{\circ}C$) tends to desorb oxygen, not absorb it. According to Mark's work this would lead to an increase in lifetime, not a decrease as was observed.

6.8 Thermally stimulated thermo electric power (T.E.P.) measurements

From ordinary T.S.C. measurements it is impossible to tell whether the peaks obtained are due to electron traps emptying into the conduction band or hole traps emptying into the valence band. A method was therefore required to try to establish which process was responsible for the various T.S.C. peaks described in section 6.2. The two standard techniques for differentiating between n type and p type behaviour in conducting materials require the measurement of the Hall coefficient or the thermo electric power. The Hall effect method was not used for two reasons (1) the flow crystals being studied were not of a suitable shape or size (2) Hall measurements on high impedance crystals are difficult to make.

The technique used was to measure the thermo emf. developed across a crystal as the various traps were emptied by heating the crystal. To do this it was necessary to establish a temperature gradient along the crystal. This was achieved by mounting the crystal on one end as shown in figure 6.8.1, the crystal being at an angle of about 45° to the cryostat block so that it could still be illuminated.

Emf's. developed were in the range 5 to 20 mv and were measured with a Vibron electrometer. Difficulty was experienced in making measurements when the crystal impedance was greater than about $10^{9}\Omega$. For these high impedances, large

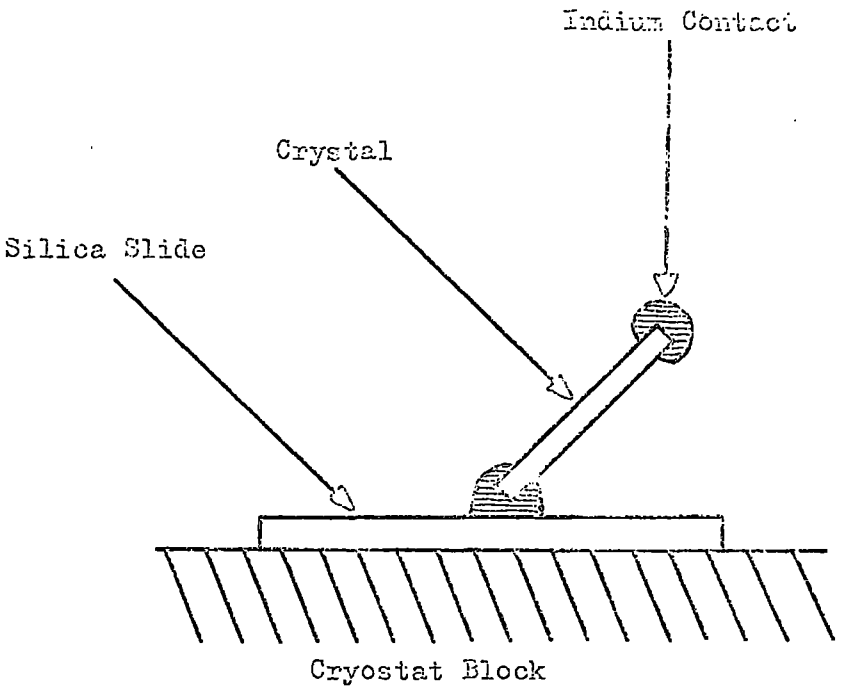

FIGURE 6.8.1 Method of mounting crystal for thermally stimulated T.E.P. measurements.

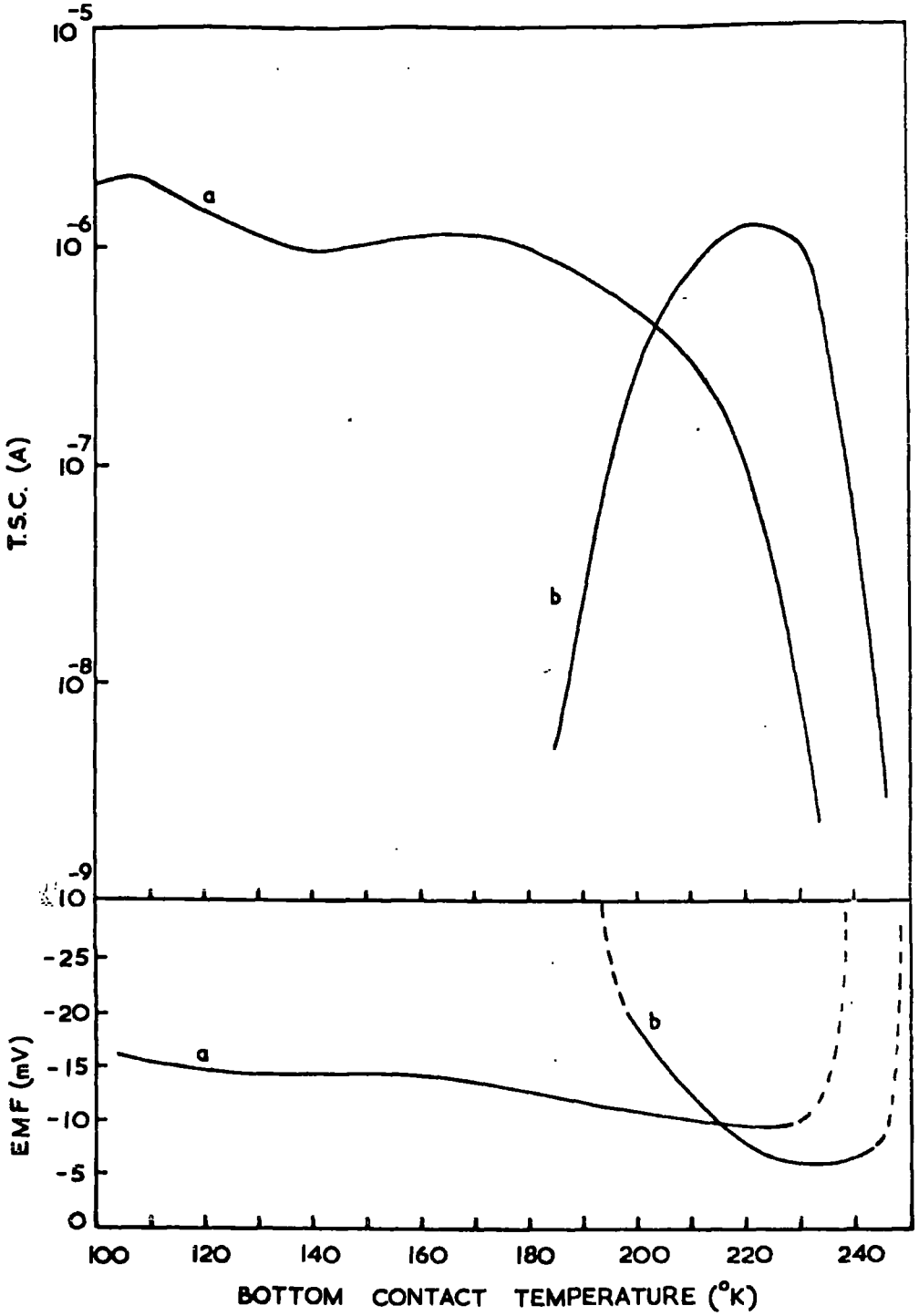

FIGURE 6.8.2. Thermally stimulated currents and the corresponding thermally stimulated e.m.fs. after (a) cooling in the dark (b) cooling from 273 °K under continuous illumination. The dashed lines signify large e.m.fs. associated with polarisation voltages.

voltages, of the order of 1 volt, were developed across the crystals. These voltages were not reproducible from one run to another. They were assumed to be due to some form of polarisation effect. In order to make satisfactory thermally stimulated T.E.P. measurements the corresponding T.S.C. had to be greater than 10^{-8}A. As a result T.E.P. measurements could not be made for the high temperature peaks or for the intrinsic crystals.

Some results for a typical crystal are given in figure 6.8.2. The separation of the contacts for this particular crystal was 2 mm. With a bottom contact temperature of 87°K the top contact was at a temperature of 118°K i.e. there was a temperature gradient of 15°K/mm along the crystal. It was found that when both the low and intermediate temperature traps were emptying the T.E.P. produced was negative. It follows, therefore, that these are electron traps.

The temperature monitored during the runs was that of the bottom contact. As this temperature approached room temperature the gradient along the crystal would gradually decrease. No measurements were made of this variation in gradient. Its effect would be to modify the observed emf. by superimposing a gradual fall in magnitude on the variations due to trap emptying.

6.9 4 probe measurements

Thermally stimulated conductivity measurements were made

using a 4 probe contact arrangement to check whether the contacts exhibited ohmic behaviour during T.S.C. runs. In addition to the usual two end current contacts there were two voltage probes equally spaced from each end of the crystal. All contacts were made in the normal way with indium. During standard T.S.C. runs the potential appearing across the voltage probes was monitored as well as the thermally stimulated current. The voltage was measured with a high input impedance (about $10^{14}\Omega$) voltmeter, type Sweeney ETVM model 1170. However some leakage resistance in the circuit meant that for crystal impedances greater than about $10^{10}\Omega$ the voltage was partially shorted out. This limited measurements to T.S.C. values greater than 10^{-9} A.

Figure 6.9.1 shows some 4 probe measurements made after a crystal had been subjected to cooling schedules that produced substantial low and intermediate temperature peaks. The crystal had a separation between current contacts of 1 cm. The voltage probes were $\frac{1}{2}$ cm apart. The applied potential was 50 volts. It was verified that varying the applied voltage changed the measured voltage correspondingly. The measured voltage was constant, at about 25 V, over the temperature range in which the low temperature traps were emptying. This is as would be expected for ohmic contacts and a uniform crystal.

When the intermediate traps were emptying, however, the

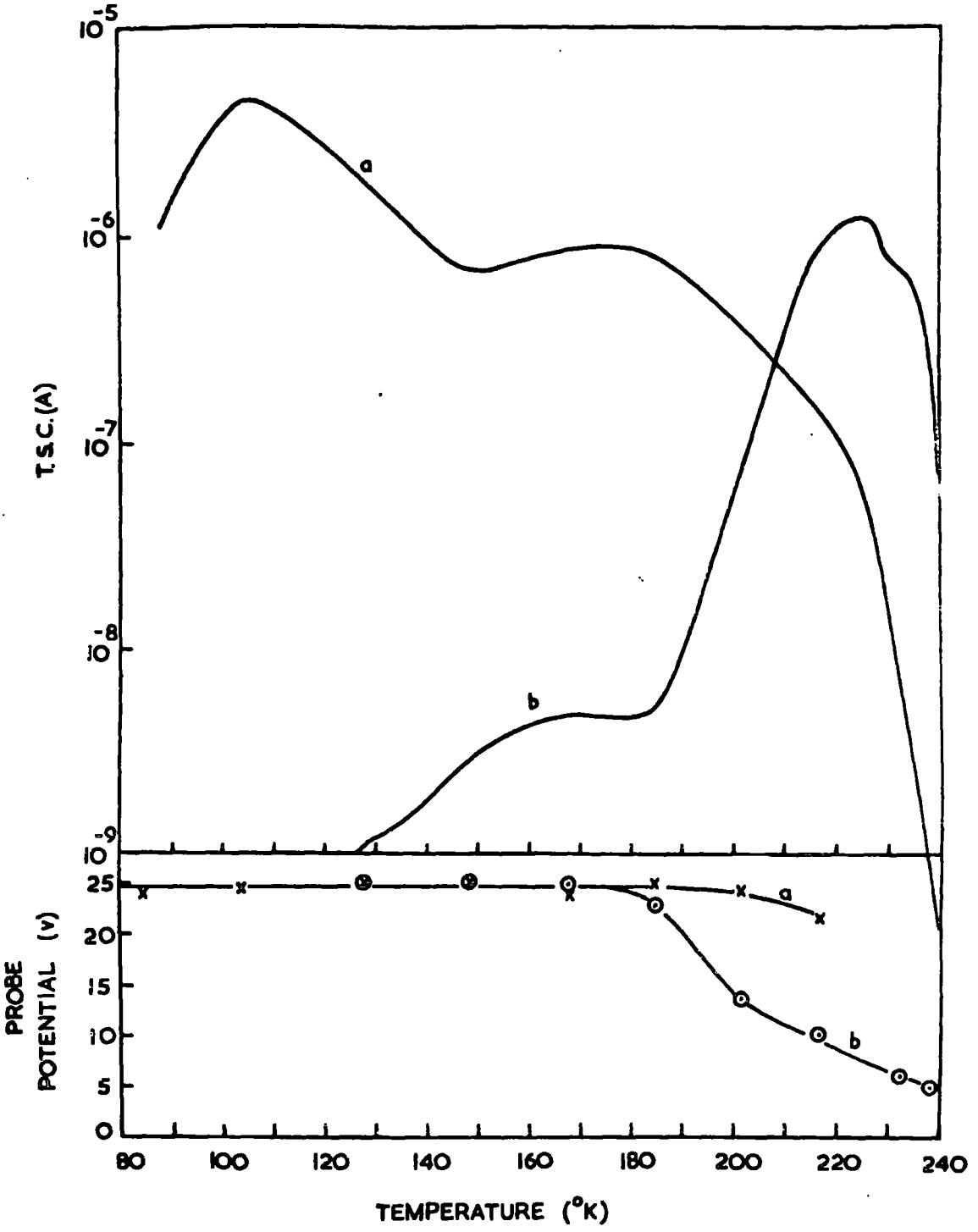

FIGURE 6.9.1. Thermally stimulated currents and the corresponding potential between the voltage probes after a) cooling in the dark b) cooling from 296 °K under continuous illumination.

probe voltage fell. Obviously the crystal in this case was non-ohmic, some of the applied potential must have been dropped across one or both of the end contacts. The traps have been shown to be electron traps (ref. 6.8). When empty they are therefore more positively charged than when full. The observed behaviour can thus be explained if, as the traps empty, positive potential barriers are formed at the contacts. This peculiar effect is discussed again in Chapter 8 when the nature of the intermediate temperature traps is examined in more detail. However one obvious result of the change in the potential appearing between the voltage probes is that strictly a correction should be applied to the T.S.C. curves to obtain their true magnitude.

6.10 Summary

In this chapter measurements of thermally stimulated currents and associated effects have been presented. The following three chapters are concerned with an analysis of the various T.S.C. peaks obtained and a discussion of the nature of the traps present in the crystals.

References

Bube, R.H., 1957, J. Chem. Phys., 27, 496.

Bube, R.H., 1963, J. Appl. Phys., 34, 3309.

Bube, R.H., et. al., 1966, J. Appl. Phys., 37, 21.

Cowell, T.A.T., and Woods, J., 1967, Phys. Stat. Sol., 24, K37.

Mark, P., 1964, J. Phys. Chem. Solids, 25, 911.

Kabayashi, A., and Kawaji, S., 1956, J. Chem. Phys., 24, 907.

Korsunskaya, N.E., et al., 1966, Phys. Stat. Sol., 13, 25.

Somorjai, G.A., 1963, J. Phys. Chem. Solids, 24, 175.

Williams, R., 1962, J. Phys. Chem. Solids, 23, 1057.

Woods, J., and Nicholas, K.H., 1964, Brit. J. Appl. Phys., 15, 1361.

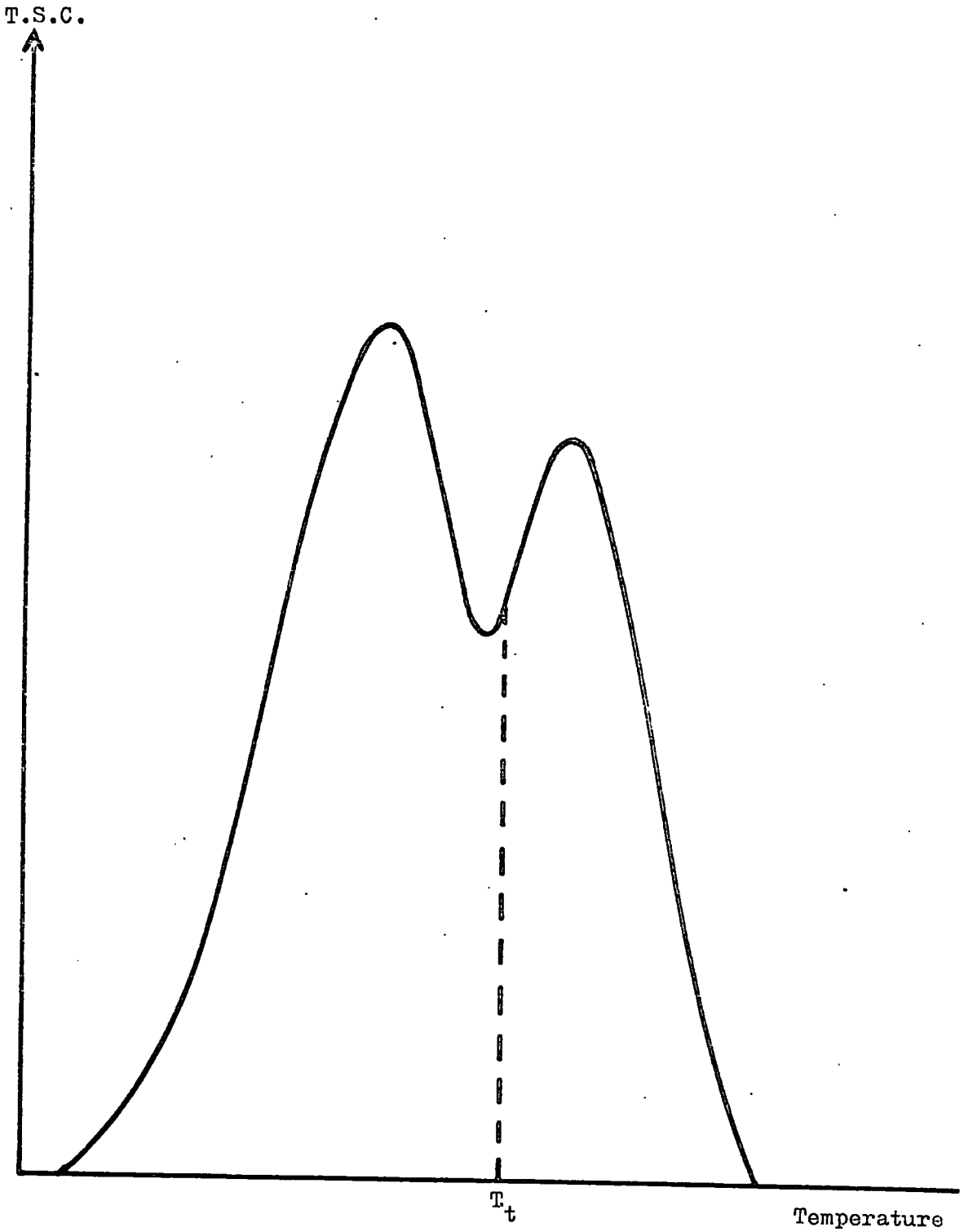

Figure 7.1.1 Thermal cleaning.

CHAPTER 7

Low temperature traps

7.1 Thermal cleaning

The low temperature traps, which emptied at temperatures up to about 210°K, gave closely spaced, overlapping T.S.C. peaks. Consequently the observed curve had broad composite peaks. Individual peaks or shoulders could only be seen when the magnitude of the peaks was reduced by cooling the crystal from a high temperature under illumination prior to the T.S.C. run (ref. figure 6.2.1 for this behaviour). In this way 7 peaks were found at temperatures (to the nearest 5°K) of 105, 115, 130, 150, 160, 175 and 200°K.

In order to determine accurately the various parameters of a particular trap, the isolated T.S.C. peak due to that trap is required. Overlapping peaks are difficult to analyse. The usual procedure to obtain separate peaks from a composite curve employs the technique of thermal cleaning (ref. figure 7.1.1).

Initially, during a T.S.C. run, the crystal is heated up to a temperature T_t in order to empty the traps responsible for the first peak. It is then recooled in the dark. On reheating in the dark the isolated second peak is obtained. This can be subtracted from the composite curve to give the first peak. Several overlapping peaks can be isolated successively in this way provided that the amount of overlap is not too great. If there is a large degree of overlap then on

the initial heating to T_t a large number of carriers are released from the traps associated with the second peak. Upon subsequent cooling and reheating a much reduced second peak is obtained. Thus the contribution of this peak to the composite curve cannot be obtained accurately and the thermal cleaning technique is not successful.

Thermal cleaning was used in an attempt to isolate the low temperature peaks in the T.S.C. curves obtained after various cooling schedules.

(1) Figure 7.1.2 shows a set of cleaned curves obtained after cooling a crystal in the dark. It was found impossible to isolate the individual peaks completely because of their high degree of overlap. However the Garlick and Gibson method of trap depth analysis (ref. section 3.3) could be applied to the rising sides of the cleaned curves. Plots of ln I against 1/T for these curves are shown in figure 7.1.3. Trap depth energies derived from the slopes of the resulting straight lines are given in table 7.1.

These energy values only give an approximate indication of the range of the depths of the traps as the cleaned curves could not be ascribed to any particular peaks.

(2) The resolution of the peaks increased as the T.S.C. magnitude fell with increasing temperature at the start of illumination during the cooling prior to the T.S.C. run. However it was not possible to reduce the amount of overlap of

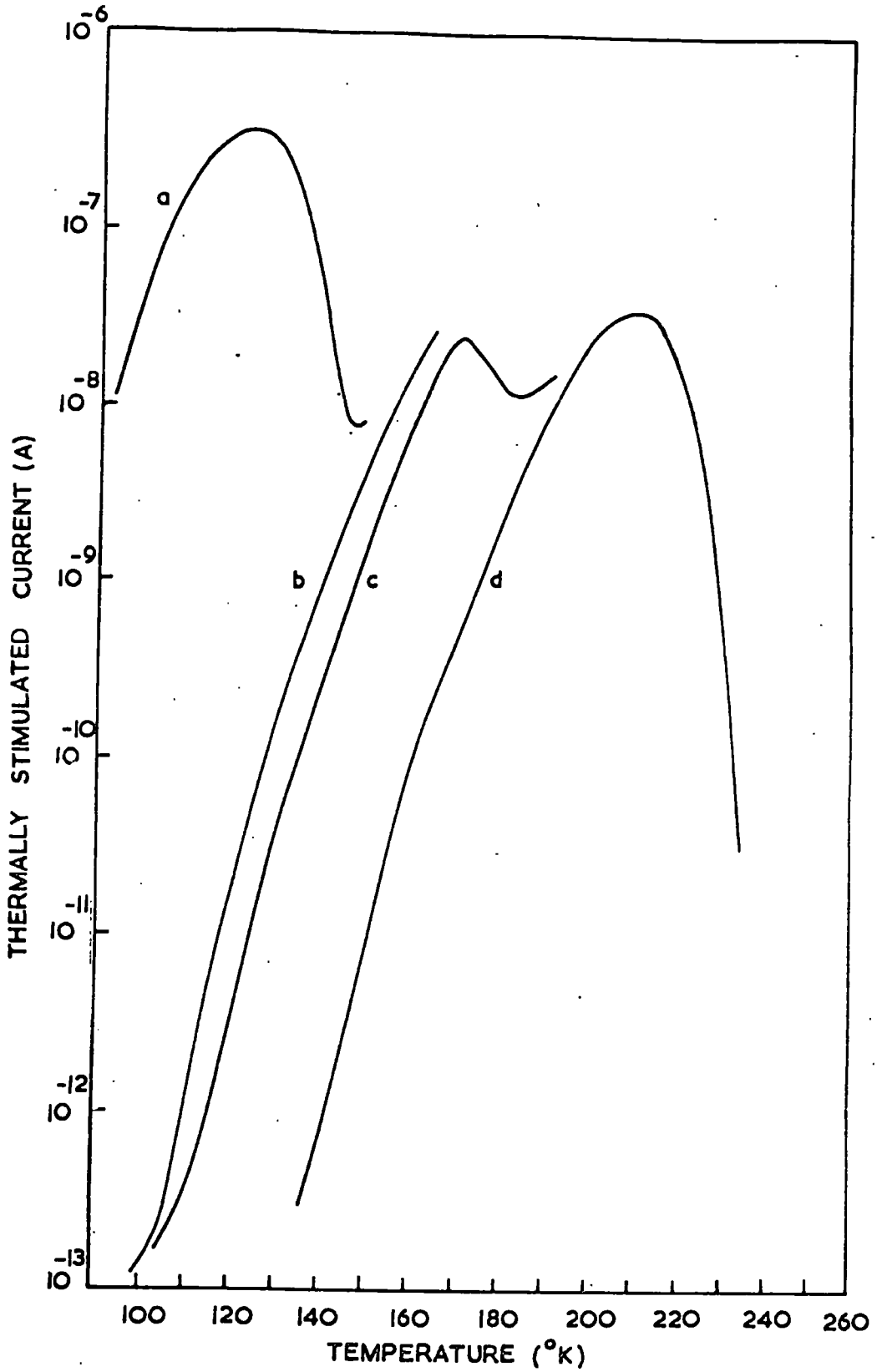

FIGURE 7.1.2. Thermally cleaned low temperature peaks.

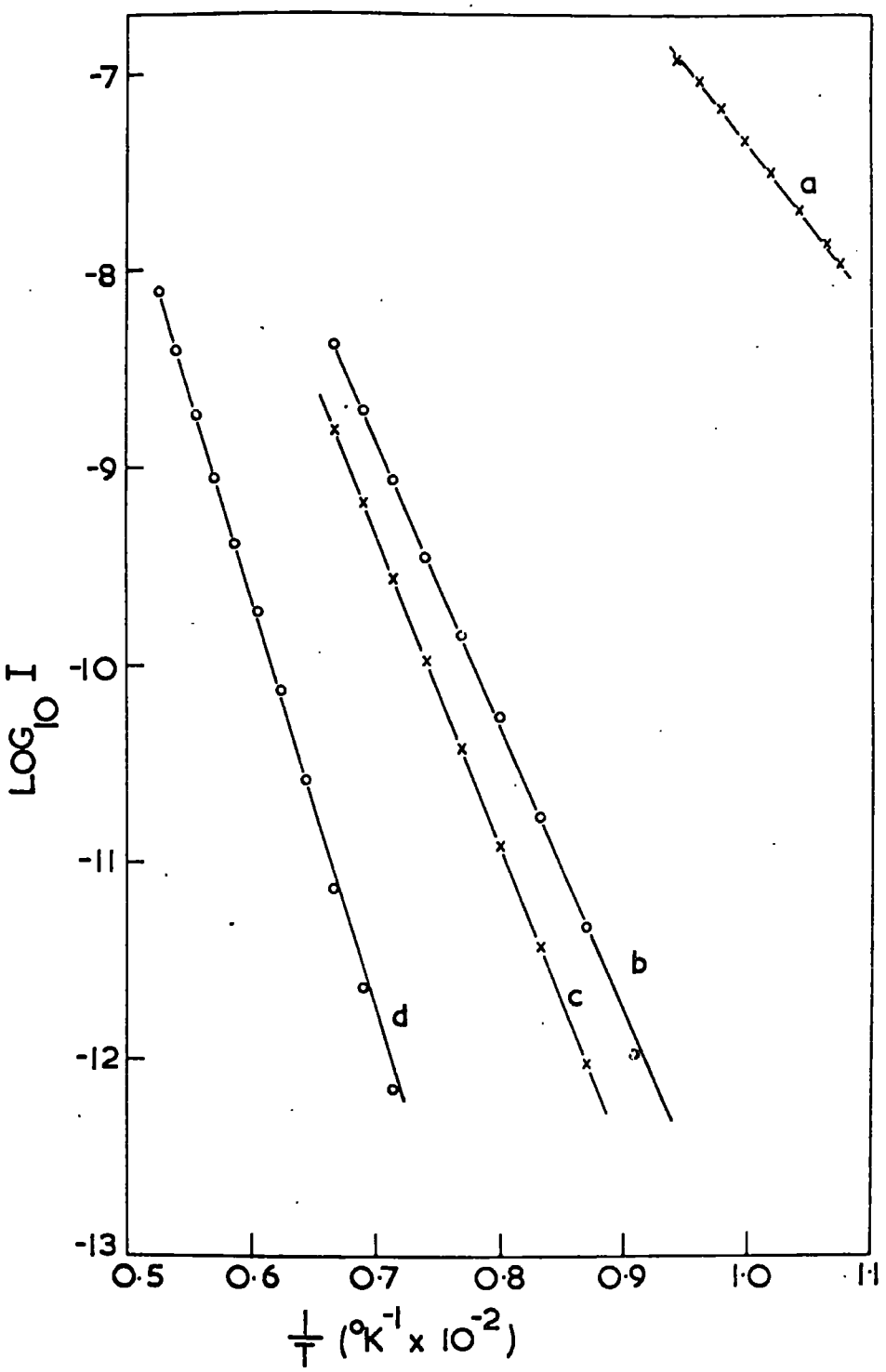

FIGURE 7.1.3. Application of the Garlick and Gibson technique to the cleaned curves of figure 7.1.2.

Table 7.1. Results of Garlick and Gibson analysis of cleaned curves.

Curve	Temperature (^{o}K) to which thermal cleaning carried out prior to obtaining particular curve	Trap depth (ev)
a	—	0.16
b	149	0.29
c	164	0.31
d	192	0.41

Table 7.2. Fermi level analysis of low temperature traps.

Nominal peak temperature	105°K		115°K		130°K		150°K	
Curve (in fig. 6.2.1)	T(°K)	E(ev)	T(°K)	E(ev)	T(°K)	E(ev)	T(°K)	E(ev)
a					126	0.19		
b			122	0.19			154	0.28
c			115	0.23			151	0.35
d	107	0.26	114	0.28*	128	0.32*	151	0.38*
e			116	0.30				

Nominal peak temperature	160°K		175°K		200°K	
Curve (in fig. 6.2.1)	T(°K)	E(ev)	T(°K)	E(ev)	T(°K)	E(ev)
a	160	0.29*	173	0.30	209	0.36
b	163	0.30	172	0.31	204	0.36
c	161	0.38			200	0.43*
d	162	0.39			198	0.45
e					196	0.52

the peaks sufficiently to permit their successful isolation.

7.2 Fermi level analysis

According to Bube (1955), as discussed in section 3.5, a calculation of the Fermi level corresponding to a T.S.C. curve maximum gives the trap depth associated with the peak if the trap empties with appreciable retrapping. This method of analysis was applied to the various peaks and shoulders found in the curves shown in figure 6.2.1. Table 7.2 records the results of this analysis.

The trap depths given in table 7.2 are subject to a possible maximum error of -0.01 ev because the overlap affects peak positions and heights to a certain extent. This applies especially to values marked * which were calculated from shoulders in the curves, and to the maxima in curves (a) and (b) at 126°K and 122°K. However it can be seen that a spread of values was obtained for the depth of any particular trap as calculated from the different curves. This suggests that the Fermi level type of analysis is not valid when applied to the low temperature traps, which implies that the traps do not empty under fast retrapping conditions. However the behaviour of these centres cannot be explained so simply as will be shown in the following section.

7.3 Decay of T.S.C.

In section 3.8 a constant temperature method of T.S.C. analysis (Haine and Carley Read, 1968) was described. This

technique was used to obtain information about the traps associated with the 105°K peak. After cooling a crystal in the dark and then illuminating it for 10 minutes to fill the traps it was placed in the dark and held at 90°K while the decay of the T.S.C. with time was monitored. A typical decay is shown in figure 7.3.1 in the form of a plot of ln current vs time.

It is first necessary to ascertain whether the observed decay of current is associated with the slow thermal emptying of shallow traps or some other process. Warschauer and Reynolds (1960), Litton and Reynolds (1962) and Kulp, Gale and Schulze (1965) have observed the phenomenon of "stored" conductivity in some CdS crystals. After being cooled to 77°K, exposed to light and then put in the dark, these CdS crystals exhibited a conductivity up to 10 orders of magnitude greater than the intrinsic dark value. This high conductivity persisted at a constant level for periods of at least 66 hours. These crystals also emitted green "tap" luminescence when knocked with a hard object. Although the maximum current in figure 7.3.1 is about 7 orders of magnitude greater than the intrinsic level, the decay of the current is not consistent with it being associated with "stored" conductivity. Further evidence that the measured current was the result of the emptying of shallow traps comes from a consideration of the T.S.C. curve measured after the 2 hour decay period. The area

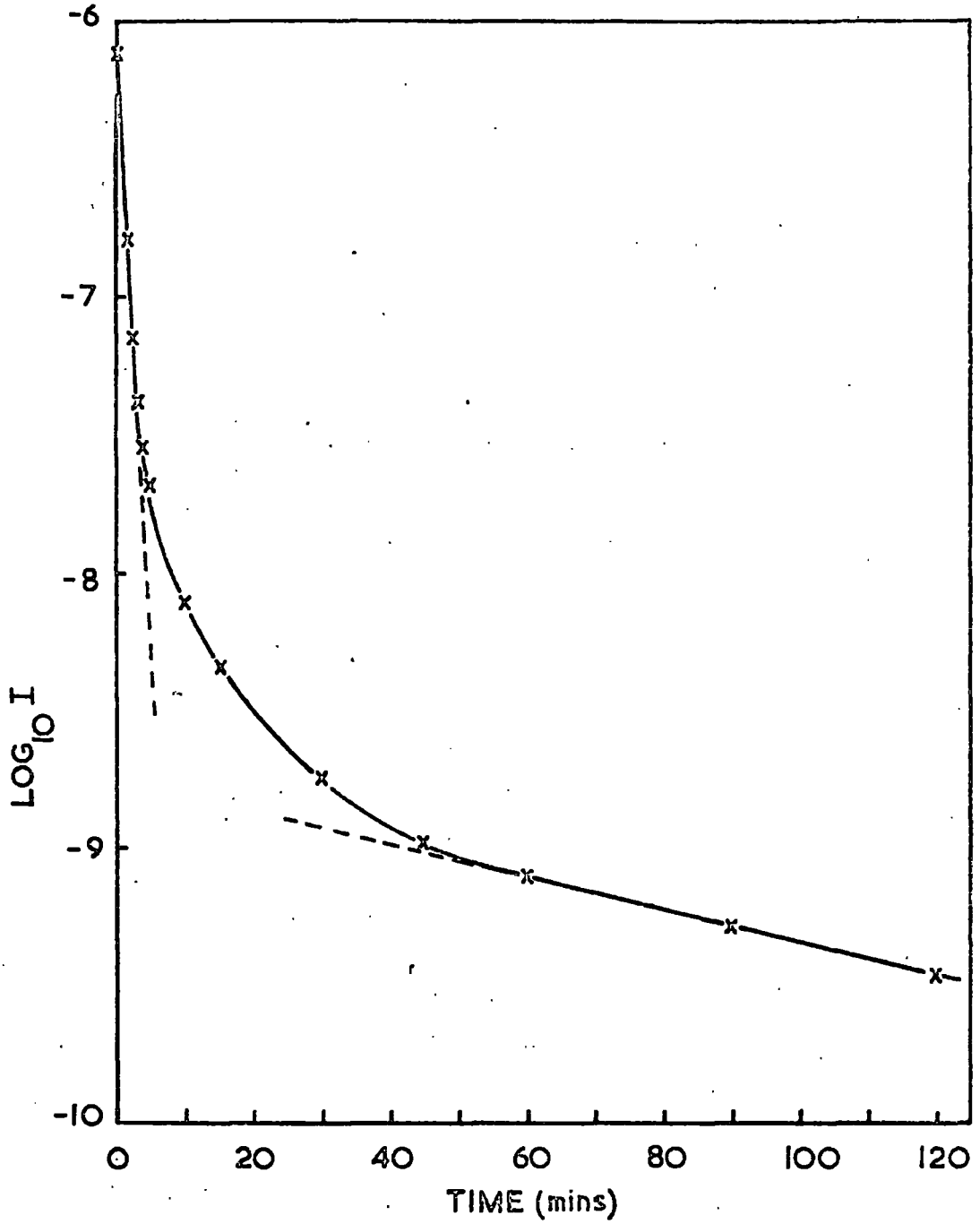

FIGURE 7.3.1. Decay of T.S.C. at 90°K associated with 105°K trap. The dashed lines are projections of the linear regions.

Table 7.3. Parameters associated with 105°K peak.

Parameter	Value
Trap depth	0.15 ev
Density of traps	2.5×10^{14} cm^{-3}
Capture cross section	4.0×10^{-18} cm^{2}
Trapping time	0.069 m secs
Free electron lifetime	5.2 m secs

under this curve, subtracted from the area under the T.S.C. curve obtained with no prior decay, shows that approximately 10^{10} electrons were freed from shallow traps during the decay. Integration of the area under the curve in figure 7.3.1, plus a knowledge of the photoconductive gain (about 10^4), indicates that the release of 10^{10}electrons completely accounts for the measured current.

The T.S.C. measurements showed that electrons were freed predominantly from the 105°K traps although it was estimated that perhaps 10% of the released electrons originated from the 115 and 130°K traps. It is therefore concluded that the decay of T.S.C. at 90°K can essentially be analysed in terms of the thermal freeing of electrons from the 105°K traps. The decay of current shown in figure 7.3.1 exhibits two linear regions. This behaviour, in terms of the Haine and Carley Read model, is typical of that for initially full traps emptying under fast retrapping conditions. From the slopes of the linear regions, together with a value of lifetime obtained from photoconductive gain measurements, the various trapping parameters associated with the 105°K peak were calculated. These are given in table 7.3.

The trapping time is about 2 orders of magnitude smaller than the free electron lifetime. This justifies the previous assertion that the traps empty with fast retrapping. However this appears to disagree with the conclusion drawn from

the Fermi level analysis in the preceding section.

This enigma can be resolved when the effect of the decrease in carrier lifetime, as evidenced by photocurrent against temperature measurements (section 6.5), is considered. It is suggested that after cooling a crystal in the dark the low temperature traps empty under fast retrapping conditions on subsequent heating. This follows because of the long free electron lifetime compared to the trapping time. However if the crystal is cooled under illumination from progressively higher temperatures the lifetime decreases. Thermally freed electrons then have less chance of being retrapped before they recombine with holes (via the recombination path created as a result of the illumination treatment). Thus there is a progressive change in the behaviour of the traps towards emptying under monomolecular conditions. The results of the Fermi level analysis of trap depth given in table 7.2 are therefore only valid for curve (a).

7.4 Trap densities

The densities of the low temperature traps were calculated utilising the areas under T.S.C. curves as described in section 3.7. The photoconductive gains used in these calculations were obtained from measurements of photocurrent against temperature.

For high resistivity, as grown crystals values of total trap density (assuming the traps to be completely filled)

between 10^{13} and 10^{15} cm^{-3} were found. Assuming equal concentrations for all seven traps, a density of between 10^{12} and 10^{14} cm^{-3} is obtained for any particular trap. This is in good agreement with the value of N_t given in table 7.3.

Total trap densities found in copper doped crystals, of the order of 10^{14} cm^{-3}, were similar to those in as grown crystals. However crystals that had been annealed in selenium vapour contained much larger trap concentrations, values of 10^{17} cm^{-3} being measured.

7.5 Discussion

The determination of the trap depths associated with the seven low temperature T.S.C. peaks was not very satisfactory as no isolated peaks could be obtained. As a result of the analysis of T.S.C. decay using the technique of Haine and Carley Read it is suggested that the Fermi level technique is only valid when applied to T.S.C. curves measured after cooling crystals in the dark. An application of this method (reference the data for curve (a) in table 7.2) gave values of trap depths in the range 0.19 to 0.36 ev. Individual trap depths could not be calculated as seven distinct peaks were not seen in the curves measured after cooling in the dark. The Haine and Carley Read technique yielded a trap depth of 0.15 ev associated with the 105°K peak. Thus it is concluded that the low temperature trapping levels lie in the range 0.15 to 0.36 ev below the conduction band. Application of the Garlick and

Gibson technique to the rising sides of incompletely cleaned peaks gave a spread of trap depths of 0.16 to 0.41 ev (reference table 7.1) which is in good agreement with these results.

It is unfortunate that this determination of trap depth depends on a Fermi level analysis as this is an inherently inaccurate method. This was discussed in section 3.5 where it was mentioned that the minimum error associated with this technique is $-\frac{1}{2}kT^*$. Thus the value of 0.36 ev associated with the upper limit of the distribution of traps is subject to an error of at least -0.01 ev.

The nature of the traps is not known. They could be associated either with native defects or impurities. The starting material for crystal growth was pure to 1 part in 10^5 or better. This is greater than the typical trap contents, which correspond to about 1 part in 10^8. Thus it is quite possible that impurities play a part in trapping effects. However it is perhaps significant that crystals that had been annealed in selenium vapour contained trap concentrations 2 to 3 orders of magnitude greater than found in either as grown crystals or material that had been copper doped. Woodbury and Hall (1966) have studied the self diffusion of selenium in CdSe and concluded that selenium interstitials are the diffusing defects in this process. Thus it is possible that the traps are selenium interstitials, perhaps in association with other

defects or impurities.

The existence of seven closely spaced traps cannot adequately be accounted for. However Curie (1960) in his book "Luminescence in Crystals" advanced an interesting explanation for the existence of a group of discrete trapping levels in zinc sulphide. He suggested that trapped electrons are captured in the field of two centres, one being a sulphur vacancy (A) and the other a luminescent centre due to substitutional copper at a zinc site (B). The various traps are formed by the interaction of A and B at different separations i.e. nearest neighbours in the lattice, next nearest neighbours and so on. In the context of the present work a corresponding model for the low temperature traps could consist of selenium interstitials located at various distances from some other centre.

More recently Faeth (1968) has analysed the trapping spectrum of CdS using an equation of the form

$$E_i = a - (bi - ci^2) \qquad 7.5.1$$

where a, b and c are constants and i is an integer. Using a = 2.406, b = 0.475 and c = 0.0238 ev, and putting i = 0, 1, 2, 3 etc., Faeth derived 10 values of E_i which correspond to the positions of all the imperfection centres found in CdS by various workers. The case of i = 0 was chosen so that E_o corresponded to the band gap of CdS. Further, Faeth pointed out that diatomic molecular spectra are defined

Table 7.4. Application of equation 7.5.2 to low temperature traps.

i	Peak temperature (^{o}K)	E_i (ev)
0	200	0.36
1	175	0.30
2	160	0.25
3	150	0.21
4	130	0.18
5	115	0.16
6	105	0.15

by an equation of similar form to 7.5.1. Of course this may just be a coincidence. However the possibility of interpreting trapping spectra in terms of different excited states of some molecular structure is intriguing. A possible energy level distribution of the 0.15 to 0.36 ev traps observed in CdSe was calculated using the format of 7.5.1. An estimation of the constants required the knowledge of three trap depths. Those used were 0.36 and 0.30 ev derived from the Fermi level analysis and 0.15 ev found using the Haine and Carley Read method. The following equation was derived.

$$E_i = 0.36 - 0.065\ i + 0.005\ i^2 \qquad 7.5.2$$

The values of E_i corresponding to the seven traps are listed in table 7.4.

Thermally stimulated current measurements in CdSe have not been widely reported. However measurements made by Bube (1954) and Bube and Barton (1958) on CdSe crystals displayed fairly featureless distributions in the range 80 to 220°K. Although these authors did not consider that their curves were composed of a large number of peaks it seems likely that they do in fact correspond to the low temperature peaks discussed in this chapter. A predominant peak at about 110°K was sometimes observed by Bube. He assigned a trap depth of 0.15 ev to this peak. This agrees with the value associated with the 105°K peak found in the present work. Shimizu (1965) observed a broad peak between 100 and 250°K in the T.S.C. spectra of

evaporated films of CdSe. He suggested that the films contained a large number of traps with a minimum depth of 0.1 ev.

References

Bube, R.H., 1954, Photoconductivity Conference, Eds. Breckenridge, R.G., Russel, B.R., and Hahn, E.E. (New York: John Wiley), P.575.

Bube, R.H., and Barton, L.A., 1958, J. Chem. Phys., 29, 128.

Curie, D., 1960, Luminescence in Crystals (Methuen), P.165.

Faeth, P.A., 1968, J. Electrochem. Soc., 115, 440.

Kulp, B.A., Gale, K.A., and Schulze, R.G., 1965, Phys. Rev., 140, A252.

Litton, C.W., and Reynolds, D.C., 1962, Phys. Rev., 125, 516.

Shimizu, K., 1965, Japan. J. Appl. Phys., 4, 627.

Warschauer, D.M., and Reynolds, D.C., 1960, J. Phys. Chem. Solids, 13, 251.

Woodbury, H.H., and Hall, R.B., 1966, Phys. Rev. Letters, 17, 1093.

CHAPTER 8

Intermediate temperature traps

8.1 Introduction

Four intermediate temperature traps were found in the as grown crystals. They gave T.S.C. maxima, to within 5°K, at 215, 230, 250 and 270°K. No crystal showed all four peaks. The effect of the cooling schedule on these traps was very pronounced. When the T.S.C. curve obtained after cooling a crystal in the dark was thermally cleaned, to remove the peaks due to the low temperature 0.15 to 0.36 ev traps, small residual peaks were found at 215, 230 or 250°K. However substantial peaks appeared only when illumination was switched on at between 250°K and 275°K during the cooling prior to the measurements (reference figures 6.2.1 and 6.2.2). Continuous illumination during cooling from temperatures greater than 275°K resulted in a decrease in the magnitude of the peaks. Heating at 400°K in the dark led to the disappearance of the traps. This behaviour must be photochemical in nature, involving the creation and destruction of the traps by radiation at different temperatures.

8.2 Effect of thermal quenching

Generally it was not possible to isolate the various peaks by thermal cleaning because of their high degree of overlap. However one crystal examined contained only one intermediate temperature trap, that associated with the 215°K peak. The

low temperature peaks, being two orders of magnitude smaller than this peak, were readily removed from the T.S.C. curve by thermal cleaning. Thus the isolated 215°K peak was obtained and is shown in figure 8.2.1 (the actual temperature at the maximum was 216°K). The dashed curve in figure 8.2.1 is a theoretical curve obtained for a trap depth of 1.7 ev assuming monomolecular emptying. This was the best fit to the experimental curve that could be obtained using the curve fitting procedure described in section 3.6. Table 8.1 summarises the values of trap depth obtained from the 215°K peak using three different methods of analysis.

Measurements of the spectral response of photoconductivity which are described in Chapter 10 show that the band gap of CdSe at 215°K is 1.76 ev (reference figure 10.5.2). Therefore the trap depths listed in table 8.1 are obviously in error. They are much too large to be associated with an electron trap and indeed the value obtained using the Grossweiner technique is greater than the band gap energy.

The fact that sensible values of trap depth could not be obtained from the 215°K peak (and presumably the other peaks if they could have been isolated) suggests that some other mechanism in addition to trap emptying contributed to the experimental curves. The intermediate temperature peaks exhibit unusually steep rising and falling edges. These characteristics can be explained by considering some results

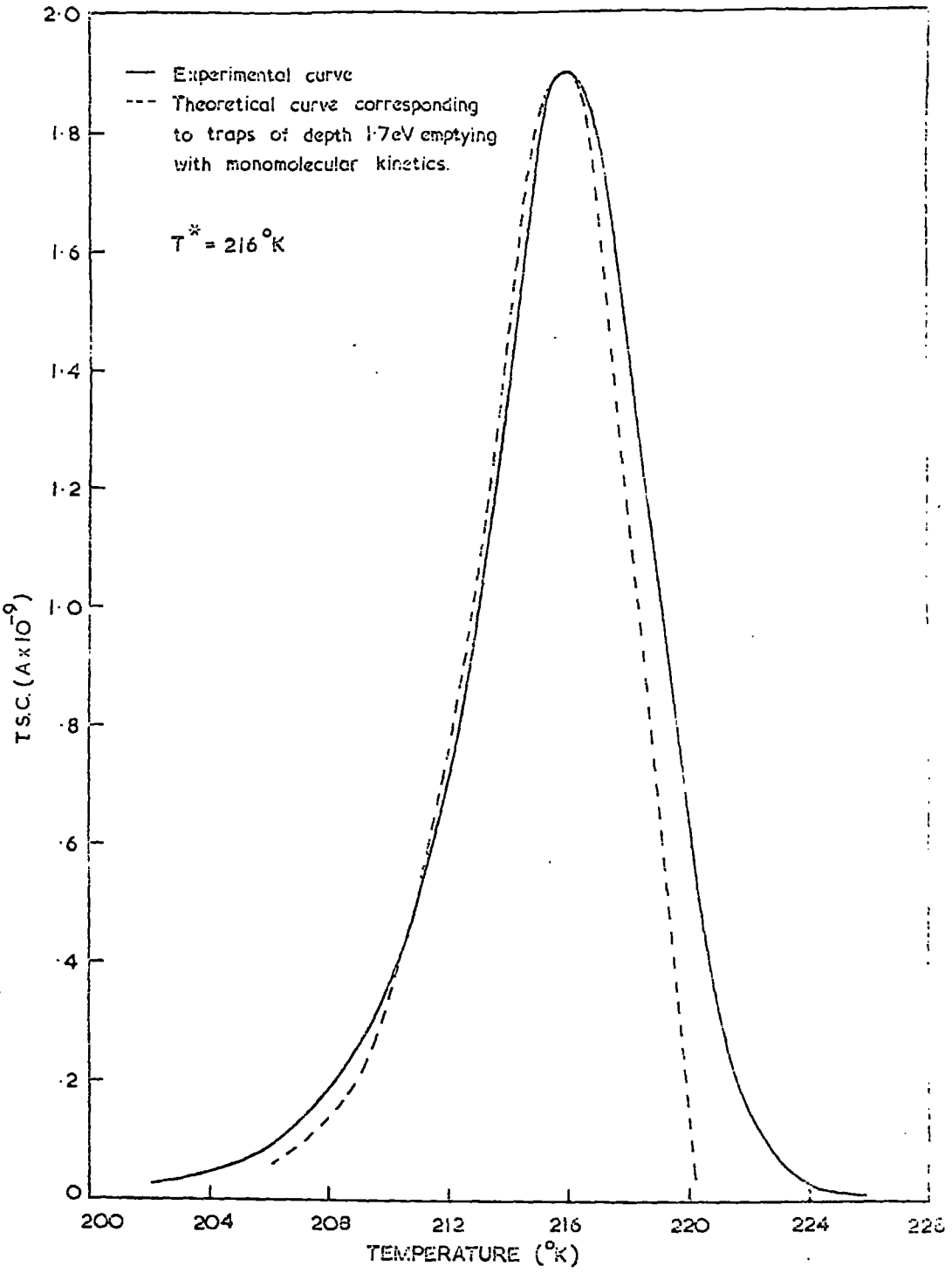

FIGURE 8.2.1. 215 °K intermediate temperature T.S.C. peak.

Table 8.1. Trap depths associated with 215°K peak

Type of analysis	Trap depth (ev)
Grossweiner	2.0
Garlick & Gibson	1.3
Cowell & Woods, curve fitting	1.7

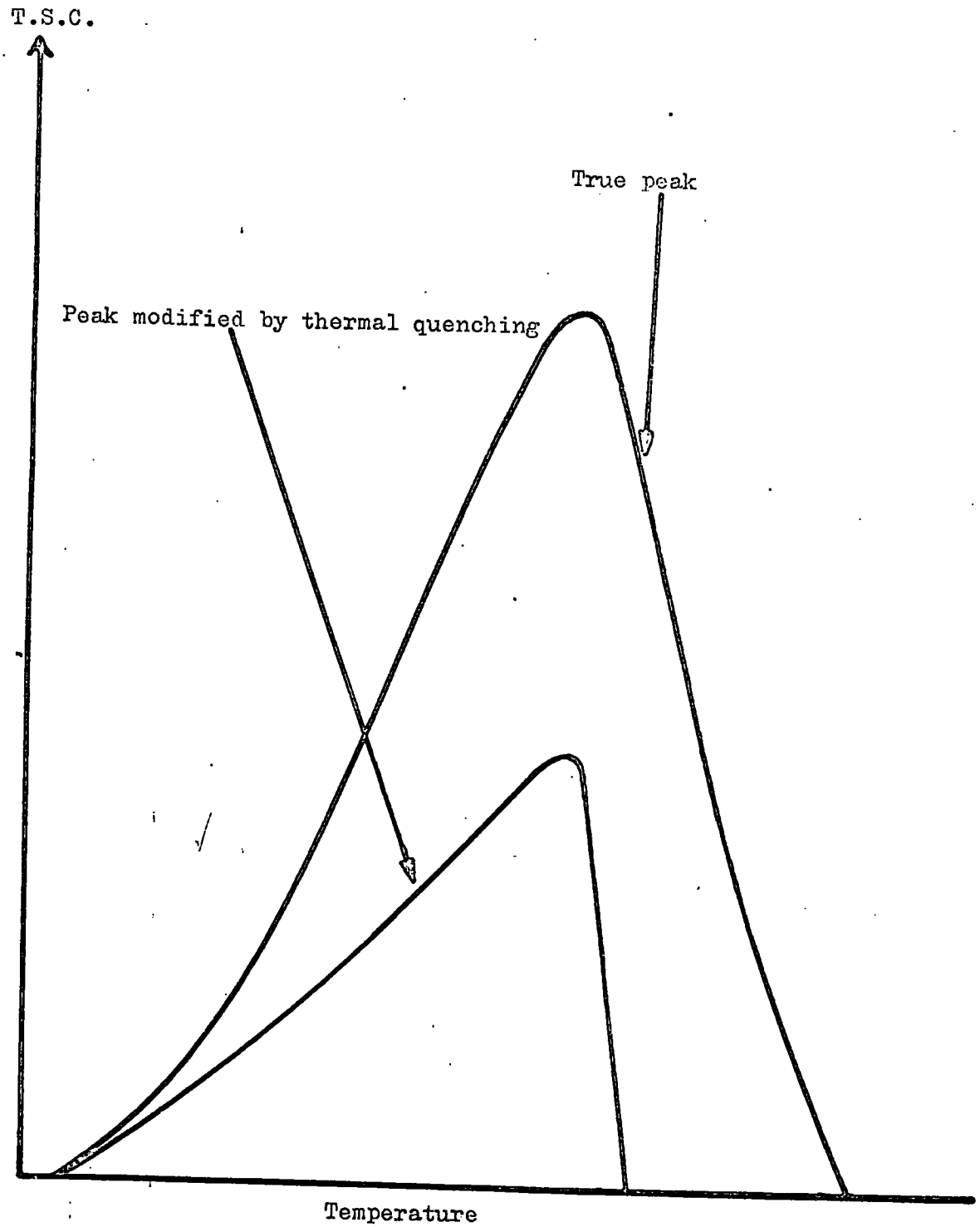

FIGURE 8.2.2 The effect of the decrease in lifetime due to thermal quenching on the shape of a T.S.C. peak.

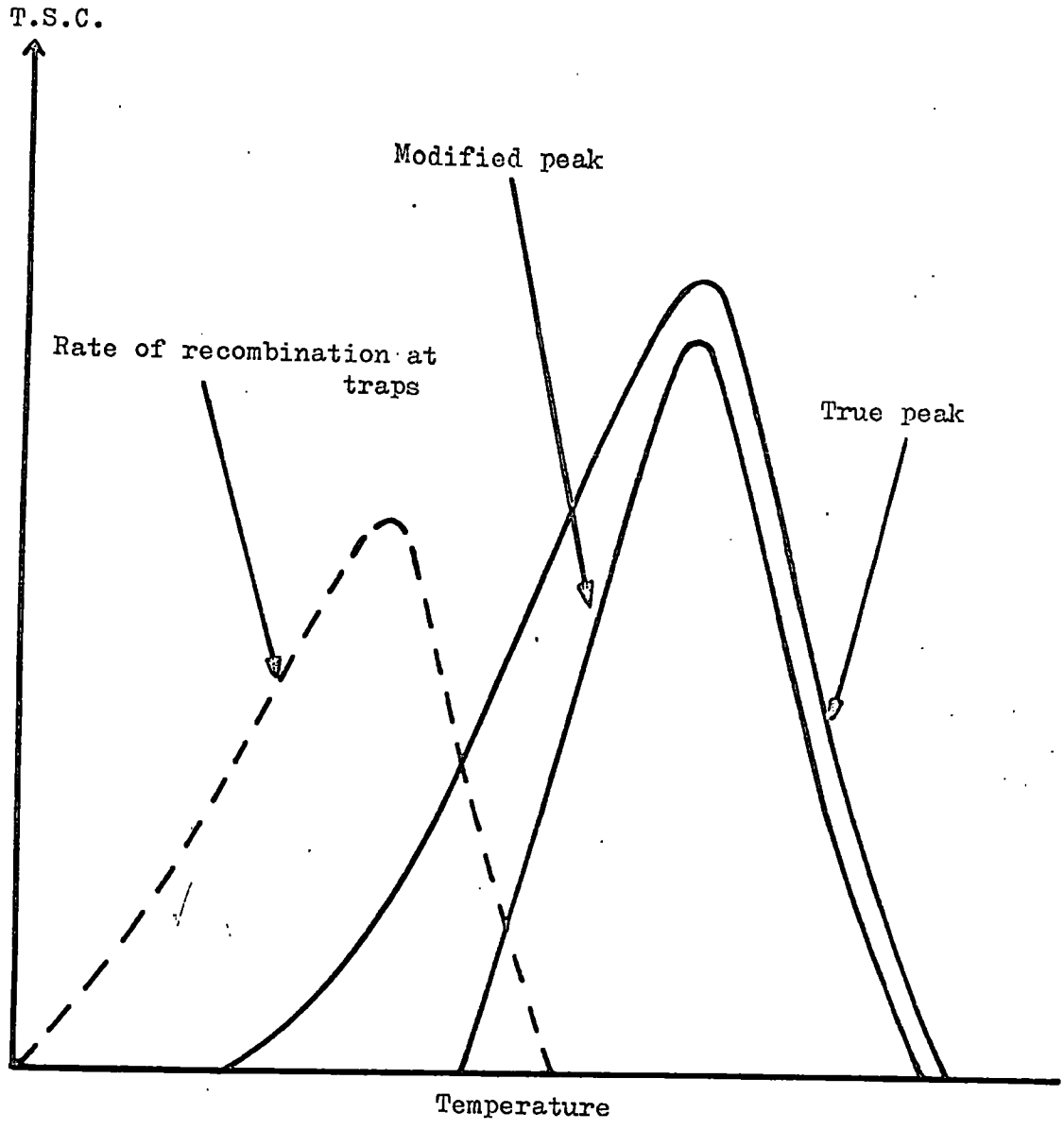

FIGURE 8.2.3 The effect of recombination at trapping centres on the T.S.C. peak shape.

of the photocurrent against temperature measurements described in section 6.5. These measurements demonstrate that thermal quenching occurs between 200 and 280°K for photocurrents of similar magnitude to the thermally stimulated currents. As a result the lifetime falls by six orders of magnitude over the temperature range in which the intermediate temperature traps empty. Thermal quenching is due to the thermal freeing of holes from sensitising centres. It is suggested that two processes, associated with this release of holes, substantially modified the shapes of the T.S.C. peaks.

(1) The effect on a T.S.C. peak of the lifetime decrease due to thermal quenching is illustrated in figure 8.2.2. This mechanism obviously accounts for the steep falling edges of the intermediate temperature peaks. However the effect of this reduction in lifetime on the rising edges should have been to lead to trap depths, as determined by the Garlick and Gibson and curve fitting methods, which were smaller than the true values. In practice these techniques gave high values. Thus simple recombination via class 1 centres between the thermally released electrons and holes cannot alone account for the shape of the experimental curves.

(2) An additional mechanism which would explain the observed steep rising sides of the peaks is that of direct recombination between free holes and trapped electrons. Such recombination would reduce the number of electrons available to be raised to

the conduction band and contribute to the current. The rate of recombination would depend on the number of holes thermally freed from the sensitising centres. The rate of release of these holes is given by

$$\frac{dp_2}{dt} = p_2 \nu_p \exp(-E_2/kT)$$

Figure 8.2.3 demonstrates the effect of recombination via the trapping centres on the shape of the T.S.C. peak.

As an example consider the case of traps emptying under monomolecular kinetics. The thermally stimulated conductivity under such conditions has been given in equation 3.2.5.

$$\sigma = n_{to} \tau_n e \mu_n \nu \exp\left[-(E/kT) - \int_{T_o}^{T} \frac{\gamma}{\beta} \exp(-E/kT)dT\right] \qquad 3.2.5$$

Because of processes (1) and (2) described above n_{to} and τ_n in 3.2.5 are no longer constant but are strongly temperature dependent. 3.2.5 no longer describes the conductivity and therefore conventional methods of T.S.C. analysis cannot be applied.

Therefore no accurate analysis could be carried out to find the trapping parameters, E_t, S_t and N_t, associated with the intermediate temperature peaks.

8.3 Density of traps

Trap densities in the range 10^{15} to 10^{16} cm^{-3} were obtained from estimates of the areas under the intermediate T.S.C. peaks. These values cannot be regarded as accurate because of the variation of lifetime over the span of the peaks.

Table 8.2. Fermi level analysis of intermediate temperature peaks.

T.S.C. peak (^{o}K)	Range of trap depths (ev)
215	0.38 to 0.46
230	0.39 to 0.50
250	0.40 to 0.48
270	0.61 to 0.68

However the value of lifetime used to obtain these trap densities was the maximum value before thermal quenching. The calculation therefore yielded the minimum trap density present in the crystals.

8.4 Fermi level analysis

The Fermi level technique of trap depth analysis is not affected by variations in lifetime. When this method was applied to the various curves obtained after different cooling schedules a spread of trap depths was found for each trap. The ranges of energies in question are listed in table 8.2.

These results demonstrate quite clearly that these particular traps do not empty under fast retrapping conditions.

8.5 Copper doped crystals

T.S.C. measurements made on copper doped crystals were described in section 6.6. The 230°K peak was observed in the spectra of these crystals. The T.S.C. curve obtained after cooling a copper doped crystal from 295°K under illumination is shown in figure 8.5.1. Also shown is the variation of photocurrent with temperature. The lifetime decreased, due to thermal quenching, by about one order of magnitude in the range 230°K to 260°K. As a result, although the falling side of the peak may have been slightly affected by thermal quenching, the peak shape was not modified in the way that the peaks exhibited by as grown crystals were.

The positions of the Fermi levels corresponding to the peak

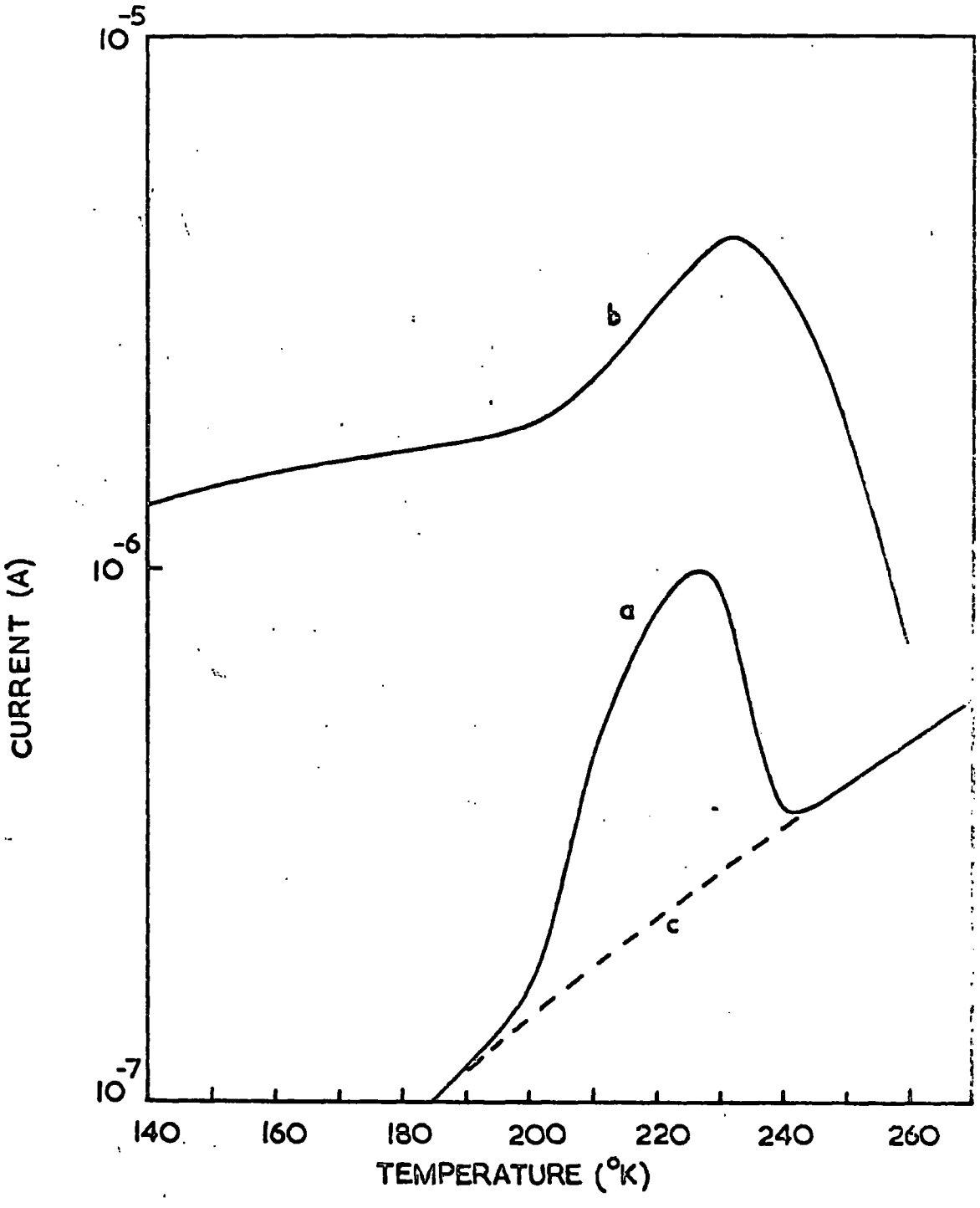

FIGURE 8.5.1. Copper doped crystal a) T.S.C. b) Photocurrent, both measured after cooling the crystal from 295 °K under continuous illumination. The dashed curve c) is the dark current.

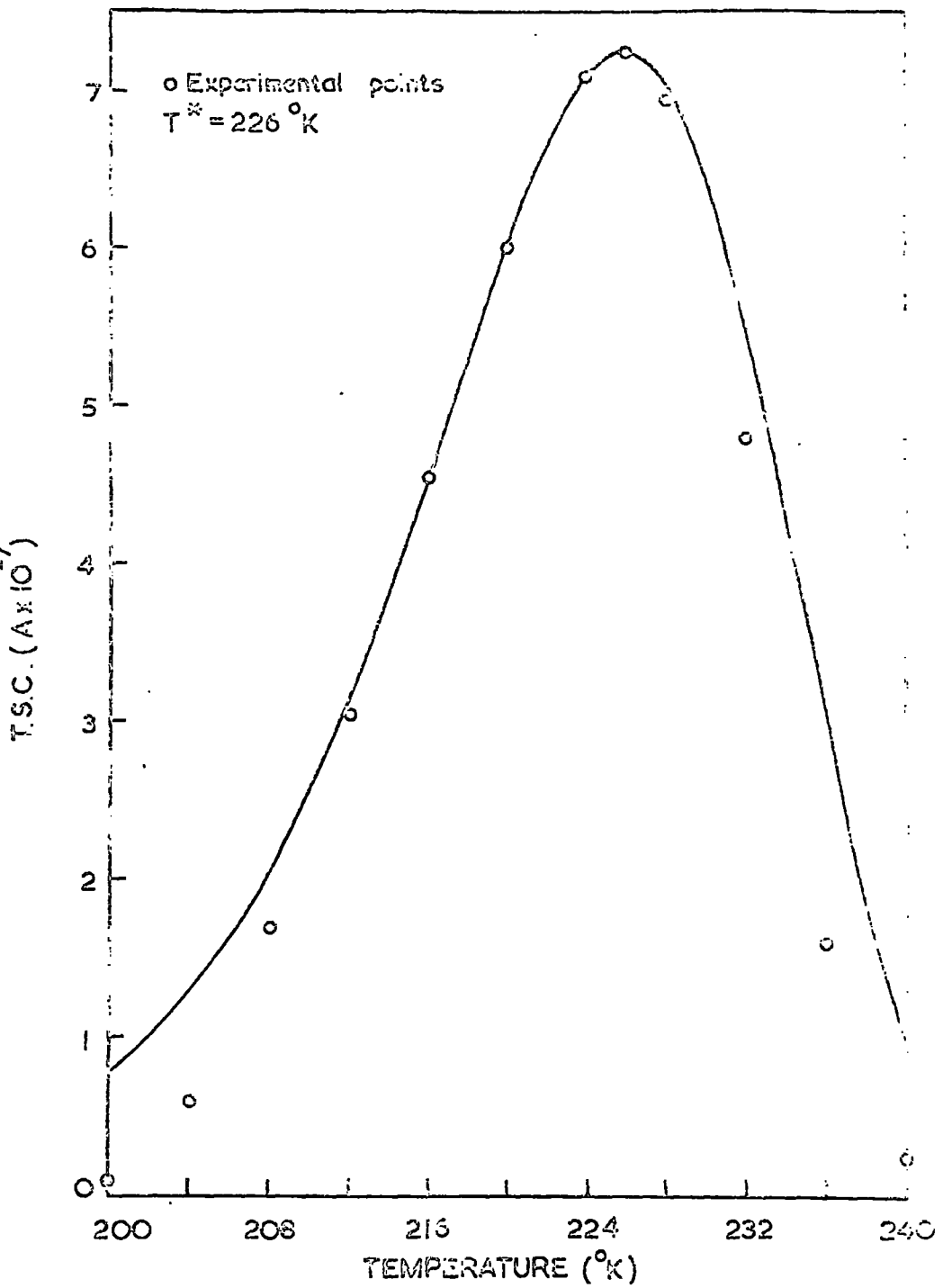

FIGURE 8.5.2. Curve fitting to the 230°K peak obtained from a copper doped crystal. The theoretical curve shown corresponds to the case of fast retrapping and a trap depth of 0·46 eV.

maxima found after cooling crystals under illumination from temperatures in the range 260 to 320°K lie between 0.34 and 0.35 ev. This is sufficiently consistent to suggest that the traps empty with appreciable retrapping. An application of the Grossweiner technique (which is strictly only valid for monomolecular kinetics) to the peak shown in figure 8.5.1 gave values of 0.5 ev for the trap depth and 1.4×10^{-16} cm^2 for the capture cross section. The high value of cross section again indicates that monomolecular kinetics are not applicable. This conclusion is in disagreement with that drawn in section 8.4, namely that the intermediate traps empty without any significant retrapping. However in the as grown crystals emptying of these traps is accompanied by a rapid fall in lifetime due to the freeing of holes from the sensitising centres. Electrons therefore have a restricted opportunity to be retrapped and the traps empty under monomolecular kinetics even though they have such a large capture cross section. In the copper doped crystals thermal quenching was not so severe. The electron lifetime in the region spanned by the 230°K peak is essentially constant as is clearly demonstrated in figure 8.5.1. Thus appreciable retrapping of electrons freed from the 230°K traps in copper doped crystals occurs.

Theoretical curves for a trap emptying with fast retrapping were calculated as described in section 3.6. A perfect fit to the experimental curve could not be obtained,

probably because of the slight effect of thermal quenching on the falling edge of the peak. Thus the best fit to the rising side of the peak was obtained and the result, corresponding to a trap depth of 0.46 ev, is shown in figure 8.5.2 together with the experimental points. These experimental values were obtained by subtracting the dark current from the measured T.S.C. curve shown in figure 8.5.1. An attempt to use the Garlick and Gibson method on the rising side of the peak was unsuccessful because the plot of ln I against 1/T did not yield a good straight line.

There is poor agreement between the values of trap depth derived from calculations of the position of the Fermi level (0.34 to 0.35 ev) and that associated with the theoretical curve (0.46 ev) shown in figure 8.5.2. This is indicative of the unreliability of the Fermi level technique.

Integration of the areas under experimental peaks showed that trap densities (assuming that all the traps were filled) of the order of 10^{15} cm^{-3} were present in these crystals.

8.6 Discussion

T.S.C. peaks at 215°K and 230°K were reported by Bube (1954) for CdSe. Bube and Barton (1958) observed a peak at 250°K. The trap depths associated with these peaks were quoted as 0.43 ev, 0.35 to 0.38 ev and 0.5 ev (in order of increasing peak temperature) and were arrived at using a Fermi level analysis. Comparison of these values with those listed in

table 8.2 shows that there is agreement for the 215°K peak only. However this is not significant as it has been shown, both in this chapter and the preceding one, that indiscriminate use of the Fermi level technique gives misleading results. Even for the case of traps that apparently empty with significant retrapping (reference section 8.5) there is only poor agreement between this method and the more sophisticated curve fitting procedure.

There has been no report in the literature of traps in CdSe being affected by illumination at different temperatures in the same way as the traps discussed in this chapter. The nearest equivalent to this behaviour is that found for the 0.41 and 0.83 ev traps in CdS by Woods and Nicholas (1964). These traps are created photochemically by irradiation in the range 220 to 295°K. However cooling crystals under illumination from higher still temperatures does not destroy these centres.

The fact that the 230°K trap appeared in copper doped crystals is not taken as indicating that this trap is associated with copper impurities. This is because copper, when present in CdSe, acts as an acceptor and produces sensitising centres (Bube, 1957). Under suitable conditions these would behave as hole traps. However the intermediate temperature traps have been shown to be electron traps (reference section 6.8).

Any explanation of the nature of the intermediate

temperature traps must include the unusual behaviour described in section 6.9. Results of 4 probe T.S.C. measurements indicate that a positive potential barrier is formed at the end contacts as the traps empty. The idea of a trap surrounded by a repulsive potential barrier (Bube et al, 1966) would be convenient in explaining this effect. However this model cannot be applied for three reasons.

(1) The traps are electron traps and as such the associated repulsive barriers are negatively charged.

(2) The T.S.C. peak height, for a trap of this nature, would progressively increase with illumination at higher temperatures. It may reach a maximum but it would not decrease.

(3) After cooling a crystal in the dark, followed by illumination at 90^{o}K, repulsive traps would be substantially empty. Therefore the potential barrier at the contacts should be observed in the subsequent T.S.C. measurements at low temperatures. This was not seen in practice.

The intermediate temperature traps must therefore be photochemical in nature. They must be positively charged when empty, hence having a large capture cross section for electrons. The value of 10^{-16} cm^{2} derived in section 8.5 agrees with this suggestion. A possible model for these traps is that under illumination native defects migrate to the vicinity of the contacts. There they associate with imperfections which are photochemically induced by the procedure employed during the

contacting of the crystals. If the resultant complex is positively charged it readily captures electrons to become neutral. When the traps empty positive barriers are formed at the contacts and these exist until the traps are thermally dissociated. Different numbers of defects composing the traps could account for four different centres being found.

The effect of different cooling treatments can be explained if the thermal dissociation of the traps increases at a faster rate with rising temperature than their photochemical creation. The result of this would be that up to a certain temperature ($280^{o}K$ in practice) a net increase in the density of the traps would occur. Above this temperature the density of traps created would decrease.

It is clear that a more intensive study of these traps is required before their nature can be properly understood. Use must be made of 4 probe T.S.C. measurements. An examination must also be carried out into the effect of the contacting procedure to establish whether photochemical changes do in fact take place. In order to do this a comparison could be made between T.S.C. measurements made on crystals contacted in the dark and those with contacts made under irradiation. Of course it is possible that any photochemical changes that do take place are due to light and heat radiation from the molybdenum boat used to evaporate the indium contacts.

References

Bube, R.H., 1954, Photoconductivity Conference, Eds. Breckenridge, R.G., Russel, B.R., and Hahn, E.E. (New York: John Wiley), P.575.

Bube, R.H., 1957, J. Phys. Chem. Solids, 1, 234.

Bube, R.H., and Barton, L.A., 1958, J. Chem. Phys., 29, 128.

Bube, R.H., et al., 1966, J. Appl. Phys., 37, 21.

Woods, J., and Nicholas, K.H., 1964, Brit. J. Appl. Phys., 15, 1361.

CHAPTER 9

High temperature traps

9.1 Introduction

The characteristic feature of the high temperature traps is that in order to observe their associated T.S.C. peaks it was necessary to cool a crystal under illumination from above a threshold temperature prior to the measurements. Increasing the temperature at which illumination was begun resulted in an increase in the magnitude of the various peaks. Maxima at 295°K, 335°K and 365°K were found, with threshold temperatures of 250°K, 285°K and 320°K respectively. No crystal investigated showed all three peaks simultaneously. The effect of the cooling schedule on the 295 and 365°K peaks has been shown previously in figures 6.2.1 and 6.2.2.

There are two explanations which would account for the observed effect of illumination at different temperatures. (1) the traps are photochemically created in increasing numbers by irradiation at progressively higher temperatures, and (2) the traps are surrounded by repulsive barriers and illumination at higher temperatures results in more efficient filling. The characteristics of this type of trap are considered in the following section.

9.2 Repulsive barriers

The model for a trap surrounded by a coulombic repulsive barrier is depicted in figure 9.2.1.

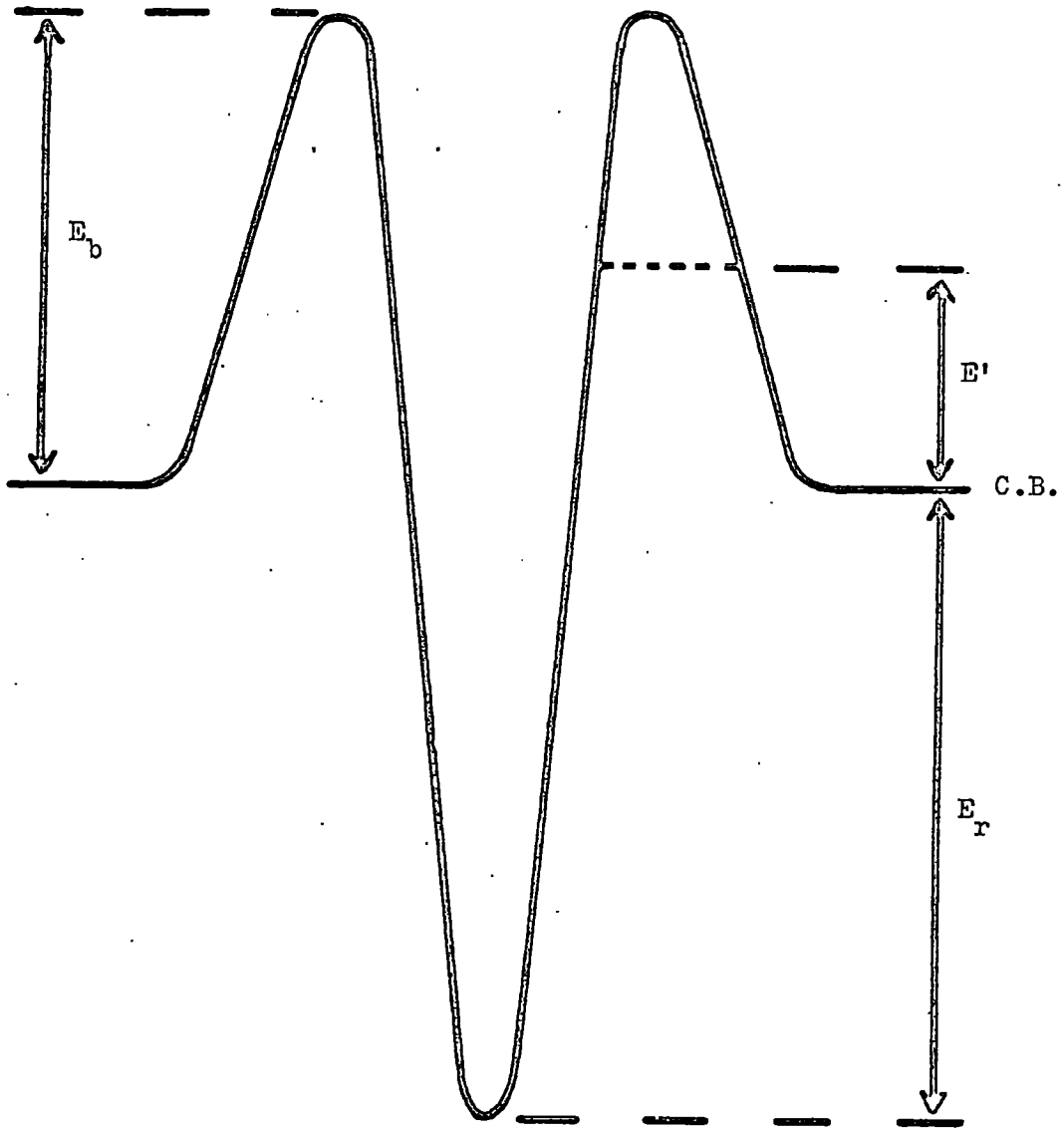

FIGURE 9.2.1 Model for a trap surrounded by a repulsive barrier.

The bottom of the trapping centre is at a depth E_r below the conduction band and is surrounded by a potential barrier of height E_b. Electrons can be released from the trap in two ways. (1) By thermal excitation over the barrier, and (2) by tunnelling through the barrier.

For a non-repulsive trap, with a level E ev below the conduction band, it can be shown that in equilibrium at a temperature T

$$\nu \exp(-E/kT) = Svn \qquad (9.2.1)$$

and

$$\nu = SvN_c \qquad (9.2.2)$$

where S is the capture cross section of the trap, N_c is the effective density of states in the conduction band and v is the thermal velocity of the electrons.

In the case of a trap surrounded by a repulsive barrier it is necessary to define two cross sections.

S_{te} = the cross section effective during escape.

S_{tc} = the cross section effective during capture.

(1) We now consider electron escape by thermal excitation over the barrier. The energy required for this process i.e. the effective trap depth, is

$$E_t = E_b + E_r$$

Equations 9.2.1 and 9.2.2 become

$$\nu \exp(-E_t/kT) = S_{tc}vn$$

$$\nu = S_{te}vN_c$$

from which it is found that

$$S_{tc} = S_{te} \exp(-E_b/kT) \qquad (9.2.3)$$

(2) The second way in which electrons can be released from the trap is by tunnelling through the barrier at a height E' above the conduction band. The effective trap depth in this case is the thermal energy required to raise the electron to E' before tunnelling can take place.

$$E_t = E_r + E'$$

It is necessary to take into account the transmission coefficient for tunnelling. This is $\exp(-\alpha/E'^{\frac{1}{2}})$ where $\alpha = (2\pi^2 e^2/\epsilon h)(2m)^{\frac{1}{2}}$.

Equation 9.2.1 becomes

$$\nu \exp(-E_t/kT) \exp(-\alpha/E'^{\frac{1}{2}}) = S_{tc} v n$$

and it follows that

$$S_{tc} = S_{te} \exp\left[-(E'/kT + \alpha/E'^{\frac{1}{2}})\right] \qquad (9.2.4)$$

In practice the value of cross section obtained from an analysis of T.S.C. data is S_{te}. A consideration of equations 9.2.3 and 9.2.4 leads to two important conclusions.

(a) The value of S_{tc} can be several orders of magnitude smaller than S_{te}. For example, if E_b = 0.3 ev and T = 360°K;

$$S_{tc} = (7 \times 10^{-5}) S_{te}$$

This fact has been used by Bube et al (1966) to explain why traps in CdS_xSe_{1-x} crystals, with a measured cross section of $10^{-14} cm^2$, emptied with no significant retrapping.

(b) The exponential dependence of S_{tc} on temperature leads to a rapid decrease in the magnitude of this cross section as the

temperature is lowered. This explains why no appreciable trap filling can be obtained at low temperatures.

9.3 The 365°K trap

When a Fermi level analysis was applied to the T.S.C. maxima associated with this trap, which were measured after various cooling schedules, a spread of trap depth energies was obtained. The results of an application of this technique to curves (d) and (e) of figure 6.2.1 are given in table 9.1. These results are taken to show that the traps probably empty under monomolecular conditions.

To obtain the true T.S.C. peak it was necessary to make two corrections to the measured curve.

(1) The dark current had to be subtracted from the experimental curve.

(2) The variation in free carrier lifetime had to be taken into account. This was estimated from a measurement of photocurrent against temperature for a current level similar to the T.S.C. level. The lifetime was found to increase by about an order of magnitude over the temperature range in which the traps empty, as is seen in figure 9.3.1. Both curves in this figure were measured after the crystal had been cooled from 400°K under illumination. The importance of this lifetime correction will be seen in the following analysis.

In figure 9.3.2 experimental T.S.C. points are shown for

the 365°K peak (the actual temperature at the maximum is 364°K). This curve was obtained after cooling a crystal from 400°K under illumination prior to the measurements. The points have not been corrected for the variation in lifetime. Also shown is the theoretical curve, assuming monomolecular emptying, that best fits the experimental curve. The corrected experimental points and the best fitting curve to these are shown in figure 9.3.3. After the lifetime correction the maximum occurs at 349°K, a significant change from the measured peak. Table 9.2 summarises the trapping parameters obtained from the curve fitting procedure.

The difference in the values of trap depth found from the two curves demonstrates the importance of the lifetime correction.

Trapping parameters obtained from the corrected experimental curve by other techniques are summarised in table 9.3. There is a good measure of agreement with the values listed in table 9.2.

The curve fitting technique was also applied to the 365°K peak obtained after cooling a crystal from 352°K under illumination. The best fitting theoretical curve and experimental points are shown in figure 9.3.4 for the uncorrected peak and in figure 9.3.5 for the peak corrected for lifetime variations. Data obtained from the theoretical curves is tabulated in 9.4.

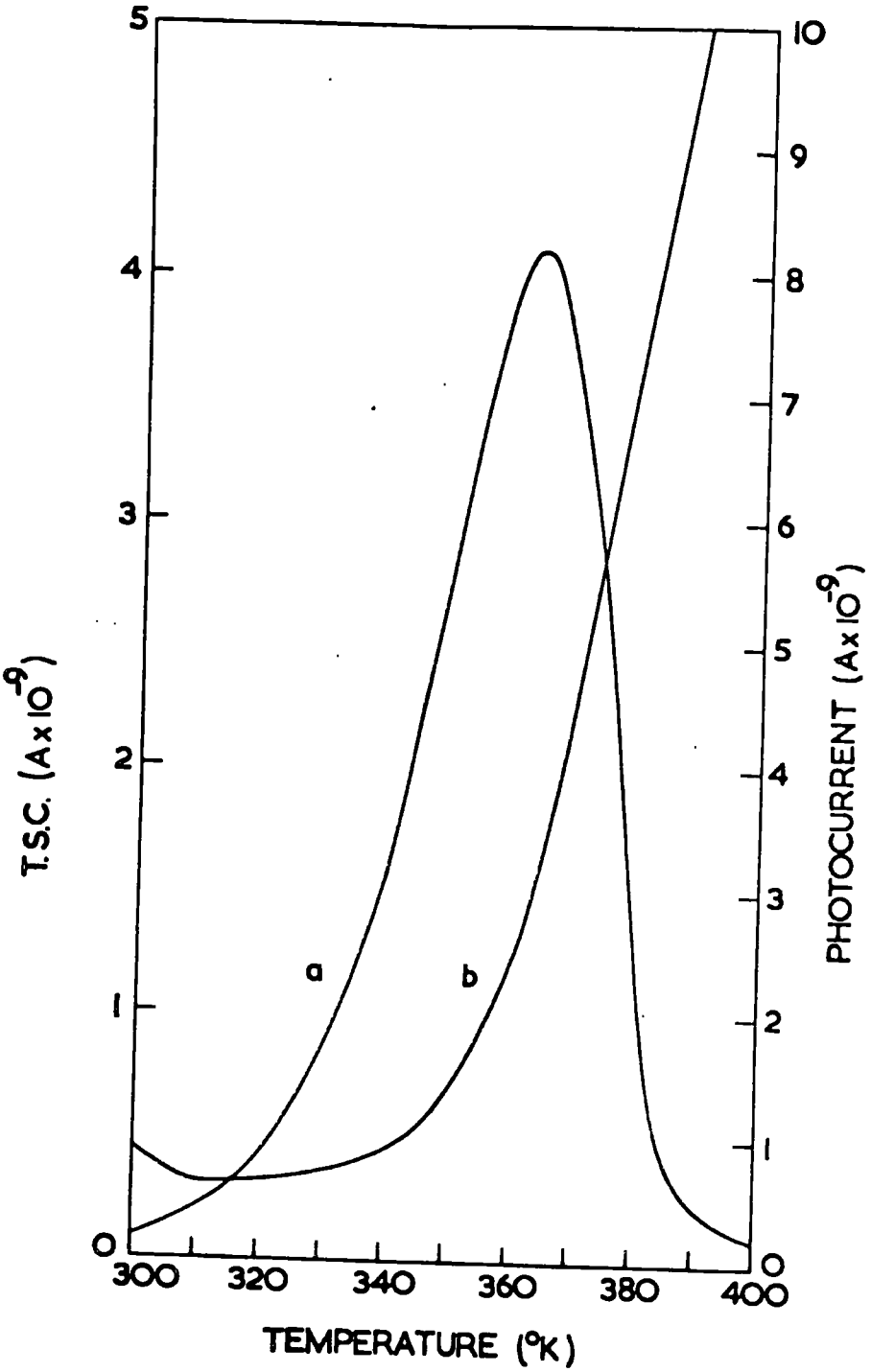

FIGURE 9.3.1. a) 365°K T.S.C. peak b) Corresponding variation in free electron lifetime as obtained from photocurrent measurements.

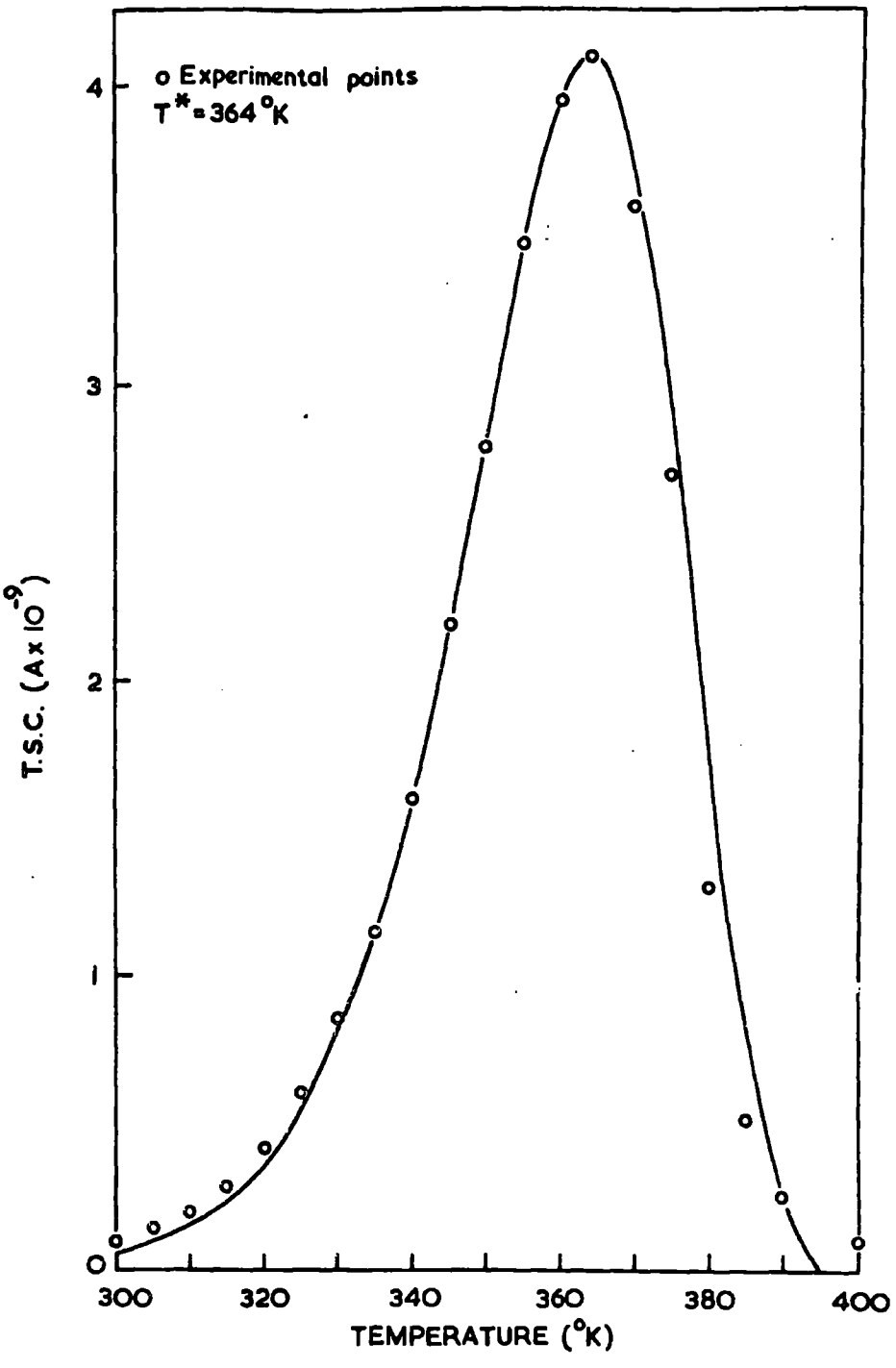

FIGURE 9.3.2. Uncorrected 365 °K peak measured after cooling the crystal from 400 °K under illumination. The theoretical curve shown is for the case of monomolecular kinetics and a trap depth of 0·76 eV

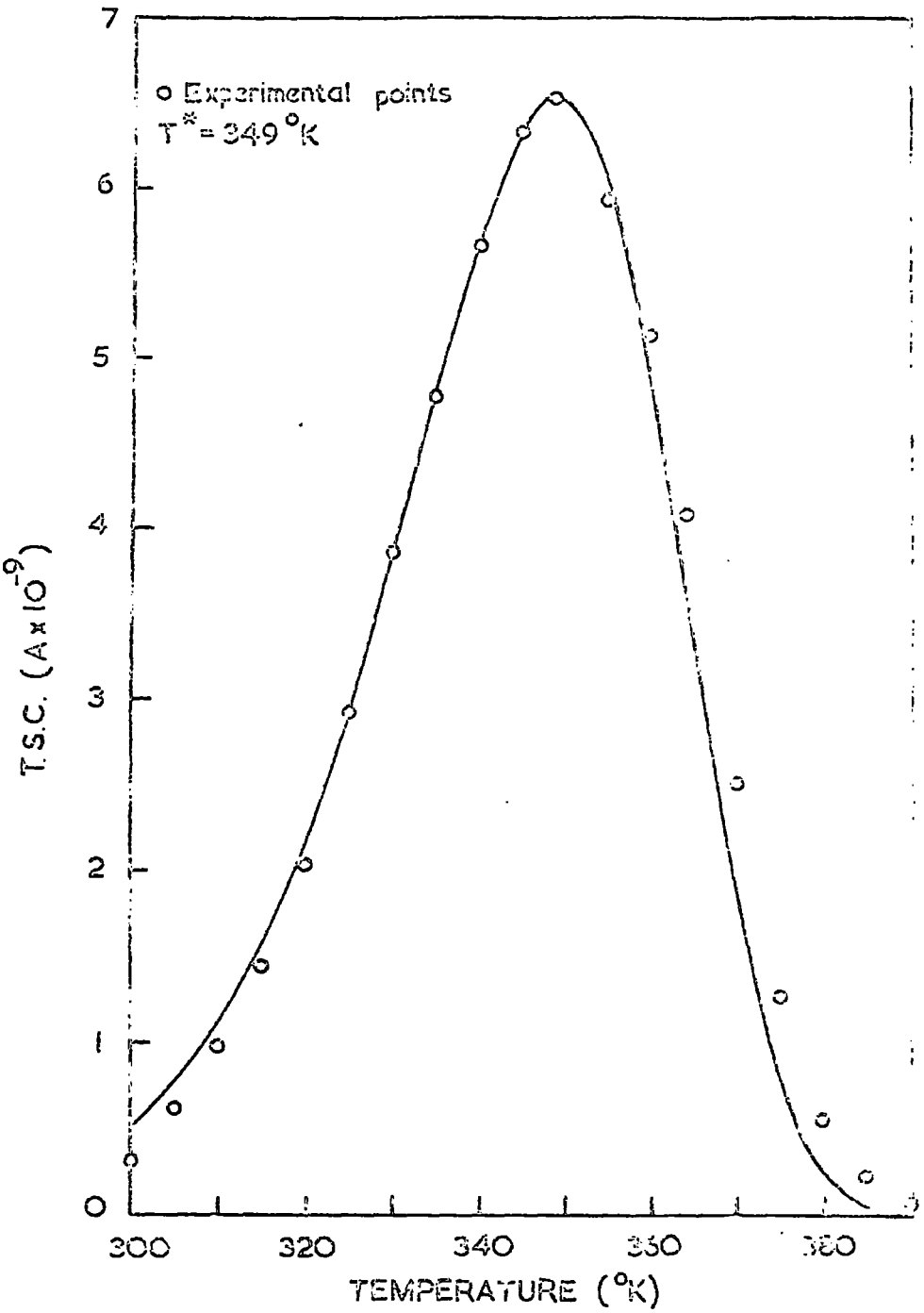

FIGURE 9.3.3. Corrected 365 °K peak measured after cooling the crystal from 400 °K under illumination. The theoretical curve shown is for the case of monomolecular kinetics and a trap depth of 0·63 eV.

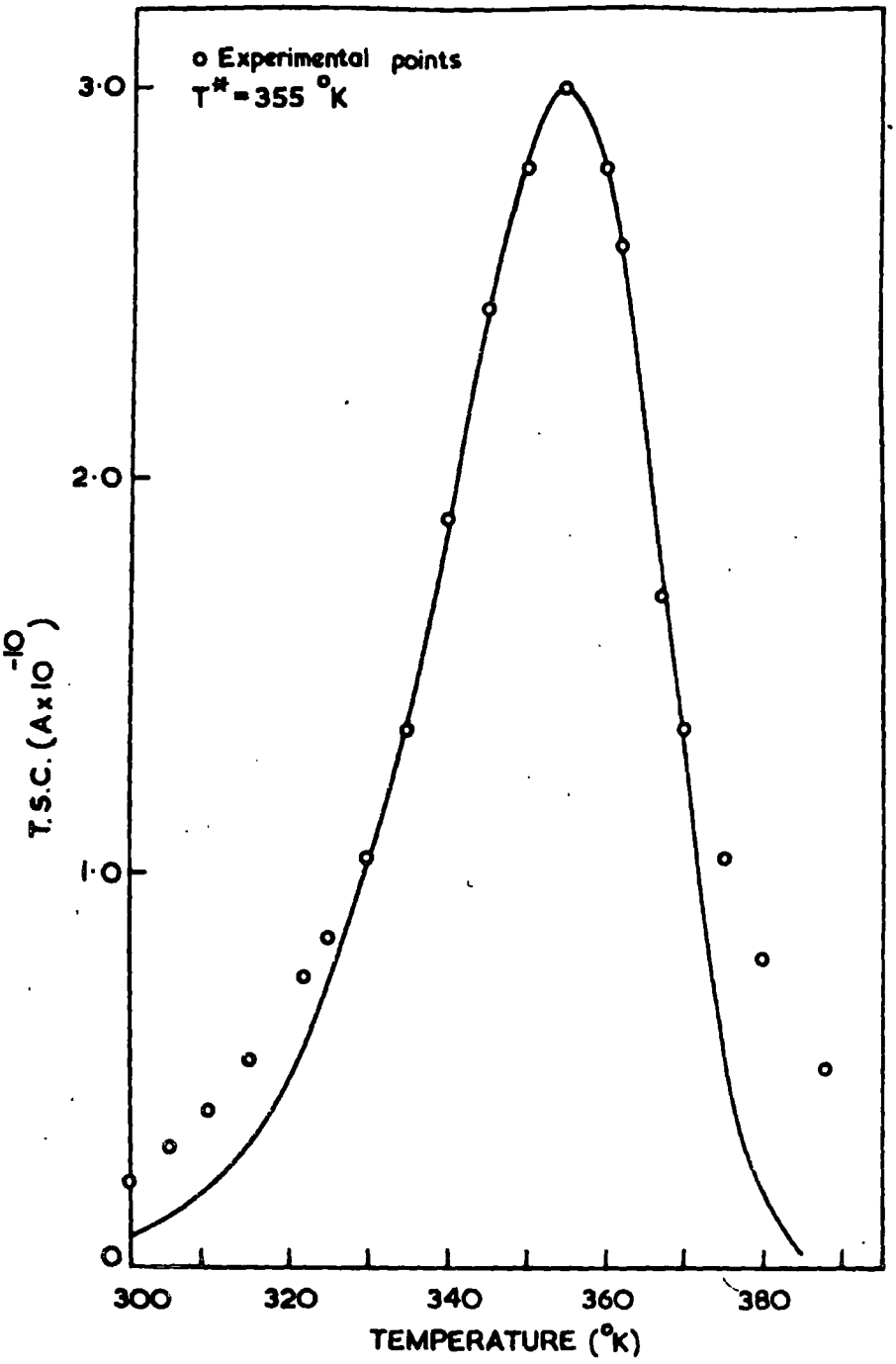

FIGURE 9.3.4. Uncorrected 365 °K peak measured after cooling the crystal from 352 °K under illumination. The theoretical curve shown is for the case of monomolecular kinetics and a trap depth of 0·76eV.

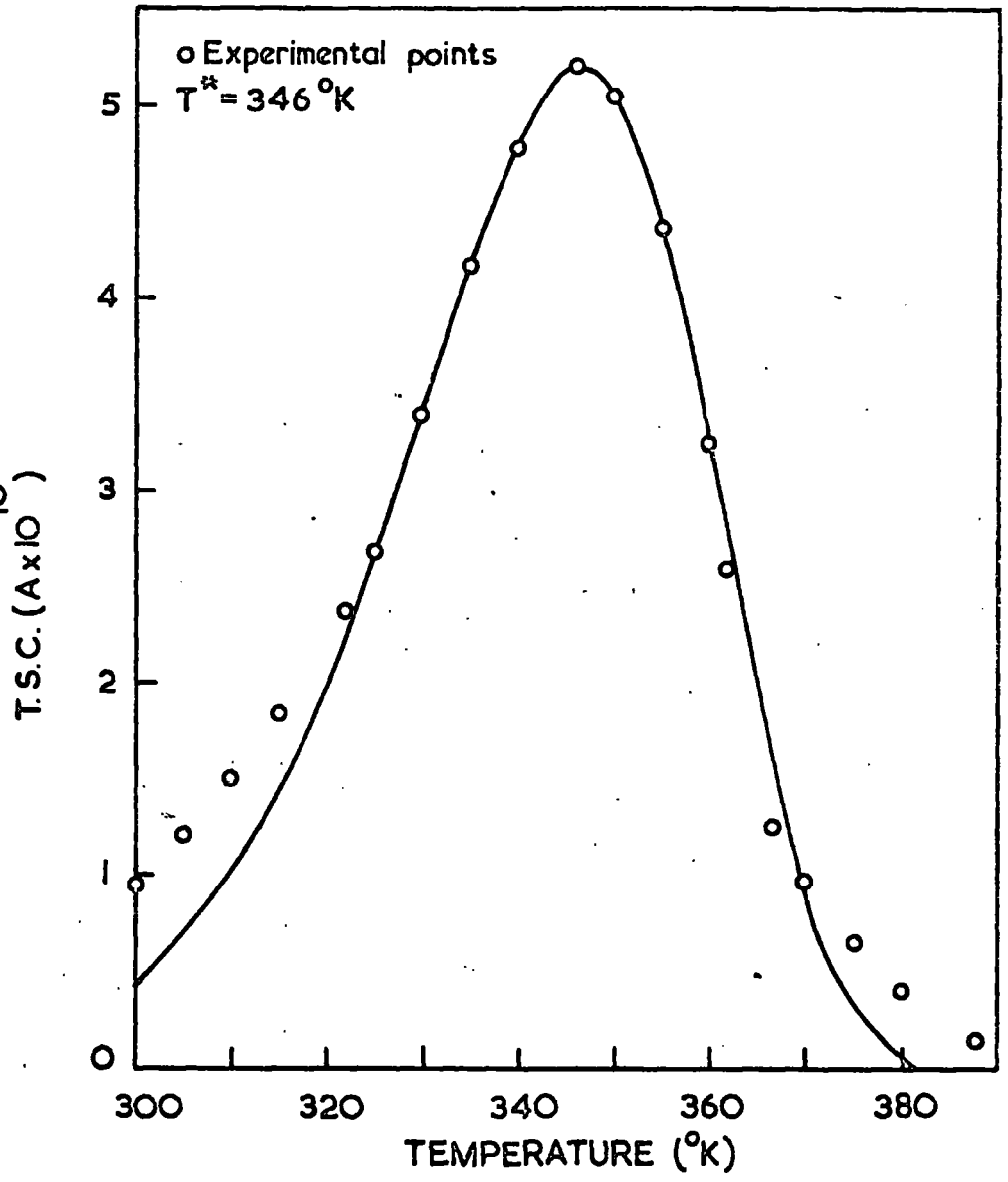

FIGURE 9.3.5. Corrected 365 °K peak measured after cooling the crystal from 352 °K under illumination. The theoretical curve shown is for the case of monomolecular kinetics and a trap depth of 0·63 eV.

Table 9.1. Fermi level analysis of 365°K trap.

Curve (ref. fig. 6.2.1)	Peak temperature (°K)	Trap depth (ev)
d	362	0.75
e	364	0.89

Table 9.2. Parameters associated with both the corrected and uncorrected 365°K peaks.

	Peak temperature (°K)	Trap depth (ev)	Cross section (cm^2)	Density (cm^{-3})
Uncorrected curve	364	0.76	6.5×10^{-20}	7.2×10^{13}
Corrected curve	349	0.63	2.4×10^{-19}	1.2×10^{19}

Table 9.3. Parameters of 365°K trap derived by techniques other than curve fitting.

Type of analysis	Trap depth (ev)	Cross section (cm^2)	Density (cm^{-3})
Grossweiner	0.67	2.6×10^{-19}	
Garlick & Gibson	0.62		
Area under curve			1.3×10^{-19}

Table 9.4. Trapping parameters associated with 365°K peak found after cooling from 352°K under illumination.

	Peak temperature (°K)	Trap depth (ev)	Cross section (cm^2)	Density (cm^{-3})
Uncorrected curve	355	0.76	1.3×10^{-17}	5.0×10^{-17}
Corrected curve	347	0.63	2.9×10^{-19}	5.9×10^{-17}

A comparison between tables 9.2 and 9.4 shows very good consistency in the trapping parameters associated with the peaks measured after the two different cooling schedules. It is therefore possible to describe the trap associated with the observed 365°K peak as having a trap depth of 0.63 ev and a cross section of 10^{-19} cm^2.

A reduction, from 400°K to 352°K, in the temperature at which illumination was begun during the cooling prior to the measurements led to a decrease in the density of filled traps by about an order of magnitude. This would fit in with either a fall in the efficiency of trap filling or a reduction in the number of traps photochemically created. It is not possible to decide which of these two processes is operative from the measurements made.

The potential barrier model described in 9.2 was used by Bube et al (1966) to explain the peculiar behaviour of traps that can only be filled at high temperatures. These traps empty under monomolecular conditions but because of their large cross section (10^{-14} cm^2) appreciable retrapping would be expected. However the cross section of the 0.63 ev traps studied in the present work is 5 orders of magnitude smaller than that found for their repulsive traps. It is reasonable to suppose that the 0.63 ev traps would empty naturally under monomolecular conditions. There is therefore no need for recourse to the model proposed by Bube. The traps could be

photochemically created by irradiation at high temperatures and then thermally destroyed in the dark above 365°K. The measured value of S would then be the capture cross section of the traps. This does not rule out the possibility of the traps being of the repulsive barrier type, nor does the fact that equal cross sections were measured after different cooling schedules. If the traps are surrounded by repulsive barriers then the observed cross section is that operative during escape and this should not change as long as the peak maxima occur at the same temperature (as was in fact found).

9.4 The 335°K trap

It was again necessary to correct the measured T.S.C. peaks for an increase in lifetime over the span of the peaks. The results of an analysis of a corrected curve are listed in table 9.5. The uncorrected curve was measured after cooling a crystal from 400°K under continuous illumination.

The agreement between the values of E obtained by the different techniques is only fair but as usual the value found from curve fitting is regarded as the most accurate. Monomolecular kinetics are assumed on the basis of a Fermi level analysis which yielded a spread of trap depth values between 0.70 and 0.74 ev. The small capture cross section found for the traps justifies this assumption. It is again not possible to decide whether the traps are

Table 9.5. Trapping parameters associated with 335°K peak (for the corrected curve $T^* = 330^\circ K$).

Type of analysis	Trap Depth (ev)	Cross section (cm^2)	Density (cm^{-3})
Curve fitting	0.52	2.4×10^{-20}	2.8×10^{17}
Grossweiner	0.55	2.6×10^{-20}	
Garlick & Gibson	0.46		
Area under curve			2.8×10^{17}

photochemically created or are surrounded by repulsive barriers.

9.5 The 295°K trap

This trap was always found together with one or other of the traps discussed in the preceding two sections. Its associated T.S.C. peak was about two orders of magnitude smaller than the higher temperature peak. Reference to figure 6.2.1 shows that as a consequence of this the 295°K peak only appears as a slight shoulder in the rising side of the second peak. There was therefore a large degree of overlap which affected the 295°K peak but it was possible to obtain well resolved 365 or 335°K peaks by thermal cleaning. However subtracting the cleaned peak from the initial curve was not effective in producing a satisfactory 295°K peak because of the overlap. When a definite 295°K peak was found in the T.S.C. curve after using a suitable cooling schedule (curve c in figure 6.2.1) it was too small to be used for determining its associated trapping parameters. The only two techniques by which it was possible to estimate the depth of the 295°K trap were (1) a Fermi level analysis, and (2) the Garlick and Gibson method. As usual the Fermi level method did not lead to consistent results, a spread of 0.66 to 0.74 ev being obtained.

A Garlick and Gibson analysis was applied to the rising edge of the most pronounced 295°K shoulder that was found in the T.S.C. curves measured after cooling several crystals from

400°K under illumination. The plot of ln I against 1/T in question is shown in figure 9.5.1. A good straight line is obtained, the slope of which yields a trap depth of 0.43 ev. Presumably the true value is slightly less than this, the observed value being high because of the effect of the rising side of the second high temperature peak. Plots of ln I vs 1/T for 295°K shoulders which are less pronounced than that shown in figure 9.5.1 give trap depths of up to 0.46 ev because of the greater effect of the second peak.

The potential barrier model put forward by Bube et al (1966) has previously been described in this chapter. Their published data was for a trap with an associated T.S.C. peak at 289°K and which occurs in $CdS_{0.73}Se_{0.27}$ crystals. They also reported that this trap occurs in crystals of composition $CdS_{0.87}Se_{0.13}$ and $CdS_{0.5}Se_{0.5}$ and in CdS. A feature of their measurements was that the Garlick and Gibson technique, when applied to the 289°K peak, yielded two activation energies, 0.43 ev and 0.75 ev. They suggested that the first of these values is associated with traps emptying by tunnelling. The larger energy, 0.75 ev, is that required to excite electrons over the potential barrier. The agreement between their value of 0.43 ev and the value obtained from the curve plotted in figure 9.5.1 is very interesting, more so as the T.S.C. maxima occur at essentially the same temperature. The wide range of crystal compositions in which the repulsive

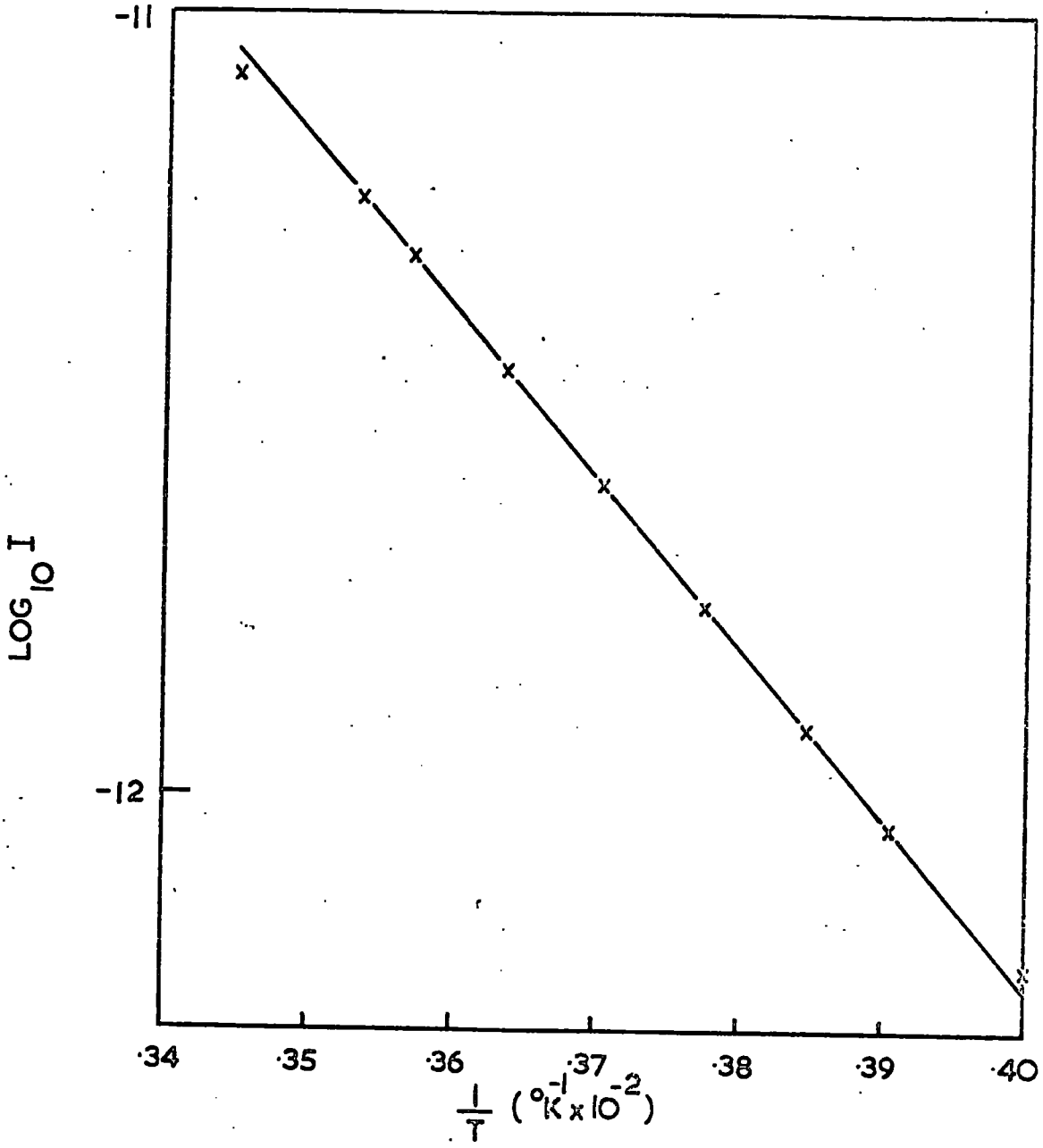

FIGURE 9.5.1. Application of the Garlick and Gibson technique to the 295 °K peak.

trap was identified suggest that it could be common to the whole range of solid solutions of CdS and CdSe. It is possible that the 295°K trap discussed in this section is the same as that described by Bube.

9.6 The effect of prolonged irradiation at 400°K

T.S.C. curves were measured after subjecting a crystal (which exhibited the 365°K peak) to the following cooling schedules after first heating to 400°K in the dark; (1) cooling in the dark then 10 minutes illumination at 90°K, (2) continuous illumination from 400°K during cooling followed by a further 10 minutes at 90°K, and (3) irradiation at 400°K for half an hour, then cooling in the dark followed by 10 minutes illumination at 90°K.

Treatment (2) resulted in the usual 4 orders of magnitude reduction in the heights of the low temperature 90 to 210°K peaks as compared with treatment (1). However the difference in the heights of these peaks after treatments (1) and (3) was only about one order of magnitude. It therefore appears that the decrease in carrier lifetime, caused by irradiation at 400°K during treatment (3), must have been reversed to a considerable degree after the illumination was switched off. This probably occurred while the crystal was still at a high temperature. The total time required to cool the crystal from 400°K to 90°K was about $2\frac{1}{2}$ minutes. This gives an idea of the time required for the photochemically induced changes to reverse. The

significant point is that treatment (3) resulted in an increase in the height of the 365°K peak by 3x compared to the peak found after schedule (2). These results indicate that if the 365°K traps are created photochemically by illumination at high temperatures then this process is not connected with that which causes the reduction in lifetime. In Chapter 11 it will be shown that this reduction in lifetime is attributable to the creation of fast recombination centres. Therefore the high temperature traps do not correspond to class 1 centres.

However any photochemical process which involves the creation of the high temperature traps could be connected with the destruction of the intermediate temperature traps. Reference to figures 6.2.1 and 6.2.2 shows that as the intermediate temperature peaks start to decrease the high temperature peaks start to increase.

9.7 Discussion

An interesting feature of the high temperature traps is their high densities. The largest concentration found, 10^{19} cm^{-3}, corresponds to a trap content in the crystals of about 1 part in 10^4. The significant point is that when electrons are trapped an equal number of holes must be captured by other centres in order to maintain charge neutrality. Thus the crystals must contain a high concentration of centres capable of capturing 10^{19} cm^{-3} holes. These

are possibly the class 1 or class 11 recombination centres. This assumes that the high temperature traps are electron traps, which has not been proved. However even if they are hole traps it is still necessary to account for the capture of an equivalent number of electrons.

A possibility to be considered is that the centres capture both electrons and holes without recombination between the oppositely charged carriers taking place. Such a centre could be a photochemically created complex. Perhaps under the action of irradiation at high temperatures two types of defect, one of which acts as an electron trap and the other as a hole trap, associate to form a complex defect. When the electrons are freed on heating in the dark, giving rise to the observed T.S.C. peaks, the complex dissociates into the two original defects. Holes are then ejected and recombine with the freed electrons via the class 1 centres. The trapping complex is thus annihilated. A similar model was advanced by Woods and Nicholas (1964) to explain how the 0.83 ev traps in CdS empty under monomolecular conditions when their large cross section of 10^{-14} cm^2 should lead to appreciable retrapping.

Another explanation could apply if the traps are surrounded by repulsive barriers. In this case it is possible that the barrier is high enough to prevent any electron trapping unless a hole is first captured. The

capture of this hole would reduce the height of the barrier.

9.8 Summary

Chapters 6, 7, 8 and 9 have dealt with T.S.C. measurements. Variations in the results obtained with different cooling treatments have been examined and an attempt made to explain them. Trapping parameters associated with the various peaks have been evaluated and the possible nature of the traps discussed. In the following three chapters measurements of photoconductivity and luminescence are presented. These measurements are considered in relation to the information obtained from the T.S.C. results.

References

Bube, R.H., et al., 1966, J. Appl. Phys., 37, 21.

CHAPTER 10

Spectral response of photoconductivity and infra red quenching

10.1 Procedure

The experimental arrangement used for these measurements has been described in section 5.5. An applied potential of 50 V was used throughout.

It was not possible to scan automatically through the spectrum of illumination and monitor the photocurrent obtained on a pen recorder because of the slow response of the photocurrent to any change in illumination. This slow response was a direct consequence of the influence of electron traps (as described in section 2.3). Times of up to ¼ hour were required for the photocurrent to stabilise. In making measurements the current was allowed to reach a steady value before taking the reading. Measurements were made at progressively shorter wavelengths during a run.

In most cases the monochromator slits and source lamp current were adjusted during a run to obtain equal dispersion (band width 480 A^{o}) and illumination energy flux (0.022 $\mu w/mm^{2}$) for each wavelength. However for measurements of the infra red quenching of photocurrent it was necessary to use a band width of 950 A^{o} and an energy flux of 2.4 $\mu w/mm^{2}$ in order to obtain an appreciable effect. An alternative technique would have been to use fixed slit widths and lamp current and then correct the photocurrent values for the variation in the lamp

spectrum. This was not done as it would have required the assumption of a linear dependence of photocurrent on light intensity. This was not justified as superlinearity was found in the highly photosensitive, as grown crystals (this phenomenon is described in Chapter 11). All measurements discussed in this chapter are for as grown crystals unless otherwise stated.

10.2 Infra red quenching of quasi dark current

The existence of a large quasi dark current after illuminating a crystal at 90°K has been described in section 7.3. This effect is attributed to the slow thermal emptying of shallow traps. In particular the decay of this current with time is illustrated in figure 7.3.1. If, during a decay of this nature, a crystal was illuminated with infra red radiation of wavelength between 1 and 2 μ there was an immediate rise in the current followed by a fast decay. This behaviour, for 1.375 μ radiation, is shown in figure 10.2.1. If the irradiation was removed the current did not rise at all towards its original level. It continued to slowly decay at a rate governed by the thermal emptying of the traps. It was possible to reduce the current to the true dark current level by continuing the irradiation for several hours (1½ hours for the example illustrated in figure 10.2.1).

This behaviour can be attributed to two effects of the infra red illumination.

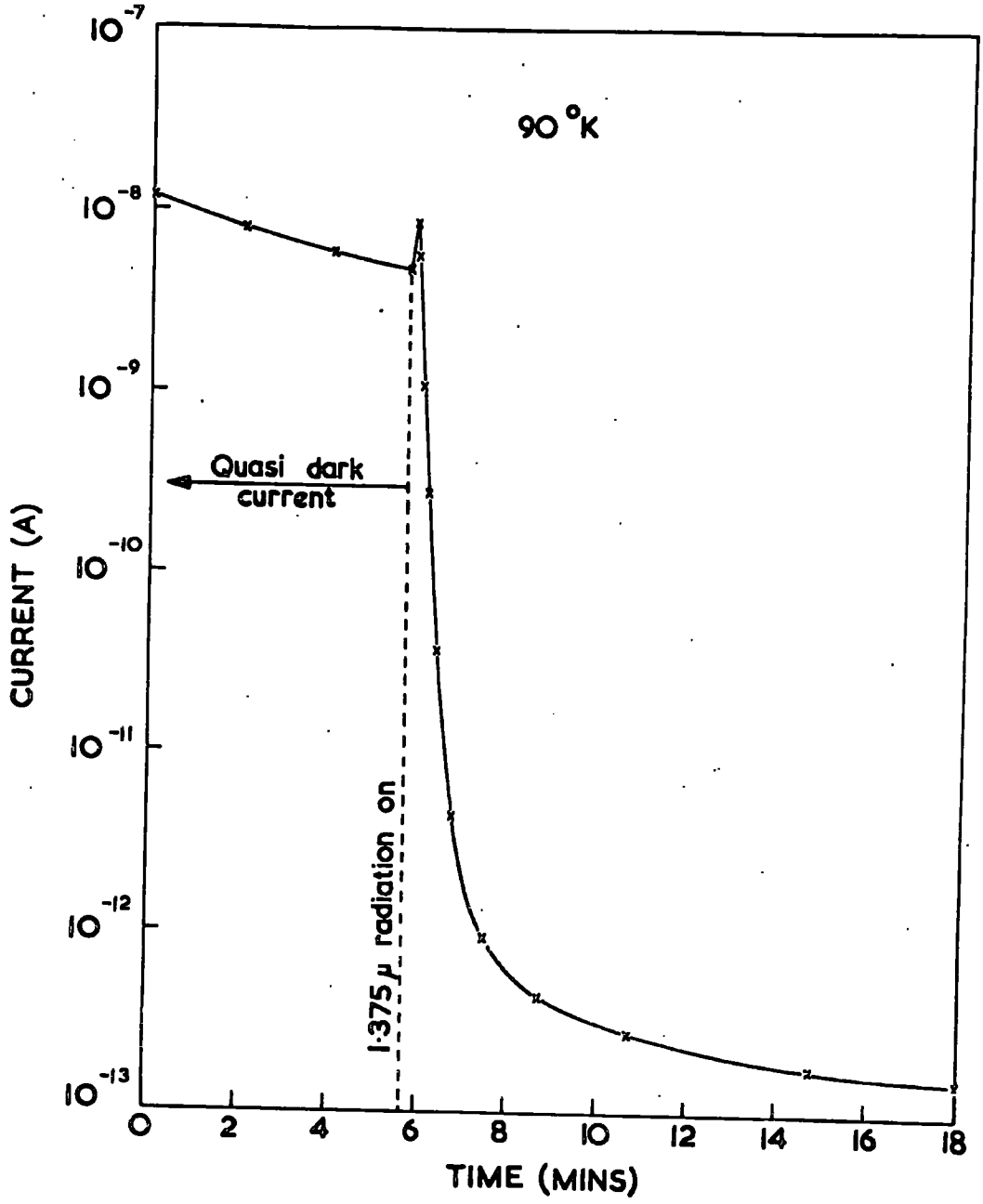

FIGURE 10.2.1. Quenching of quasi dark current by 1·375 μ radiation.

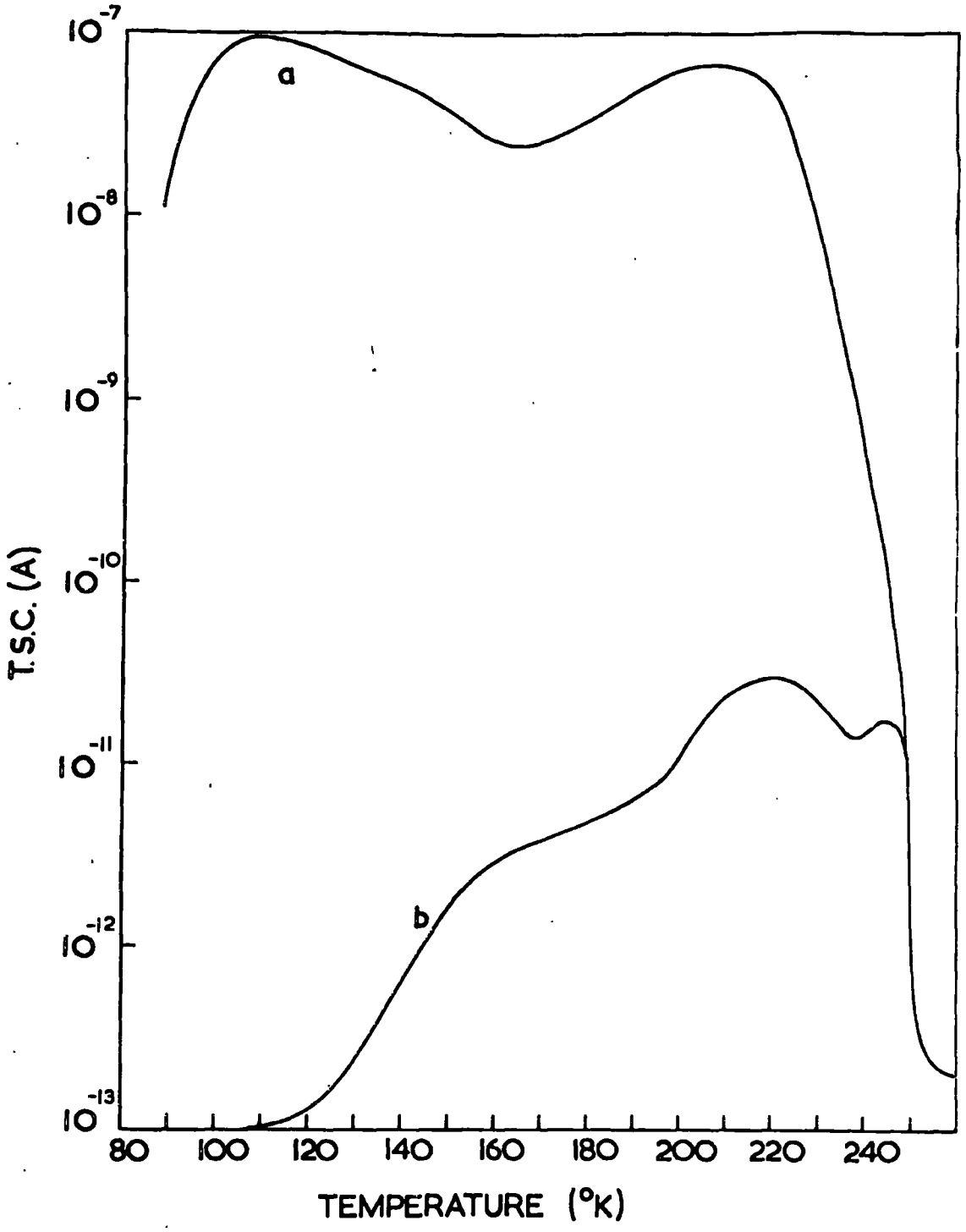

FIGURE 10.2.2. T.S.C. curves after a) 20 minutes illumination at 90°K to fill the low temperature traps b) As a) but followed by 1½ hours illumination with 1·375μ quenching radiation at 90°K.

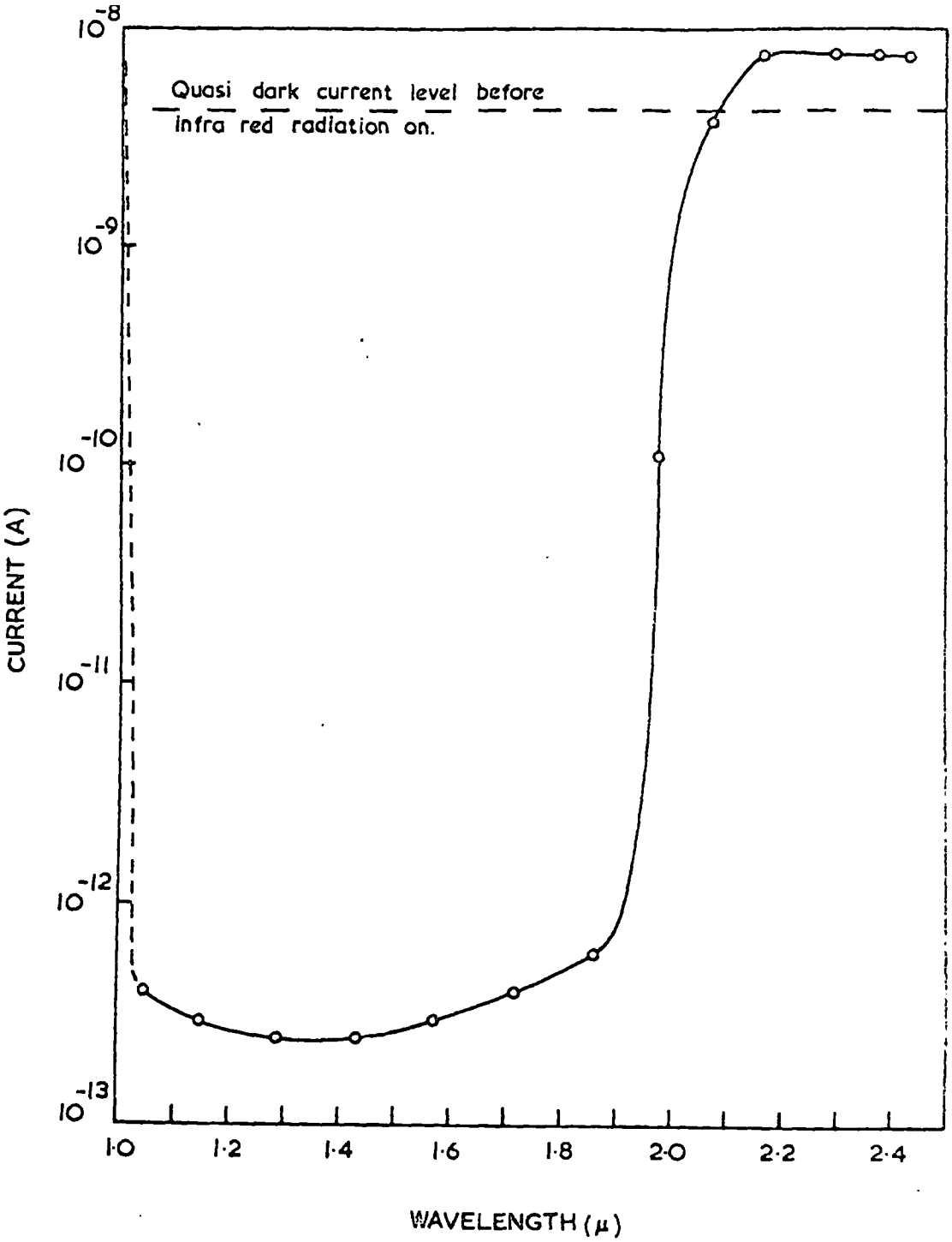

FIGURE 10. 2. 3. Spectral distribution of the I.R. quenching of the quasi dark current at 90°K.

(1) The direct excitation of electrons from traps, resulting in the observed rise in current.

(2) The release of holes from sensitising centres with a consequent quenching of the current due to (1) i.e. the observed sharp fall in the current.

The quenching could be achieved in two ways.

(a) Recombination between the free holes and trapped electrons, thus reducing the density of carriers available to be raised to the conduction band.

(b) Recombination between the free carriers released from the traps and the holes, probably via fast recombination centres i.e. a decrease in the free electron lifetime.

Thermally stimulated current measurements were made following a prolonged quenching of the quasi dark current. Figure 10.2.2. shows a curve (b) obtained after a crystal had been irradiated with infra red of wavelength 1.375 μ for $1\frac{1}{2}$ hours. For comparison a curve (a) obtained without prior quenching is also shown. These measurements demonstrate that the infra red radiation substantially empties the 0.15 to 0.36 ev traps. However it must be noted that part of the reduction in height of curve (b) compared with curve (a) may be due to a lifetime effect. Some of the holes freed by the I.R. illumination may be captured at class 1 centres without taking part in recombination. They would then recombine with electrons freed during the subsequent heating with a resultant

decrease in the lifetime of these electrons.

Figure 10.2.3 shows the spectral distribution of the quenching of the quasi dark current. This current was allowed to decay for a period of 10 minutes to reach a fairly steady value. The crystal was then illuminated with infra red radiation of decreasing wavelength. With each wavelength 5 minutes were allowed for the current to stabilise appreciably before its value was noted. A long wavelength threshold of quenching was found to occur at about 2.1 μ. Therefore the energy levels of the sensitising centres are situated at about 0.59 ev above the valence band. Illumination with radiation of a longer wavelength than the quenching threshold gave rise to a small photocurrent due to optical trap emptying. The large photocurrent (shown by the dashed line in figure 10.2.3) obtained for wavelengths shorter than 1.03 μ will be discussed in section 5 of this chapter.

10.3 Optical trap emptying

Measurements described in the above section showed that it was possible to empty traps by direct excitation of electrons to the conduction band with infra red radiation. This effect was examined further to see if it was possible to obtain thresholds of response, in curves of current vs wavelength, corresponding to the emptying of the various traps found from T.S.C. measurements. The technique did not give satisfactory results. Small photocurrents were obtained, at the most 2x

greater than the quasi dark currents. However there was no structure in the curves.

10.4 Infra red quenching of photoconductivity

No infra red quenching of photoconductivity was found at room temperature. This is to be expected as the class 11 centres do not contain holes at this temperature except at very high incident light intensities. Quenching at 90°K was therefore investigated.

It was difficult to study the quenching of photoconductivity in crystals that had been cooled in the dark. This was because of the masking effect of the high residual dark current and the quenching of this current described in section 10.2. When the primary excitation was sufficiently intense to give a photocurrent large enough to dominate this dark current then the secondary radiation available from the monochromator was not intense enough to cause appreciable quenching.

I.R. quenching was therefore studied in crystals that had been cooled from 400°K under illumination with intense white light prior to the measurements. The quasi dark current was then negligible compared with the primary photocurrent (which was of the order of 10^{-7} A). The spectral dependence of the quenching is shown in figure 10.4.1. A long wavelength threshold was observed at 2.03 μ. From this the position of the sensitising centres was calculated to be 0.61 ev above the

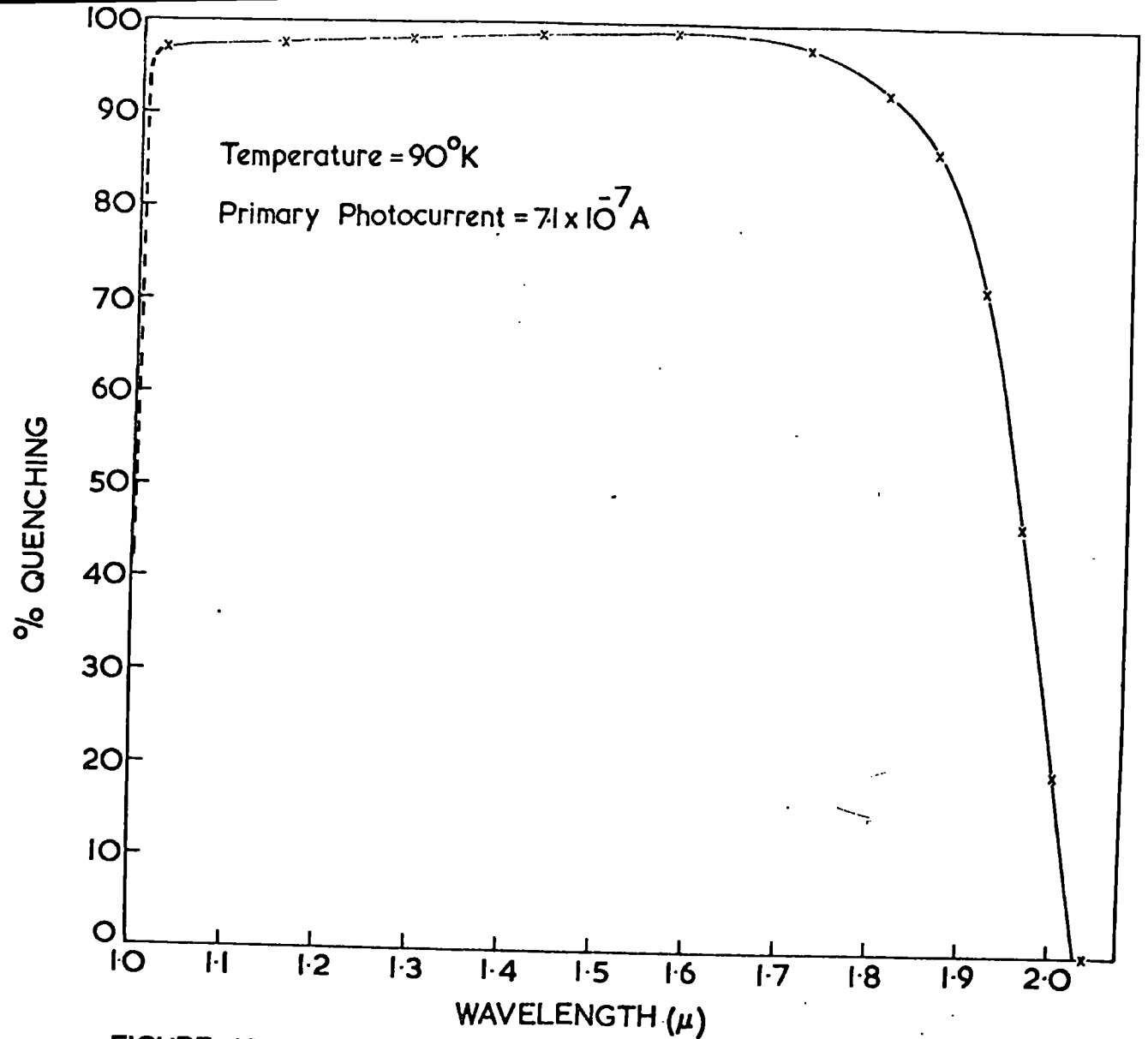

FIGURE 10.4.1. Spectral distribution of I.R. quenching of photoconductivity.

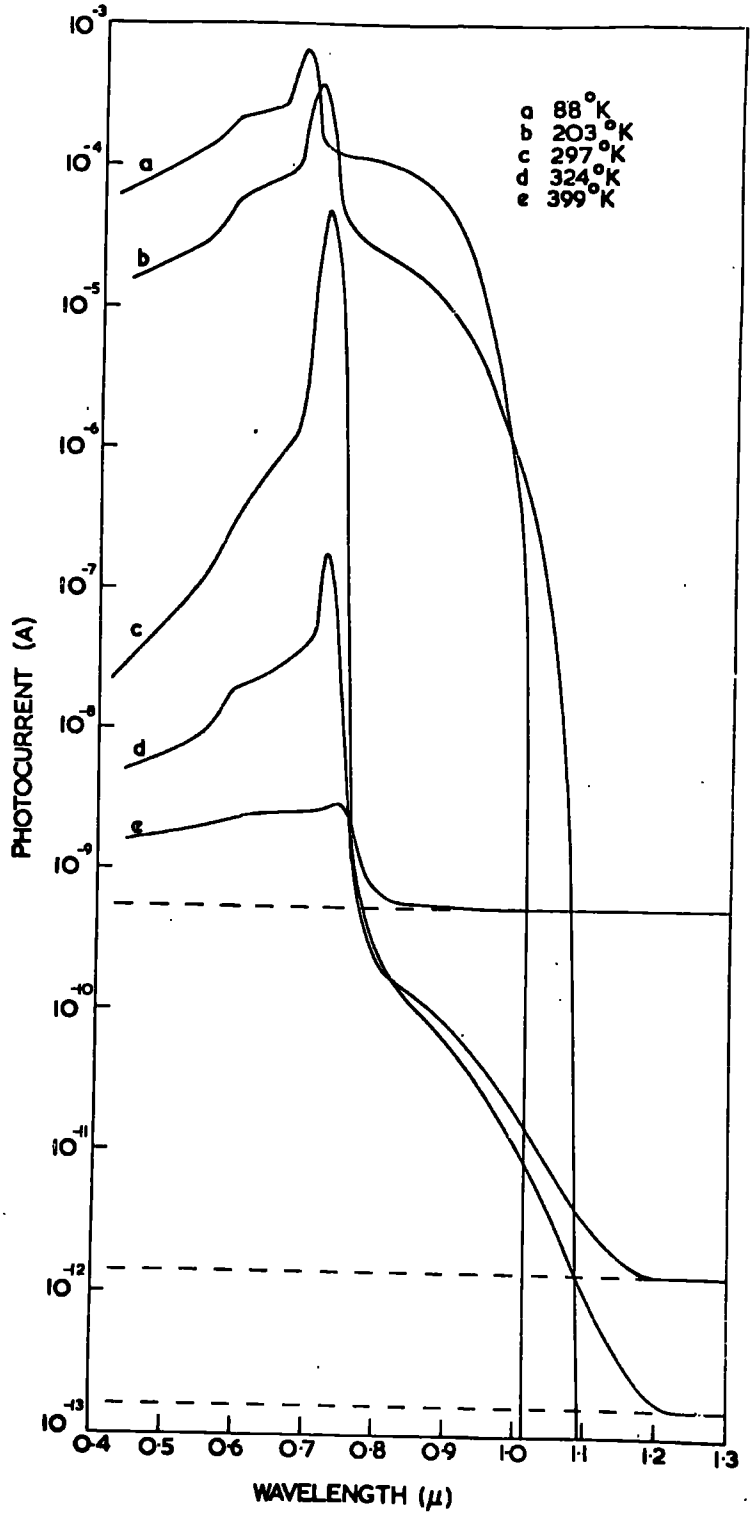

FIGURE 10.5.1. Spectral response of photoconductivity at various temperatures. The dashed lines indicate the dark current levels.

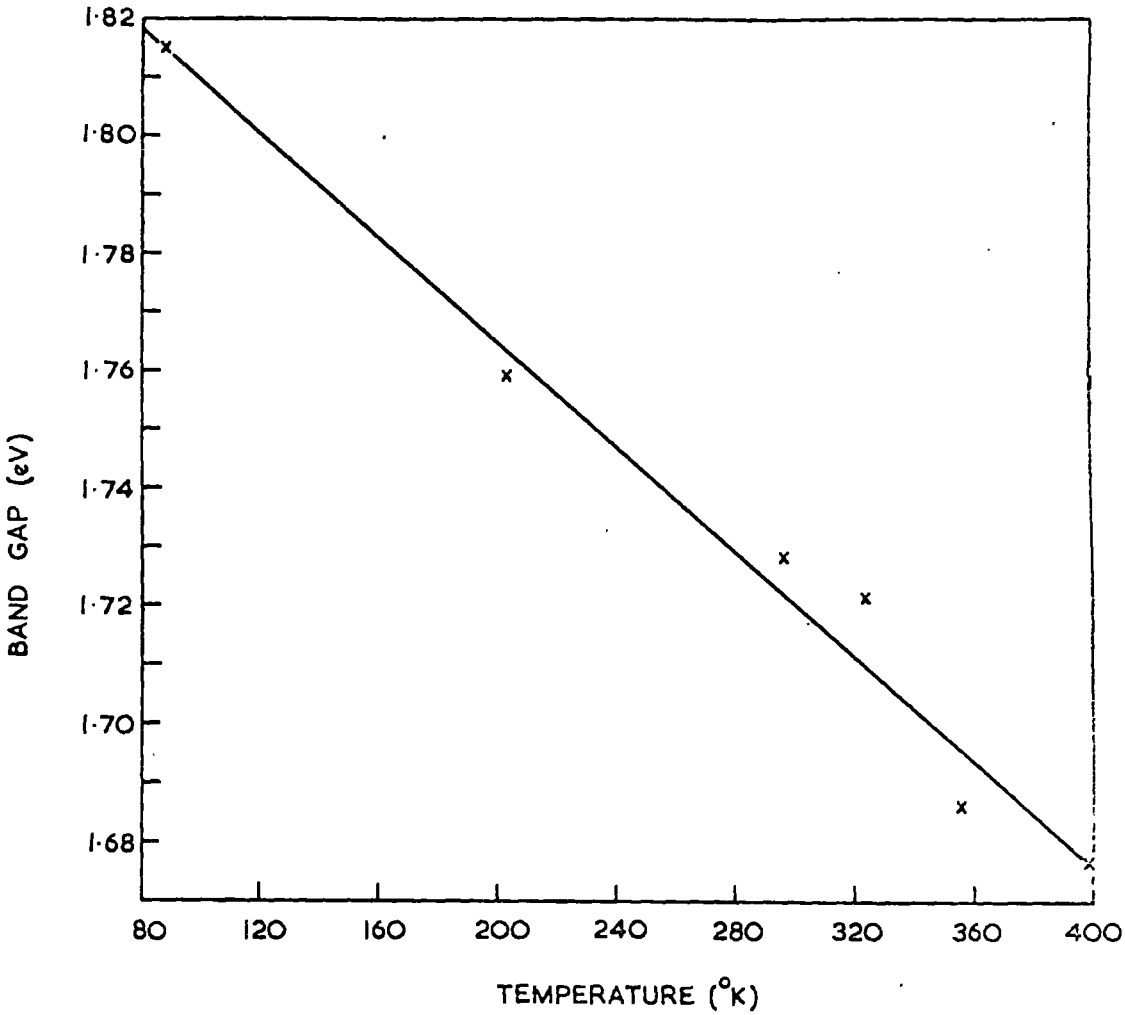

FIGURE 10.5.2. Temperature dependence of band gap energy as found from measurements of the spectral dependence of photoconductivity.

valence band. This is in good agreement with the value of 0.59 ev found from the results discussed in section 10.2.

The fact that appreciable quenching was found in crystals that had been cooled from 400°K under irradiation is perhaps significant when it is considered with reference to the reduction in lifetime caused by this treatment (reference section 6.5). Measurements of I.R. quenching do not yield quantitative values of the density of sensitising centres. However it is reasonable to suppose that if the photochemical decrease in lifetime is associated with a large reduction in the number of these centres then pronounced I.R. quenching would not be observed.

10.5 Spectral response of photoconductivity

The curves in figure 10.5.1 show the spectral dependence of photocurrent at several temperatures for a typical crystal. The measurements were made after the crystal had been heated to 400°K and then cooled to the required temperature in the dark, thus ensuring that the various traps were empty. There are three regions of interest in the curves.

(1) The maxima found in the curves at about 0.7 μ. The energies corresponding to the wavelengths at these maxima are taken as a measure of the band gap at the various temperatures. As the temperature is increased there is a corresponding decrease in the band gap. In figure 10.5.2 a plot of band gap energy against temperature shows a linear relationship.

From the slope of this line a variation of band gap with temperature of - 4.4×10^{-4} ev/^{o}K is obtained.

(2) There is a shoulder on the short wavelength side of the maxima, at about 0.59 μ. The position of the shoulder is essentially independent of temperature. This shoulder appears as a separate peak in the spectral response curves of some crystals which had been annealed in selenium vapour (reference section 10.7). An example of this is shown in figure 10.7.2 where the wavelength at the maximum is 0.58 μ, corresponding to a photon energy of 2.14 ev. The presence of a third valence band in CdSe, lying 2.27 ev below the conduction band at 4.2^{o}K, has been discussed in section 1.3. It is possible that the short wavelength shoulder is associated with transitions from this valence band. However if this is the case it is difficult to understand why the position of this shoulder does not shift to longer wavelengths with increasing temperature.

(3) A long wavelength photo-response was observed which exhibited a very sharp threshold at temperatures of 88^{o}K and 203^{o}K (curves a and b in figure 10.5.1). The threshold at 88^{o}K is at 1.01 μ, corresponding to a photon energy of 1.23 ev. A similar threshold is seen in figure 10.2.3.

Infra red quenching experiments (sections 2 and 3 of this chapter) showed the presence of sensitising centres with levels at 0.6 $\pm$ 0.01 ev above the valence band. From figure 10.5.2

the band gap at 88°K was calculated to be 1.82 ev. Thus the energy levels of the sensitising centres must lie 1.22 ev below the conduction band. It is therefore very probable that photoconductivity excited by the long wavelength radiation is due to electrons excited from the sensitising centres to the conduction band. This is reasonable because, before the spectral response measurements were made, the crystals were heated to 400°K and then cooled without being subjected to any illumination. Therefore no free holes would be produced to be captured by the sensitising centres and these latter would be substantially filled with electrons.

Some electrons excited from these levels would also be captured by the empty 0.15 to 0.36 ev traps. This accounts for the 1.18 ev threshold of trap filling observed in the T.S.C. measurements made after illumination with monochromatic light described in section 6.3.

Curves (c), (d) and (e) in figure 10.5.1 do not exhibit such sharp long wavelength thresholds or large long wavelength photo-response as are found in curves (a) and (b). This can be attributed to the low photoconductive gains pertaining as a result of the former measurements being made at temperatures above the region of thermal quenching of photoconductivity. At these temperatures the class 11 centres act as hole traps in thermal equilibrium with the valence band. Some of the holes left in these centres by the optical excitation of

electrons to the conduction band are freed thermally to the valence band. They then recombine with the excited electrons via fast recombination centres with a resultant short free electron lifetime.

However the magnitudes of the maxima found in curves (c) and (d) at wavelengths corresponding to band to band excitation are larger than was expected from a consideration of the small long wavelength responses. This is particularly apparent in the measurements made at 297°K. The maximum photocurrent obtained at this temperature was only one order of magnitude smaller than that observed at 88°K whereas the long wavelength response was about six orders of magnitude smaller. It is known that the greater the magnitude of a photocurrent then the higher is the temperature at which thermal quenching of this current sets in. It is therefore probable that the rise in current which results from band to band excitation at 297°K and 324°K causes a shift in thermal quenching to temperatures such that the crystal is no longer fully desensitised. Thus the gains during excitation with light of approximately band gap energy are greater than those operating at longer wavelengths.

Spectral response measurements were also made on crystals that had been cooled under intense white light prior to the measurements. After this treatment a long wavelength photo-response was still observed although both this and the response due to band to band excitation were reduced in magnitude by a

factor of about 10 times as a result of the decrease in lifetime caused by the irradiation during cooling.

10.6 Photo-stimulated thermo electric power measurements

In section 6.8 a technique of measuring thermally stimulated thermo-electric power is described. This involves establishing a temperature gradient along a crystal by mounting it on one end. Photo-stimulated T.E.P. measurements were also made on crystals mounted in this way. They were illuminated with monochromatic light. Figure 10.6.1 shows the spectral dependence of the T.E.P. obtained at 91°K (bottom contact temperature). The crystal had been heated to 400°K and cooled in the dark prior to these measurements. The temperature drop along the crystal was 30°K. For all wavelengths shorter than the threshold of the photo-response a negative T.E.P. was found. This indicates that the photoconductivity, due to both band to band excitation and excitation from the sensitising centres, is predominantly n type as would be expected. At about 0.7 μ, when band to band excitation becomes dominant, there is a sharp change in the positive direction. This is presumably due to the onset of a small p type photocurrent associated with the holes left in the valence band.

10.7 Crystals annealed in selenium vapour

No infra red quenching, at either room temperature or at 90°K, was observed in crystals which had been annealed in selenium vapour. This suggests that these crystals contain

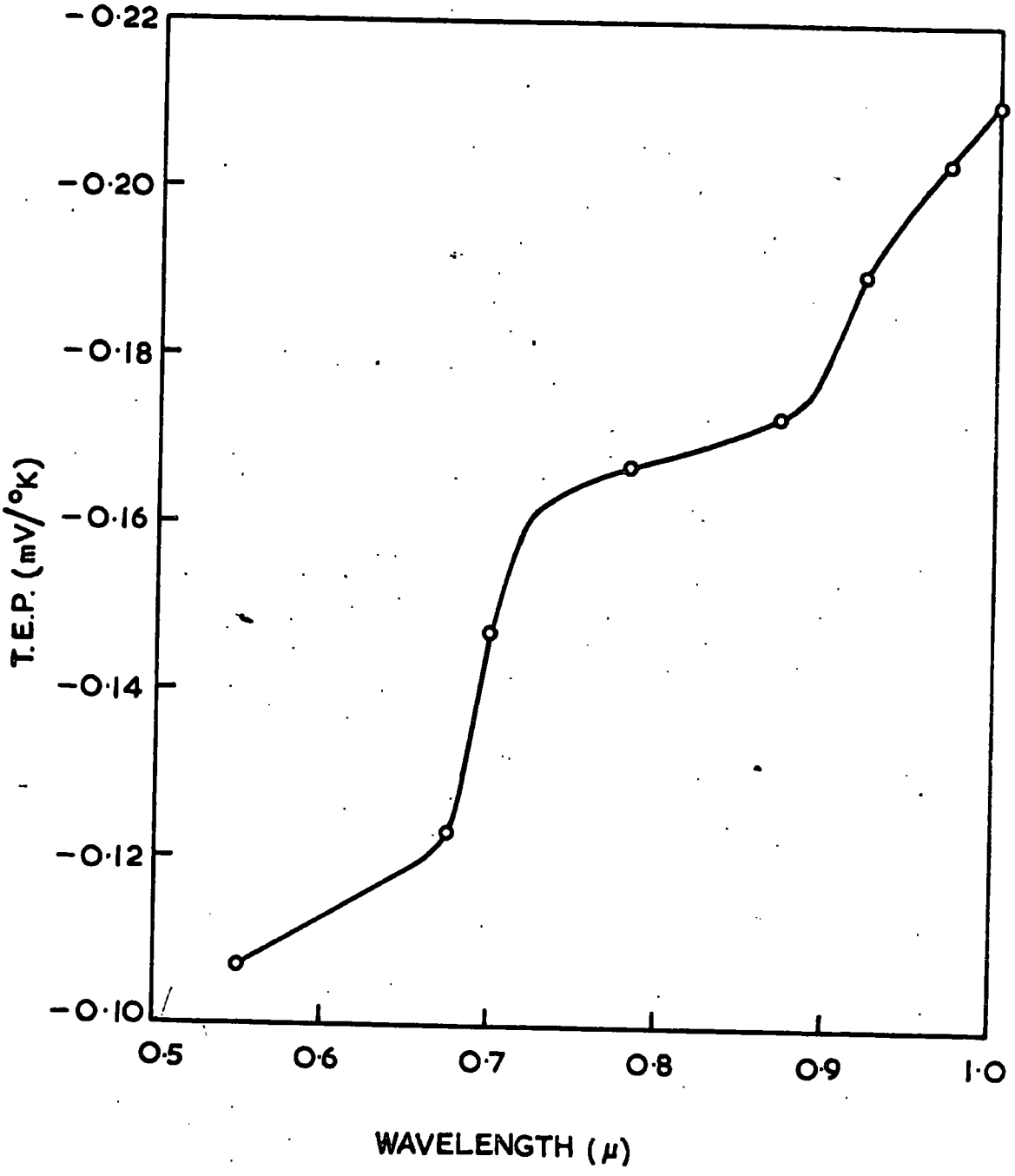

FIGURE 10.6.1. Spectral dependence of photo-stimulated T.E.P.

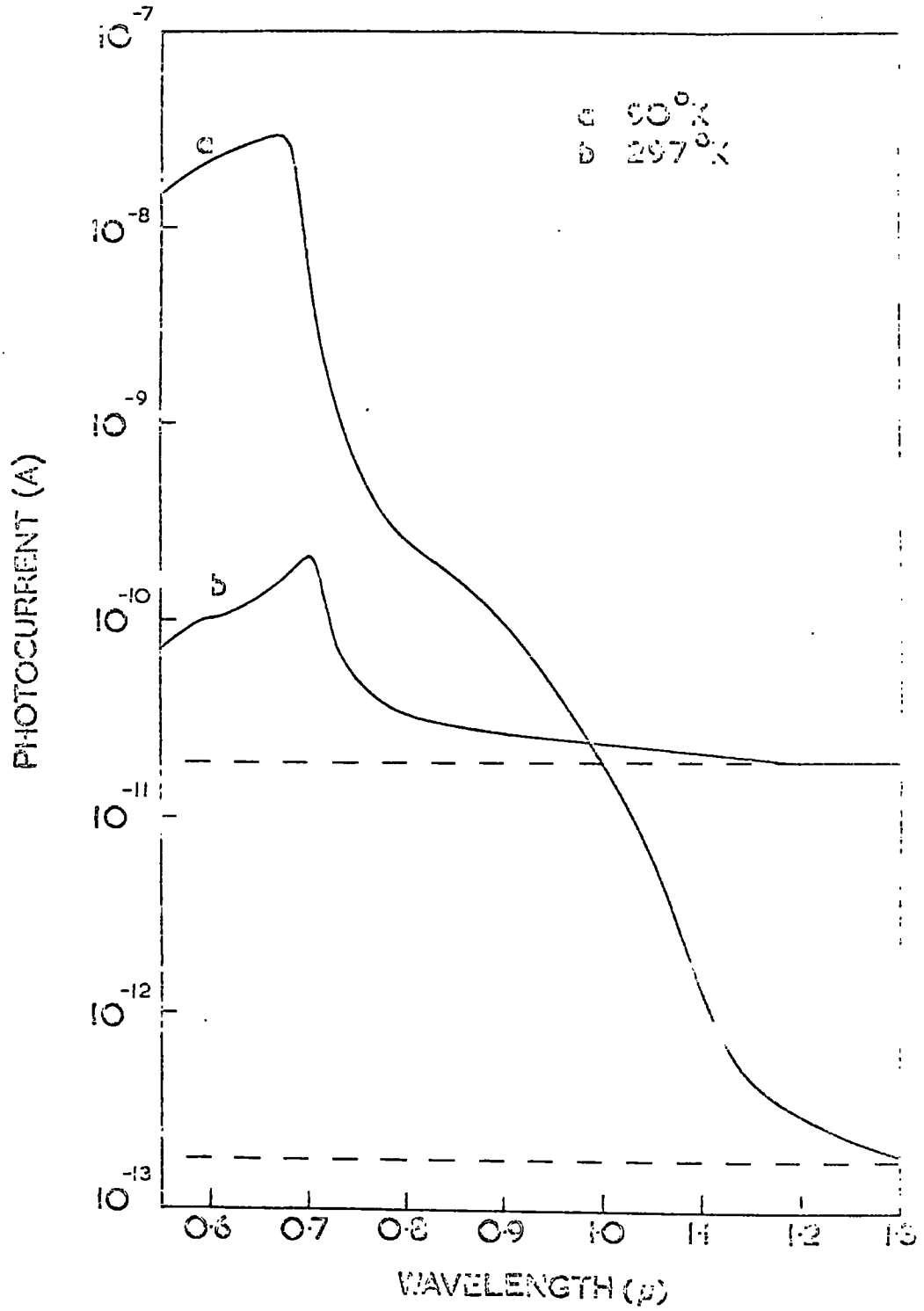

FIGURE 10.7.1. Spectral response of photoconductivity of a crystal annealed in saturation vapour. The dashed lines denote the dark current levels.

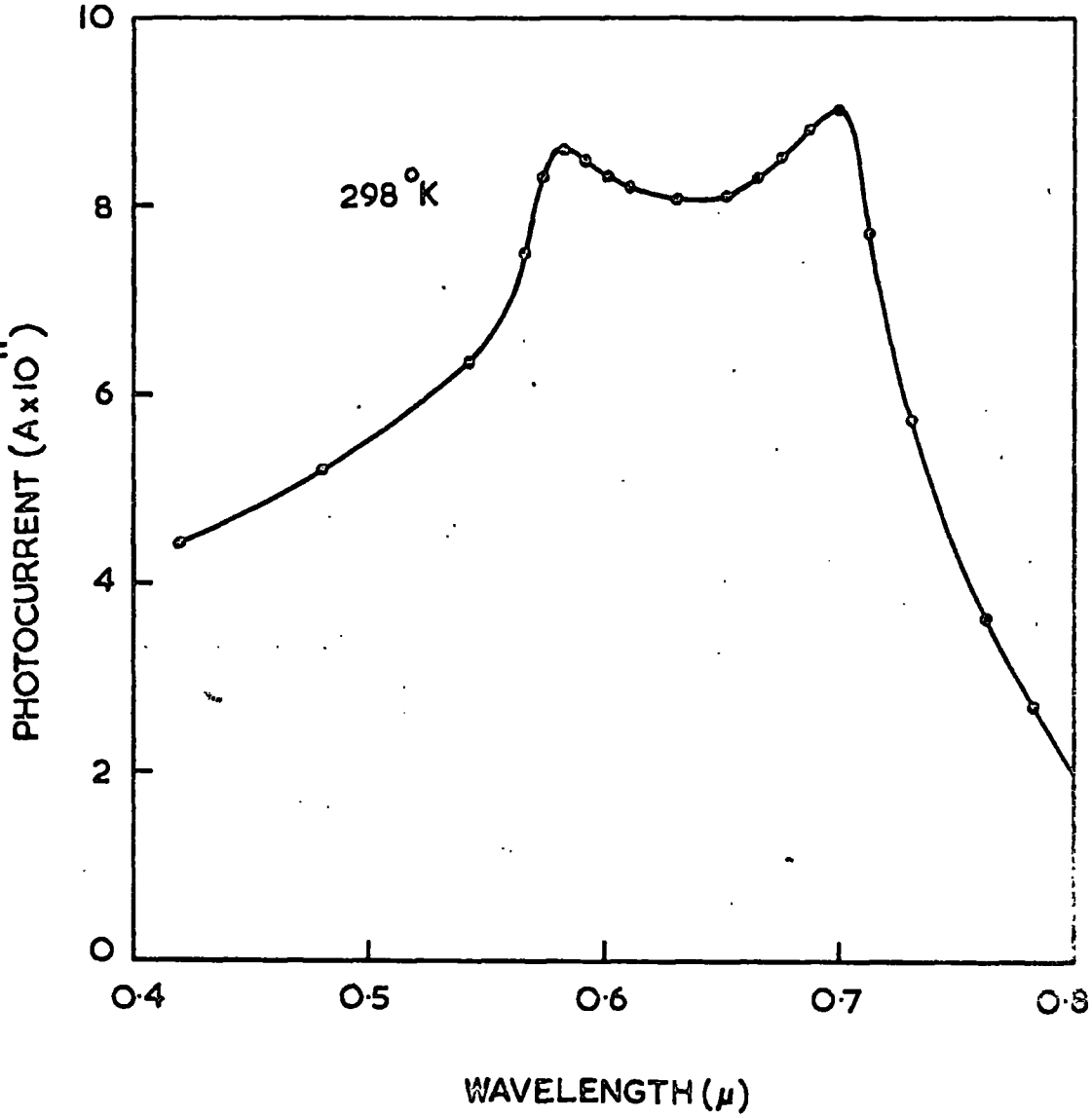

FIGURE 10.7.2. Spectral response of photoconductivity, exhibiting two maxima, of a crystal heat treated in Se vapour.

either only a small number of sensitising centres or none at all. Further evidence to support this conclusion comes from measurements of the photoconductive gains of such crystals. They exhibited poor photosensitivity with gains of about 0.1. This conclusion is interesting because cooling these crystals from progressively higher temperatures under illumination resulted in a reduction of the free electron lifetime (reference section 6.6). A similar effect was of course observed with as grown crystals. However infra red quenching measurements showed the presence of an appreciable density of sensitising centres in as grown crystals. The logical deduction from these results is that the change in lifetime is not due to a change in the density of sensitising centres.

Figure 10.7.1 shows the spectral dependence of photocurrent measured at 90°K and 297°K for a crystal that had been heat treated in selenium vapour. A long wavelength response was observed at wavelengths up to about 1.3 μ. The threshold of this response was not very sharp, making it difficult to estimate its true value. Taking a value of 1.3 μ for the threshold means that the long wavelength response is due to excitation from levels about 0.95 ev below the conduction band.

It is pertinent at this point to discuss the possibility of a long wavelength response attributable to the optical excitation of electrons from class 1 fast recombination centres. Such electrons would immediately recombine with the holes left

in the centres because of the associated large capture cross section. Consequently the electrons would only have a short lifetime and the resultant photocurrent would be small, possibly too small to be detected. This accounts for the lack of any such long wavelength response in as grown crystals. However it is possible that the 1.3 μ response in crystals which had been annealed in selenium vapour is due to the excitation of electrons from class 1 centres lying 0.95 ev below the conduction band. The lack of a sharp threshold is compatible with the short lifetimes associated with this type of excitation. It should also be noted that the 1.3 μ response may be superimposed upon a 1 μ response associated with excitation from a small number of sensitising centres present in these crystals.

In some instances the room temperature spectral response curve exhibits two maxima, the usual one at about 0.7 μ and an additional one at 0.58 μ. This behaviour, which is illustrated in figure 10.7.2, has been discussed in section 10.5.

10.8 Discussion

The main feature of the results discussed in this chapter is the identification of the sensitising centres in the highly photosensitive crystals. The energy levels of these centres are situated 0.6 ± 0.01 ev above the valence band. The existence of these centres in CdSe has been fairly widely reported. Bube (1955 and 1964), Bube and Barton (1958) and

Stupp (1963) have studied the centres in undoped crystals. Bube and Barton regarded these centres as being due to cadmium vacancies (which act as acceptors). Bube (1957) identified sensitising centres lying at 0.6 ev above the valence band in copper doped crystals. Stupp found levels at a similar position in both copper and silver doped crystals. Copper and silver act as acceptors in CdSe. Because of the coincidence of the positions of the centres in both doped and undoped material Stupp suggested that the dominant sensitising centre in CdSe is an activator, presumably a native defect, always present in the lattice. Impurity acceptors may introduce subsidiary sensitising centres.

The crystals studied in the present work were not deliberately doped but this does not mean that no impurities were present (no analysis of impurity content was carried out). However no evidence of the existence of a high density of sensitising centres in crystals which had been annealed in selenium vapour was found. If these centres are associated with impurities it is probable that they would have been found in these crystals. This evidence supports the model postulated by Stupp. The two simple types of defect which can act as acceptors in CdSe are cadmium vacancies and selenium interstitials. Woodbury and Hall (1967) suggested that selenium interstitials constitute the mobile defects during selenium self diffusion in CdSe. If this model is

correct then heat treatment of crystals in selenium vapour should increase the selenium interstitial content. As no sensitising centres were found in such crystals it appears that these cannot be associated with selenium interstitials. Further, if interstitials are the diffusing defects, the concentration of cadmium vacancies should not be appreciably altered by the annealing treatment. Therefore it is possible that the sensitising centres are cadmium vacancies as suggested by Bube and Barton.

Results have been presented in sections 10.4 and 10.7 which suggest that the changes in free electron lifetime described in section 6.5 cannot be attributed to variations in the density of the 0.6 ev sensitising centres. This phenomenon is discussed further in the following chapter where it is shown that the reduction in lifetime is due to the photochemical creation of fast recombination centres.

References

Bube, R.H., 1955, Phys. Rev., 99, 1105.

Bube, R.H., 1957, J. Phys. Chem. Solids, 1, 234.

Bube, R.H., 1964, J. Appl. Phys., 35, 586.

Bube, R.H., and Barton, L.A., 1958, J. Chem. Phys., 29, 128.

Stupp, E.H., 1963, J. Appl. Phys., 34, 163.

Woodbury, H.H., and Hall, R.B., 1966, Phys. Rev. Letters, 17, 1093.

CHAPTER 11

Superlinearity measurements

11.1 Introduction

Measurements of photocurrent as a function of intensity of illumination were used to investigate the nature of the reduction in lifetime which occurred when crystals were irradiated at progressively increasing temperatures. Only two cooling schedules were considered (a) cooling a crystal from 400°K in the dark, and (b) cooling from 400°K under intense white light. These were the treatments which produced the greatest difference in lifetime. In each case, after cooling, the crystal was held at 90°K under irradiation for 10 minutes before making the measurements. This was to ensure that the measurements were not affected by time dependent trap filling.

The measurements were obtained from crystals illuminated by monochromatic light of wavelength 0.70 μ (band width 720 A°) i.e. radiation of approximately band gap energy. This radiation was derived from a monochromator with a tungsten lamp source. Variation of the illumination intensity was achieved by altering the lamp filament current. The procedure, after suitably cooling a crystal, was to set the required intensity and then to heat the crystal while monitoring the current. These measurements of photocurrent against temperature were later converted to show the

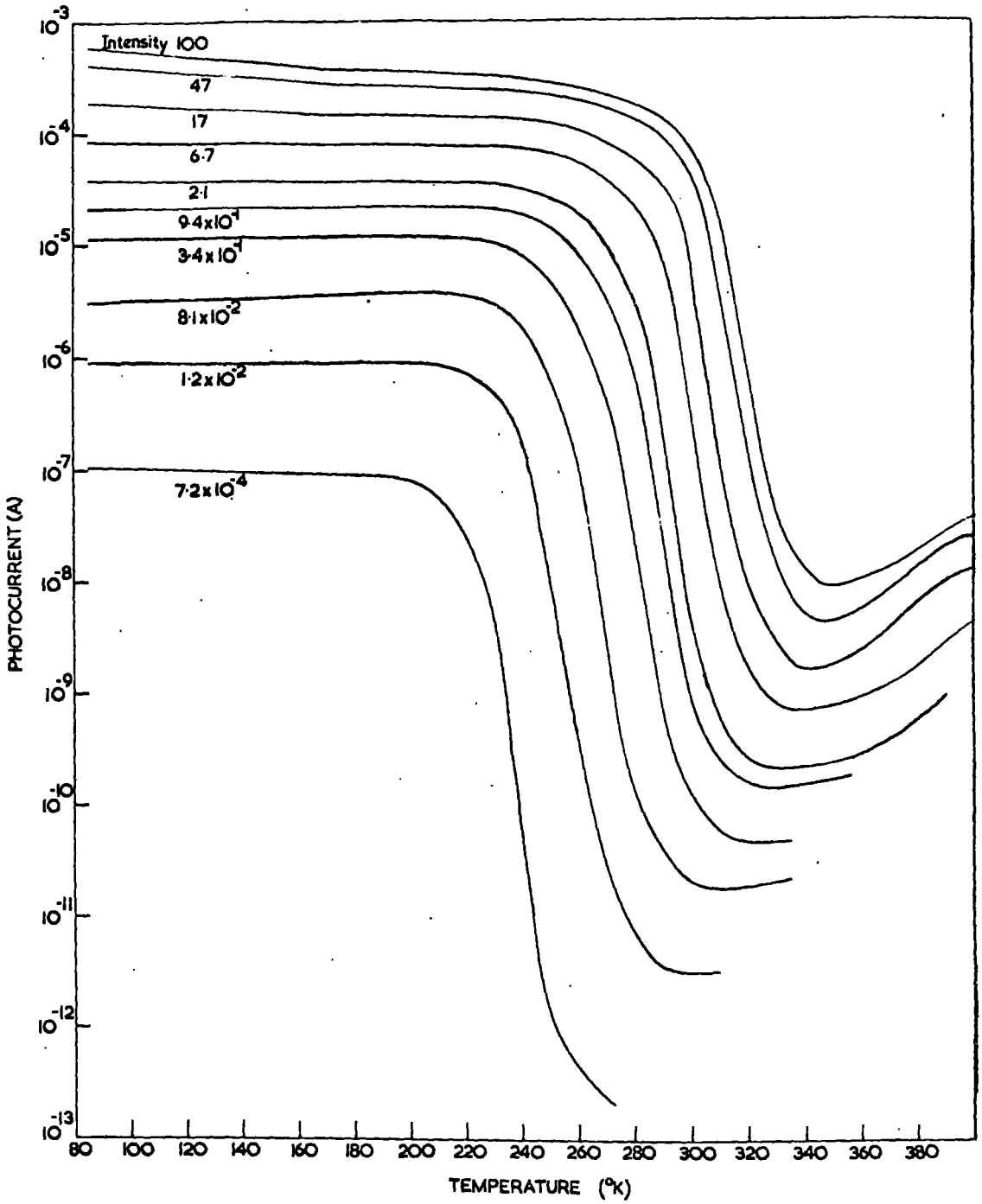

FIGURE II.2.1. Photocurrent vs temperature measurements obtained after cooling a crystal in the dark.

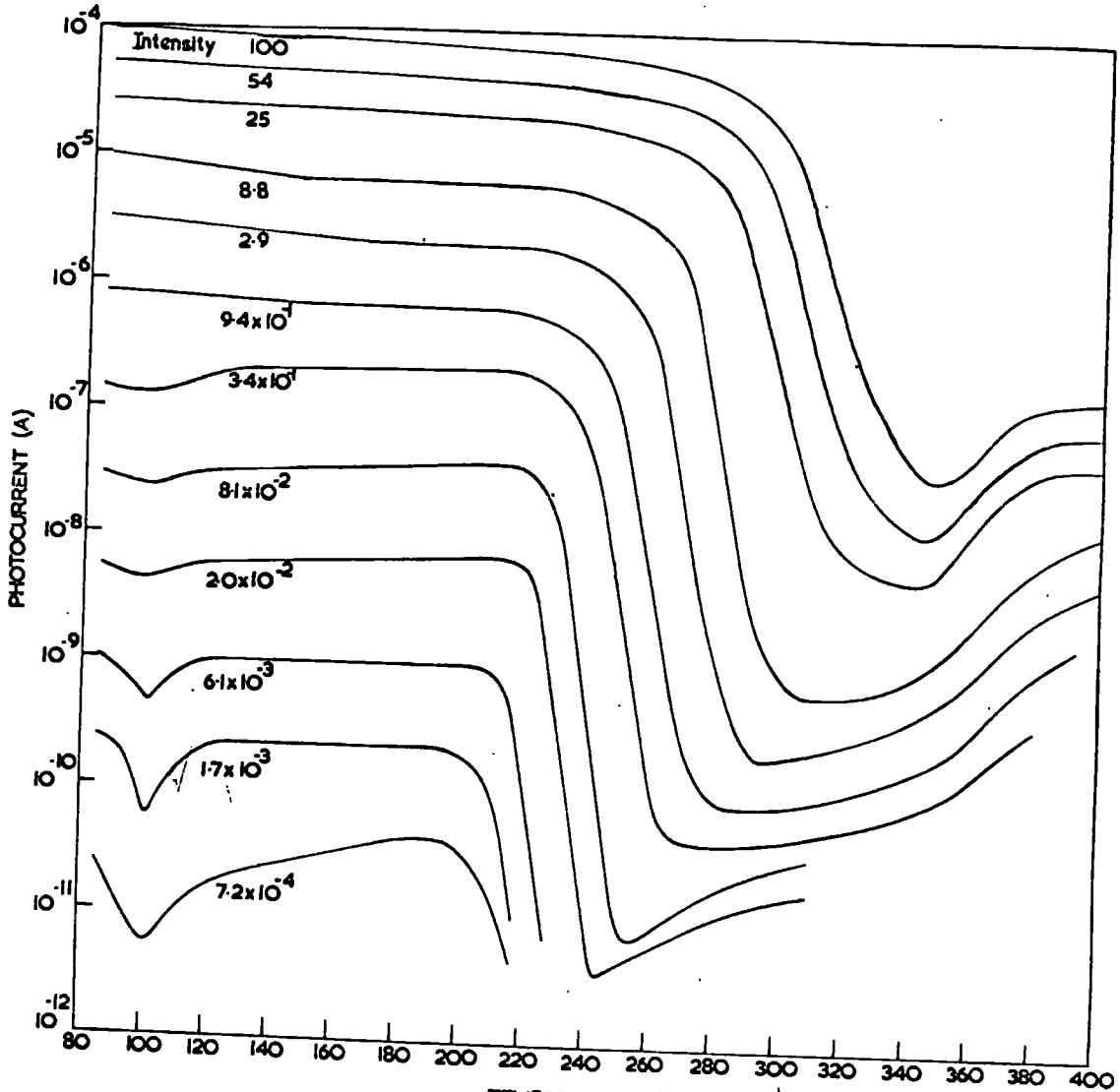

FIGURE II.2.2. Photocurrent vs temperature measurements obtained after cooling a crystal from 400°K under illumination.

dependence of photocurrent on illumination intensity at fixed temperatures.

11.2 Photocurrent vs temperature measurements

In figure 11.2.1 a set of curves at different light intensities, obtained after cooling an as grown crystal from 400°K in the dark, are presented. Figure 11.2.2 shows the curves measured after cooling the crystal from 400°K under illumination. In both cases the appropriate dark currents were subtracted from the measured photocurrents to obtain the true values. The light intensities quoted in figures 11.2.1 and 11.2.2 are in arbitrary units (one arbitrary unit corresponds to approximately 10^{11} photons per second).

The curves in figure 11.2.2 demonstrate an unusual feature. For light intensities less than about 1 arbitrary unit there is a minimum in the current at about 100°K. It is likely that this is due to a decrease in lifetime caused by the emptying of shallow hole traps.

11.3 Superlinearity after cooling in the dark

The measurements illustrated in figure 11.2.1 were converted to display values of electron density as a function of illumination intensity at different temperatures and are presented in figure 11.3.1. A superlinear dependence of photocurrent upon light intensity, with slopes between 2.3 and 3.4, is found in the temperature range 240 to 320°K. However the upper and lower breakpoints of superlinearity are not very

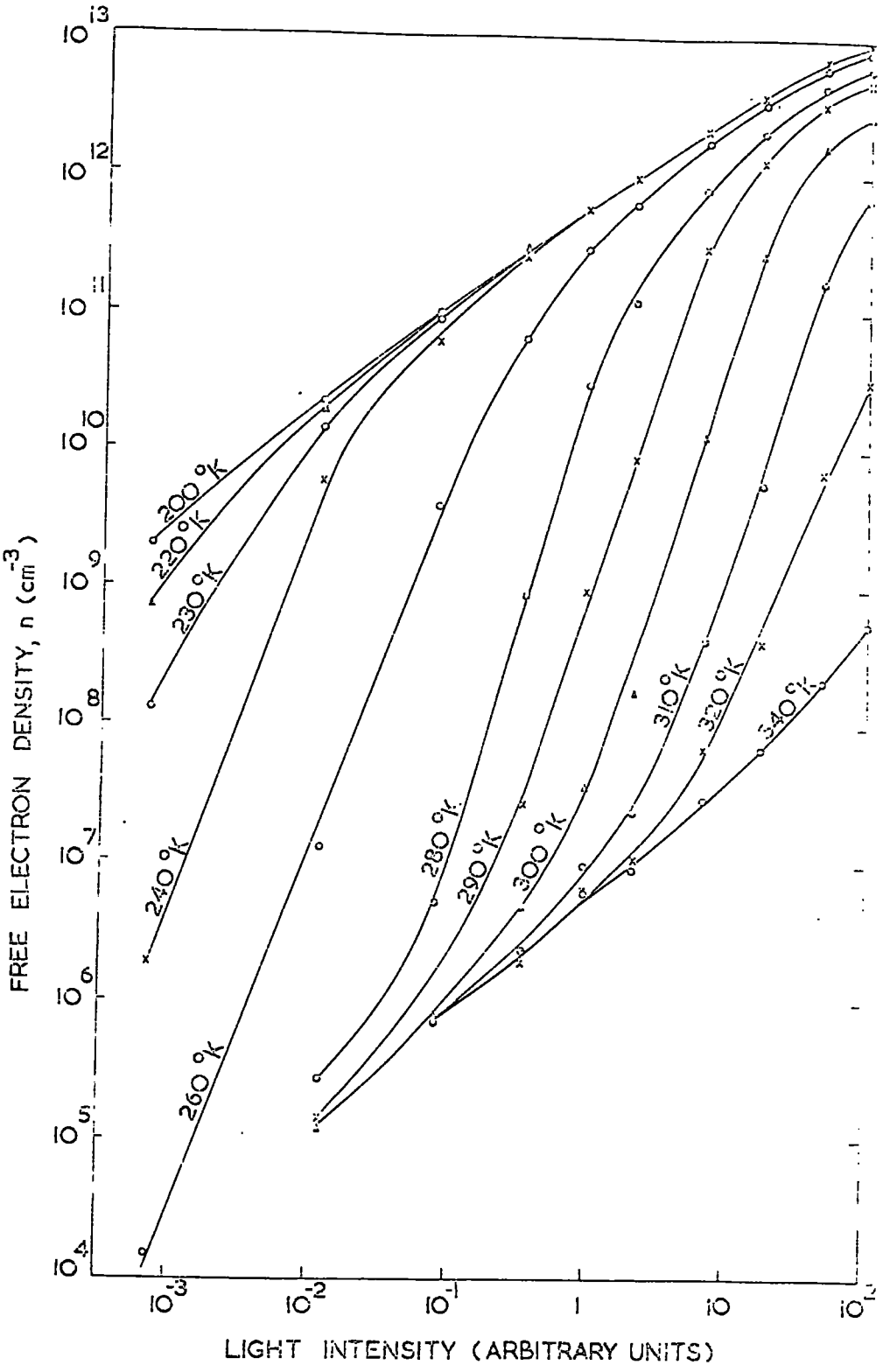

FIGURE II.3.1. Superlinearity of photocurrent obtained after cooling a crystal in the dark prior to the measurements.

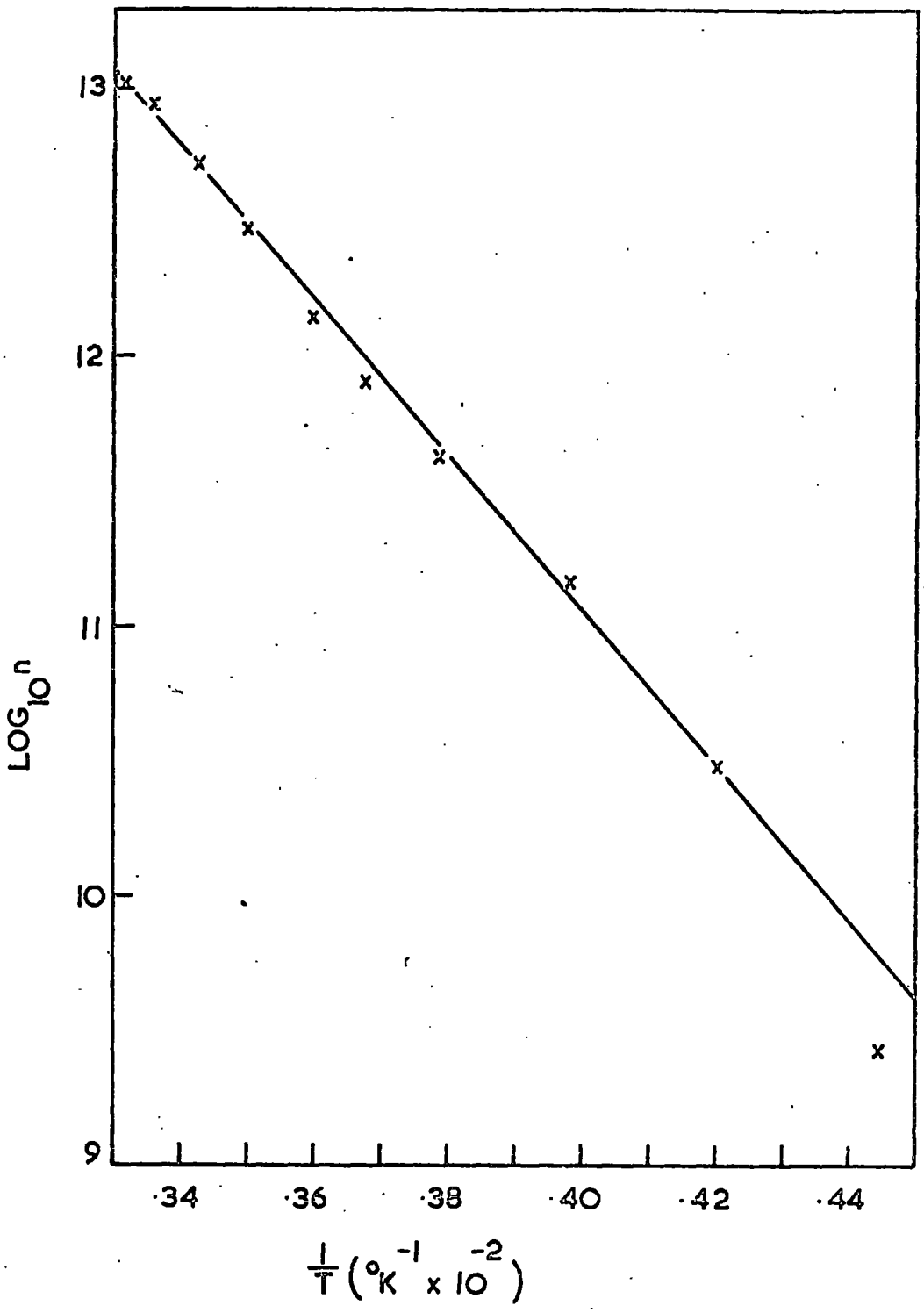

FIGURE II.3.2. Upper breakpoints of superlinearity after cooling in the dark.

clearly defined. Two unusual features are observed.

(a) In the range 240 to 320°K an increase in temperature results in a quenching of the photocurrent above the upper breakpoint.

(b) Below 240°K this quenching is not observed but the degree of superlinearity decreases until by about 200°K the response is completely sublinear.

Stupp (1963) found similar results to (a) and (b) from measurements made on CdSe sintered layers but could not account for the effects. Dussel and Bube (1966) suggested that the effects observed by Stupp are associated with the onset of significant recombination via shallow trapping centres.

The breakpoints in figure 11.3.1 are not sufficiently well defined for them to be estimated with any reasonable accuracy. However the upper breakpoints can be derived from figure 11.2.1. They are taken to be the intersections of the projected curves prior to and following the onset of thermal quenching. It is again difficult to estimate the positions of the lower breakpoints. The upper breakpoints obtained in this way are plotted in the form of ln n (free electron density) against reciprocal temperature in figure 11.3.2. The slope of this line corresponds to an energy of 0.58 ev. This is in good agreement with the value of 0.6 ev found for the position of the sensitising centres above the valence band from the measurements described in Chapter 10.

The conditions which are associated with the upper breakpoints of superlinearity, after Dussel and Bube (1966), have been summarised in section 2.7. For discrete trapping levels two conditions lead to a plot of ln n vs 1/T having a slope associated with the height of the class 11 levels above the valence band. These conditions are (1) $n > P_{h2}/\beta_{e2}$, and (2) $R_2 > R_1$. It is not possible to distinguish which of these conditions applies to the data plotted in figure 11.3.2.

11.4 Superlinearity after cooling under illumination

When the measurements presented in figure 11.2.2 are replotted as free electron density against intensity of illumination the curves are very similar to those in figure 11.3.1 with the exception that superlinearity is still observed at temperatures down to 90°K. A dependence of $n \propto F^{1.3}$ is observed at this temperature.

Figure 11.4.1 depicts the dependence of photocurrent on intensity at 90°K after the two different cooling schedules. The fact that superlinearity is observed after cooling under illumination but not after cooling in the dark is well demonstrated. In the superlinear region the effect of a decrease in temperature on the occupancy of the various recombination centres is to increase the transfer of holes from the class 1 to the class 11 centres. Thus the recombination traffic is shifted away from the class 1 centres. It is the end of this transfer process which essentially determines the

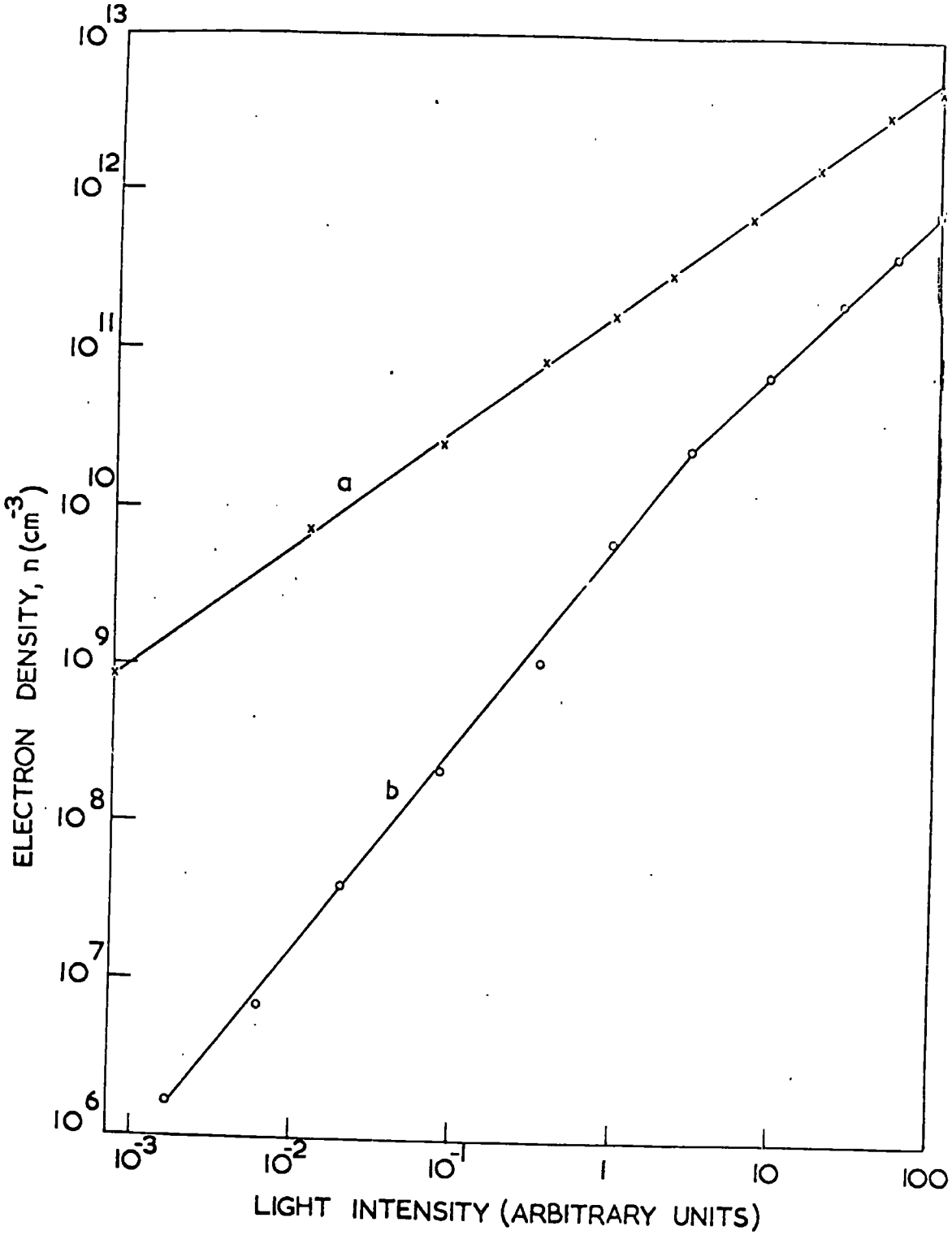

FIGURE 11.4.1. The dependence of photocurrent upon light intensity at 90°K after cooling a) in the dark b) from 400°K under illumination.

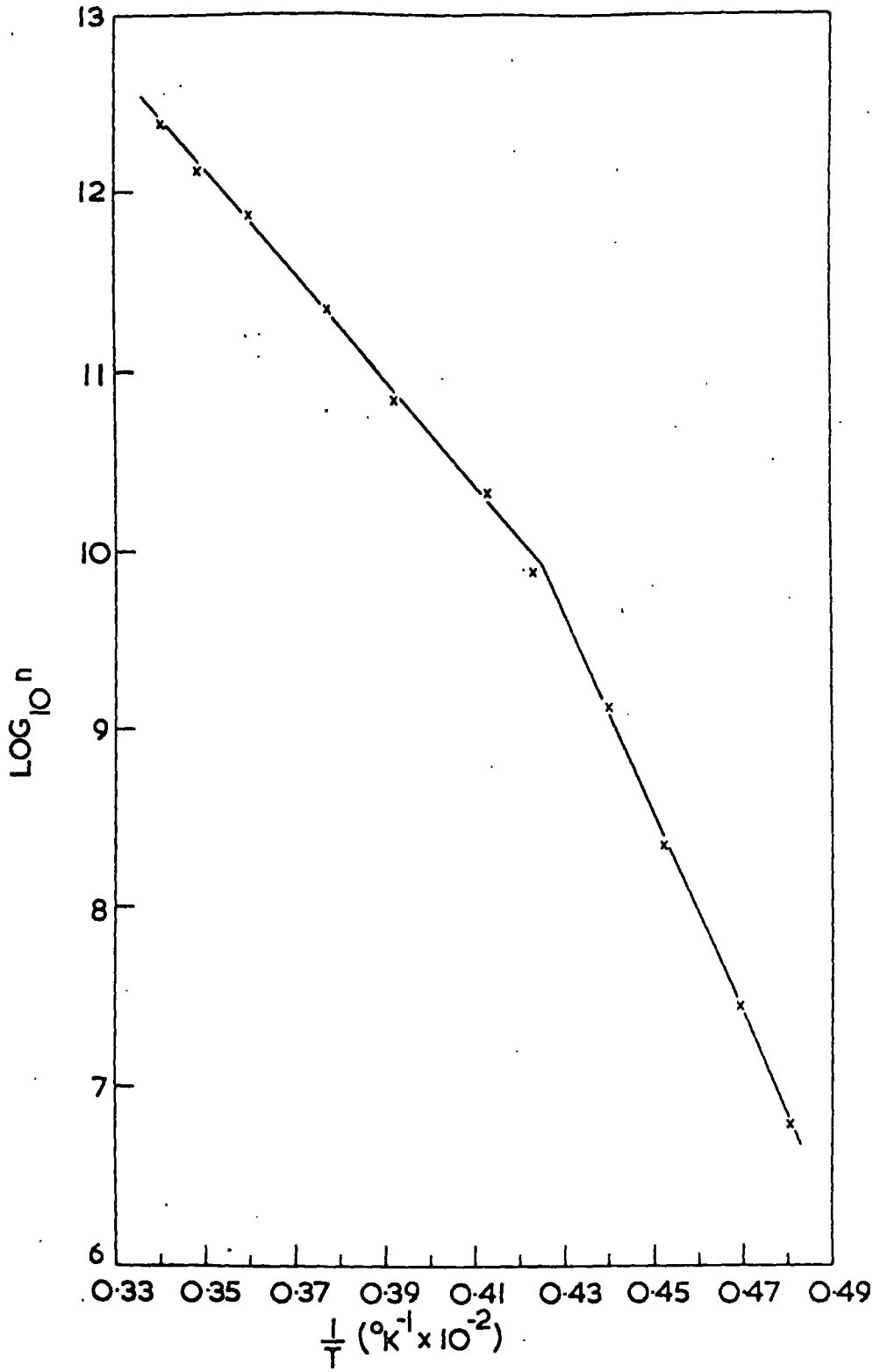

FIGURE II.4.2. Upper breakpoints of superlinearity after cooling from 400°K under continuous illumination.

end of superlinearity. The occurrence of superlinearity at 90°K after cooling the crystal under illumination therefore indicates that after this treatment there is an increase in the class 1 recombination traffic. It is suggested that this is due to the photochemical creation of class 1 centres as a result of the illumination at elevated temperatures during cooling. This could take three forms.

(1) An increase in the density of those centres already present. However this is not thought to be the case. This is because the effect of heating to 400°K in the dark is to dissociate the new centres. If these are of the same nature as the original centres then it is to be expected that such heating would destroy the original centres also. This did not happen.

(2) The creation of an extra density of centres which are of a different nature from those already present.

(3) A further possibility is that under irradiation the original centres associate with other defects. There would not be an increase in the density of fast recombination centres in this case. However an increase in recombination would still occur if the new centres have larger capture cross sections for electrons and holes than the original centres.

Whichever of the above processes does in fact occur the creation of the new class 1 centres results in the observed reduction in free electron lifetime. This model explains two

effects mentioned in Chapter 10 which are incompatible with the idea of the decrease in lifetime being due to a significant change in the density of sensitising centres. These effects are (a) the fact that crystals cooled from 400°K under irradiation exhibit infra red quenching, and (b) the observation that the variation in lifetime also occurs in crystals annealed in selenium vapour and which do not appear to have any appreciable density of sensitising centres.

Upper breakpoints of superlinearity, after cooling from 400°K under continuous illumination, were derived from the thresholds of thermal quenching of the curves in figure 11.2.2. These are plotted in the form of ln n against 1/T in figure 11.4.2. A twofold linear dependence is found. The slope of the line at high illumination intensities (high values of n) has an associated energy of 0.58 ev. This is in agreement with the value derived from figure 11.3.2. However at low light intensities the slope yields an energy of 1.13 ev. It is difficult to assign this energy to any particular level as it does not correspond to either the depth of electron traps or the height of the sensitising centres. According to Dussel and Bube (1966) these are the only energies which can be derived from data associated with the upper breakpoints of superlinearity. However the model put forward by these authors does not predict the possibility of a twofold dependence such as is illustrated in figure 11.4.2. Thus it

appears that their analysis is incomplete. It may be significant that the particular cooling schedule under consideration results in the creation of new class 1 centres. These would influence lifetime to a greater extent at low light intensities than at high light levels. Therefore it is possible that the value of 1.13 ev derived from figure 11.4.2 is associated with these new centres.

11.5 Saturation of photoconductivity

It is possible, using high levels of illumination (above the superlinear range), to obtain a saturation of photoconductivity. Measurements of this type were made but their interpretation proved difficult. They have therefore not been included in the main part of the thesis but are briefly discussed at the end in Appendix 11.

References

Dussel, G.A., and Bube, R.H., 1966, J. Appl. Phys., 37, 13.

Stupp, E.H., 1963, J. Appl. Phys., 34, 163.

CHAPTER 12

Photoluminescence

12.1 Introduction

The experimental arrangement used for the measurement of photoluminescence has been described in section 5.6. Spectra were recorded on a chart and later corrected for the variation with wavelength of the sensitivity of the lead sulphide detector. As described in 5.6 the filtered radiation from a high pressure mercury lamp was used to excite the luminescence. However when luminescence was studied after a crystal had been cooled from a particular temperature under illumination the irradiation during cooling was provided by the 750 Watt tungsten lamp used in the T.S.C. work. This was to ensure the validity of a comparison between the luminescence measurements and results described in the preceding chapters. After cooling the mercury lamp was again used to excite the luminescence.

12.2 High resistivity crystals

After cooling a high resistivity crystal in the dark the subsequent luminescence spectrum measured at $90^{o}K$ usually exhibited a peak at $0.95 \pm 0.02\ \mu$ with a long wavelength tail or shoulder. This is shown in curve (a) of figure 12.2.1. When the crystal was cooled under illumination from progressively higher temperatures prior to the measurements the $0.95\ \mu$ emission band decreased in intensity slightly and the long

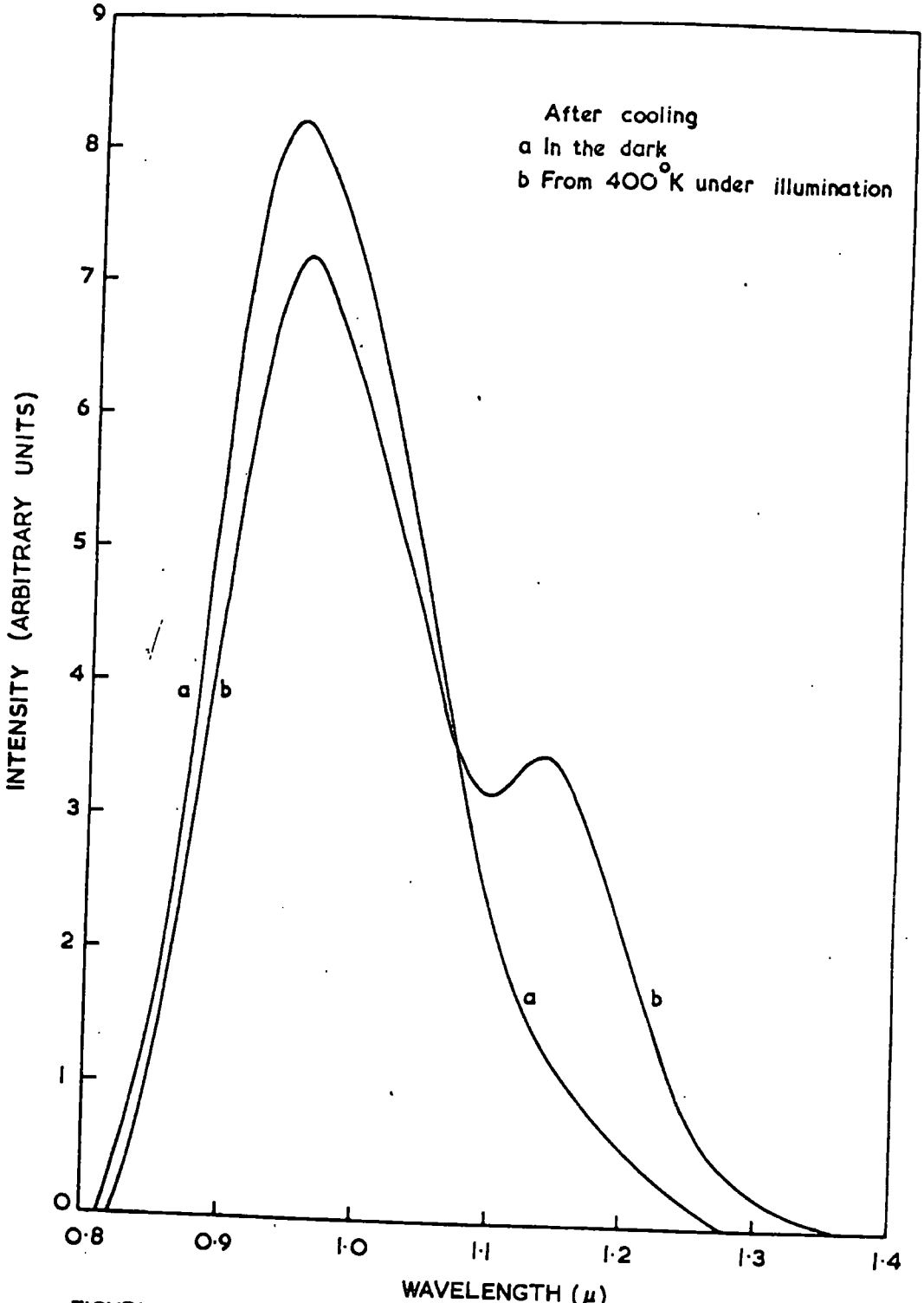

FIGURE 12.2.1. Photoluminescence of high resistivity crystal at 90°K

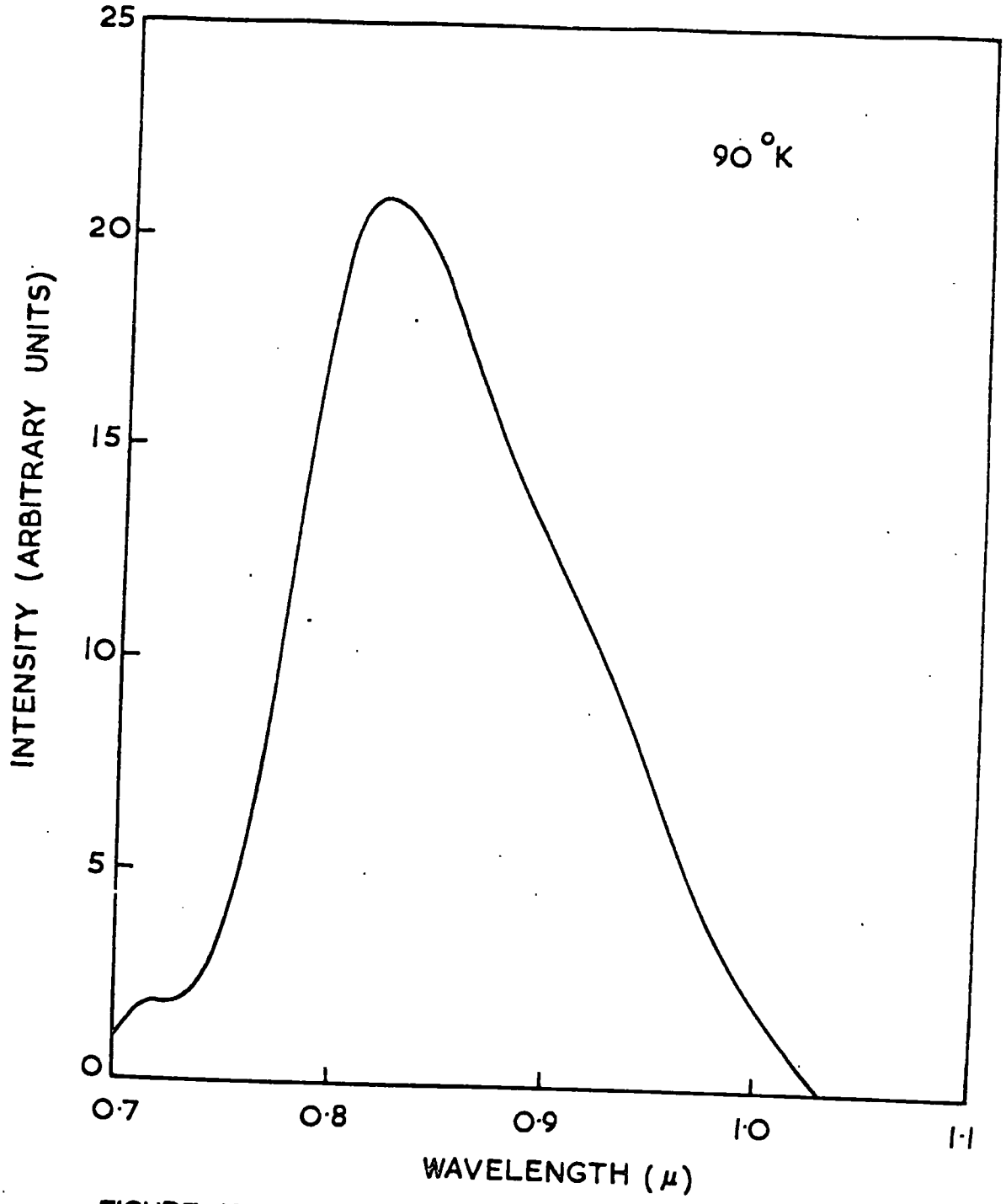

FIGURE 12.3.1. Photoluminescence of low resistivity crystal

wavelength shoulder increased until it was resolved as a separate peak. This second maximum occurred at 1.15 ± 0.03 μ. Curve (b) in figure 12.2.1 shows the luminescence spectrum obtained after cooling the crystal from 400°K under continuous illumination. However some crystals did not exhibit any detectable 1.15 μ luminescence, the 0.95 μ band only being found. No detectable band edge luminescence or other infra red emission up to 3 μ was observed in the high resistance crystals.

12.3 Low resistivity crystals

An example of the luminescent spectra at 90°K of low resistivity (about 1Ωcm) crystals is shown in figure 12.3.1. There is a predominant peak at 0.82 ± 0.01 μ with a shoulder at about 0.9 μ. This shoulder is probably due to a small overlapping 0.95 μ band i.e. the same as that discussed in section 12.2. There is also a small peak at 0.72 μ corresponding to band edge emission. The effect of illumination during cooling on the luminescence of these crystals was not examined. However it was found that after copper doping or annealing in selenium vapour these crystals emitted no detectable luminescence of any wavelength.

12.4 Temperature dependence of luminescence intensity

The temperature dependence of the intensity of the various emission bands was measured by heating crystals at a similar rate to that used in T.S.C. measurements and monitoring the

luminescence under consideration. Results of these measurements are presented in figures 12.4.1 and 12.4.2. In these curves 100% efficiency is equivalent to the maximum intensity measured. It was found that the 0.95 μ emission was thermally quenched above about 150°K. Thermal quenching of the 0.82 μ emission occurred above 100°K. However there was appreciable 1.15 μ luminescence over the whole temperature range considered (i.e. up to 400°K).

In the Schon-Klasens model of luminescence thermal quenching is controlled by the occupancy of the ground state luminescence centres. As the temperature is raised the number of centres occupied by electrons increases because of the increase in the probability that an electron in the valence band can be thermally excited to the c entres. Since electrons in the excited state cannot make transitions into electron occupied levels the luminescence efficiency, η , decreases. The thermal quenching of the luminescence is described by

$$\eta = \frac{1}{1 + C \exp(-W/kT)} \qquad 12.4.1$$

Where W is the energy of the levels of the luminescent centres above the valence band and C is a constant. A plot of $\ln\left(\frac{1}{\eta} - 1\right)$ against 1/T should give a straight line of slope W. This criterion was applied to the regions of thermal quenching in the durves of figure 12.4.1 and the results are plotted in figure 12.4.3. In each case a linear dependence over a substantial part of the curve was obtained. The values of W

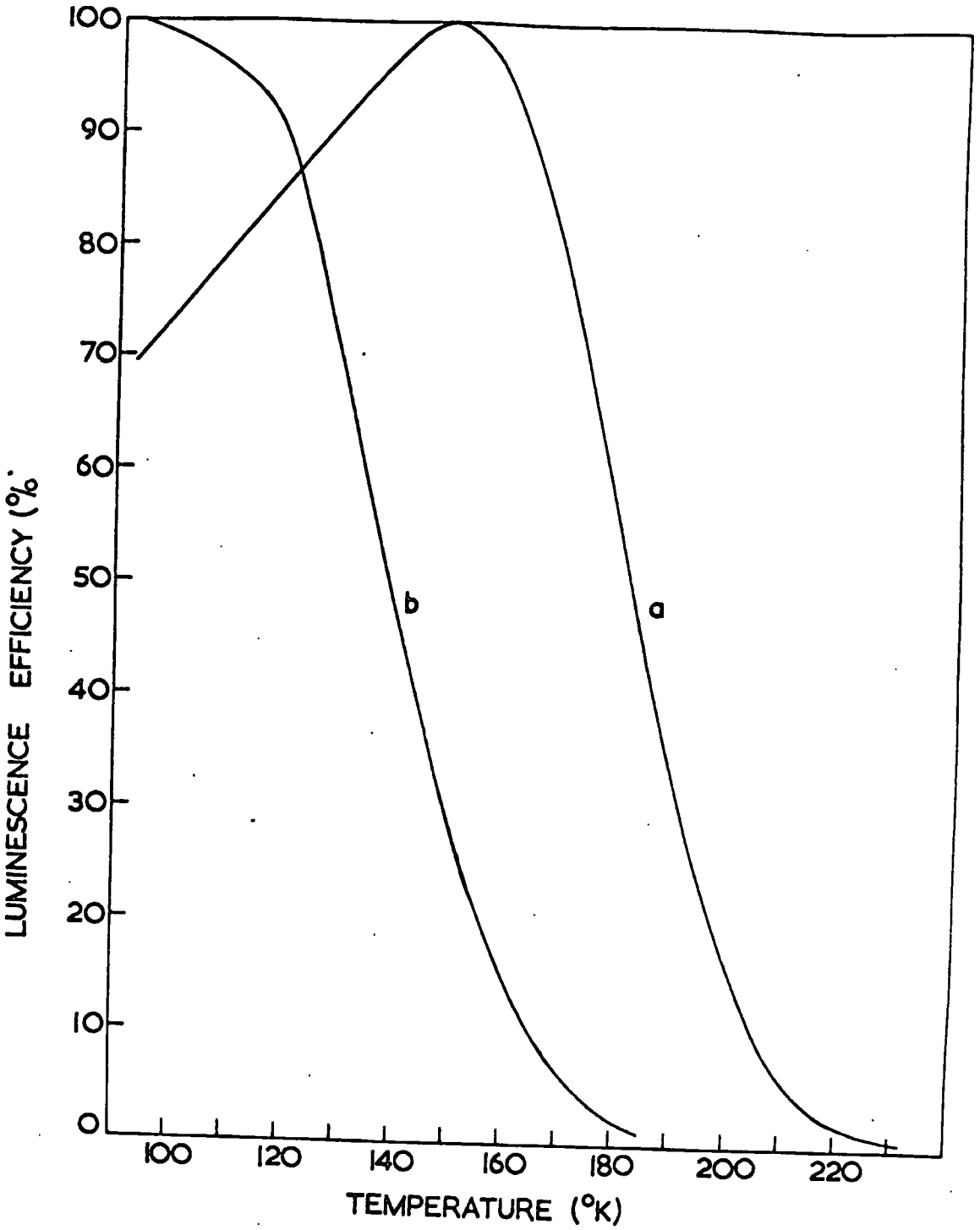

FIGURE 12.4.1. Temperature dependence of the intensity of the a)0·95μ and b)0·82μ luminescence bands.

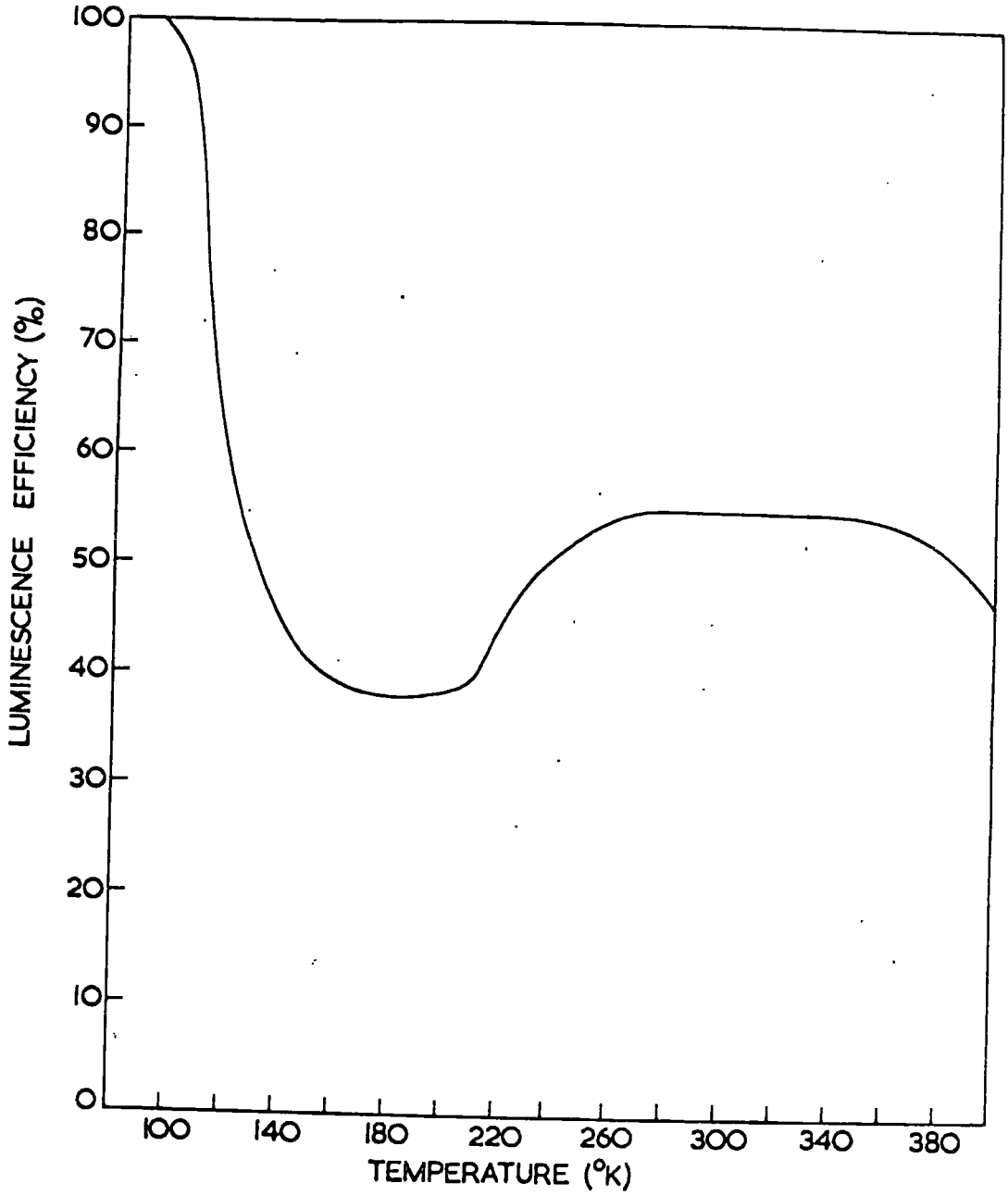

FIGURE 12.4.2. Temperature dependence of the 1·15μ luminescence intensity.

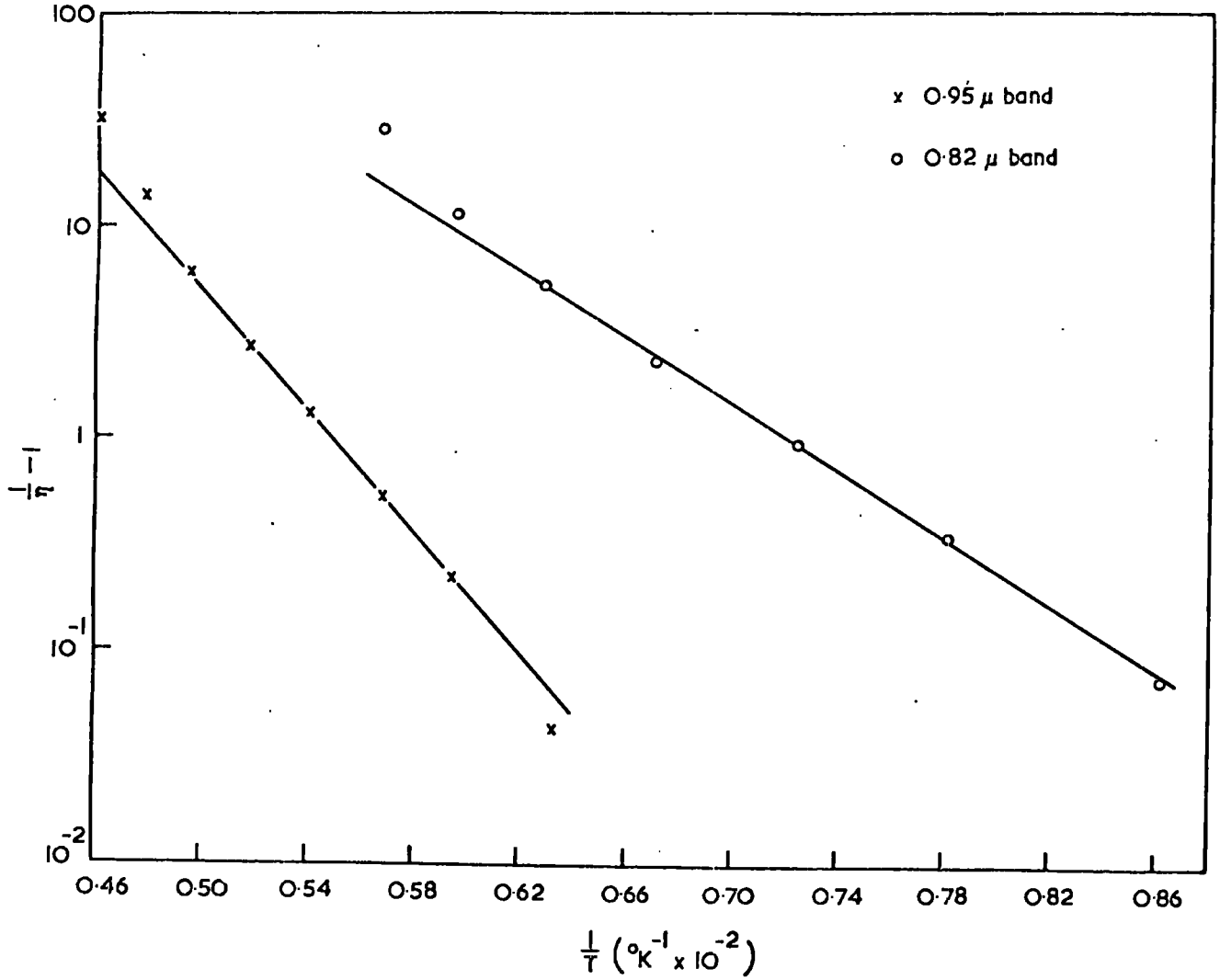

FIGURE 12.4.3. Application of equation 12.4.1. to the thermal quenching of luminescence.

derived from the respective slopes are

(a) For the 0.95 μ emission, W = 0.28 ev.

(b) For the 0.82 μ emission, W = 0.15 ev.

A suitable application of equation 12.4.1 could not be made in the case of the 1.15 μ luminescence because of the absence of any well defined region of thermal quenching.

12.5 Other published results on I.R. luminescence in CdSe

Infra red luminescence has been reported by other workers for both CdSe phosphors and crystals. Garlick and Dumbleton (1954) found luminescence at 0.9 and 1.2 μ in copper activated phosphors at 90°K. The 1.2 μ emission only was observed at room temperature. Avinor and Meijer (1960) studied the luminescence of phosphors activated by various dopants. They attributed the 0.92 μ emission to silver impurities and a 1.2 μ band to copper impurities (both these dopants were introduced in conjunction with indium used as a donor). A further peak at 1.46 μ was found in the spectra of gold doped phosphors. Hoschl and Konak (1963) observed 0.97 μ emission in flow crystals grown from the elements by a technique similar to that described in Chapter 4. Their crystals were not deliberately doped. Luminescence bands centred at 0.81 and 0.86 μ were observed in the spectra of undoped crystals by Halsted, Aven and Coghill (1965).

The effect of electron radiation damage, with electron energies up to 1 Mev, on the luminescent emission of CdSe

crystals has been reported by Kulp (1966) and Schulz and Kulp (1967). Kulp found a 0.93 μ band at 77°K prior to bombardment. Electron bombardment at this temperature produced a further emission peak at 1.25 μ. The 0.93 μ luminescence was thermally quenched above 170°K whereas the 1.25 μ emission intensity decreased above 375°K. Both of these bands disappeared after crystals had been annealed at temperatures above 500°C in an excess of either cadmium or selenium vapour. Kulp quoted impurity contents of less than 1 ppm. of both silver and copper in his crystals. Schulz and Kulp carried out radiation damage experiments on crystals at liquid helium temperature. The luminescence band produced by bombardment at this temperature had a peak in the range 1.08 to 1.17 μ. This emission could be removed by annealing the crystal above 62°K. The 0.93 μ luminescence was generally found to disappear when a crystal was cooled from 77 to 4.2°K. Considering the results of the electron bombardment damage at both temperatures Schulz and Kulp suggested that the 1.08 to 1.17 μ damage band is associated with the displacement of cadmium atoms and the 1.25 μ emission is related to the displacement of selenium atoms. They concluded that the luminescence centres are probably complex associations of defects.

12.6 Discussion of luminescence in high resistivity crystals

It would be convenient to assign the 0.95 μ and 1.15 μ

luminescence bands to transitions involving either the class 1 or class 11 centres. However such a simple energy level picture cannot be obtained.

The class 11 centres lie at levels 0.6 ev above the valence band. Transitions from the conduction band to these levels, if radiative, would result in the emission of photons of energy 1.22 ev at 90°K (the band gap at this temperature is 1.82 ev). This is fairly close to the photon energies of both the 0.95 μ and 1.15 μ luminescence, which correspond to 1.30 ev and 1.08 ev respectively. However it is probable that the 1.15 μ emission is not due to transitions to the sensitising centres because the intensity of the luminescence increased as a result of irradiation at high temperatures. Such irradiation creates fast recombination centres. The resultant increased recombination via these centres should cause a decrease in recombination via the class 11 centres (and via any other centres present). There should be no increase in the number of transitions to the sensitising centres.

Illumination at elevated temperatures brought about a decrease in the intensity of the 0.95 μ luminescence. This is compatible with this emission being due to transitions involving the class 11 centres. However if such is the case then the Schon-Klasens model of thermal quenching should apply. The results of this type of analysis, given in section 12.4, indicate that the 0.95 μ luminescence is associated with levels

lying at 0.28 ev above the valence band. This energy does not correspond to that of the class 11 centres. No account has so far been taken of a possible difference between thermal and optical activation energies. However there is agreement for the position of the sensitising centres deduced from both optical (infra red quenching and spectral dependence of photoconductivity) and thermal (superlinearity and thermal quenching of photoconductivity) measurements. It therefore appears that there is no optical/thermal shift and thus the 0.95 μ emission cannot be attributed to transitions to the sensitising centres.

Developing the results of the thermal quenching analysis, it is suggested that the 0.95 μ emission is due to transitions from excited states lying 0.24 ev below the conduction band to ground state centres at 0.28 ev above the valence band. In such a model thermal quenching would be at least partially determined by the thermal release of electrons from the shallow centres and thus the Schon-Klasens model would not be strictly applicable. However the slope of a plot of ln $(\frac{1}{\eta} - 1)$vs 1/T should be a combination of 0.24 and 0.28 ev. This is very close to the value of 0.28 ev actually obtained. Further, the excited states at 0.24 ev below the conduction band may correspond to one of the groups of low temperature traps discussed in Chapter 7, most probably to the group associated with either the 150°K, 160°K or 175°K T.S.C. peak.

Although a simple thermal quenching behaviour was not observed for the 1.15 μ luminescence it seems that the onset of true thermal quenching occurs at about 360°K. This suggests that the associated centres are quite deep. Two simple models would be consistent with this result. These are (1) transitions from the conduction band to luminescent centres with levels lying at 0.74 ev above the valence band, and (2) transitions to the valence band from excited states lying at 0.74 ev below the conduction band.

A possibility is that the 1.15 μ centres correspond to the class 1 centres. Two pieces of evidence support this conclusion.

(a) The increase in the intensity of luminescence following a cooling treatment which causes an increase in recombination via the class 1 centres.

(b) From one of the linear ranges of figure 11.4.2 an energy of 1.13 ev, possibly associated with the class 1 centres, was obtained. There is a reasonable measure of agreement between this value and the photon energy, 1.08 ev, of the 1.15 μ emission.

However it is difficult to explain why, if the 1.15 μ luminescence is due to transitions involving the fast recombination centres, some crystals were found which did not display this emission.

12.7 0.82 μ Luminescence

The thermal quenching of the 0.82 μ (1.51 ev) emission occurs at quite low temperatures. This shows that the associated centres are shallow. From curve (b) in figure 12.4.3 the position of the ground state centres was deduced to lie at 0.15 ev above the valence band. The excited states in this case would lie at 0.16 ev below the conduction band. This does in fact correspond quite well to the depth (0.15 ev) of the 105°K low temperature traps. If these levels are associated with the excited luminescence states then the emptying of the traps could also account for the observed thermal quenching. A further interesting point is that in section 11.2 evidence was seen, from measurements of photocurrent against temperature, of the release of holes from shallow centres at about 100°K. Such centres could well be the ground states of the 0.82 μ emission.

12.8 Other materials

In conclusion it is interesting to try to relate the I.R. luminescence found in CdSe with the emission observed in the more widely studied CdS and ZnS.

It has recently been suggested by Bryant and Cox (1965) that some of the I.R. luminescence bands in CdS and ZnS are due to transitions from a luminescent centre to the various branches of the valence band. The band structure of CdSe has been discussed in section 1.3 where it was seen that a third

valence band lies at a position 0.43 ev below the upper band. Transitions from an excited state with levels lying at 1.08 ev above the upper valence band and also the third valence band could result in the observed 1.15 and 0.82 μ emission. However such a model is not consistent with the difference in the thermal quenching found for these two luminescence bands.

Halsted, Aven and Coghill have considered the possibility of luminescence bands in different II-VI compounds being related to similar centres. They considered measurements made by both themselves and other workers and tried to find correspondence between the various emission bands. The so called "blue" (0.43 μ) and "green" (0.52 μ) emission in ZnS is of interest. A study of the emission from ZnS-CdS solid solutions showed that the corresponding bands in CdS occur at 0.78 and 1.02 μ. There have been no reported measurements of the corresponding luminescence wavelengths in the CdS_xSe_{1-x} system. However Halsted et al suggested that the 1.2 μ emission reported by Avinor and Meijer corresponds to the 0.52 and 1.02 μ luminescence in ZnS and CdS respectively. All these bands are associated with copper impurities. There is some doubt as to the emission in CdSe that is equivalent to the "blue" emission in ZnS. This is because only one centre associated with copper has been identified in CdSe. However, with reference to the present work, it is suggested that the

0.95/1.15 μ luminescence may be analagous to the "blue" and "green" bands in zinc sulphide.

References

Avinor, M., and Meijer, G., 1960, J. Chem. Phys., 32, 1456.

Bryant, F.J., and Cox, A.F.J., 1965, Brit. J. Appl. Phys., 16, 463.

Garlick, G.F.J., and Dumbleton, M.J., 1954, Proc. Phys. Soc., B67, 442.

Halsted, R.E., Aven, M., and Coghill, H.D., 1965, J. Electrochem. Soc., 112, 177.

Hoschl, P., and Konak, C., 1963, Czech. J. Phys. B, 13, 364.

Kulp, B.A., 1966, J. Appl. Phys., 37, 4936.

Schulz, H.J., and Kulp, B.A., 1967, Phys. Rev., 159, 603.

CHAPTER 13

Summary and suggestions for further work

13.1 General Considerations

In Chapters 6 to 12 various measurements made on CdSe flow crystals have been described. An attempt has been made to interpret and discuss the results of these measurements in the appropriate chapters. It is hoped that the order of presentation has been such that reasonable continuity has been achieved and the relationship between the various results has become progressively apparent. However it is the purpose of this chapter to briefly summarise the implications of the results. Also, as a consequence of these results, suggestions for future work are made.

13.2 Trapping levels

Three different groups of traps were found, with a total of 14 discrete levels being identified. In some instances an analysis of the parameters associated with the different traps proved difficult. This was because either the overlapping of the T.S.C. peaks or large changes in free carrier lifetime prevented the measurement of true, isolated peaks. However the data that has been obtained concerning the various traps is listed in table 13.1. Also summarised in this table are the values of E_i calculated using the equation

$$E_i = 0.63 - 0.04046\ i + 0.00027\ i^2 \qquad 13.2.1$$

This is the procedure adopted by Faeth (1968), previously

Table 13.1. Traps in CdTe.

Trap group	Peak temperature (^{o}K)	Trap depth (ev)	Cross section (cm^2)	Density (cm^{-3})	i	E_i (ev)
Low temperature	105	0.15	10^{-18}	10^{12} to 10^{14}	13	0.15
	115			"	12	0.18
	130			"	11	0.22
	150	to		"	10	0.25
	160			"	9	0.29
	175			"	8	0.32
	200	0.36		"	7	0.36
Intermediate temperature	215			At least 10^{15}	6	0.40
	230	0.46	10^{-16}	"	4	0.47
	250			"	2	0.55
	270			"	1	0.59
High temperature	295	0.43			5	0.43
	335	0.52	10^{-20}	10^{17}	3	0.51
	365	0.63	10^{-19}	10^{19}	0	0.63

mentioned in Chapter 7, in which the trapping spectrum is described in a similar way to that used in the evaluation of molecular spectra. The trap depths used to calculate the constants in 13.2.1 were 0.63, 0.36 and 0.15 ev. It can be seen that the 0.43, 0.46 and 0.52 ev traps fit into the pattern quite well. Further, it is reasonable that some of the intermediate temperature traps have deeper energy levels than traps which empty at higher temperatures. This is simply a consequence of the respective cross sections. However these considerations do not definitely prove that 13.2.1 does indeed accurately describe the trapping distribution in CdSe.

13.3 Sensitising centres

The high resistivity, as grown crystals exhibited typical photoconductive gains of 10^4. Corresponding free electron lifetimes were of the order of m secs. The high photosensitivity of these crystals can be attributed to the presence of sensitising centres. These were identified as having energy levels lying at 0.6 $\pm$ 0.02 ev above the valence band. Crystals which had been annealed in selenium vapour did not appear to contain a significant density of these centres.

13.4 Luminescence

Although the positions of trapping levels and sensitising centres have been deduced it has not been possible to formulate an overall picture of the defect (and impurity) centre distribution. This is largely because of an inability to fit

luminescence data in with other measurements i.e. the transitions corresponding to the 0.82, 0.95 and 1.15 μ emissions can not be ascribed to any particular levels. More work on luminescence is required and this must include a determination of the excitation and infra red quenching spectra of the various bands. An attempt was in fact made during the present work to measure excitation spectra. However with the equipment available the intensity of monochromatic light that could be obtained was insufficient to excite any detectable luminescence.

13.5 Photochemical changes in trap density

There are two interesting points concerning the behaviour of the intermediate temperature traps.

(a) The photochemical changes in the density of these traps which occur as a result of illumination at different temperatures.

(b) The appearance of potential barriers at the end contacts as the traps are thermally emptied.

These effects show the relevance of making four probe T.S.C. measurements rather than using the more conventional two probe technique. Also an investigation into the effect of different contacting procedures on these traps, especially the part played by illumination during contacting, should prove of value in gaining more insight into their nature. It may also be possible to study the ohmic nature of the contacts at

temperatures low enough so that although the intermediate temperature traps are empty they have not dissociated. Another variation of experimental technique would be to vary the polarity of an applied potential during the photochemical creation of the centres to see if migration of the defects can be influenced by an external field. This would give information about their charge state and also show whether they move ionically.

13.6 High temperature traps

On the basis of the measurements made it is not possible to decide whether the high temperature traps are created photochemically or are of the type surrounded by repulsive barriers. In order to establish the nature of these centres a technique which permits the measurement of their capture cross section at different temperatures is needed. In this way the existence or otherwise of a potential barrier would be shown. Standard types of T.S.C. measurements and analysis only lead to the cross section effective during the escape of carriers. A possible method to identify traps surrounded by repulsive barriers is given in Appendix 1 at the end of this thesis. This technique is based on the number of traps filled by illumination at different temperatures. In this way an indirect estimate of the variation of capture cross section with temperature would be obtained.

An extension of the four probe measurements to the high

temperature traps may also be significant if they are surrounded by repulsive barriers.

13.7 Photochemical changes in lifetime

It was observed that illuminating a crystal at progressively higher temperatures resulted in a corresponding reduction in free electron lifetime. This was found to be associated with the photochemical creation of fast recombination centres. A comparison with the lifetime variations observed in CdS by other workers is interesting. Cowell and Woods (1967) found that the irradiation of CdS crystals at increasing temperatures brought about an increase in lifetime. These authors attributed this phenomenon to the photochemical creation of sensitising centres. Korsunskaya et al (1966) also found new sensitising centres created in CdS following illumination in the temperature range + 20 to - 100°C.

CdS and CdSe have the same crystal structure and one would also expect them to contain similar defects. The different changes in lifetime described above may be related to the respective positions of defect levels in the two materials. For example in CdSe the sensitising centres lie at 0.6 ev above the valence band whereas the corresponding energy in CdS is 1 ev. Thus these centres empty at a higher temperature in CdS than in CdSe. If such centres take part in photochemical changes then their charge state would be important in determining whether they associate with other defects.

Therefore similar photochemical changes may take place at different temperatures in the two materials. It would be relevant to investigate such effects in mixed CdS_xSe_{1-x} crystals to see whether the transition from the CdS to the CdSe mode of behaviour yields any information concerning the nature of the defect centres. Such measurements should be coupled with T.S.C., infra red quenching and other standard types of measurement.

Luminescence measurements made on mixed crystals would also resolve whether the 0.95/1.15 μ luminescence described in Chapter 12 is analagous to the 0.78/1.02 μ emission in CdS and the "blue" and "green" bands in ZnS.

13.8 Mobility

It is considered that any future work on the properties of CdSe should include measurements of the electron mobility in the high resistivity crystals as there are no published results for such material. Also measurements of mobility made prior to and following the various photochemical changes could be used to gain information concerning the charge states of the centres involved. In order to make mobility measurements, however, larger crystals than can be grown with the flow method described in Chapter 4 will be required. Recently, in this laboratory, a technique has been developed (Clark and Woods, to be published) by which large boules (1 cm diameter x 3 cms long) of CdS can be grown under controlled partial pressures of

the components. Preliminary trials using this technique have shown that it is suitable for growing both CdSe and $CdS_x Se_{1-x}$ crystals also. Such crystals should be used in future work.

References

Clark, L., and Woods, J., to be published.

Cowell, T.A.T., and Woods, J., 1967, Phys. Stat. Sol., 24, K37.

Faeth, P.A., 1968, J. Electrochem. Soc., 115, 440.

Korsunskaya, N.E., et al., 1966, Phys. Stat. Sol., 13, 25.

Appendix 1

A possible method to identify traps surrounded by repulsive barriers

This technique is based on the measurement of the number of traps filled by illumination at different temperatures.

The rate of capture of electrons by a set of discrete traps is given by $S_{tc}v(N_t-n_t)n$, where:

S_{tc} is the capture cross section of the traps.

N_t is the density of the traps.

n_t is the density of filled traps.

v is the thermal velocity of the free electrons.

n is the free electron density.

If illumination is carried out at temperatures below that of the T.S.C. peak maximum, so that the escape of electrons from the filled traps can be ignored, we obtain the rate of trap filling.

$$dn_t/dt = S_{tc}v(N_t - n_t)n \qquad A1$$

During the filling of traps n is not constant as the steady state condition is not reached until all the traps are full. However an approximation that the steady state condition can be considered is used. Thus

$$n = F\tau_n$$

where F is the rate of excitation of electrons per unit volume and τ_n is the free electron lifetime in the steady state.

At each temperature the irradiation to fill the traps is

carried out for the same time and at such an intensity that $F\tau_n$ is the same. Further, if the time of excitation is short then $n_t \ll N_t$. A1 then becomes

$$dn_t/dt = S_{tc} v N_t F \tau_n \qquad A2$$

The solution of A2 gives the density of traps, n_t, filled in time t.

$$n_t = S_{tc} v N_t F \tau_n t \qquad A3$$

A trap surrounded by a repulsive barrier can be filled by an electron either being excited over the barrier or tunnelling through it. The relationships between the two cross sections of such a trap, S_{tc} and S_{te}, in the different cases have been given in equations 9.2.3 and 9.2.4. For convenience these equations are repeated below.

Excitation over the barrier:

$$S_{tc} = S_{te} \exp(-E_b/kT) \qquad (9.2.3)$$

Tunnelling through the barrier:

$$S_{tc} = S_{te} \exp\left[-(E'/kT + \alpha/E'^{\frac{1}{2}})\right] \qquad (9.2.4)$$

In order to obtain the temperature dependence of S_{tc} for the case of tunnelling it is necessary to take into account the temperature dependence of E' (the height above the conduction band at which tunnelling takes place). If the exponential term in 9.2.4 is differentiated with respect to E', at constant T, then the value of E' for the minimum value of the exponential is:

$$E' = (\tfrac{1}{2}\alpha kT)^{3/2}$$

Table 1.

Temperature (^{o}K)	Excitation over the barrier $\exp(-E_b/kT)$	Tunnelling through the barrier $\exp -1.09 \; {}^{3}/(kT)^{\frac{1}{2}}$
400	3×10^{-3}	7×10^{-6}
200	9×10^{-6}	3×10^{-7}
100	8×10^{-11}	6×10^{-9}
50	7×10^{-21}	5×10^{-11}

9.2.4 becomes:

$$S_{tc} = S_{te} \exp\left[-1.89 \alpha^{\frac{2}{3}}/(kT)^{\frac{1}{3}}\right] \qquad A4$$

The variation of S_{tc} with temperature for the two different methods of capture is described by the exponential terms in 9.2.3 and A4. This assumes that S_{te} does not vary with temperature which is not strictly true. However this variation of S_{te} is neglected for the sake of simplicity. Values of the two exponential terms at different temperatures are listed in table A. In calculating these terms values used were $E_b = 0.2$ ev and $\alpha = (2\pi^2 e^2/\epsilon h)\ (2m)^{\frac{1}{2}} = 3.66 \times 10^{-6}$ erg$^{\frac{1}{2}}$.

It is to be expected that the largest value of S_{tc} will be effective at any particular temperature. Thus at low temperatures trap filling by tunnelling should predominate and S_{tc} will be determined by equation A4. At higher temperatures a significant number of electrons should be excited directly over the potential barrier. The dependence of S_{tc} on temperature, governed now by equation 9.2.3, will become stronger.

For the case of excitation over the barrier, substitution of 9.2.3 into A3 gives

$$\ln n_t = \ln(vN_t F \gamma_n t S_{te}) - E_b/kT$$

For the case of tunnelling, substitution of A4 into A3 gives

$$\ln n_t = \ln(vN_t F \gamma_n t S_{te}) - 1.89 \alpha^{\frac{2}{3}}/(kT)^{\frac{1}{3}}$$

Both v and S_{te} are temperature dependent; v is proportional to $T^{\frac{1}{2}}$ and S_{te} is usually assumed to vary as T^{-2}. Therefore we can write

$$l_n(vN_tF\gamma_n tS_{te}) = \ln(CT^{-3/2})$$

where C is a constant.

Therefore:

At high temperatures a plot of $\ln(n_t T^{3/2})$ against $1/T$ should yield a straight line of slope $-E_b/k$.

At low temperatures a plot of $\ln(n_t T^{3/2})$ against $1/T^{\frac{1}{3}}$ should yield a straight line of slope $-1.89\alpha^{\frac{2}{3}}/k^{\frac{1}{3}}$.

In the case of photochemically created traps a simpler situation than that described above for traps of the repulsive barrier type is expected. If the creation process has an activation energy, E_c, then N_t is proportional to $\exp(-E_c/kT)$. A plot of $\ln(n_t T^{3/2})$ against $1/T$, for all temperatures, should give a straight line of slope $-E_c/k$.

Appendix 11

Saturation of photoconductivity

Bube (1960 and 1966) has studied the phenomenon of saturation of photoconductivity in CdS and $CdS_{0.5}Se_{0.5}$ crystals. He considered that at a high enough intensity of illumination all of the sensitising centres become filled by holes. With illumination which produces band to band excitation additional holes excited by still higher intensities are captured by fast recombination centres which can then quickly capture electrons. With illumination which directly excites electrons from the class 11 centres to the conduction band the rate of absorption decreases to zero once these centres are filled by holes. In both cases a saturation of the measured photocurrent results.

An attempt was made to observe saturation of photoconductivity in highly photosensitive, as grown crystals. A helium-neon D.C. gas laser (type Nelas model G3) was used in order to obtain high intensity monochromatic radiation. This light, of wavelength 6328 A^{o}, would be strongly absorbed by the crystals and directly excite electrons from the valence band to the conduction band. The emission energy of the laser, $1\frac{1}{2}$ mW, corresponded to 1.5×10^{15} photons per second incident on the crystal. The intensity of the incident radiation was varied by interspersing neutral density filters between the laser and the crystal.

Measurements of photocurrent as a function of illumination intensity at 90°K are presented in figure 1. Curve (a) was obtained after the crystal had been cooled from 400°K in the dark. Curve (b) was measured after the crystal had been cooled from 400°K under intense white light. Also shown in curve (c) are measurements obtained at 297°K after cooling the crystal from 400°K in the dark. Only partial saturation of the photocurrent was observed in case (a) and no saturation was found in cases (b) and (c). Clearly higher intensities of illumination are required before complete saturation under all conditions can be observed. However an analysis of the measurements obtained provides sufficient information to throw some doubt on the explanation of saturation as postulated by Bube.

In Bube's model of the saturation of photoconductivity, recombination via class 1 and class 11 centres is considered. The rate equation in the steady state is

$$F = \beta_{e1} n (N_1 - n_1) + \beta_{e2} n (N_2 - n_2) \qquad A5$$

where the notation used has previously been defined in section 2.7.

Also the density of sensitising centres, N_2, is given by the sum of the free electron density at saturation and the density of trapped electrons above the dark equilibrium Fermi level.

Although curve (a) in figure 1 does not exhibit complete saturation the maximum current measured can be reasonably taken

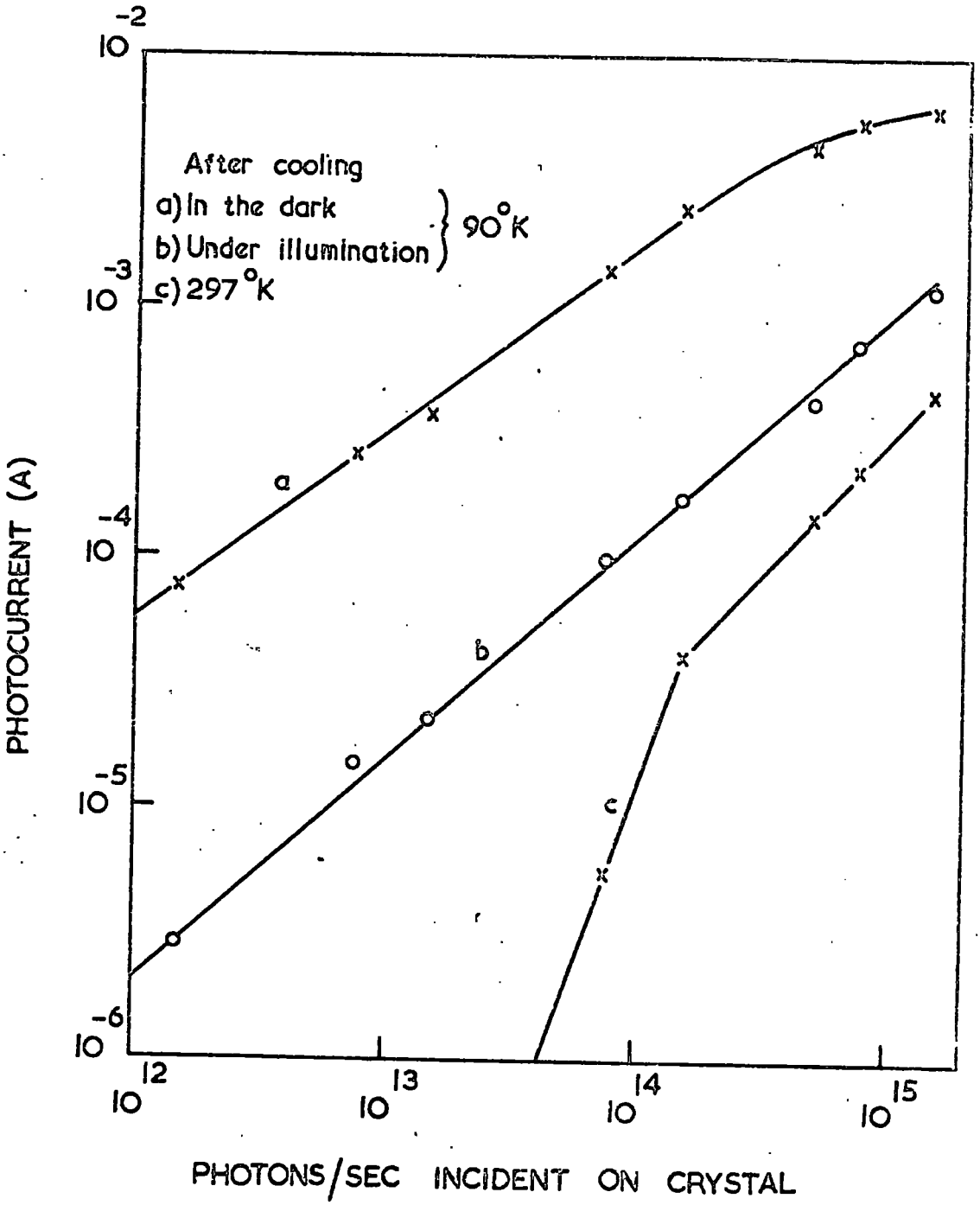

FIGURE 1. Photocurrent vs Intensity using laser excitation.

Table B Saturation data from curve (a).

Free electron density	1.3×10^{13} cm^{-3}
Incident photon intensity	1.5×10^{15} photons/sec
Density of electrons trapped in the 0.15 to 0.36 ev traps	4.9×10^{13} cm^{-3}

as the current at saturation in order to obtain an order of magnitude estimate of N_2. The conditions at this approximate saturation point are given in table B. After cooling from $400^{o}K$ in the dark before carrying out the measurements only the 0.15 to 0.36 ev traps would be filled. The density of electrons trapped in these centres was obtained from T.S.C. measurements. Thus, applying Bube's criterion, we obtain a value for the density of the sensitising centres, $N_2 = 10^{14} cm^{-3}$.

At saturation $n_2 = 0$. Typical values of the electron capture probabilities are $\beta_{e1} = 10^{-6} cm^3$ sec and $\beta_{e2} = 10^{-14} cm^3$ sec. Thus at the saturation point A5 becomes

$$10^{18} = 10^{7}(N_1 - n_1) + 10^{13} \qquad A6$$

In deriving A6 order of magnitude approximations for the various values have been used. The incident photon intensity given in table B has been corrected for the crystal volume to obtain F (assuming the creation of one free pair per incident photon).

The term in A6 associated with recombination via the sensitising centres, 10^{13}, is negligible. This does not make sense because the equation reduces to that describing recombination via a single set of centres. It has been shown in section 2.7 that in such a case the photocurrent varies as the square root of the illumination intensity. Thus curve (a) in figure 1 should exhibit a half power relationship over a large range of intensities and no saturation should be seen.

No such half power law was observed. Further, if recombination via the class 1 centres is predominant, then the filling of the sensitising centres by holes cannot affect the recombination kinetics appreciably. Thus again no onset of saturation should be observed.

A possibility examined is that the high intensity laser illumination creates excitons rather than free electron-hole pairs (the role of excitons in photoconductivity has been discussed in section 1.5). If, under these conditions, only one in 10^4 or 10^5 of these excitons dissociate to give free carriers at 90^oK then the value of F in A6 will be too large by a similar factor. Thus the class 11 term will no longer be negligible. However at room temperature all the excitons should dissociate and thus saturation should occur at a lower incident illumination intensity than at 90^oK. Curve (c) in figure 1 shows that at room temperature no saturation was observed. Thus this explanation cannot account for the discrepancy in A6.

No adequate explanation for the discrepancy could be found. It is therefore concluded that when photoconductivity occurs as a result of band to band excitation then saturation is not caused by the sensitising centres becoming filled by holes. Some other mechanism is involved. Thus the calculated value of N_2, 10^{14} cm^{-3}, is incorrect. The process by which saturation occurs possibly involves free electron-hole recombination or

recombination at shallow trapping centres. Further investigations into the nature of this mechanism are required.

Curve (b) in figure 1 was measured after a cooling treatment which results in a decrease in the free electron lifetime due to the photochemical creation of fast recombination centres (ref. section 11.4). Whatever mechanism is responsible for the saturation of photoconductivity the additional recombination via the new class 1 centres would result in the shift of saturation to a higher intensity of illumination. Therefore the fact that after this treatment (compared to that for curve (a) which produces no change in lifetime) no saturation was observed confirms the results discussed in 11.4.

References

Bube, R.H., 1960, J. Appl. Phys., 31, 1301.

Bube, R.H., 1966, J. Appl. Phys., 37, 4132.

APPENDIX 111

Computer programme used to calculate theoretical curves for fitting to T.S.C. peaks.

```
//     EXEC  NPL1FCLG
//C.SYSIN   DD  *
 TSC: PROCEDURE OPTIONS(MAIN);
 DCL (A,B,C,D,IT1,IT2,IMAX,TS,EP,T,K,TT,TTS) FLOAT;
 Q: GET LIST(N,M,IMAX,TTS);
 BEGIN; DCL AA(N) FLOAT;
 GET LIST(AA); PUT SKIP(3) DATA(TTS,IMAX); PUT SKIP(2);
 L: DO I=1 TO M BY 1;
 GET LIST(EP); PUT DATA(EP); PUT SKIP(2);
 LL: DO II=1 TO N BY 1;
 TT=AA(II);
 K=8.61E-05;
 T=EP/(K*TT); TS=EP/(K*TTS);
 B=EXP(TS)*TS**(2);
 D=EXP(TS)*TS**(7/2);
 A=IMAX*EXP(TS+B*EXP(-TS)*TS**(-2)*(1-2*TS**(-1)+6*TS**(-2)
 -24*TS**(-3)));
 C=IMAX*EXP(TS+D*EXP(-TS)*TS**(-7/2)*(1-7/2*TS**(-1)+1.575
 E01*TS**(-2)-8.663E01*TS**(-3)));
 IT1=A*EXP(-T-B*EXP(-T)*T**(-2)*(1-2*T**(-1)+6*T**(-2)-24*T**
 (-3)));
 IT2=C*EXP(-T-D*EXP(-T)*T**(-7/2)*(1-7/2*T**(-1)+1.575E01*T**(-2)
```

```
 -8.663E01*T**(-3)));
 PUT DATA(TT,IT1,IT2); PUT SKIP(2);
 END LL;
 END L;
 END;
 GO TO Q;
 END TSC;
/*
//G.SYSIN  DD  *
/*
```